

**SYNTHESIS OF IMIDAZOLE SCHIFF BASE LIGANDS, THEIR
SILVER(I) COMPLEXES AND THEIR ACTIVITIES AGAINST
*CANDIDA ALBICANS***

Theresa M. Tallon, B.Sc.

**A THESIS SUBMITTED TO THE NATIONAL UNIVERSITY OF IRELAND IN
FULFILMENT OF THE REQUIREMENT FOR THE DEGREE OF
DOCTOR OF PHILOSOPHY**



NUI MAYNOOTH

Ollscoil na hÉireann Má Nuad

**Department of Chemistry,
The National University of Ireland,
Maynooth,
Co. Kildare**

[2010]

Research Supervisors:

Dr. Malachy McCann.
Dr. John Briody.
Dr. John McGinley.

Head of Department:

Professor John Lowry.


Table of Contents

	Page number
Table of contents	I
Dedication	XI
Abstract	XII
Declaration	XIII
Acknowledgements	XIV
Symbols and Abbreviations	XVI
Chapter 1 Introduction	1
1.1 Description of Fungi and Fungal Infections	2
1.2 Current Prescription Antifungal Drugs	5
1.2.1 Polyenes	6
1.2.2 Synthetic Antifungal Agents	8
1.2.3 Azoles	9
1.2.4 Echinocandins	11
1.2.5 Allylamines	13
1.2.6 Latest Additions to the Arsenal of Antifungal Drugs	13
1.3 Metals in Medicine and Metal-Based Drugs	14
1.3.1 Elements Essential for Life	14
1.3.2 A Brief History of Metals in Medicine with Particular Emphasis on Silver	15
1.3.3 Current and Possible Future Metallopharmaceuticals	17
1.4 Previous Work in this Research Group	19
1.5 Silver Coordination Chemistry and Bioinorganic Chemistry	24
1.6 Mechanism of Silver Transport and Bioactivity	27

1.7	Imidazole Chemistry	33
1.8	Aim of the Present Work	41
Chapter 2 Experimental (part 1) Organic Synthesis		43
2.0	Chemicals and Instrumentation	44
2.1	Instrumentation	44
2.2	Synthesis of Starting Materials	45
2.2.1	1- <i>H</i> -Imidazol-2-amine hemisulphate (1)	45
2.2.2	1-Methyl-1 <i>H</i> -imidazole-2-carboxaldehyde	46
2.2.2.1	1-Methyl-2-hydroxymethyl-1 <i>H</i> -imidazole (2)	46
2.2.2.2	1-Methyl-1 <i>H</i> -imidazole-2-carboxaldehyde (3)	46
2.2.3	1-Benzyl-1 <i>H</i> -imidazole-2-carboxaldehyde	47
2.2.3.1	1-Benzyl-1 <i>H</i> -imidazole (4)	47
2.2.3.2	1-Benzyl-2-hydroxymethyl-1 <i>H</i> -imidazole (5)	48
2.2.3.3	1-Benzyl-1 <i>H</i> -imidazole-2-carboxaldehyde (6)	49
2.2.4	4(5)-Methyl-1 <i>H</i> -imidazole-5(4)-carboxaldehyde (8)	50
2.3	Schiff Base Ligands Derived from 1<i>H</i>-Imidazol-2-amine (1)	51
2.3.1	(<i>E</i>)- <i>N</i> -(4-[(1 <i>H</i> -Imidazol-2-yl)methyl]benzylidene)]-1 <i>H</i> -imidazol-2-amine (22)	51
2.3.2	(<i>E</i>)-3-[(1 <i>H</i> -Imidazol-2-ylimino)methyl]phenol (23)	52
2.3.3	(<i>E</i>)-2-[(1 <i>H</i> -Imidazol-2-ylimino)methyl]phenol (24)	53
2.3.4	<i>N</i> -[(<i>E</i>)-1 <i>H</i> -Imidazol-2-ylmethylidene]-1 <i>H</i> -imidazol-2-amine (25)	53
2.3.5	<i>N</i> -[(<i>E</i>)-1 <i>H</i> -Imidazol-4-ylmethylidene]-1 <i>H</i> -imidazol-2-amine (26)	54
2.3.6	<i>N</i> -[(<i>E</i>)-(5-Methyl-1 <i>H</i> -imidazol-4-yl)methylidene]-1 <i>H</i> -imidazol-2-amine (27)	55
2.3.7	<i>N</i> -[(<i>E</i>)-(1-Methyl-1 <i>H</i> -imidazol-2-yl)methylidene]-1 <i>H</i> -imidazol-2-amine (28)	56



2.4. Schiff Base Ligands Derived from Histamine	57
2.4.1 2-([2-(1 <i>H</i> -Imidazol-5-yl)ethyl]iminomethyl)phenol (29)	57
2.4.2 <i>N</i> -[2-(1 <i>H</i> -Imidazol-5-yl)ethyl]- <i>N</i> -[(<i>E</i>)-1 <i>H</i> -imidazol-2-ylmethylidene]amine (30)	58
2.4.3 <i>N</i> -[2-(1 <i>H</i> -Imidazol-4-yl)ethyl]- <i>N</i> -[(<i>E</i>)-(5-methyl-1 <i>H</i> -imidazol-4-yl)methylidene]amine (31)	58
2.4.4 <i>N</i> -[2-(1 <i>H</i> -Imidazol-4-yl)ethyl]- <i>N</i> -[(<i>E</i>)-(1-methyl-1 <i>H</i> -imidazol-2-yl)methylidene]amine (32)	59
2.4.5 <i>N</i> -[2-(1 <i>H</i> -Imidazol-4-yl)ethyl]- <i>N</i> -[(<i>E</i>)-1 <i>H</i> -imidazol-5-ylmethylidene]amine (33)	60
2.4.6 (<i>E</i>)- <i>N</i> -[[(1-Benzyl-1 <i>H</i> -imidazol-2-yl)methylene]-2-(1 <i>H</i> -imidazol-2-yl)]ethanamine (34)	61
2.4.7 <i>N</i> -[2-(1 <i>H</i> -Imidazol-4-yl)ethyl]- <i>N</i> -(<i>E</i>)-[4-(1 <i>H</i> -imidazol-1-yl)phenyl]methylideneamine (35)	62
2.5 Schiff Base Ligands Derived from Apim	63
2.5.1 2-([3-(1 <i>H</i> -Imidazol-1-yl)propyl]iminomethyl)phenol (36)	63
2.5.2 <i>N</i> -[(<i>E</i>)-1 <i>H</i> -Imidazol-5-ylmethylidene]- <i>N</i> -[3-(1 <i>H</i> -imidazol-1-yl)propyl]amine (37)	64
2.5.3 <i>N</i> -[(<i>E</i>)-1 <i>H</i> -Imidazol-2-ylmethylidene]- <i>N</i> -[3-(1 <i>H</i> -imidazol-1-yl)propyl]amine (38)	65
2.5.4 3-(1 <i>H</i> -Imidazol-1-yl)- <i>N</i> -[(<i>E</i>)-(5-methyl-1 <i>H</i> -imidazol-4-yl)methylidene]-1-propanamine (39)	66
2.5.5 3-(1 <i>H</i> -Imidazol-1-yl)- <i>N</i> -[(<i>E</i>)-(1-methyl-1 <i>H</i> -imidazol-2-yl)methylidene]-1-propanamine (40)	67
2.6 Schiff Base Ligands Derived from 1,2-Diaminoethane, 1,3-Diaminopropane and 1,4-Diaminobutane	68

2.6.1	<i>N</i> -[(<i>E</i>)-1 <i>H</i> -Imidazol-2-ylmethylidene]- <i>N</i> -(2-[(<i>E</i>)-1 <i>H</i> -imidazol-2-ylmethylidene]aminoethyl)amine (41)	68
2.6.2	<i>N</i> -[(<i>E</i>)-1 <i>H</i> -Imidazol-2-ylmethylidene]- <i>N</i> -(3-[(<i>E</i>)-1 <i>H</i> -imidazol-2-ylmethylidene]aminopropyl)amine (42)	69
2.6.3	<i>N</i> -[(<i>E</i>)-1 <i>H</i> -Imidazol-2-ylmethylidene]- <i>N</i> -(4-[(<i>E</i>)-1 <i>H</i> -imidazol-2-ylmethylidene]aminobutyl)amine (43)	70
2.6.4	<i>N</i> -[(<i>E</i>)-(4-Methyl-1 <i>H</i> -imidazol-5-yl)methylidene]- <i>N</i> -(2-[(<i>E</i>)-(4-methyl-1 <i>H</i> imidazol-5-yl)methylidene]aminoethyl)amine (44)	71
2.6.5	<i>N</i> -[(<i>E</i>)-(5-Methyl-1 <i>H</i> -imidazol-4-yl)methylidene]- <i>N</i> -(3-[(<i>E</i>)-(5-methyl-1 <i>H</i> -imidazol-4-yl)methylidene]aminopropyl)amine (45)	72
2.6.6	<i>N</i> -[(<i>E</i>)-(5-Methyl-1 <i>H</i> -imidazol-4-yl)methylidene]- <i>N</i> -(4-[(<i>E</i>)-(5-methyl-1 <i>H</i> -imidazol-4-yl)methylidene]aminobutyl)amine (46)	73
2.6.7	2-[[(<i>E</i>)-(2-Hydroxyphenyl)methylidene]aminoethyl]imino]methylphenol (47)	74
2.6.8	2-[[3-[(<i>E</i>)-(2-Hydroxyphenyl)methylidene]aminopropyl]imino]methylphenol (48)	75
2.6.9	2-[[4-[(<i>E</i>)-(2-Hydroxyphenyl)methylidene]aminobutyl]imino]methylphenol(49)	76
2.6.10	<i>N</i> -[(<i>E</i>)-1 <i>H</i> -Imidazol-4-ylmethylidene]- <i>N</i> -(2-[(<i>E</i>)-1 <i>H</i> -imidazol-4-ylmethylideneaminoethyl])amine (50)	77
2.6.11	<i>N</i> 1-[(<i>E</i>)-1 <i>H</i> -Imidazol-5-ylmethylidene]- <i>N</i> -(3-[(<i>E</i>)-1 <i>H</i> -imidazol-5-ylmethylidene])-1,3-propanediamine (51)	78
2.6.12	<i>N</i> -[(<i>E</i>)-1 <i>H</i> -Imidazol-5-ylmethylidene]-5-[(<i>E</i>)-(1 <i>H</i> -imidazol-5-ylmethyl)imino]-1-butylamine (52)	79
2.6.13	<i>N</i> -[(<i>E</i>)-(1-Methyl-1 <i>H</i> -imidazol-2-yl)methylidene]- <i>N</i> -(2-[(<i>E</i>)-(1-methyl-1 <i>H</i> -imidazol-2-yl)methylidene]aminoethyl)amine (53)	80
2.6.14	<i>N</i> -[(<i>E</i>)-(1-Methyl-1 <i>H</i> -imidazol-2-yl)methylidene]- <i>N</i> -(3-[(<i>E</i>)-(1-methyl-1 <i>H</i> -imidazol-2-yl)methylidene]aminopropyl)amine (54)	81
2.6.15	4-[(<i>E</i>)-2-(1-Methyl-1 <i>H</i> -imidazol-2-yl)diazenyl]- <i>N</i> -[(<i>E</i>)-(1-methyl-1 <i>H</i> -imidazol-2-yl)methylidene]-1-butanamine (55)	82
2.6.16	<i>N</i> -[(<i>E</i>)-(1-Benzyl-1 <i>H</i> -imidazol-2-yl)methylidene]- <i>N</i> -(2-[(<i>Z</i>)-(1-benzyl-1 <i>H</i> -imidazol-2-yl)methylidene]aminoethyl)amine (56)	83

2.6.17	<i>N</i> -[(<i>E</i>)-(1-Benzyl-1 <i>H</i> -imidazol-2-yl)methylidene]- <i>N</i> -(3-[(<i>E</i>)-(1-benzyl-1 <i>H</i> -imidazol-2-yl)methylidene]aminopropyl)amine (57)	84
2.6.18	<i>N</i> -[(<i>E</i>)-(1-Benzyl-1 <i>H</i> -imidazol-2-yl)methylidene]- <i>N</i> -(4-[(<i>E</i>)-(1-benzyl-1 <i>H</i> -imidazol-2-yl)methylidene]aminobutyl)amine (58)	85
2.7	Schiff Base Ligands Derived from 1,2-Phenylenediamine, 1,3-Phenylenediamine and 1,4-Phenylenediamine	86
2.7.1	<i>N</i> -[(<i>E</i>)-1 <i>H</i> -Imidazol-2-ylmethylidene]- <i>N</i> -(2-[(<i>E</i>)-1 <i>H</i> -imidazol-2-ylmethylidene]aminophenyl)amine (59)	86
2.7.2	<i>N</i> 1-[(<i>E</i>)-1 <i>H</i> -Imidazol-2-ylmethylidene]- <i>N</i> -(3-[(<i>E</i>)-1 <i>H</i> -imidazol-2-ylmethylidene]-1,3-benzenediamine (60)	87
2.7.3	<i>N</i> -[(<i>E</i>)-1 <i>H</i> -Imidazol-2-ylmethylidene]- <i>N</i> -(4-[(<i>E</i>)-1 <i>H</i> -imidazol-2-ylmethylidene]aminophenyl)amine (61)	87
2.7.4	2-[(2-[(<i>E</i>)-(2-Hydroxyphenyl)methylidene]aminophenyl)]imino methylphenol (62)	88
2.7.5	2-[(3-[(<i>E</i>)-(2-Hydroxyphenyl)methylidene]aminophenyl)]imino methylphenol (63)	89
2.7.6	2-[(4-[(<i>E</i>)-(2-Hydroxyphenyl)methylidene]aminophenyl)]imino methylphenol (64)	90
2.7.7	<i>N</i> -[(<i>E</i>)-(5-Methyl-1 <i>H</i> -imidazol-4-yl)methylidene]- <i>N</i> -(2-[(<i>E</i>)-(5-methyl-1 <i>H</i> -imidazol-4-yl)methylidene]aminophenyl)amine (65)	91
2.7.8	<i>N</i> -[(<i>E</i>)-(4-Methyl-1 <i>H</i> -imidazol-5-yl)methylidene]- <i>N</i> -(3-[(<i>E</i>)-(5-methyl-1 <i>H</i> -imidazol-4-yl)methylidene]aminophenyl)amine (66)	92
2.7.9	<i>N</i> -[(<i>E</i>)-(4-Methyl-1 <i>H</i> -imidazol-5-yl)methylidene]- <i>N</i> -(4-[(<i>E</i>)-(4-methyl-1 <i>H</i> -imidazol-5-yl)methylidene]aminophenyl)amine (67)	93
2.7.10	<i>N</i> -[(<i>E</i>)-1 <i>H</i> -Imidazol-4-ylmethylidene]- <i>N</i> -(2-[(<i>E</i>)-1 <i>H</i> -imidazol-5-ylmethylidene]aminophenyl)amine (68)	94
2.7.11	<i>N</i> -[(<i>E</i>)-1 <i>H</i> -Imidazol-4-ylmethylidene]- <i>N</i> -(3-[(<i>E</i>)-1 <i>H</i> -imidazol-4-ylmethylidene]aminophenyl)amine (69)	95
2.7.12	<i>N</i> -[(<i>E</i>)-1 <i>H</i> -Imidazol-4-ylmethylidene]- <i>N</i> -(4-[(<i>E</i>)-1 <i>H</i> -imidazol-4-ylmethylidene]aminophenyl)amine (70)	95



2.7.13	<i>N</i> -[(<i>E</i>)-(1-Methyl-1 <i>H</i> -imidazol-2-yl)methylidene]- <i>N</i> -(2-[(<i>E</i>)-(1-methyl-1 <i>H</i> -imidazol-2-yl)methylidene]aminophenyl)amine (71)	96
2.7.14	<i>N</i> -[(<i>E</i>)-(1-Methyl-1 <i>H</i> -imidazol-2-yl)methylidene]- <i>N</i> -(3-[(<i>E</i>)-(1-methyl-1 <i>H</i> -imidazol-2-yl)methylidene]aminophenyl)amine (72)	97
2.7.15	<i>N</i> -[(<i>E</i>)-(1-Methyl-1 <i>H</i> -imidazol-2-yl)methylidene]- <i>N</i> -(4-[(<i>E</i>)-(1-methyl-1 <i>H</i> -imidazol-2-yl)methylidene]aminophenyl)amine (73)	98
2.7.16	<i>N</i> -[(<i>E</i>)-(1-Benzyl-1 <i>H</i> -imidazol-2-yl)methylidene]- <i>N</i> -(2-[(<i>E</i>)-(1-benzyl-1 <i>H</i> -imidazol-2-yl)methylidene]aminoethyl)amine (74)	99
2.7.17	<i>N</i> -[(<i>E</i>)-(1-Benzyl-1 <i>H</i> -imidazol-2-yl)methylidene]- <i>N</i> -(3-[(<i>E</i>)-(1-benzyl-1 <i>H</i> -imidazol-2-yl)methylidene]aminophenyl)amine (75)	100
2.7.18	<i>N</i> -[(<i>E</i>)-(1-Benzyl-1 <i>H</i> -imidazol-2-yl)methylidene]- <i>N</i> -(4-[(<i>E</i>)-(1-benzyl-1 <i>H</i> -imidazol-2-yl)methylidene]aminophenyl)amine (76)	101
Chapter 2 Experimental (part 2) Synthesis of Ag(I) Complexes		102
2.8	Synthesis of Ag(I) Complexes of the Schiff Base Ligands Derived from 1<i>H</i>-Imidazol-2-amine (1)	103
2.8.1	[Ag(22) ₂]ClO ₄	103
2.8.2	[Ag(23) ₂]ClO ₄ ·H ₂ O	104
2.8.3	[Ag(24) ₂]ClO ₄ ·2H ₂ O	105
2.8.4	[Ag(25)]ClO ₄ ·2H ₂ O	105
2.8.5	[Ag(26)]ClO ₄ ·H ₂ O	106
2.8.6	[Ag(27)]ClO ₄ ·H ₂ O	107
2.8.7	[Ag(28)]ClO ₄ ·H ₂ O	108
2.9	Synthesis of Ag(I) Complexes of the Schiff Base Ligands Derived from Histamine	109
2.9.1	[Ag(29)]ClO ₄ ·H ₂ O	109



2.9.2	[Ag _{1.5} (30)](ClO ₄) _{1.5}	110
2.9.3	[Ag _{1.5} (31)](ClO ₄) _{1.5}	111
2.9.4	[Ag _{1.5} (32)](ClO ₄) _{1.5} ·H ₂ O	111
2.9.5	[Ag _{1.5} (33)](ClO ₄) _{1.5}	112
2.9.6	[Ag(34)]ClO ₄ ·H ₂ O	113
2.9.7	[Ag ₂ (35)](ClO ₄) ₂ ·H ₂ O	114
2.10	Synthesis of Ag(I) Complexes of the Schiff Base Ligands Derived From Apim	115
2.10.1	[Ag(36) ₂]ClO ₄ ·H ₂ O	115
2.10.2	[Ag(37)]ClO ₄	116
2.10.3	[Ag(38)]ClO ₄	117
2.10.4	[Ag(39)]ClO ₄	118
2.10.5	[Ag(40)]ClO ₄	119
2.11	Synthesis of Ag(I) Complexes of the Schiff Base Ligands Derived From 1,2-Diaminoethane, 1,3-Diaminopropane and 1,4-Diaminobutane	120
2.11.1	[Ag _{1.5} (41)](ClO ₄) _{1.5}	120
2.11.2	[Ag _{1.5} (42)](ClO ₄) _{1.5}	121
2.11.3	[Ag ₂ (43)](ClO ₄) ₂	122
2.11.4	[Ag ₂ (44)](ClO ₄) ₂	123
2.11.5	[Ag ₂ (45)](ClO ₄) ₂	124
2.11.6	[Ag ₂ (46)](ClO ₄) ₂	125
2.11.7	[Ag(47)]ClO ₄	126
2.11.8	[Ag(48)]ClO ₄	127
2.11.9	[Ag ₂ (49)](ClO ₄) ₂	128
2.11.10	[Ag(50)]ClO ₄	129
2.11.11	[Ag ₂ (51)](ClO ₄) ₂	130
2.11.12	[Ag ₂ (52)](ClO ₄) ₂	131



2.11.13	[Ag _{1.5} (53)](ClO ₄) _{1.5}	132
2.11.14	[Ag _{1.5} (54)](ClO ₄) _{1.5}	133
2.11.15	[Ag ₂ (55)](ClO ₄) ₂	134
2.11.16	[Ag _{1.5} (56)](ClO ₄) _{1.5}	135
2.11.17	[Ag ₂ (57)](ClO ₄) ₂	136
2.11.18	[Ag ₂ (58)](ClO ₄) ₂	137
2.12	Synthesis of Ag(I) Complexes of the Schiff Base Ligands Derived from 1,2-Phenylenediamine, 1,3-Phenylenediamine and 1,4-Phenylenediamine	138
2.12.1	[Ag _{1.5} (59)](ClO ₄) _{1.5}	138
2.12.2	[Ag(60)]ClO ₄ ·2H ₂ O	139
2.12.3	[Ag(61)]ClO ₄	140
2.12.4	[Ag _{1.5} (62)](ClO ₄) _{1.5}	141
2.12.5	[Ag ₂ (63)](ClO ₄) ₂	141
2.12.6	[Ag(64)]ClO ₄ ·2H ₂ O	142
2.12.7	[Ag _{1.5} (65)](ClO ₄) _{1.5}	143
2.12.8	[Ag _{1.5} (66)](ClO ₄) _{1.5}	144
2.12.9	[Ag _{1.5} (67)](ClO ₄) _{1.5}	145
2.12.10	[Ag _{1.5} (68)](ClO ₄) _{1.5} ·3H ₂ O	146
2.12.11	[Ag(69)]ClO ₄ ·H ₂ O	147
2.12.12	[Ag(70)]ClO ₄ ·H ₂ O	147
2.12.13	[Ag(71)]ClO ₄ ·H ₂ O	148
2.12.14	[Ag(72)]ClO ₄ ·2H ₂ O	149
2.12.15	[Ag(73)]ClO ₄ ·H ₂ O	150
2.13	Anti-Candida Testing	152
2.13.1	Biological Preparations	152
2.13.2	Fungal Isolates	152
2.13.3	Sterilisation	152

2.13.4	Cell Density	152
2.13.5	Minimal Growth Media (MM)	152
2.13.6	Commercial Anti-Fungal Agents	152
2.13.7	Fungal Cell Culture Conditions	153
2.14	Susceptibility Testing Methods	153
2.14.1	Preparation of Complexes for Susceptibility Testing	153
2.14.2	Determination of Yeast Cell Minimum Inhibitory Concentrations (MIC)	153
Chapter 3	Results and Discussion	155
3.1.	Schiff Base Ligands	156
3.1.1	The Formation of Schiff Bases	156
3.2	Aldehydes Used for the Synthesis of Schiff Bases	157
3.3	Schiff Base Ligands Derived from 1 <i>H</i> -Imidazole-2-amine (1)	160
3.3.1	Synthesis of 1 <i>H</i> -Imidazole-2-amine (1)	160
3.3.2	Synthesis of Schiff Base Ligands Derived from 1 <i>H</i> -Imidazole-2-amine (1)	162
3.4	Schiff Base Ligands Derived from Histamine	167
3.4.1	Synthesis of Schiff Base Ligands Derived from Histamine	167
3.5	Synthesis of Schiff Base Ligands Derived from 1-(3-Aminopropyl)imidazole (Apim)	173
3.6	Synthesis of Schiff Base Ligands Derived from 1,2-Diaminoethane, 1,3-Diaminopropane and 1,4-Diaminobutane	181
3.7	Synthesis of Schiff Base Ligands Derived from 1,2-Phenylenediamine, 1,3-Phenylenediamine and 1,4-Phenylenediamine	186
3.8	Synthesis of Ag(I) Complexes	192
3.9	Synthesis of the Ag(I) Complexes of the Schiff Base Ligands Derived from 1 <i>H</i> -Imidazole-2-amine (1)	200
3.10	Synthesis of the Ag(I) Complexes of the Schiff Base Ligands Derived from Histamine	205
3.11	Synthesis of the Ag(I) Complexes of the Schiff Base Ligands Derived from Apim	210

3.12	Synthesis of the Ag(I) Complexes of the Schiff Base Ligands Derived from 1,2-Diaminoethane, 1,3-Diaminopropane and 1,4-Diaminobutane	214
3.13	Synthesis of the Ag(I) Complexes of the Schiff Base Ligands Derived from 1,2-Phenylenediamine, 1,3-Phenylenediamine and 1,4-Phenylenediamine	227
3.14	Biological Activity	237
3.14.1	The Fungal Growth Curve	237
3.14.2	Anti- <i>Candida</i> Activity of the Imidazole Ligands and their Metal Complexes	237
3.14.3	Anti- <i>Candida</i> Activity of the Ag(I) Complexes of the Schiff Base Ligands Derived from 1 <i>H</i> -Imidazole-2-amine (1)	241
3.14.4	Anti- <i>Candida</i> Activity of the Ag(I) Complexes of the Schiff Base Ligands Derived from Histamine	244
3.14.5	Anti- <i>Candida</i> Activity of the Ag(I) Complexes of the Schiff Base Ligands Derived from Apim	247
3.14.6	Anti- <i>Candida</i> Activity of the Ag(I) Complexes of the Schiff Base Ligands Derived from 1,2-Diaminoethane, 1,3-Diaminopropane and 1,4-Diaminobutane	249
3.14.7	Anti- <i>Candida</i> Activity of the Ag(I) Complexes of the Schiff Base Ligands derived from 1,2-, 1,3- and 1,4-Phenylenediamine	254
3.15	Summary of anti- <i>Candida</i> Activity	257
Chapter 4	Conclusions	258
	Bibliography	261
	Appendix 1	273
	Appendix 2	282
	Epilogue	291


Abstract

The work described in this thesis concerns the synthesis of *ca.* 50 new imidazole-containing Schiff base ligands, the formation of their Ag(I) complexes and their evaluation as agents for inhibiting the growth of the fungal pathogen, *Candida albicans*. The synthesis of some Schiff base ligands proved problematic and the products were characterized using standard IR and NMR spectroscopic methods, micro-analysis and, in two instances, by X-ray crystallography. Compared to the synthesis of the ligands the preparation of the Ag(I) complexes was relatively simple and pure products were isolated in moderate to good yields. The Ag(I) complexes were also characterized using standard IR and NMR spectroscopic methods, micro-analysis and, in two cases, by mass spectrometry. All of the Schiff base ligands and their corresponding Ag(I) complexes were tested for their anti-*Candida* activity. While the metal-free Schiff base ligands were essentially inactive, the corresponding Ag(I) complexes showed excellent activity. The set of Ag(I) complexes based on the Apim (Apim = 1-(3-aminopropyl)imidazole) Schiff base ligands were the most potent. A progressive improvement in activity of the Ag(I) complexes was seen on going from Schiff base ligands derived from 1*H*-imidazole-2-amine to histamine to Apim, corresponding to the increase in spacer chain length of the respective ligand sets. A notable reduction in activity was observed in the Ag(I) complexes of di-Schiff base ligands derived from 1,2-diaminoethane, 1,3-diaminopropane and 1,4-diaminobutane. The extra imine group in the spacer chain may have had a negative impact on activity and negate any positive effect due to the progressive increase in spacer chain length. The set of Ag(I) complexes containing di-Schiff base ligands derived from 1,2-, 1,3- and 1,4-phenylenediamine had similar activity to those complexes with ligands derived from 1,2-diaminoethane, 1,3-diaminopropane and 1,4-diaminobutane. In this instance, the resulting increase in the level of aromaticity does not appear to affect the anti-*Candida* activity.



Acknowledgements

I would like to extend my thanks to my supervisors, Dr. M. McCann, Dr. J. Briody and Dr. J. McGinley. I would also like to thank Prof. M. Quinn for giving me the opportunity to pursue my Ph.D. research and to Prof. J. Lowry for making it possible to continue that work. To all the staff of the Chemistry Department, particularly Ria, Noel, Barbra, Ann and Niamh my sincere thanks.

I would like to acknowledge the financial support provided by Kildare County Council, and to thank all their staff, especially Ronan for all his help throughout the years. I would also like to express my appreciation for the bursary form *BOC* it was gratefully received.

I like to take this opportunity to say thank you, to my family, particularly my partner Robert, my sons, Brian, David and Robert and my princess, Aoife. To my parents, James and Sheila, my sisters and brothers, especially Patrick, Thomas and Moya, a big thank you.

Thanks to all the postgrads, both past and present for the daily group therapy sessions in the coffee-room and the more in-depth sessions in the Roost. Your sensitivity, reverence and compassion during those sessions were deeply felt and appreciated and were, without doubt, the source of some of the high points of my time in Maynooth. Special thanks to Carol, Ciaran, Declan, Denis, Edel, Elaine, Fiachra, Garry McR, John W, Kenneth, Linda, Marcia, Margaret, Maryann R, Niall, Niamh, Owen, Paul, Rachel, Rob, Saidhbhe, Sinead and Suaad for their encouragement and friendship.

A measure of a person is the company they keep, and with this I would like to thank my wider family of friends for their support throughout the duration of this project. Granted my measure as a person might now be a little weird because of you, but you are all special in your own special way.

I reserve a very special thank you to Martin for picking up all those pieces and putting them back together and sending me back into the fray when I wanted to take the more



sensible and less painful option and walk away, without you, this work would never have been finished, Martin you kept me sane, well near sane as I will ever be! Thank you!

Finally, I leave you with these immortal words, and wish all *saol gon aifeal*.

“A man would do nothing if he waited until he could do it so well that no one would find fault with what he has done.”

John Henry Cardinal Newman

Symbols and Abbreviations

AIDS	Acquired Immunodeficiency Syndrome
AmB	Amphotericin B
Apim	1-(3-Aminopropyl)imidazole
ATP	Adenosine triphosphate
BBB	Blood-brain barrier
bdoaH ₂	Benzene-1,2-dioxyacetic acid
bib	1,3-Bis(4,5-dihydro-1H-imidazole-2-yl)benzene
1-Bimi	Bis(1 <i>H</i> -Imidazole-1-ylmethyl)-1 <i>H</i> -imidazole
2-Bimi	2-(1 <i>H</i> -Imidazole-2-ylmethyl)-1 <i>H</i> -imidazole
2-BIM(Me)	1-Methyl-2-(1-methyl-1 <i>H</i> -imidazole-2-yl)methane
bipy	2,2'-Bipyridine
DCM	Dichloromethane
CDC	Centre for Disease Control and Prevention
CHN	% Carbon, hydrogen and nitrogen
d, m, s, t	Doublet, multiplet, singlet, triplet
DMSO	Dimethylsulfoxide
DNA	Deoxyribonucleic acid
ECG	Electrocardiogram
FDA	The U.S. Food and Drug Administration
fumH ₂	Fumaric acid
GSSG	Anti-oxidant molecule glutathione
HIV	Human Immunodeficiency Virus
Hz	Hertz
iphaH ₂	Isophthalic acid
IR	Infrared
LFSE	Ligand field stabilization energy
MgSO ₄	Magnesium sulphate
malH ₂	Malonic acid
MBS	Metal binding site
2-mBIM	Bis(2-methyl-1 <i>H</i> -imidazole-1-yl)methane
MeCN	Acetonitrile

MIC	Minimum inhibitory concentration
MIC ₅₀	The minimum inhibitory concentration that results in a 50% kill
MIC ₁₀₀	The minimum inhibitory concentration that results in a 100% kill
MM	Minimal medium
MOF	Metal-organic frameworks
MRI	Magnetic resonance imaging
mRNA	Messenger ribonucleic acid
MRSA	Methicillin-resistant <i>Staphylococcus aureus sp.</i>
MT	Metallothionins
NIH	U.S. National Institute of Health
norbH ₂	<i>cis</i> -5-Norborene-endo-2,3-dicarboxylic acid
NO ₂ imiH	4(5)-nitroimidazole
1,10-phen	1,10-Phenanthroline
1,10-phendio	1,10-Phenanthroline-5,6-dione
phaH ₂	Phthalic acid
RPMI	Roswell Park Memorial Institute
salH ₂	Salicylic acid
sal-imi	Salicylic acid-imidazole Schiff base ligands
SDA	Sabouraud Dextrose Agar
SSD	Silver sulfadiazine
T.B.	Tuberculosis
THF	Tetrahydrofuran
TSIL	Task specific ionic liquids
URDIP	Unit for Research and Development of Information Products India
VRSA	Vancomycin-resistant <i>Staphylococcus aureus sp.</i>
ZVED	National Centre for Zoonotic, Vector-Borne, and Enteric Diseases

Introduction

1.1 Description of Fungi and Fungal Infections

Fungi^{1,2} are ubiquitous in nature, where they are found free-living on plants, in soil and in salt water. They are major plant pathogens and are one of the main causes of crop damage and spoilage of foods (Figure 1).³

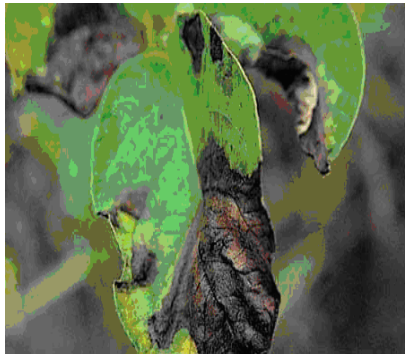


Figure 1 Potato blight caused by *Phytophthora infestans*.

Fungi are very versatile organisms that live in and on animals as part of their natural flora, but they can also be the cause of numerous infections. These infections are classified as follows: (a) Superficial mycoses: infections that are limited to the outermost layers of the skin and hair (Figure 2).⁴



Figure 2 Superficial fungal infection of the skin.

(b) Cutaneous mycoses: infections that extend deeper into the epidermis as well as invasive hair and nail diseases (Figure 3).⁴



Figure 3 Fungal infection of the nail.

(c) Subcutaneous mycoses: infections involving the dermis, subcutaneous tissues, muscle and fascia (Figure 4).⁴



Figure 4 Fungal infection of the oral cavity.

(d) Systemic mycoses: infections that originate primarily in the lungs, but may spread to many organs (Figure 5).⁴

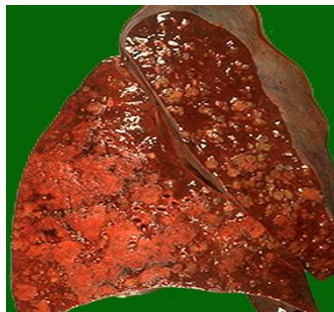


Figure 5 Fungal infection of the lung.

Almost all fungal organisms involved in human diseases are free-living, but humans have a high level of innate immunity to infection due to innate natural barriers. Most infections

are mild and self-limiting. The skin protects us against colonization by fungi that attack superficial, cutaneous and subcutaneous layers. Mucosal surfaces protect against organisms that attack the pulmonary system, while humoral factor protects against systemic infection. Consequently, very few fungi can cause infection in an otherwise healthy individual. However, in cases where the immune system has been compromised, either by disease or by therapies, fungal infection can become a problem. The emergence of new diseases and infections, such as Human Immunodeficiency Virus (HIV), Acquired Immunodeficiency Syndrome (AIDS), and the re-emergences of old ones, like Tuberculosis (T.B.), have led to an increase in the incidence of fungal infections. Also, the emergence of fungi which are resistant to the current prescription drugs is a matter of urgent concern, and it is this challenge that is driving the demand for new drugs.

One of the most common fungal species to affect humans is the yeast *Candida albicans*. This yeast is dimorphic, that is to say, it exists as single, oval yeast cells, and reproduces by budding (Figure 6). It also has the ability to produce pseudohyphae, where the buds elongate forming a structure known as the germ tube. Germ tubes remain attached to each other to form root-like rhizoids (Figure 7). Rhizoids can penetrate mucosae and intestinal walls causing microscopic holes, which then allow toxins, undigested food, bacteria and fungi to enter the blood stream, giving rise to a condition called Leaky Gut Syndrome.⁵

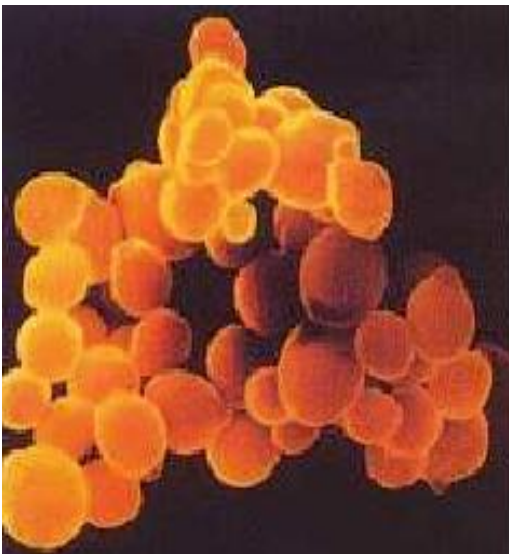


Figure 6 Yeast or budding form of *C. albicans*.



Figure 7 Pseudohyphae, the invasive form of *C. albicans*.

C. albicans is found in humans as a normal part of the bowel flora. In a healthy person, *C. albicans*, in their millions, perform many functions inside the digestive tract, one of which is to destroy harmful bacteria. Our immune system, together with bacteria, such as *Lactobacillus acidophilus sp.*, helps to keep the growth of *Candida sp.* and other fungal cells under control. However, if the immune system is compromised and the numbers of “friendly” bacteria are reduced, then an overgrowth of *Candida sp.* can occur, giving rise to a condition known as candidiasis.

1.2 Current Prescription Antifungal Drugs^{1,2,5-7,9}

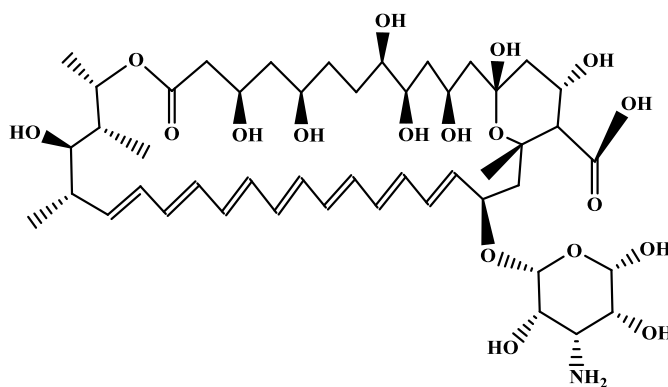
In contrast to anti-bacterial chemotherapy there are relatively few antifungal agents available. This is because, up to the 1970’s, fungal infections were less common. This was due to either a lack of diagnosis or occurrence, and historically was much less likely to cause fatality, at least in the “developed world.” This, coupled with the extreme difficulty in developing a drug that is selective against the fungal cells, which are very similar to the mammalian cell, has been attributed to the scarcity of prescription fungicides.^{5b}

This thesis concerns itself with the fungal species *C. albicans*. However, other fungi, especially *Aspergillus sp.*, *Pneumocystis carinii sp.*, *Cryptococcus neoformans sp.* and *Histoplasma sp.*, all pose at least the same, if not an even greater risk to human health.

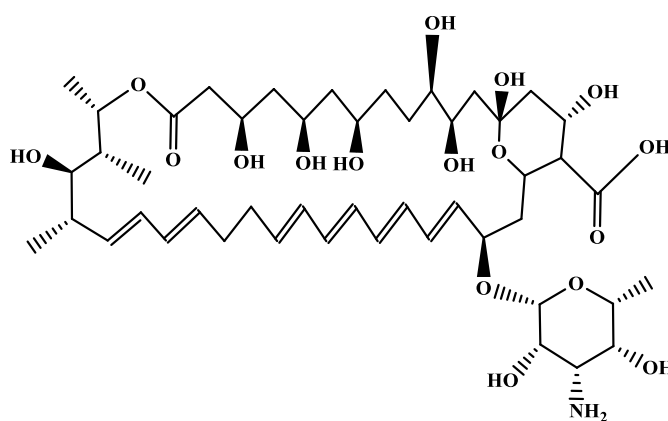
The treatment of candidiasis is dependent on the nature of the infection. Superficial mycoses’s, involving skin or cutaneous tissue, requires different treatment regimes from systemic mycosis, which involves organ disease. Some of the current prescription drugs, such as amphotericin B (AmB),⁶ nystatin and griseofulvin,⁷ also have broad spectrum antimicrobial effects (Figure 8).

1.2.1 Polyenes

The first of the polyenes, nystatin (Figure 8), was discovered in 1949 by Hazen and Brown.⁸ Polyenes are metabolites produced by various species of *Streptomyces*. The compounds are cyclic, macrolide lactones containing a variable number of hydroxyl groups and from 2-7 conjugated double bonds. These compounds are classified by their degree of unsaturation. The mechanism of their action is thought to be based on their ability to bind to sterols in the cytosolic membrane of fungal cells. Although mammalian cells also contain the sterol, cholesterol, polyenes tend to preferentially bind to the fungal sterol, ergosterol (Figure 9).



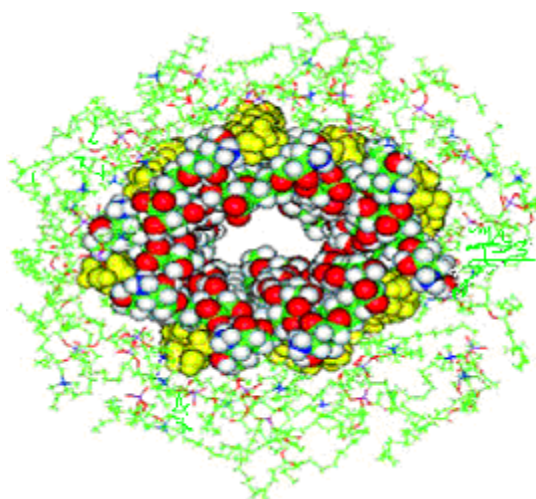
Amphotericin B (AmB)



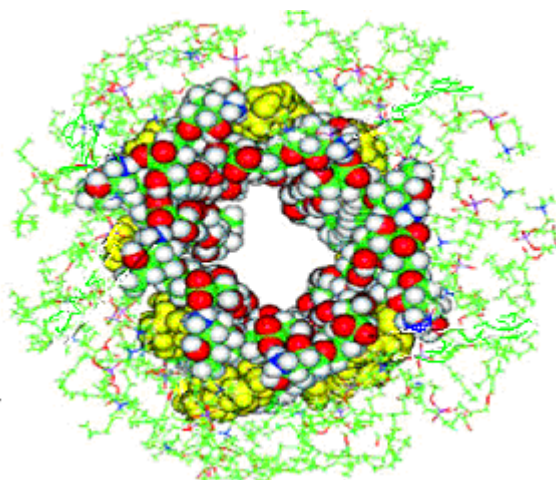
Nystatin

Figure 8 The polyenes.

Amphotericin B (AmB)^{6,9} (Figure 8) is a heptaene macrolide and is one of the few polyenes that is clinically useful. The mechanism of action of AmB is complex and not totally understood, despite the clinical use of AmB for over 50 years (1956).¹⁰ Lack of a complete understanding of its mechanism of action makes it difficult to modify its structure in order to decrease its mammalian cytotoxicity. It has been suggested that several molecules of AmB insert into the cytoplasmic membrane of the fungal cell to form pores that allow leakage of essential ions from the cytosol and which eventually leads to cell death.^{6,10}



AmB-cholesterol channel



AmB-ergosterol channel

Figure 9 The AmB-cholesterol pore and the AmB-ergosterol pore.¹¹

The proposed molecular simulations of the AmB-cholesterol pore and the AmB-ergosterol pore are shown in Figure 9. AmB's nitrogens are shown in blue, and the nitrogens of the sterol are shown in yellow.¹¹ A seemingly minor difference in the size and shape of the two pores has a catastrophic effect on the fungal cell, as the different size and shape allows leakage of fungal cell contents.

AmB is insoluble in water at normal pH and is too toxic to be given parenterally. As a consequence, it is administered either as a sodium deoxycholate-lipid complex or it is encapsulated in liposomes. It can also be given topically. As it is capable of crossing the blood-brain barrier it is effective against cryptococcal meningitis. As yet, there are no known cases of resistance to AmB. The adverse side-effects of AmB are that it interacts with plasma proteins and binds to cholesterol in lipoproteins, which are then deaminated in the liver. The consequence is renal toxicity in up to 80% of patients, although most recover when the treatment is complete. The spleen, lungs and kidneys may also be affected and some impairment of glomerular filtration may remain.

1.2.2 Synthetic Antifungal Agents

5-Flucytosine⁹ (Figure 10) is a fluorinated pyrimidine analogue. It is converted to the antimetabolite 5-fluorouracil (5-FU) in fungal cells but, not in mammalian cells. 5-FU inhibits the enzyme thymidylate synthetase and so affects DNA replication. 5-Flucytosine is used in conjunction with AmB as a treatment for severe systemic fungal infections such as cryptococcal meningitis. 5-Flucytosine is not prescribed alone as resistance commonly arises during treatment.

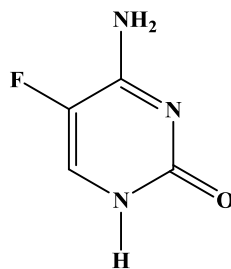
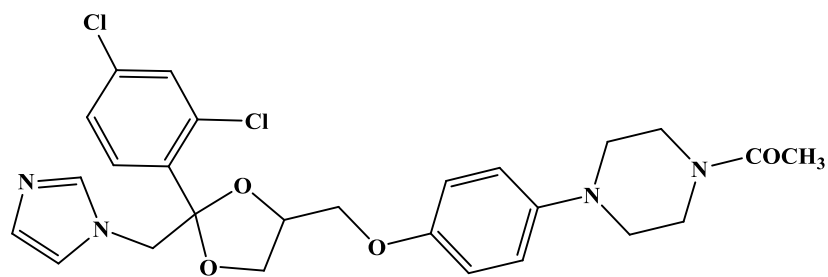


Figure 10 5-Flucytosine.

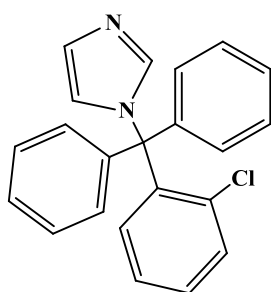
1.2.3 Azoles^{3,4,9,11,12}

Two clinically useful azole families, the imidazoles and the triazoles, have good antimicrobial activity. The most commonly prescribed drugs are fluconazole, itraconazole, ketoconazole, miconazole and econazole (Figure 11). The azoles act by inhibiting the P450 enzymes (14 α -sterol demethylase (CYP51s)) responsible for the synthesis of ergosterol, which is the main sterol in the fungal cell membrane. The depletion of ergosterol causes a loss in fluidity of the membrane thereby making it brittle. The membrane can fracture leading to leakage of cell contents and ultimately to cell death. It should be noted that the depletion of the membrane ergosterol reduces the number of binding sites available for AmB. As a result, azoles and AmB cannot be used together in combination therapy.

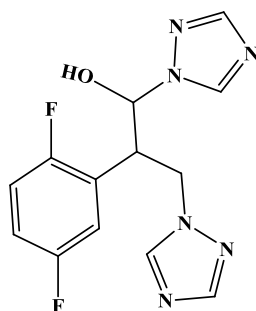
Ketoconazole was the first azole that could be given orally to treat systemic fungal infections. It is effective against several types of fungi, but it is highly toxic to mammalian cells and relapse is common even after seemingly successful treatment. Also, it does not reach therapeutic levels in the central nervous system (CNS) unless administered in very high doses. The main adverse effect of ketoconazole is liver toxicity,⁴ which can be fatal. Organ damage can progress even after the treatment has stopped. Ketoconazole can also have adverse reactions with other drugs. The extensive use of the azoles has led to the emergence of fungal resistance, with many fungal strains now resistant to all azoles.³



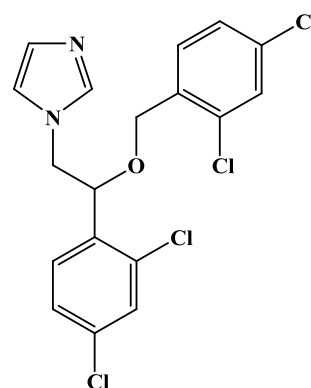
Ketoconazole



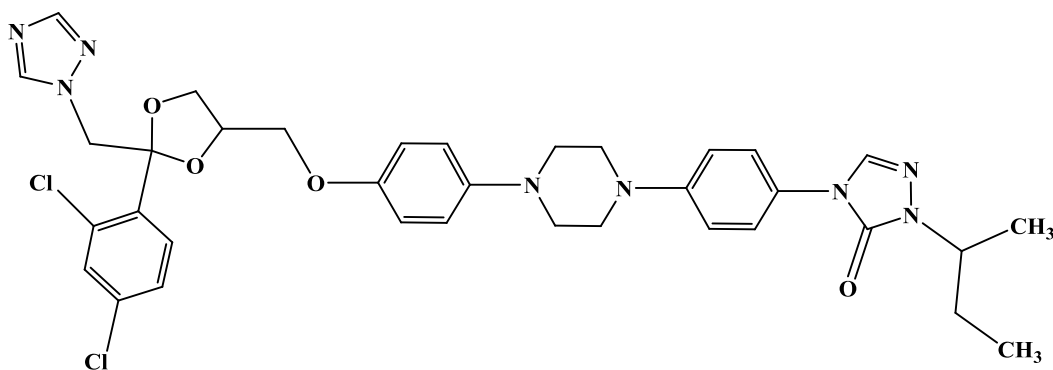
Clotrimazole



Fluconazole



Miconazole



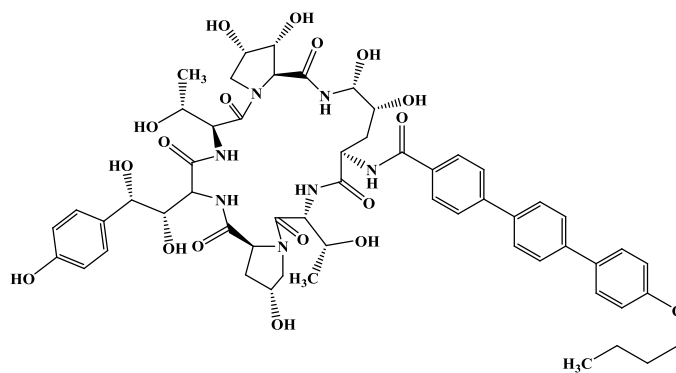
Itraconazole

Figure 11 Some examples of azole antifungal drugs.^{4,12}

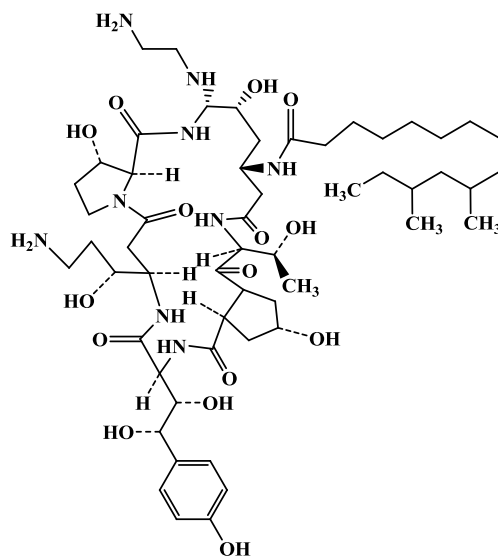
Fluconazole, unlike virtually all other commercially available azoles, is essentially water-soluble and therefore can be given either orally or intravenously. Due to the fact that it reaches high concentrations in the CNS and ocular fluids, it is frequently used in the treatment of fungal meningitis. Fluconazole can also be used for the treatment of fungal infections involving the vagina, mouth, skin tissues and nails. Despite not being a potent antifungal, as judged by *in-vitro* susceptibility tests, it is nevertheless, remarkably effective against a variety of mycoses. Fluconazole is not hepatotoxic at normal dosage levels and side-effects are usually mild. Rare side-effects are hepatitis and exfoliative skin lesions.

1.2.4 Echinocandins

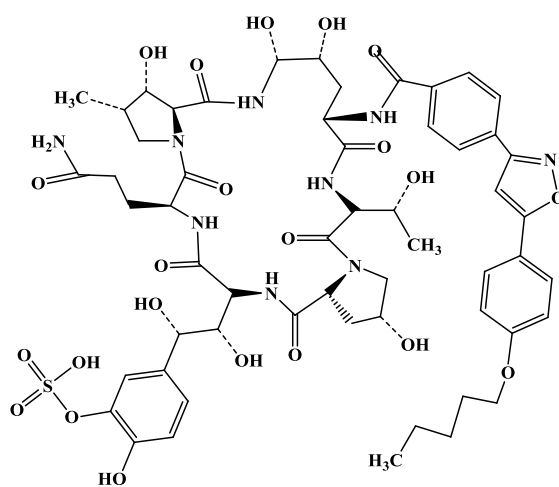
Echinocandins^{4,6,7,12} are synthetically modified, cyclic lipopeptides (Figure 12) and were originally derived from fermentation broths of various fungi. They are the first new class of antifungal drugs to be introduced in over a decade (licensed in 2002) and are thought to exert their antifungal activity by inhibiting the enzyme 1,3- β -glucan synthase. This enzyme is needed for the syntheses of 1,3- β -glucan which is required for fungal cell wall rigidity and hence structural integrity. Thus, exposure to this class of compound leads to catastrophic failure of the fungal cell wall. The adverse side-effects of the echinocandins seem to be mild and no appreciable difference in pharmacokinetics was observed in patients of different age, sex, race or renal impairments.^{4,6,7} It should be noted that the costs of the echinocandins are up to 50 times greater than the current azole prescription drugs.



Anidulafungin



Caspofungin

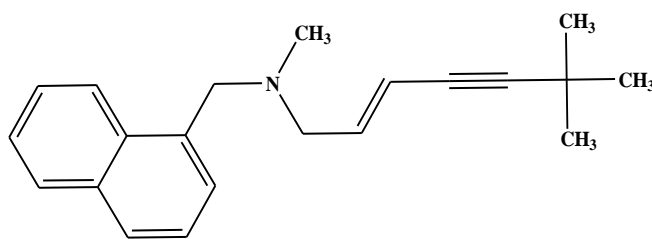


Micafungin

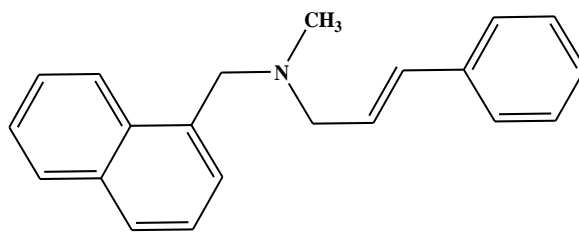
Figure 12 Echinocandins.^{4,6,12}

1.2.5 Allylamines

Terbinafine and naftifine^{9,12} (Figure 13) are highly lipophilic, keratinophilic, fungicidal compounds which are active against a wide range of skin and nail fungal pathogens. They act by inhibiting the enzyme squalene epoxidase, which is involved in the synthesis of ergosterol from squalene within the fungal cell membrane. This inhibition leads to an accumulation of squalene within the cell, which is toxic to the organism.



Terbinafine



Naftifine

Figure 13 Terbinafine and naftifine.

1.2.6 Latest Additions to the Arsenal of Antifungal Drugs

There are several antifungal drugs that are either new to the market or in late stage clinical trials. They include some new azoles, e.g. Ravuconazole¹³ (Figure 14), a triazole structurally related to fluconazole (Figure 11), which showed very promising results in clinical trials in a salvage therapy drug trial. Sordarin¹⁴ (Figure 14) is a natural product

obtained from the fungi *Sordaria araneosa* sp. and acts by inhibiting the elongation step of protein synthesis in the target organism.

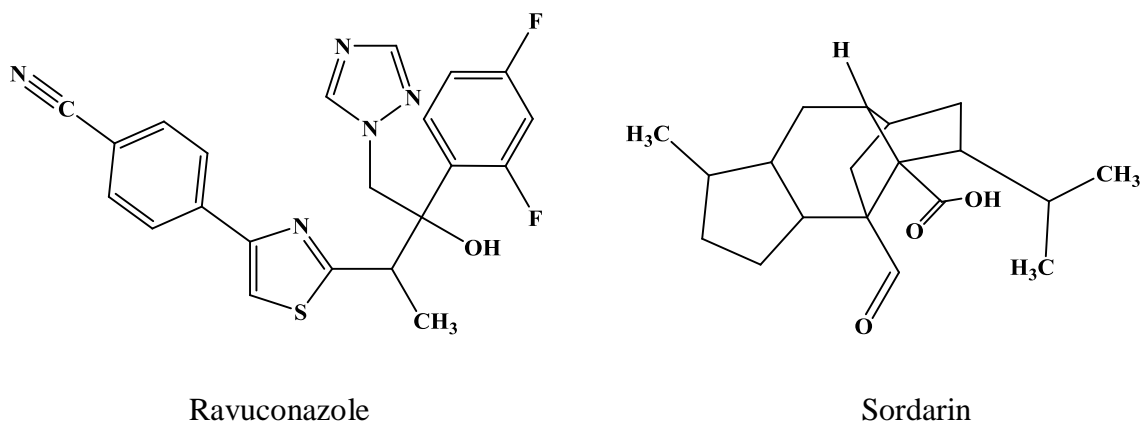


Figure 14 Ravuconazole and sordarin.

1.3 Metals in Medicine and Metal-Based Drugs

1.3.1 Elements Essential for Life

Currently, it is believed that there are approximately thirty elements which are essential to life.¹⁵ As might be expected, the elemental components of proteins, carbohydrates and bone are required in relatively large amounts, including H, Na, K, Mg, Ca, C, N, O, P, S and Cl. Other elements that are integral components of metalloproteins, such as haemoglobin and carboxypeptidases, are required in much smaller amounts. These include Fe, Zn and Cu. Several other elements are required in trace amounts to maintain a normal metabolism, and these are Li, B, F, Si, V, Cr, Mn, Co, Ni, As, Se, Mo, I and W.

Research^{15,16} into the role of metals in cell structure, function and metabolism has shown potential for the therapeutic use of metals to treat disorders or promote healthy activity. Normal metabolism appears to maintain “free” metal ion concentrations at very low levels, with metals being delivered selectively to their sites of activity and extremely tight

controls being maintained over their reactivity. Although the roles of most trace metals are known, some still remain unclear. The homeostatic control mechanisms for metal ions and their transport, the roles of trace elements in inter- and intra-cellular regulation, signal transduction and metal responsive transcriptional and translational regulation of mRNA are only beginning to be unravelled. The unique properties of metals and metal complexes, i.e. redox activity, acidity, electrophilicity, cationic, anionic, radical species, magnetic, spectroscopic and radioactivity, offer some tantalizing possibilities for the future development of metallopharmaceuticals.

1.3.2 A Brief History of Metals in Medicine with Particular Emphasis on Silver

Silver: Chemical symbol Ag, from the Latin, *argentum*, from the ancient Greek: argyros meaning “white”, “shining”.

Early medicine appears to have been largely based on superstition with treatments such as an amulet charged with magical powers being commonplace.¹⁷ A papyrus scroll, the *Ebers papyrus*, believed to date from 1550 B.C., and discovered by the Egyptologist Ebers in 1872,^{17a} describes the medicinal use of antimony sulfide, copper acetates, sulfates, carbonates and also sodium carbonates. Chinese medics were incorporating gold into cures over 4000 years ago and also prized mercury as an elixir. Indian Brahman physicians used mercury for skin diseases, smallpox and later for syphilis, a practice that continued in favour until the end of the First World War when penicillin was found to be more efficacious. Hippocrates, the father of medicine, made use of silver, alum, copper and lead derivatives. Galen favoured various copper compounds from Cyprus, and later the Greeks and Romans used silver vessels to keep water and other liquids from spoiling. Silver has a long traditional in European folklore. It was believed to be an antidote to many maladies and monsters.

In the Middle Ages,^{17b,c} the use of silver tableware was thought to protect the wealthy from plague, with mortality amongst the rich being recorded as significantly lower than

amongst the poor. Children from wealthy families fed with silver cutlery were believed to be at an advantage and this gave rise to the adage “born with a silver spoon in his/her mouth”. The Imperial Russian army used silver-lined wooden water casks to keep water fresh during the Napoleonic wars, a practice that continued to some degree during both World Wars. Settlers in Australia and pioneers in America used silver or copper coins and sometimes silver tableware in their drinking water vessels and also to keep milk fresh.

Raulin^{17d} described the sterilizing effect of silver on water in 1869. In 1884, Crede prescribed a silver nitrate solution to protect against gonorrheal ophthalmia in neonates, a practice that is still in use today. In 1861, Thomas Graham discovered what he called “colloidal silver” and by the end of the 1900s the use of silver was widespread. By the 1940s, there were almost 100 different silver-containing medicinal products on the market. Silver lost favour with the discovery of the antibiotic, penicillin, but continued to be used in alternative medicine. Despite its lack of favour, some research continued into the antimicrobial properties of silver,¹⁸ and in 1968 this led to the introduction of the first new silver product, silver sulfadiazine (SSD) (Figure 15).¹⁹ Polymeric SSD is a combination of a sulfa drug and silver and it has both antibacterial and antifungal properties. SSD is prescribed for the prevention and treatment of infection in patients with severe burns. Also, around this time, Johnson & Johnson introduced a silver-impregnated cotton fabric wound dressing for the treatment of burns.^{19b}

The cavalier use of antibiotics, including their use as feed additives for growth promotion and prophylaxis in agriculture, has led to the emergence of resistant strains of fungi and bacteria.²⁰ For example, MRSA (methicillin-resistant *Staphylococcus aureus* sp.) and VRSA (vancomycin-resistant *Staphylococcus aureus* sp.) are resistant to some of the most powerful antibiotics available. This resistance has renewed interest in the possible use of silver in the battle against antibiotic-resistant, pathogenic microbes. Currently, there are a large number of silver-containing products on the market, including silver-lined catheters, Ag/AgCl disposable ECG electrodes, clean-room paints, wound plasters, and even toothbrushes, washing machines, hair dryers, bedding and clothing.²⁰

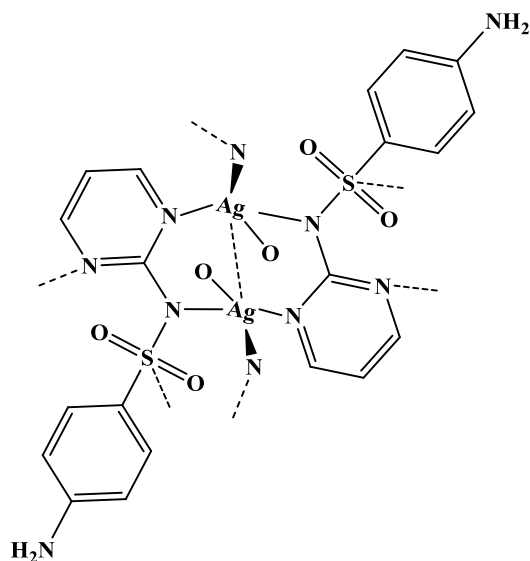


Figure 15 Silver Sulfadiazine (SSD).

A cautionary note²⁰ on the widespread use of these “new” antimicrobial silver products is the inevitable emergence of silver-resistant bacteria and yeast.²¹ Whilst the exact mechanism of microbiological resistance has not yet been elucidated, there is evidence to suggest that it is plasmid-mediated and that it is conjugally transferable.^{16,21} There is also evidence that an ATP-dependent process controlled by a gene, homologous to the gene that confers copper resistance, is involved. The removal of silver ions from the microbial cell is mediated by an efflux pump system similar to the copper efflux pump system.²² Although, silver has no known role in the human body, its antimicrobial activity, together with its very low toxicity to mammalian cells, makes it an ideal candidate for drug research.

1.3.3 Current and Possible Future Metallopharmaceuticals

As is the case with antifungal drugs, there are relatively few metal-based drugs in use, in spite of some notable successes, such as the revolutionary cancer drug, cisplatin. This may be partly due to perceptions¹⁵ that there is an increased risk of toxicity with metal-based drugs or simply that there is relatively limited inorganic expertise within the

pharmaceutical industry. As the regulatory and screening processes are the same for both metal and non-metal agents, this should not be an issue. Metallopharmaceuticals were previously confined to a small number of drugs. These included silver sulfadiazine (Figure 15), carboplatin (Figure 16) and cisplatin (Figure 16). The range of metals in use in medicine is rapidly expanding. Complexes of some infamous toxic metals, such as lead,^{15a} nickel,^{15b} chromium^{15c} and even arsenic,^{15d} are currently either under investigation or in clinical trials, despite of the fact that some are also known carcinogens. Their toxicity is being exploited as possible anticancer drugs.

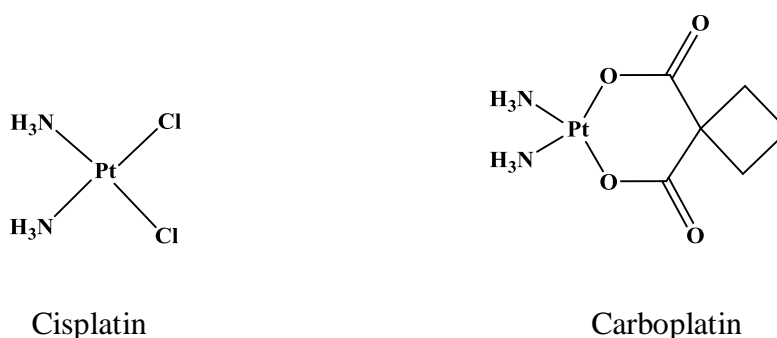


Figure 16 Cisplatin and carboplatin.

Some of the metal-based drugs used in the area of targeted radiotherapy, imaging and photodynamic therapy include metals such as Re, Y, In, Lu, and Cu,^{15a} although the drugs of choice in this area are still Te-containing complexes. Gd-complexes^{15e} are used as MRI (magnetic resonance imaging) contrast agents. Some metals, whose roles were either unknown or poorly understood, are being developed as both drug and dietary supplements, and include complexes containing Cr and V. Some of these Cr and V complexes appear to have significant effects on certain metabolic disorders, such as diabetes. The FDA (The U.S. Food and Drug Administration) and E.F.S.A (The European Food Safety Authority) have approved some vanadium complexes, such as vanadium pentoxide and vanadium citrate, as food additives.^{23d} These vanadium complexes have shown rapid and sustained correction of hyperglycemia, although they are not effective if there is a complete absence of insulin, as they act by enhancing the

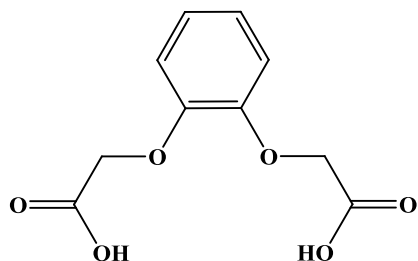
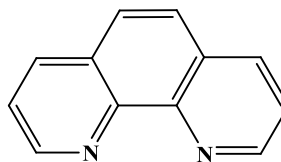
responsiveness of insulin receptors. Currently, researchers are working on a new generation of platinum complexes, and some of these new potential drugs are currently in phase 2 clinical trials. The drug *trans*-platin has been revisited. As the source of *trans*-platin's anticancer potency is also the cause of its toxicity, efforts are now concentrated on making it less toxic by decreasing its reactivity while maintaining its anticancer potency.¹⁵

The success of metallopharmaceuticals drugs, such as cisplatin and SSD, has encouraged research into the possible use of other metals in drugs. One such example is ferrocifen, the organometallic analogue of the antitumour drug tamoxifen, which has already reached the market place.²⁴ Similarly, chloroquine-ferrocene,^{24b} the organometallic analogue of the anti-malaria drug, chloroquine, has an activity comparable to that of chloroquine against non-resistant malaria parasites. The addition of the metal in both of the above cases has a positive effect on activity.

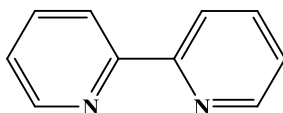
1.4 Previous Work in this Research Group

In the search for drugs active against *C. albicans*, our research group initially focused on the diacid, benzene-1,2-dioxyacetic acid (bdoaH₂) (Figure 17) and its Co(II), Mn(II) and Cu(II) complexes. The diacid ligand and its metal complexes were synthesised and screened for activity against three clinical isolates of *C. albicans*.²⁵ An improvement in activity was observed upon metal complexation compared to the metal-free ligand. In the case of 1,10-phenanthroline (1,10-phen) (Figure 17) and its metal complexes, this improvement in activity was considerable when compared to bdoaH₂ and its metal complexes. When 1,10-phen and bdoaH₂ were both complexed to a metal, there was a dramatic increase in activity, with the Mn(II) complex, [Mn(1,10-phen)₂(bdoa)]·H₂O, being the most active. Interestingly, the related binuclear Cu(II) complex, [Cu₂(bipy)₄(bdoa)]bdoa·6H₂O, which contains 2,2'-bipyridine (bipy) (Figure 17) instead of 1,10-phen, was found to be inactive. Furthermore, whereas metal-free 1,10-phen was highly cytotoxic towards *C. albicans*, bipy did not inhibit fungal growth. This latter

observation suggested that the increased aromaticity and rigidity of the 1,10-phen ligand, compared to bipy, may be important factors in its anti-*Candida* activity.

Benzene-1,2-dioxyacetic acid (bdoaH₂)

1,10-Phenanthroline (1,10-phen)



2,2'-Bipyridine (bipy)

Figure 17 Benzene-1,2-dioxyacetic acid, 1,10-phenanthroline and 2,2'-bipyridine.

Cu(II) and Mn(II) complexes containing both 1,10-phen and the dianionic ligand, norb²⁻ (norbH₂ = *cis*-5-norbornene-endo-2,3-dicarboxylic acid), were also tested for their anti-*Candida* activity. While both complexes arrested fungal growth, [Mn(1,10-phen)₂(norb)]·C₂H₅OH·H₂O was the most active.^{26,27} Cu(II) and Mn(II) complexes containing 1,10-phen and salicylic acid (salH₂) ligands were also screened,^{26,27} and whereas [Cu(1,10-phen)(sal)] was inactive, [Mn(1,10-phen)(sal)₂] was found to be a potent growth inhibitor.

The unsaturated diacid, fumaric acid (HO₂C(CH)₂CO₂H) (fumH₂) (Figure 18), and its polymeric Mn(II) complex, [Mn(fum)]_n, were reported to have negligible effect on the growth of *C. albicans*.^{27a,b} However, the 1,10-phen complexes, [Mn₂(1,10-phen)_{2.5}(H₂O)₂](fum)₂]·3H₂O and [Mn(1,10-phen)₂(CH₃COO)₂]·4H₂O, were moderately

active. Similarly, the inclusion of 1,10-phen into the formulations of simple Mn(II) complexes of phthalic acid (phaH₂) and isophthalic acid (iphaH₂) (Figure 18), to give [Mn(1,10-phen)(pha)]·2H₂O, [Mn(1,10-phen)₂(pha)(H₂O)]·4H₂O and [Mn(1,10-phen)₂(ipha)₂]·4H₂O, significantly enhanced their antifungal activity.^{27b}

Malonic acid (malH₂) (Figure 18) and its Mn(II), Co(II), Ni(II), Cu(II) and Zn(II) complexes had little activity when screened against *C. albicans*. However, the Ag(I) complex, [Ag₂(mal)], was a potent anti-*Candida* agent, suggesting that the Ag⁺ ion is the active species.^{27c}

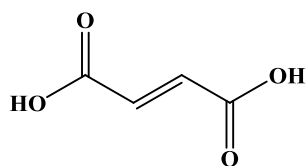
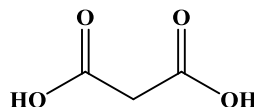
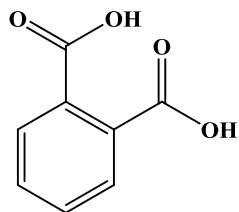
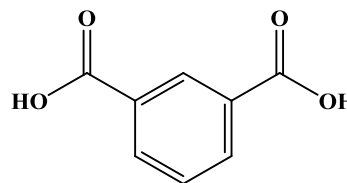
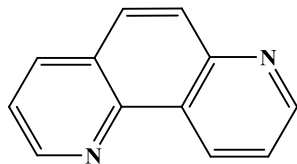
Fumaric acid (fumH₂)Malonic acid (malH₂)Phthalic acid (phaH₂)Isophthalic acid (iphaH₂)

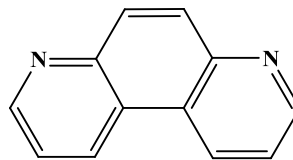
Figure 18 Fumaric acid (fumH₂), malonic acid (malH₂), phthalic acid (phaH₂) and isophthalic acid (iphaH₂).

In contrast to the high activity of the metal-free, chelating 1,10-phen ligand, the non-chelating 1,7- and 4,7-phenanthroline molecules (Figure 19) were found to be inactive against *Candida* in both the metal-free state and as the metal complexes. The anti-*Candida* activity of the metal-free 1,10-phen has been attributed to the position of the

nitrogens that enables it to chelate a metal ion *in situ*. It is the resulting 1,10-phen-metal complexes that are believed to be the source of its anti-*Candida* activity.^{27c}



1,7-Phenanthroline



4,7-Phenanthroline

Figure 19 1,7-Phenanthroline and 4,7-phenanthroline.

Work on 1,10-phenanthroline-5,6-dione²⁸ (1,10-phendio) (Figure 20) and its Cu(II) and Ag(I) metal complexes, $[\text{Cu}(1,10\text{-phendio})_3](\text{ClO}_4)_2 \cdot 4\text{H}_2\text{O}$ and $[\text{Ag}(1,10\text{-phendio})_2]\text{ClO}_4$, respectively, showed that both the metal-free 1,10-phendio and the metal complexes are potent anti-*Candida* agents, with the metal complexes showing superior activity. The salicylic acid (salH_2), 1,10-phendio mixed ligand complexes, $[\text{Cu}(1,10\text{-phendio})(\text{sal})] \cdot 1.5\text{H}_2\text{O}$ and $[\text{Ag}_2(1,10\text{-phendio})(\text{sal})]$, were found to be more active than their 1,10-phen analogues. This suggests that there is an advantageous biochemical role for the carbonyl oxygen atoms of the 1,10-phendio molecule in its anti-*Candida* activity.

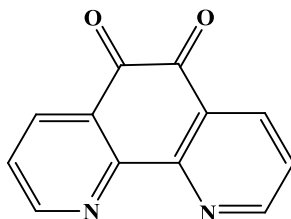


Figure 20 1,10-Phenanthroline-5,6-dione (1,10-phendio).

The most aggressive anti-*Candida* Ag(I) complex²⁹ was $[\text{Ag}_2(\text{NH}_3)_2(\text{salH})_2]$. The closely related Ag(I) complex, $[\text{Ag}_2(\text{salH})_2]$, was less active, suggesting the involvement of the NH_3 in the enhancement of the anti-*Candida* activity of the complex.

Studies into the mode of action of $[\text{Mn}(1,10\text{-phen})_2(\text{mal})]\cdot 2\text{H}_2\text{O}$ on *Candida* cells suggests that the cells must be metabolically active before the administered metal complex can take effect.^{27b} Biochemical analysis of the drug-treated cells suggested that apoptosis occurred as a result of oxidative stress, as indicated by the increased levels of lipid peroxidation and the elevated amounts of the oxidised form of the anti-oxidant molecule glutathione (GSSG).

A recent development in the area of metal-based antifungal drugs has seen the use of ligands containing the imidazole moiety (Figure 21).^{30,31} Derivatives of 2-(1*H*-imidazole-2-ylmethyl)-1*H*-imidazole (2-BIM)³⁰ (Figure 22) and 2-aminoimidazole with salicylaldehyde and *N*-hydroxyimidazoles have been synthesized and coordinated to



Figure 21 Imidazole.

Cu(II), Zn(II) and Ag(I).³¹ The metal-free ligand, bis(1-methyl-1*H*-imidazole-2-yl)methane (2-BIM(Me)), and its metal complexes, $[\text{Cu}(2\text{-BIM}(\text{Me}))_2](\text{ClO}_4)_2$ and $[\text{Zn}(2\text{-BIM}(\text{Me}))_2](\text{ClO}_4)_2$, were inactive against *C. albicans*, while the Ag(I) species, $[\text{Ag}_2(2\text{-BIM}(\text{Me}))_2](\text{ClO}_4)_2$, showed moderate activity.³¹

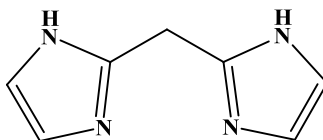


Figure 22 2-(1*H*-imidazole-2-ylmethyl)-1*H*-imidazole (2-BIM).

1.5 Silver Coordination Chemistry and Bioinorganic Chemistry

Silver is found in nature both as the pure metal and in mineral form, mainly as argentite (Ag_2S), and in smaller amounts as horn silver (AgCl) and bromargyrite (AgBr). However, the main source of silver are the ores of copper, copper-nickel and lead.³² Silver is a white, lustrous and malleable transition metal with the highest known thermal and electrical conductivities. Silver metal is used in the electronic industry, in mirrors and for silver plating. Its compounds are used in the photographic industry and, more recently, as an antimicrobial additive to clean-room paints, as medical device coatings and in antimicrobial medications (see Figure 15).^{17,21}

Silver exists in the five oxidation states, $\text{Ag}(0)$, $\text{Ag}(I)$, $\text{Ag}(II)$, $\text{Ag}(III)$ and the subvalent state,³² with $\text{Ag}(I)$ being the most common.^{33,34} The most common coordination number for $\text{Ag}(I)$ is two, as in $[\text{Ag}(\text{NH}_3)_2]^+$, in which the ligands are in a linear configuration. Other $\text{Ag}(I)$ coordination numbers are also possible, e.g. three-coordinate, as in the complex, $[\text{AgI}(\text{PR}_3)_2]$, which is trigonal planar; four-coordinate, seen in the complex, $[\text{Ag}(\text{SCN})_4]^{3-}$ which is tetrahedral; and as six-coordinate in octahedral, $[\text{AgCl}_6]^{5-}$. Four-coordinate $\text{Ag}(II)$ complexes, such as AgF_2 , are usually square planar, but the rarer, six-coordinate, distorted octahedral geometry is also found e.g. $[\text{Ag}(\text{OSO})][\text{Al}\{\text{OC}(\text{CF}_3)_3\}_4]$.^{34c} The four-coordinate, square planar complex anion, $[\text{AgF}_4]^-$, contains silver in the $\text{Ag}(III)$ oxidation state.

The atomic structure of silver shows that there is a small energy difference between the filled d-orbitals and the empty 5s and 5p orbitals, this allows the latter orbitals to accommodate additional electrons, leading to subvalent oxidation states. An example of

such a subvalent state is seen in Ag_5SiO_4 . Given that the silicate ion formulates as SiO_4^{4-} , the five silver ions together have an overall charge of $(\text{Ag}_5)^{4+}$ and implying a formal oxidation state of +0.8 for each silver.³⁴

A metallophilic interaction has been observed amongst the d^{10} monovalent ions of the Group 11 elements (Cu, Ag, Au). The term “aurophilicity” refers to the tendency of the closed-shell Au(I) ions to aggregate at distances shorter than the sum of the Van der Waals radii and with an interaction energy that is comparable in strength to hydrogen bonds.^{32,33} “Argentophilicity” and “cuprophilicity” are analogous phenomena found in silver and copper chemistry, respectively.

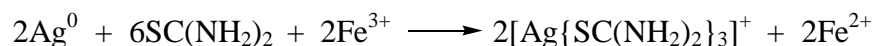
Because of its d^{10} electronic configuration, silver is at the borderline between the main group elements and the transition metals.³⁵ Metallic silver ($\text{Ag}(0)$) is relatively unreactive, but under certain conditions oxidation to Ag(I) can occur and it is this ion that is generally considered to be the bioactive species.³⁶ The interplay between $\text{Ag}(0)$ and $\text{Ag}(I)$ can be understood by studying the reduction potential for this couple in water.³²



The value of +0.799 V indicates a relatively strong thermodynamic driving force for the reduction of free, uncomplexed Ag(I) ions to the $\text{Ag}(0)$ state. However, this reduction potential varies considerably depending on the anion that accompanies the Ag(I) ion and also on the type of ligand(s) present. For example, when the Ag(I) ion is ligated with two ammonia ligands, the reduction to $\text{Ag}(0)$ becomes more difficult and it becomes even less feasible when ligated by cyanide.³²



The complexity of silver chemistry can be further illustrated by looking at the $\text{Ag(I)} \leftrightarrow \text{Ag(0)}$ interconversion. In the presence of thiocarbamide and Fe(III) ions, oxidation of Ag(0) occurs, along with subsequent formation of the soluble, tris(thiocarbamide)silver(I) complex ion.^{32,37}



In contrast, bacteria, such as *Pseudomonas stutzeri*, can develop resistance to Ag(I) accumulation by conversion of the Ag^+ ion into reduced, bioinactive Ag(0) .^{21,38} A non-biological example illustrating the reversibility of the $\text{Ag(I)} \leftrightarrow \text{Ag(0)}$ system is that of phototropic glass.³⁹ This material contains an Ag(I) halide salt which darkens on exposure to sunlight, as the Ag(I) halide salt acquires enough energy for the reduction of Ag(I) to metallic Ag(0) . The reduced silver aggregates into tiny particles, scattering the light and turning the glass dark. The reaction is reversible upon removal of the light source. The redox chemistry of silver has shown that on addition of a macrocyclic, cyclam ligand, (L), to an aqueous methanolic solution of AgClO_4 , Ag(I) has the ability to disproportionate into a mixture of Ag(II) and Ag(0) .⁴⁰



This reaction may offer a possible explanation as to how some bacteria, such as *Pseudomonas stutzeri*, can develop resistance to the build up of ionic silver Ag(I) , by converting Ag(I) to Ag(0) . The Ag(I) may be catalytically reduced in the micro-environment of an existing metallothionein (i.e. proteins that are involved in the transport, storage, and detoxification of essential and non-essential trace metals in the body).^{37,41}

For transition metals, the factors that influence how fast ligands can be exchanged are the size and charge of the central metal ion and also its electronic configuration. Ag(I) , as a

soft Lewis acid, has a low affinity for relatively hard oxygen donors, a high affinity for soft S, Se, and P, and a moderate affinity for nitrogen donors.⁴² In experiments on ligand exchange reactions, the relative order of Ag(I) bond strengths was found to be as follows: Ag-P > Ag-S >> Ag-Cl > Ag-N >> Ag-O.⁴³ In addition, the Ag(I) ion, with its d^{10} electron configuration, has zero ligand field stabilization energy (LFSE), and thus forms labile complexes which will allow rapid ligand exchange with a new ligand from within the biological environment. Proteins and nucleic acids offer many potential metal-binding sites, including sulphur, nitrogen and oxygen.⁴⁴

Silver is associated with an extensive and diverse array of reactions in organic chemistry. The Ag(I) ion can act as a σ -Lewis acid and/or a π -Lewis acid, and the applications of Ag(I) salts in organic synthesis are mostly driven by this Lewis acidity.³⁵ However, in several applications it is the insolubility properties of the silver salts, which precipitate as reaction products, that are driving the reactions. In many reactions where halogens play a key role, silver salts often activate reactions by specifically interacting with the halogen atom and forming insoluble silver halides. This is the so-called halogenophilicity of Ag(I). This effect has been widely used in organic synthesis, mainly in nucleophilic substitution, including glycosylations, in some elimination processes and in processes involving organometallics. Complexes containing coordinated Ag(I) have been known to act as catalysts for various processes, including carbene-insertion,⁴⁵ hydrogenation,⁴⁶ oxidation/reduction reactions,⁴⁷ imination,⁴⁸ and hydrogen generation,⁴⁹ to name but a few. Metallic silver also exhibits high catalytic activity in a variety of organic π conversions, such as olefin oxidation⁵⁰ and the oxidative dehydrogenation of alcohols.⁵¹

1.6 Mechanism of Silver Transport and Bioactivity

Currently, the indications are that there are no biochemical or physiological roles for silver in the human body, even though it is found to interact with several essential elements, including zinc and calcium.⁵² Silver is readily inhaled and absorbed from food and drink at concentrations consistent with environmental levels. It is commonly found in key tissues, such as the liver, kidney, brain and the blood and currently has no known

association with disease or disability.^{53,54} However, prolonged exposure to silver at very high levels, either occupationally or therapeutically, can lead to argyria or argyrosis, conditions where silver is lysosomally sequestered as silver sulfide or silver selenide in the liver, kidneys, vascular tissues, connective tissues of the blood-brain barrier (BBB) and the skin.⁵⁵ Silver ions bind strongly to sulfhydryl (-SH) moieties in the collagen of connective tissues and have been found in close proximity to peripheral nerves but not within neurological tissue. Silver ions are also absorbed into soft tissues where it binds to cysteine-rich metallothionins (MT). MTs have regulatory and cytoprotective roles⁵⁵ and are integral in the metabolism of silver in normal and damaged tissue. MTs may also contribute to the action of silver in wound repair.⁵⁶ MTs are present in all living cells and have a unique structure which enables them to sequester metals, such as zinc and silver. There are four MTs involved in the control of the following three main mammalian cell processes: (i) release of mediators, such as hydroxyl radicals and nitric oxide, (ii) apoptosis and (iii) binding and exchange of heavy metals, such as zinc, cadmium, copper and silver among others.^{55,57} The sequestering of silver in tissues, including those of the BBB, mitigates any potentially toxic influence silver may exert on neurological tissue.⁵⁸ It has been suggested that silver should be classed alongside zinc, iron and gold as a “choroids plexus toxicant,” i.e. a metal that is sequestered by the tissues but is not associated with any pathological change or pathophysiological consequences.⁵⁹

The mode of action of silver and its method of transport in the human body has not yet been fully elucidated, but then it was only recently that the active transport of Mn(II) was reported.⁶⁰ It was not until 1997 that the *trans*-membrane protein, *DCT1*, was identified as being involved in the transport of Mn(II).⁶¹ It was also discovered that *DCT1* is selective for divalent metal ions and was insensitive to the electron configuration of the metal ion that it transports. It was suggested that the protein provides a microenvironment where the metal charge is balanced by the charge on the protein positioned on or near optimum Debye lengths.⁶² Movement of metal ions along the protein is coupled to both H⁺ transport and the electrochemical potential across the cell membrane. To what extent,

the protein allows the transport of metal-bound ligands is, as yet, unknown. This discovery (*DCT1*), provides an example of a possible entry route into the cell for the Ag(II) ions but not to the more common Ag(I) ion.

Research on the transport of Fe(II) ions has shown that it is influenced by the nature of the ligand bound to the metal. When Fe(II) ions are bound to low molecular mass hydrophilic ligands the cells do not take them up, but when bound to similar mass hydrophobic ligands uptake is consistent with diffusion across the membrane lipid bilayer. It is not known if it is the magnitude of the binding constant of the Fe(II) ions to the hydrophobic ligand that is actually preventing the trans-membrane protein *DCT1* from actively transporting Fe(II). However, when the Fe(II) is bound to a high molecular mass sugar it is transported by endocytosis with the ligand intact. This would suggest that there are several possible modes by which Fe(II) may enter the cell, and that these are influenced by the ligand bound to the metal and/or the oxidation state of the metal.⁶³

From the point of view of the ligand exchange reactions of Ag(I) complexes, several possible mechanisms have been suggested for the bioactivity of the aqueous Ag(I) ion. The first mechanism involves the interference of the Ag(I) ion with electron transport, particularly the membrane bound monooxygenase system, cytochrome P450, and nitric oxide reductase (P450nor), a P450 enzyme involved in denitrification within several fungi.^{64,65} The transfer of electrons in the P450 system is not always coupled to a substrate. Monooxygenation P450 and its electron transfer proteins may transfer electrons to other acceptors, such as O₂, or indeed, to a suitable metal. This uncoupling or “leaky electron transport” has been observed in mitochondrial and microsomal systems.⁶⁶ The second possible mechanism is the binding of the Ag(I) ion to DNA.^{66b} The third mechanism is the interaction of Ag(I) ions with the cell membrane’s protein synthesis pathways.⁶⁴ These mechanisms also suggest the possibility of having Ag-biomolecular targets. The ability of Ag(I) to rapidly exchange its original ligands for new ones (zero ligand LFSE) means that Ag(I) can form labile complexes from within the biological environment even under the strict physiological constraints. Proteins or nucleic acids offer potential metal binding sites, including nitrogen and oxygen donors on the bases,

hydroxyl groups on sugars, negatively charged oxygen atoms on the phosphate residues, and the sulphur atoms of some amino acids.⁶⁴

At least three other additional mechanisms for the bioactivity of silver have been suggested.⁶⁷ They are: (iv) catalytic oxidation of the silver ions with nascent oxygen, (v) reaction with bacterial cell membranes through the attachment of silver ions to surface radicals, and (vi) the preferential binding of the silver ions with the cellular DNA, preventing it from unwinding, thus inhibiting protein synthesis and replication.⁶⁷ These hypotheses are contrary to the first two mechanisms previously outlined,⁶⁴ which require silver to be the positive ions reacting with electron-rich O- and S-containing biomolecules. If any of the above methods are correct, it would suggest that increasing the concentration of administered silver ions should result in a corresponding increase in antimicrobial activity. In work carried out on *Pseudomonas aeruginosa sp.*, using a “free” silver ion solution, this was found not to be the case.⁶⁸ Chelated Ag(I) was found to be more effective by several orders of magnitude than the free silver ions and it has been proposed that Ag(I) ions are actively transported intracellularly by the chelating ligand(s) in a protected complex and not as a free ion. The complexation of the Ag(I) ion prevents its interaction with a host of possible substances in the cell or in the cell membranes of the microorganisms, such as oxygen, thiol or other electron-rich centres, and thus precluding its biocidal activity. This theory is supported by *in vitro* experiments using isotopically labelled SSD (¹¹⁰Ag and ³⁵S) on *Pseudomonas aeruginosa sp.*⁶⁸ The experimental results showed that silver was present in the DNA and RNA fraction at levels of up to 15%, but only 0.5% in the lipid fraction, with the remainder found in proteins and polysaccharides.⁶⁸ Similarly, work on bacterial cultures taken from SSD-treated burns patients showed that the SSD dissociated, and that it was the Ag(I) ion alone that was bound to the various components of the bacterial cell.⁶⁹ When the silver was removed from the DNA, by treating the complex with chloride or bromide, regeneration occurred and full function was restored.^{68,70} Although mechanisms (iv) and (v) may not be as effective as mechanism (vi), i.e. the prevention of DNA unwinding, it seems likely that they work synergically, otherwise the free Ag(I) ion would be much more effective when applied on its own.

The silver-DNA binding proposal opens up the possible use of silver in the treatment of neoplasia, especially for some of the more challenging types (e.g. pancreatic, breast and ovarian), since within the intra- and inter-regions of solid tumours the network of capillaries are too small for some of the current high molecular weight chemotherapy agents to be delivered at therapeutic levels.^{64b,71}

Work on simple Ag(I)-imidazole complexes suggested that, despite their insolubility, the broad range of bioactivity (bacterial and fungal) of silver is as a result of the Ag(I)-N bond in these complexes.^{42,43} A comparative study was also conducted into the activities of complexes containing Ag(I)-N bonds, complexes containing Ag(I)-P bonds and those containing N-Ag(I)-P bonds.⁷² The simple salt, AgNO₃, was also included in the study. The Ag(I)-P complexes and the mixed-ligand N-Ag(I)-P complexes were found to be essentially inactive. AgNO₃ showed good activity against Gram-negative bacteria (such as *Escherichia coli*) and moderate activity against Gram-positive bacteria (such as *Streptomyces*). However, the Ag(I)-N complexes displayed superior activity and against a wider range of bacteria, yeast and moulds. Similar work on thiosalicylate silver(I) complexes, which contain Ag(I)-S moieties, showed that these were also quite active but were only functional within a narrow range of microbes.⁷² It has been suggested that this activity is dependent on the nature of the bonding atom, with superior activity for the complexes containing the more weakly bonded Ag(I)-N moiety and to a lesser extent, Ag(I)-O, and finally, the least active is the strongly bonded Ag(I)-S moiety. This suggests that the more weakly bonded metal-complexes may allow easier ligand exchange with biological ligands, thus facilitating the interruption of the fungal cells normal biochemical pathways.⁷³

Bacteria resistant to silver have been found, not surprisingly, in hospital burns units and also in areas where the clinical use of silver or silver-coated devices, such as catheters, is common. Silver-resistant bacteria have also been found in areas associated with the mining and industrial use of silver.⁷⁰ A silver-resistant bacterium, recovered from a burn unit, lead to the isolation of the genes thought to control resistance to Ag(I). The genes were isolated from a bacterial plasmid.^{16,21,72} The gene (silE) determines an extracellular metal-binding protein comprising 123 amino acids and which contains ten histidine

residues that are implicated in Ag(I) binding. SilE is homologous to the gene responsible for copper resistance. The next two genes of the 123 amino acid sequence are the histidine-kinase membrane sensor and the aspartyl phosphate transcriptional responder and these are similar to the genes that determine cobalt, zinc and cadmium resistance. The remaining four genes determine Ag(I) efflux, a cation/proton antiporter and a histidine-rich, cation-specific region.⁷⁴

However, studies on metal tolerance and resistance in bacteria, using *E. coli* as a model,⁷⁵ found that the gene determining resistance to Cu(I), namely CopA, is a Cu(I)-translocation P-type ATPase that is involved in Cu(I) export, tolerance and resistance. It is an orthologue of the human Menkes and Wilson disease-related protein. P-type ATPases belong to a large family of cation-transporting pumps. One subgroup transports monovalent and divalent cations of hard Lewis acids, such as H⁺, Na(I), K(I), Mg(II) and Ca(II).⁷⁶ The second subgroup are thought to transport divalent soft Lewis acids, such as Zn(II), Cd(II) and Pb(II),⁷⁷ and the monovalent soft metal cations such as Ag(I) and Cu(I).⁷⁸ The characteristic feature of these proteins is the presence of cysteine motifs, which have been termed metal binding sites (MBS).⁷⁵ Although MBS have been shown to be capable of binding copper and other soft metals, such as Ag(I),⁷⁹ it is not clear if the MBS serve as a metal sensor to regulate the pump,⁸⁰ an initial binding site where the ion would be transferred later to a translocation domain,⁸¹ or if it is the site of interaction with metal chaperones.⁷⁹ In studies on the role of cysteine in CopA, sequences of CopA were altered by site-directed mutagenesis of alanine residues for the cysteine residues.⁷⁵ Whilst no loss in activity was observed, the exact mode of metal ion specificity, tolerance and resistance was not deciphered. It is known that these CopA genes and other gene orthologues are widely distributed in nature, being found in animals, bacteria and fungi, and they may play a similar role in the development of tolerance and resistance.⁷⁵

The pattern of distribution of these genes may explain how resistance to drugs or metals develop in humans, bacteria and fungi. Subtle changes or mutations in the primary structures of proteins that determine resistance or tolerance to one metal or drug can occur randomly. These minor mutations can confer resistance or tolerance to similar

metals or drugs. It has been suggested that this mechanism of resistance allows bacteria and fungi to develop multi-drug or indeed multi-metal resistance, simultaneously.

Of particular concern is the suggestion that microbes, such as MRSA, that are resistant to antibiotics, develop resistance to silver much more readily than the non-antibiotic resistant microbes and, importantly, that silver-resistant microbe also develop antibiotic resistance more readily. This would suggest that once the microbe develops a mechanism of resistance it is able to adapt this mechanism rapidly to any further threats.^{21b}

1.7 Imidazole Chemistry

As much of the work outlined in this thesis involves the synthesis and coordination chemistry of imidazoles, an introduction to the general chemistry of imidazole follows.

Imidazole and imidazolium compounds can be found in biological and chemical systems and it is these widespread occurrences that have led to interest in imidazole chemistry. Imidazole^{31,32,45,46} (Figures 21, 23) is a cyclic, planar molecule that consists of a five-membered ring containing three carbons and two nitrogens, with the nitrogens arranged in the 1 and 3 positions. The nitrogen in the 1 position is a “pyrrole” type nitrogen and the nitrogen in the 3 position is a “pyridine” type nitrogen.³¹

The imidazole molecule (Figure 24) exhibits aromaticity associated with its six π -electron system. Each carbon in the ring has a p orbital perpendicular to the ring and the π cloud contains three pairs of π electrons. The lone-pair of electrons on N-1 are part of the cloud as they are in a p orbital, while the lone-pair on N-3 are not part of the cloud as they are in an sp^2 orbital, perpendicular to the p orbitals, and thus providing a point of attack for protons and other electrophiles.

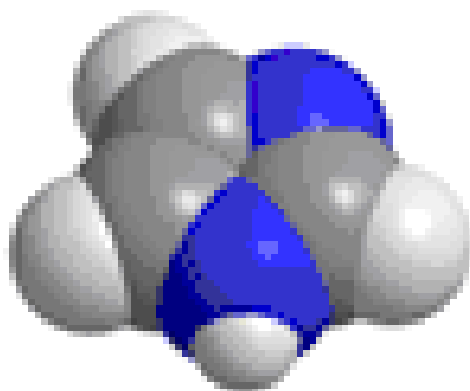
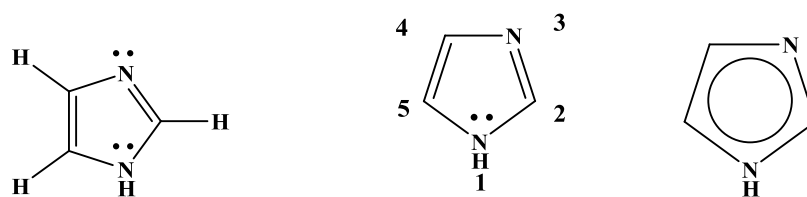


Figure 23 Imidazole.³³

The presence of two nitrogens in the ring results in a lowering of the energy levels of the π -orbital compared to that of benzene or pyridine, which makes electrophilic attack on the carbons more difficult than the corresponding pyrrole or furan. On the other hand, the inductive, electron-withdrawing effect of nitrogen has a stabilizing effect on negatively charged reaction intermediates, such as those occurring during nucleophilic addition-elimination reaction.

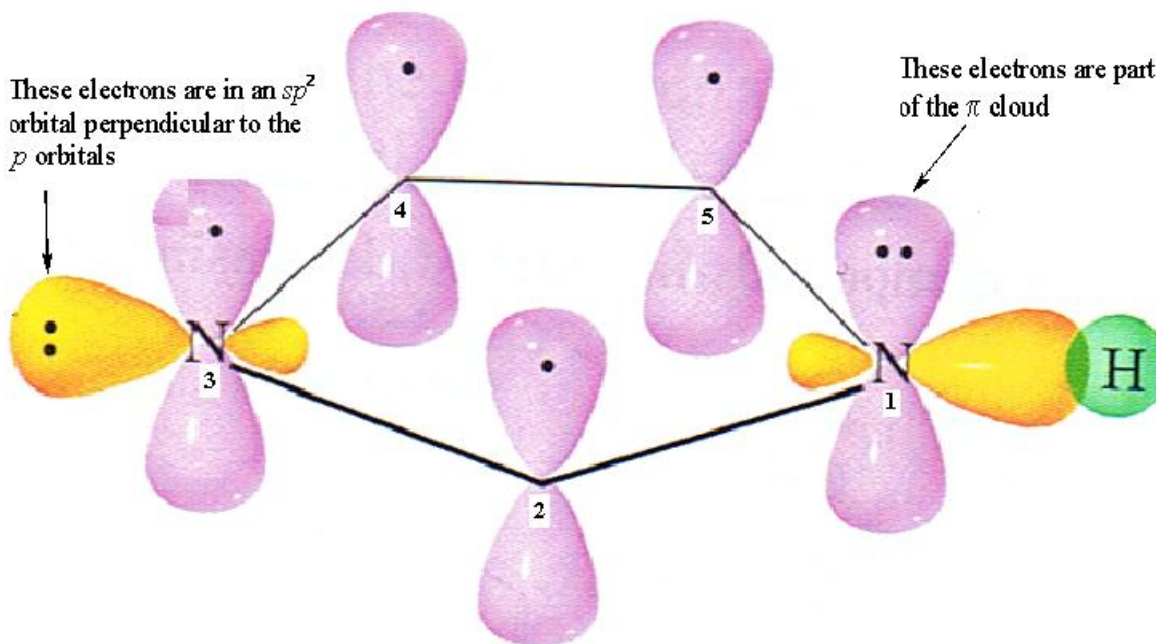
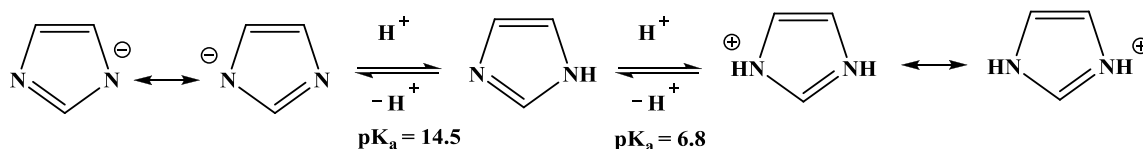


Figure 24 Orbital structure of imidazole.³³

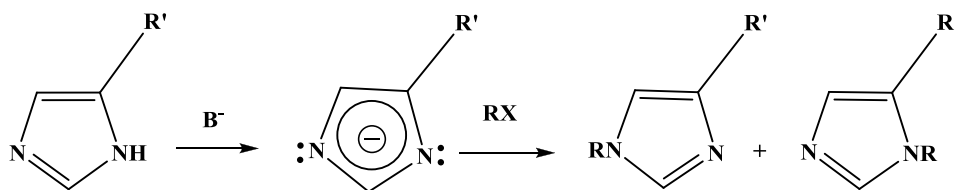
The resonance energy of imidazole is 60.9 kJ/mol, which is significantly less than the 151.2 kJ/mol of benzene. Because the pyridine-like nitrogen's electrons are not part of the π -electron cloud, imidazole gets protonated at this N atom in acid solutions. Imidazole is amphoteric, which means that it can act as a base and as an acid. As a base, the imidazole has a pK_a value of 6.8, making it approximately sixty times more basic than pyridine. The basic site is N-3. As an acid, imidazole has a pK_a value of 14.5, making the imidazole less acidic than carboxylic acids, phenols and imides, but more acidic than alcohols. The acidic proton is located on N-1. Therefore, imidazole can exist in both the protonated and deprotonated forms at the physiological pH of 7.3. In fact, appreciable amounts of both protonated and neutral imidazole units are likely to be present. Thus, both species can be present at the active site of target enzymes. As both protonated and deprotonated imidazoles have two equivalent resonance contributors, the two nitrogens become equivalent, as do the hydrogen atoms on the 4 and 5 position (Scheme 1).



Scheme 1

Imidazole is very soluble in water which indicates hydrogen-bonding with the solvent, and its high boiling point (~ 250 °C) indicates intermolecular hydrogen-bonding.^{31,82,83}

Imidazole may be substituted at each of the five positions, either individually or at all five positions. In cases where both nitrogens have substituents present, the imidazole exists as an imidazolium salt, with the delocalized positive charge on the imidazole balanced by a negative counter ion. The pyrrole-type hydrogen is the most acidic and therefore must be protected before the 2-, 4- and 5-positions can be substituted. *N*-substituted imidazoles, including alkyl-, aryl-, acyl- and vinyl-imidazoles, can be synthesized. In these reactions, the imidazole acts as an attacking nucleophile. It is sometimes necessary to convert the imidazole to the more reactive anion by deprotonation (Scheme 2), and if regioselectivity is also required, a protecting group might be put on the pyrrole nitrogen. In *N*-protected imidazoles deprotonation occurs in the order C-2 > C-5 > C-4.

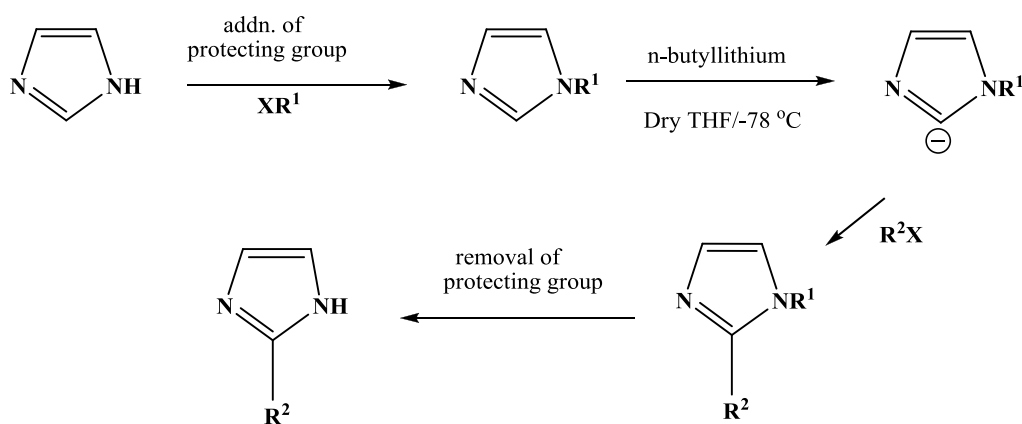


R = alkyl, aryl, acyl

X = Cl, Br, I

Scheme 2

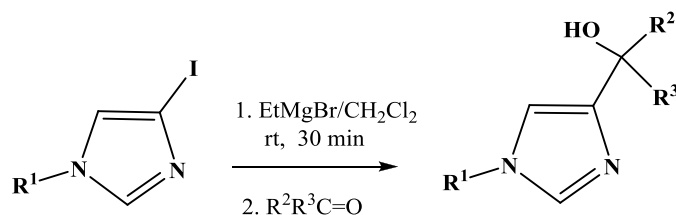
Nucleophilic substitution at imidazole carbons is mainly confined to displacement of halogens or sulfo-groups. Electrophilic substitution at the carbons of the imidazole ring is largely restricted to nitration, sulfonation and halogenation. Acidic electrophiles tend to protonate the imidazole, producing the much less reactive imidazolium salt. Most electrophilic reactions occur at the 4-(5) position, rather than the less reactive 2-position. Halogenation occurs at all three positions. One of the more common electrophilic reactions involves the formation of metallic derivatives. Provided the pyrrole nitrogen is protected, the imidazole carbanion can be formed by reaction with a strong base, such as a lithium derivative or a Grignard reagent. The carbanion can then react with a variety of electrophiles, such as aldehydes, ketones, esters or organic nitriles, which can introduce various functional groups. Scheme 3 shows one of the more common methods of mono-deprotonation, i.e. the reaction of the *N*-protected imidazole with *n*-butyllithium at -78 °C in dry THF. If the 2-position is already substituted then lithiation occurs readily at the 5-position. Di-lithiation will occur at the 2- and 5-positions if two moles of base are used with one mole of imidazole substrate. Because the 5-anion is more reactive than the 2-anion, it is possible to introduce different substituents onto firstly the 5-position and then onto the 2-position if sequential reactions are carried out using different electrophiles.



R^2X = alkyl halides, aldehydes, ketones, acid derivatives, carbon dioxide, organic nitriles, halogens

Scheme 3

For imidazole, it is much more difficult to substitute at the 4-position. Lindell⁸⁴ reported the synthesis of the imidazole-4-yl anion at room temperature by the addition of ethyl magnesium bromide to *N*-protected 4-iodoimidazoles. These iodoimidazoles were, in turn, reacted with a variety of aldehydes and ketones to give carbinols (Scheme 4).



Scheme 4

An alternative approach for the preparation of substituted imidazoles is the synthesis of the imidazole ring with the substituent already in place. One of the earliest examples of the synthesis of imidazoles was in 1858, when Debus⁸⁵ reacted glyxol with formaldehyde and ammonia. Modification of the Debus⁸⁵ method was used by Bu and Gunner⁸⁶ in the development of thermally stable optical chromophores. A more recent development of the Bu and Gunner⁸⁶ method is the microwave-assisted synthesis of substituted imidazoles in solvent-free conditions.⁸⁷

Histidine residues containing imidazole rings are important ligating centres around the catalytic sites of many enzymes, for example, chymotrypsin, trypsin and elastin, where the imidazole acts as a proton transfer agent.^{31,88} The nitrogen donor atoms of imidazole in the histidyl residue are common binding sites in various metalloenzymes, such as in the Zn-containing carbonic anhydrase where the Zn(II) ion is coordinated to three imidazoles, and in the enzyme carbonic peptidase where the Zn(II) ion is coordinated to two imidazoles. Therefore, ligands containing two or more imidazole moieties might be

able to mimic the binding sites of some enzymes. Such examples includes 2-BIM²⁹ (Figure 22) and tris(imidazole-2-yl)carbinol³⁰ (Figure 25).

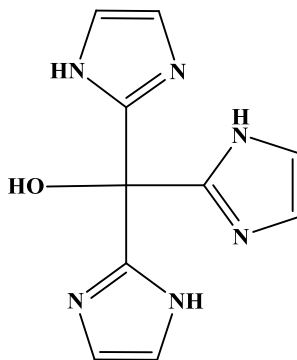


Figure 25 Tris(imidazole-2-yl)carbinol.

L(-)-Histidine (Figure 26) is an essential amino acid for some mammals, such as rats, but not for humans. The complexing power of histidine is involved in the transportation of oxygen in haemoglobin. The iron atom of the haem group in haemoglobin is linked to the protein through the nitrogen of a histidyl group.⁸⁸

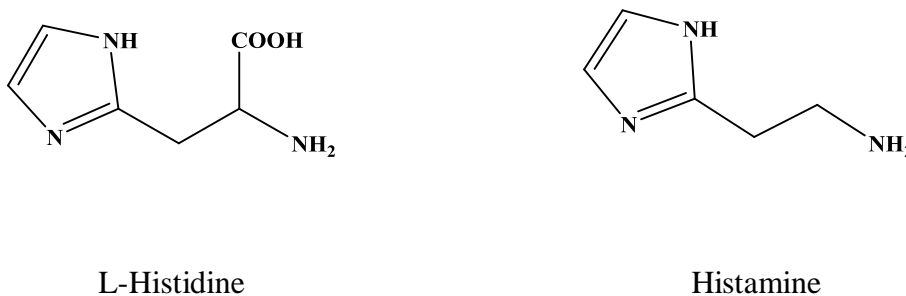


Figure 26 L-Histidine and histamine.

Histamine (Figure 26) is involved in many regulatory responses, such as the control of gastric acid in the stomach, with an over-expression resulting in the over-production of acid as part of an allergic response. The imidazole-based drug, cimetidine (trade name, Tagamet) (Figure 27), acts as an antagonist by blocking the histamine receptor site, thus

reducing the production of gastric acid. Histamine is also involved in the inflammatory response. The release of histamine triggers both dilation and increased permeability of capillaries in the vicinity of the injury, allowing increased blood flow to the site of injury and easing the release of leukocytes.³³

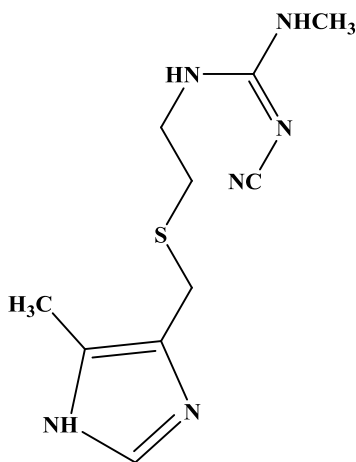


Figure 27 Tagamet.

The imidazole ring is also present in the nucleotides adenine and guanine in DNA and also in biotin (also known as Co-enzyme R), a member of the B group of vitamins. Imidazole-containing compounds can also be found as polymers, and which are used in the paint industry as optical brighteners.⁸⁹ Current research is focused on the possible use of imidazoles as ionic liquids as an alternative to toxic solvents.⁹⁰ Imidazole is also found as an entity in natural compounds, such as theophylline (Figure 28),⁹¹ which is a stimulant found in tea and coffee

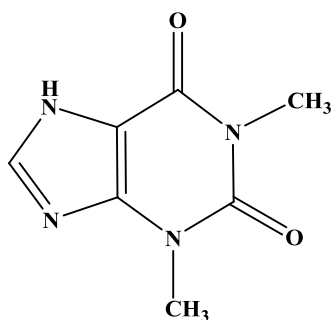
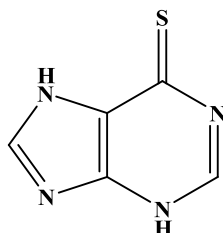
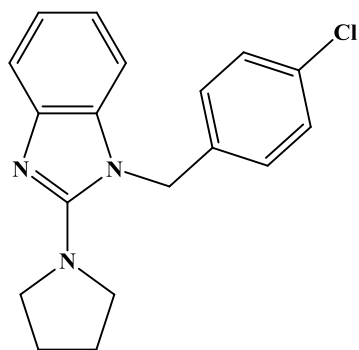


Figure 28 Theophylline.

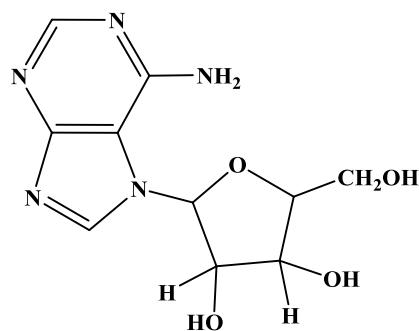
A large range of pharmaceutical products containing the imidazole moiety have been synthesised and include the antifungal azole drugs (Figure 11), anticancer medication, mercaptopurine, the antihistamine drug clemizole,⁴ and the antiviral drug vidarabine⁴ (Figure 29) to name but a few.



Mercaptopurin



Clemizole



Vidarabine

Figure 29 Mercaptopurine, Clemizole and Vidarabine.

1.8 Aim of the Present Work

Currently, the most widely used antifungal drugs are the imidazole derivatives, such as ketoconazole and miconazole. Work previously carried out on Cu(II) metal complexes of some of these prescription azoles showed that the metal complexes were more active antifungal agents than the metal-free azole drugs.⁹² The enhancing effect of metals,



particularly Cu(II) and Ag(I), on the antifungal activity has also been found in studies on a number of other drugs.^{24-28,30}

The aim of the present work was to design and synthesise novel imidazole ligands, complex the ligands to Ag(I) and then screen both the ligands and the metal complexes for their anti-*Candida* activity. The objective was to develop new, silver-imidazole antifungal drugs, or families of drugs, that would become the next generation in the fight against fungal infections. The strategy of developing families of drugs, rather than concentrating on a single wonder drug, is that by rotating the drugs a subtle change in the structure might halt, or at least slow, the inevitable process of fungal drug resistance.

Experimental (part 1)
Organic synthesis

2.0 Chemicals and Instrumentation

Chemicals were purchased from commercial sources and, unless specified, were used without further purification. Note: *Caution is required when handling perchlorate salts as they are extremely reactive and can be explosive under certain conditions.*

All ligand synthesis reactions were carried out in solvents that were purified and dried before use, using standard literature methods.

2.1 Instrumentation

Infrared spectra of solids (in a KBr matrix) were recorded in the 3700-370 cm^{-1} region on a Nicolet FT-IR Impact 400D infrared spectrometer.

^1H and ^{13}C NMR spectra were run on a Bruker Advance 300 MHz instrument.

Microanalytical data were provided by the Microanalytical Laboratory, National University of Ireland, Cork, Ireland and UCD, National University of Ireland Dublin, Belfield, Dublin 4, Ireland.

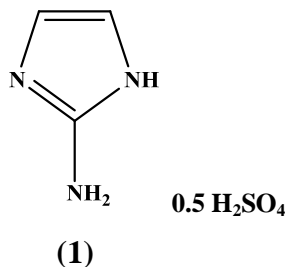
X-ray crystallography work was carried out by Prof. Vickie McKee, Chemistry Department, Loughborough University, Loughborough, Leicester, LE11 3TU, UK.

Microtitre plates were read using a Labsystems iEMS Reader MF (absorbance at $\lambda = 540$ nm).

Mass spectrometry work was carried out by Ms. B. Woods N.U.I. Maynooth using an Agilent Technologies 6210 Time-of-Flight LC/MS.

2.2 Synthesis of starting materials⁹³⁻¹⁰⁰

2.2.1 1-*H*-Imidazol-2-amine hemisulphate (1)⁹³



o-Methylisourea hemisulphate (88.74 g, 0.72 mol) was weighed into a reaction vessel. Under nitrogen, deionised water (150 cm³) and 2-amino-acetaldehyde-diethylacetate (105.3 g, 1.00 mol) were added and the reaction mixture stirred for 4 h at 50 °C. TLC monitoring of the reaction showed complete transformation. The reaction mixture was then cooled to 20 °C and the pH adjusted to 2.5 with concentrated sulphuric acid (7 cm³). The mixture was then heated to 100 °C for 2 h. (TLC monitoring of the reaction showed complete transformation). The reaction mixture was cooled to 20 °C and slowly added to ice-cold ethanol (3000 cm³), over a 1 h period, while maintaining the temperature between 0-5 °C. The resulting suspension was stirred for an additional 1 h at 0-5 °C. The product was filtered off, washed twice with ice-cold ethanol (50 cm³) and dried in a vacuum drying piston at 40 °C.

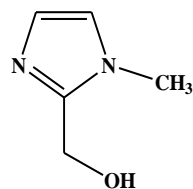
Yield: 85.00 g (86%).

¹H NMR: (D₂O): 6.80 (s, 2H).

IR (KBr): 3154, 2991, 2750, 1673, 1100, 819 cm⁻¹.

2.2.2 1-Methyl-1*H*-imidazole-2-carboxaldehyde⁹⁵

2.2.2.1 1-Methyl-2-hydroxymethyl-1*H*-imidazole (2)

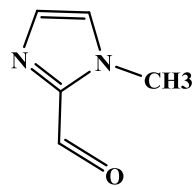


(2)

The following is a modification of the literature method.⁵ 1-Methyl-1*H*-imidazole (20 g, 24.3 mmol), paraformaldehyde (7.29 g, 24.0 mmol) and toluene (50 cm³) were heated in a pressure vessel at 110 °C for 18 h. The bomb was cooled and allowed to stand for 24 h. The resulting transparent crystals were washed with ethyl acetate and ether and then air-dried.

<u>Yield:</u>	15.8 g (58%).
<u>Mp:</u>	92-94 °C (Lit. 91-92 °C). ⁹⁴
<u>¹H NMR:</u>	(ppm d ₆ -DMSO): 3.65 (s, 3H), 4.45 (s, 2H), 5.28 (s,b, 1H), 6.75 (s, 1H), 7.05 (s, 1H).
<u>¹³C NMR:</u>	(ppm d ₆ -DMSO): 32.7, 55.8, 122.2, 126.4.
<u>IR (KBr):</u>	3136, 3115, 2827, 2022, 1499, 1360, 1146, 1021, 963, 746 cm ⁻¹ .

2.2.2.2 1-Methyl-1*H*-imidazole-2-carboxaldehyde (3)⁹⁵



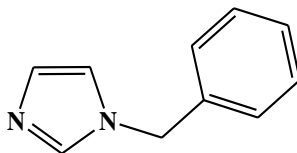
(3)

1-Methyl-2-hydroxymethylimidazole (**2**) (10 g, 9.00 mmol) was dissolved in 1,4-dioxane (150 cm³). Activated manganese dioxide (20 g) was added to the solution and the suspension was stirred under reflux for 4 h. The reaction was monitored by TLC (MeOH: ethyl acetate: 1:5). The suspension was filtered hot and the MnO₂ washed with boiling 1,4-dioxane. The solvent was removed on a rotary evaporator and the resultant yellow oil was distilled on a Kuglrohr apparatus at 78 °C.

<u>Yield:</u>	7.50 g (74 %).
<u>Bp:</u>	85-87 °C (Lit. 89-95 °C). ⁹⁴
<u>¹H NMR:</u>	(ppm d ₆ -DMSO): 3.95 (s, 3H), 7.25 (s, 1H), 7.60 (s, 1H), 9.69 (s, 1H).
<u>¹³C NMR:</u>	(ppm d ₆ -DMSO): 30.6, 128.5, 130.9, 143.2, 181.8.
<u>IR (KBr):</u>	3427, 3113, 2959, 2849, 1688, 1513, 1485, 1412, 1385, 1336, 1293, 1158, 960, 860 cm ⁻¹ .

2.2.3 1-Benzyl-1*H*-imidazole-2-carboxaldehyde (**6**)⁹⁶

2.2.3.1 1-Benzyl-1*H*-imidazole (**4**)



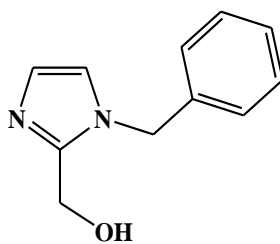
(**4**)

To a solution of imidazole (60.0 g, 1.00 mol) in ethylene glycol dimethyl ether (300 cm³) was added sodium methoxide (180 g, of a 30% solution). Benzyl bromide (171.00 g, 1.00 mol) was then added drop-wise. The solution was stirred and cooled in ice for 1 h. The solid was filtered off and washed with ethyl acetate. The filtrate was evaporated under reduced pressure. De-ionized water (200 cm³) was added to the residue and this was

acidified with 6 M HCl (200 cm³) and extracted with dichloromethane (4 x 50 cm³). The pH of the aqueous layer was adjusted to pH 8-9 with saturated Na₂CO₃ solution and the product extracted with DCM. The DCM solution was dried with MgSO₄ and the solvent was removed under reduced pressure to give an off-white solid. The solid was recrystallised from ethyl acetate yielding clear crystals. The product was washed with dry ethyl acetate and air dried.

<u>Yield:</u>	77.5 g (77 %).
<u>Mp:</u>	67-69 °C (Lit. 68-70 °C). ⁹⁴
<u>¹H NMR:</u>	(ppm d ₆ -DMSO): 5.10 (s, 2H), 6.85 (s, 1H), 7.10 (m, 3H), 7.35 (s, 3H), 7.50 (s, 1H).
<u>¹³C NMR:</u>	(ppm d ₆ -DMSO): 52.4, 119.9, 123.3, 127.8, 128.7, 128.9, 129.2, 136.6.
<u>IR (KBr):</u>	3461, 3099, 1602, 1562, 1497, 1455, 1278, 1233, 1208, 1157, 1108, 1073, 1030 cm ⁻¹ .

2.2.3.2 1-Benzyl-2-hydroxymethyl-1*H*-imidazole (**6**)⁹⁶



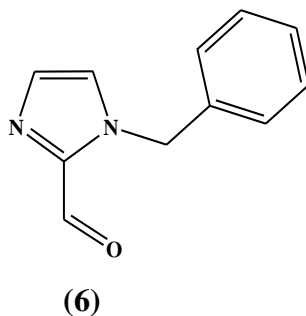
(5)

1-Benzyl-1*H*-imidazole (**4**) (20 g, 0.127 mol) and 37% formaldehyde (50 cm³, 0.61 mol) were heated in a pressure vessel at 140 °C for 18 h. The resulting oil was concentrated on a rotary evaporator and then dissolved in DCM. The solution was washed with a saturated solution of Na₂CO₃ (3 x 50 cm³), then dried over MgSO₄. After filtration the

solvent was removed under reduced pressure to yield a golden oil, which was recrystallised from ethyl acetate to yield a gold oil which over time yielded a semi-solid.

<u>Yield:</u>	16 g (71 %).
<u>Mp:</u>	93-95 °C (Lit. 94-95 °C). ⁹⁴
<u>¹H NMR:</u>	(ppm d ₆ -DMSO): 3.31 (s, 2H), 5.05 (s, 2H), 6.85 (s, 1H), 7.25 (m, 5H), 7.35 (s, 1H).
<u>¹³C NMR:</u>	(ppm d ₆ -DMSO): 48.9, 56.1, 121.4, 126.7, 127.0, 127.7, 127.9, 128.9, 129.5.
<u>IR (KBr):</u>	3469, 3168, 1690, 1563, 1497, 1454, 1356, 1234, 1208, 1159, 1108, 1073 cm ⁻¹ .

2.2.3.3 1-Benzyl-1*H*-imidazole-2-carboxaldehyde (**6**)⁹⁶

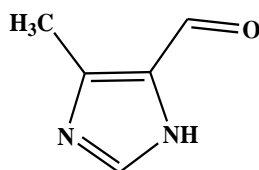


1-Benzyl-2-hydroxymethyl-1*H*-imidazole (10.0 g, 5.30 mmol) and selenium dioxide (2.60 g, 2.30 mmol) were dissolved in 1,4-dioxane (100 cm³). De-ionized water (16.5 cm³) was added and the mixture refluxed for 3 days. The reaction was monitored by TLC (MeOH: ethyl acetate 1:5). The suspension was filtered and the solvent removed under reduced pressure. The resultant yellow oil was distilled on a Kugrohr apparatus at 108 °C.

<u>Yield:</u>	7.5 g (88 %).
<u>Bp:</u>	106-107 °C (Lit. 109-111 °C). ⁹⁴

<u>^1H NMR:</u>	(ppm $\text{d}_6\text{-DMSO}$): 5.45 (s, 2H), 6.92 (s, 1H), 7.45 (m, 5H), 7.90 (s, 1H), 9.70 (s, 1H).
<u>^{13}C NMR:</u>	(ppm $\text{d}_6\text{-DMSO}$): 51.8, 122.8, 128.5, 128.6, 128.8, 135.3, 136.3, 185.8.
<u>IR (KBr):</u>	3470, 3168, 1659, 1563, 1497, 1455, 1278, 1208, 1157, 1108, 1030, 977, 845, 798, 713, 664 cm^{-1} .

2.2.4 4(5)-Methyl-1H-imidazole-5(4)-carboxaldehyde (8)⁹⁶⁻⁹⁸



(8)

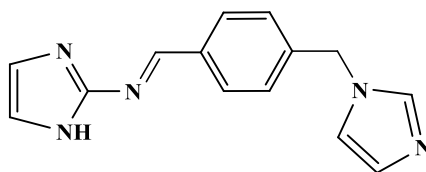
The pH of a solution of 4-methyl-1H-imidazolemethanol hydrochloride (20 g, 13.40 mmol) in de-ionized water (50 cm^3) was adjusted with a saturated solution of Na_2CO_3 to 7.0 and the water then removed under reduced pressure. The solid product was extracted with ethanol (25 $\text{cm}^3 \times 4$), and the solvent evaporated. Nitric acid (112 cm^3 , d 1.42) was added to the resultant yellow crystals. When the brown fumes had cleared, the pH of the yellow solution was adjusted to pH 8-9 with a saturated solution of Na_2CO_3 and allowed to stand for 4 h. The resulting yellow crystals were filtered off, washed with cold water and dried *in vacuo*.

<u>Yield:</u>	10.5 g (71 %).
<u>Mp:</u>	166-169 $^\circ\text{C}$ (Lit. 168-170 $^\circ\text{C}$). ⁹⁵
<u>^1H NMR:</u>	(ppm $\text{d}_6\text{-DMSO}$): 2.43 (s, 3H), 7.75 (s, 1H), 9.75 (s, 1H).
<u>^{13}C NMR:</u>	(ppm $\text{d}_6\text{-DMSO}$): 11.3, 133.9, 137.6, 140.6, 184.0.
<u>IR (KBr):</u>	3290, 3040, 2970, 2920, 2860, 1660, 1510, 1350, 1250, 960 cm^{-1} .

2.3 Schiff Base Ligands Derived from 1*H*-Imidazole-2-amine (1)⁹³⁻¹⁰¹

Prior to its use in Schiff base condensation reactions, the free amine (1) was released from the hemisulphate salt using barium hydroxide.

2.3.1 (*E*)-*N*-(4-[(1*H*-Imidazol-2-yl)methyl]benzylidene)-1*H*-imidazol-2-amine (22)



(22)

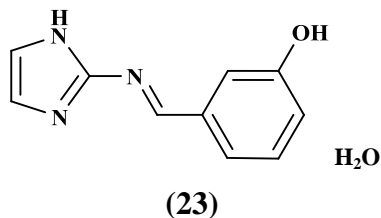
To a solution of 1*H*-imidazole-2-amine (1.00 g, 1.20 mmol) in a mixture of dry methanol:benzene (10:30 cm³)⁹⁵ was added 4-(1*H*-imidazol-1-yl)-benzaldehyde (2.07 g, 1.20 mmol). Molecular sieve (4A) was added and the mixture was refluxed for 6 h and then stirred overnight at room temperature. The reaction was monitored by TLC (MeOH: ethyl acetate 1:5). The molecular sieve was removed by filtration and solvent extraction of the crude reaction residue with hot ethanol obtained the product. The solvent was removed under reduced pressure to yield a brown solid (22). The product (22) was washed with cold methanol and air dried.

<u>Yield:</u>	1.75 g (58 %).
<u>Mp:</u>	Decomposition > 210 °C.
<u>% Found:</u>	C: 66.58, H: 5.63, N: 28.12.
<u>% Calculated:</u>	C: 66.92, H: 5.21, N: 27.87 (C ₁₄ H ₁₃ N ₅ mol. wt. 251.29).
<u>¹H NMR:</u>	(ppm d ₆ -DMSO): 3.10 (s, 2H), 7.10 (s, 2H), 8.00 (m, 6H), 8.48 (s, 1H), 9.20 (s, 1H) 11.39 (s, b, 1H).
<u>¹³C NMR:</u>	(ppm d ₆ -DMSO): 50.6, 117.0, 119.7, 120.3, 127.7, 129.7, 130.2, 135.4, 139.0, 150.5, 158.0.

IR (KBr): 3114, 1603, 1578, 1545, 1523, 1489, 1302, 1252, 1179, 1107, 1054, 961 cm^{-1} .

Solubility: Hot methanol, sparingly in ethanol, DMSO.

2.3.2 (*E*)-3-[(1*H*-Imidazol-2-ylimino)methyl]phenol (**23**)



This solid was prepared in a similar way to (**22**) using 1*H*-imidazole-2-amine (**1**) (1.00 g, 1.20 mmol)⁹³ and 3-hydroxybenzaldehyde (1.46 g 1.20 mmol). A yellow/brown solid (**23**) was obtained.

Yield: 1.28 g (58 %).

Mp: Decomposition > 200 °C.

% Found: C: 59.00, H: 4.97, N: 20.26.

% Calculated: C: 58.53, H: 5.40, N: 20.48 (C₁₀H₁₁N₃O₂, mol. wt. 205.21).

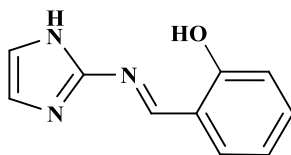
¹H NMR: (ppm d₆-DMSO): 6.95 (m, 1H), 6.85 (s, 1H), 7.53 (m, 4H), 9.05 (s, 1H) 12.35 (s, b, 1H).

¹³C NMR: (ppm d₆-DMSO): 98.6, 114.1, 119.0, 120.4, 130.0, 137.0, 151.0, 157.7, 159.4.

IR (KBr): 3170, 1682, 1603, 1581, 1547, 1455, 1376, 1313, 1283, 1248, 1169, 1110, 998 cm^{-1} .

Solubility: Methanol, ethanol, DMSO.

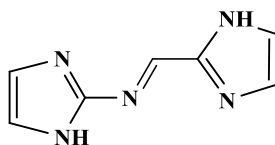
2.3.3 (*E*)-2-[(1*H*-Imidazol-2-ylimino)methyl]phenol (**24**)¹⁰¹

**(24)**

This solid was prepared in a similar way to (**22**) using 1*H*-imidazole-2-amine (**1**) (1.00 g, 1.20 mmol)^{31,93,101} and salicylaldehyde (1.46 g, 1.20 mmol). A yellow/brown solid (**24**) was obtained.

<u>Yield:</u>	1.28 g (58 %).
<u>Mp:</u>	Decomposition > 180 °C.
<u>% Found:</u>	C: 63.95, H: 5.16, N: 22.62.
<u>% Calculated:</u>	C: 64.16, H: 4.85, N: 22.45 (C ₁₀ H ₉ N ₃ O ₁ , mol. wt. 187.2).
<u>¹H NMR:</u>	(ppm d ₆ -DMSO): 7.16 (s, 1H), 7.86 (d, 2H), 8.07 (d, 2H), 8.39 (s, 1H), 9.19 (s, 1H) 12.29 (s, b, 1H).
<u>¹³C NMR:</u>	(ppm d ₆ -DMSO): 118.0, 120.0, 130.1, 134.0, 135.6, 139.0, 150.5, 158.0.
<u>IR (KBr):</u>	3141, 1606, 1574, 1492, 1457 1345, 1272, 1199, 1152, 1112, 1004, 900 cm ⁻¹ .
<u>Solubility:</u>	Methanol, ethanol, DMSO.

2.3.4 *N*-[(*E*)-1*H*-Imidazol-2-ylmethylidene]-1*H*-imidazol-2-amine (**25**)³¹

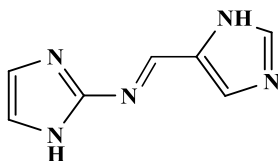
**(25)**

This solid was prepared in a similar way to **(22)** using 1*H*-imidazole-2-amine (**1**) (1.00 g, 1.20 mmol)⁹³ and imidazole-2-carboxyaldehyde (1.15 g, 1.20 mmol). A brown solid **(25)** was obtained.

<u>Yield:</u>	1.25 g (65 %).
<u>Mp:</u>	Decomposition > 180 °C.
<u>% Found:</u>	C: 52.56, H: 4.65, N: 43.90.
<u>% Calculated:</u>	C: 52.17, H: 4.35, N: 43.45 (C ₇ H ₇ N ₅ , mol. wt. 161.16).
<u>¹H NMR:</u>	(ppm d ₆ -DMSO): 7.00 (s, 2H), 7.29 (s, 2H), 8.85 (s, 1H), (12.30 (s, b, 2H).
<u>¹³C NMR:</u>	(ppm d ₆ -DMSO): 144.5, 148.9, 150.2.
<u>IR (KBr):</u>	3144, 1612, 1566, 1431, 1346, 1303, 1112, 998, 849 cm ⁻¹ .
<u>Solubility:</u>	Methanol, sparingly in ethanol, DMSO.

Poor solubility of the complex prevented complete ¹³C NMR analysis.

2.3.5 *N*-[(*E*)-1*H*-Imidazol-4-ylmethylidene]-1*H*-imidazol-2-amine (**26**)



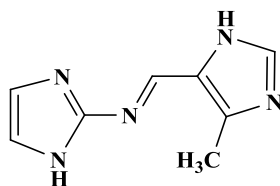
(26)

This solid was prepared in a similar way to **(22)** using 1*H*-imidazole-2-amine (**1**) (1.00 g, 1.20 mmol)⁹³ and 4(5)-imidazolecarboxyaldehyde (1.32 g, 1.20 mmol). A light brown solid **(26)** was obtained.

<u>Yield:</u>	1.93 g (70 %).
<u>Mp:</u>	Decomposition > 200 °C.
<u>% Found:</u>	C: 52.55, H: 4.23, N: 43.31.

<u>% Calculated:</u>	C: 52.17, H: 4.35, N: 43.45 (C ₇ H ₇ N ₅ , mol. wt. 161.16).
<u>¹H NMR:</u>	(ppm d ₆ -DMSO): 7.95 (s, 1H), 7.75 (s, 1H), 7.85 (m, 2H), 9.00 (s, 1H), 12.00 (s, 2H).
<u>¹³C NMR:</u>	(ppm d ₆ -DMSO): 118.6, 128.2, 138.3, 144.5, 148.9, 150.2.
<u>IR (KBr):</u>	3140, 2595, 1877, 1610, 1570, 1438, 1341, 1175, 1107, 850, 798 cm ⁻¹ .
<u>Solubility:</u>	Methanol, sparingly in ethanol, DMSO.

2.3.6 *N*-[(*E*)-(5-Methyl-1*H*-imidazol-4-yl)methylidene]-1*H*-imidazol-2-amine (27)



(27)

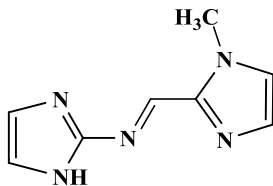
This solid was prepared in a similar way to (22) using 1*H*-imidazole-2-amine (1) (1.00 g, 1.20 mmol)⁹³ and 4-methyl-5-imidazolecarboxaldehyde (1.32 g, 1.20 mmol).⁹⁵ A light brown solid (27) was obtained.

<u>Yield:</u>	1.25 g (65 %).
<u>Mp:</u>	Decomposition > 180 °C.
<u>% Found:</u>	C: 54.60, H: 5.39, N: 40.36.
<u>% Calculated:</u>	C: 54.85, H: 5.18, N: 39.98 (C ₈ H ₉ N ₅ , mol. wt. 175.19).
<u>¹H NMR:</u>	(ppm d ₆ -DMSO): 2.45 (s, 3H), 6.95 (s, 2H), 7.65 (s, 1H), 9.00 (s, 1H), (11.90 (s,b, 2H).
<u>¹³C NMR:</u>	(ppm d ₆ -DMSO): 33.0, 118.6, 128.0, 137.5, 144.5, 148.4, 152.0.
<u>IR (KBr):</u>	3218, 1610, 2662, 1570, 1513, 1443, 1250, 1312, 1261, 1163, 1073, 945, 869, 810 cm ⁻¹ .

Solubility: Methanol, sparingly in ethanol, DMSO.

Poor solubility of the complex prevented complete ^{13}C NMR analysis.

2.3.7 *N*-[(*E*)-(1-Methyl-1*H*-imidazol-2-yl)methylidene]-1*H*-imidazol-2-amine (28)



(28)

This solid was prepared in a similar way to (22) using 1*H*-imidazole-2-amine (1) (1.00 g, 1.20 mmol)⁹³ and 1-methyl-2-imidazolecarboxaldehyde (1.32 g, 1.20 mmol).⁹⁴ A light brown solid (28) was obtained.

Yield: 1.25 g (65 %).

Mp: Decomposition > 210 °C.

% Found: C: 54.62, H: 5.46, N: 40.46.

% Calculated: C: 54.85, H: 5.18, N: 39.98 (C₈H₉N₅, mol. wt. 175.19).

^1H NMR: (ppm d₆-DMSO): 3.45 (s, 3H), 7.15 (s, 2H), 7.45 (s, 2H), 9.00 (s, 1H), (11.90 (s, b, 1H).

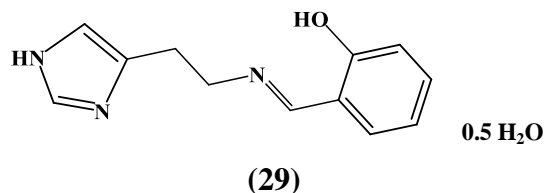
^{13}C NMR: (ppm d₆-DMSO): 35.0, 116.8, 118.5, 133.8, 134.5, 139.3, 148.4.

IR (KBr): 3218, 2613, 1610, 1570, 1513, 1443, 1250, 1312, 1261, 1073, 945, 869, 810, 727, 640 cm⁻¹.

Solubility: Methanol, sparingly in ethanol, DMSO.

2.4. Schiff Base Ligands Derived from Histamine^{102,104}

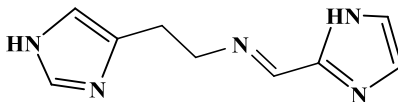
2.4.1 2-([2-(1*H*-Imidazol-5-yl)ethyl]iminomethyl)phenol (**29**)^{102,104}



To a solution of histamine (0.60 g, 5.4 mmol) in dry methanol:benzene (40 cm³, 3:1) was added salicylaldehyde (0.66 g, 5.4 mmol). The resulting yellow solution was refluxed for 4 h and the reaction was monitored by TLC (MeOH: hexane, 1:5). Molecular sieve (4A) was added and the reaction stirred overnight at room temperature. The molecular sieve was filtered off and the solvent removed under reduced pressure to yield a yellow/brown solid (**29**). The solid was washed with cold, dry ethanol and air-dried.

<u>Yield:</u>	0.9 g (77 %).
<u>Mp:</u>	Decomposition > 200 °C.
<u>% Found:</u>	C: 64.37, H: 6.28, N: 18.64
<u>% Calculated:</u>	C: 64.60, H: 6.30, N: 18.76 (C ₁₂ H ₁₄ N ₃ O _{1.5} mol. wt. 224.25).
<u>¹H NMR:</u>	(ppm d ₆ -DMSO): 2.97 (m, 2H), 3.85 (m, 2H), 6.69 (m, 3H), 7.09 (m, 2H), 7.11 (s, 1H), 7.48 (s, 1H), 11.99 (s, b, 1H), 13.66(s, b, 1H).
<u>¹³C NMR:</u>	(ppm d ₆ -DMSO): 27.7, 31.7, 48.6, 115.4, 115.9, 118.1, 126.4, 128.0, 128.5, 129.0, 133.6, 157.0.
<u>IR (KBr):</u>	3406, 2851, 2621, 1633, 1494, 1456, 1279, 1257, 1151, 964, 824, 756 cm ⁻¹ .
<u>Solubility:</u>	Soluble in hot water, MeOH, DMSO and hot EtOH.

2.4.2 N-[2-(1*H*-Imidazol-5-yl)ethyl]-N-[(*E*)-1*H*-imidazol-2-ylmethylidene] amine (30)

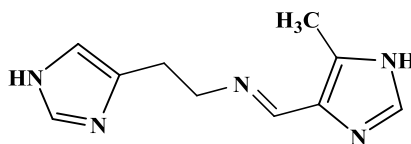


(30)

This solid was prepared in a similar manner to (29) using histamine (0.60 g, 5.4 mmol) and imidazole-2-carboxaldehyde (0.52 g, 5.4 mmol). A yellow solid (30) was obtained.

<u>Yield:</u>	0.84 g (89 %).
<u>Mp:</u>	158-160 °C.
<u>% Found:</u>	C: 57.43, H: 5.76, N: 36.97
<u>% Calculated:</u>	C: 57.13, H: 5.86, N: 37.01 (C ₉ H ₁₁ N ₅ mol. wt. 189.22).
<u>¹H NMR:</u>	(ppm d ₆ -DMSO): 2.76 (t, 2H), 3.70 (t, 2H), 7.45 (s, 1H), 7.52 (s, 1H), 7.57 (s, 2H), 8.20 (s, 1H), 11.81 (s, b, 2H).
<u>¹³C NMR:</u>	(ppm d ₆ -DMSO): 29.7, 59.9, 118.2, 128.3, 133.3, 134.5, 144.5, 149.0, 152.3.
<u>IR (KBr):</u>	3113, 2850, 2664, 1649, 1615, 1554, 1449, 1386, 1292, 1103, 932, 822, 756 cm ⁻¹ .
<u>Solubility:</u>	Soluble in water, MeOH, DMSO and hot EtOH.

2.4.3 N-[2-(1*H*-Imidazol-4-yl)ethyl]-N-[(*E*)-(5-methyl-1*H*-imidazol-4-yl)methylidene]amine (31)

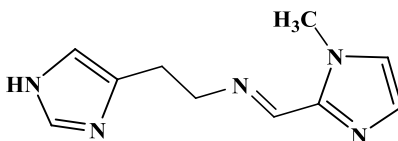


(31)

This solid was prepared in a similar manner to **(29)**, using histamine (0.60 g, 5.4 mmol) and 4-methyl-5-imidazolecarboxaldehyde (0.60 g, 5.4 mmol). A yellow/tan solid **(31)** was obtained.

<u>Yield:</u>	1.00 g (91%).
<u>Mp:</u>	178-180 °C.
<u>% Found:</u>	C: 59.35, H: 6.81, N: 34.66.
<u>% Calculated:</u>	C: 59.10, H: 6.45, N: 34.46 (C ₁₀ H ₁₃ N ₅ mol. wt. 203.24).
<u>¹H NMR:</u>	(ppm d ₆ -DMSO): 2.29 (s, 3H), 2.82 (t, 2H), 3.74 (t, 2H), 6.78 (s, 1H), 7.52 (s, 1H), 7.58 (s, 1H), 8.22 (s, 1H), 11.90 (s, b 2H).
<u>¹³C NMR:</u>	(ppm d ₆ -DMSO): 32.1, 43.6, 60.6, 125.1, 128.3, 134.4, 144.7, 150.
<u>IR (KBr):</u>	3331, 2603, 1626, 1598, 1526, 1438, 1347, 1324, 1237, 1149, 1090, 958 cm ⁻¹ .
<u>Solubility:</u>	Soluble in hot water, MeOH, DMSO and hot EtOH.

2.4.4 *N*-[2-(1*H*-Imidazol-4-yl)ethyl]-*N*-[(*E*)-(1-methyl-1*H*-imidazol-2-yl)methylidene]amine (**32**)¹⁰⁴

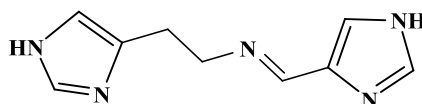


(32)

This compound was prepared using a modification of the literature procedure.¹⁰⁴ The solid was synthesised in a similar manner to **(29)** using histamine (0.60 g, 5.4 mmol) and 1-methyl-2-imidazolecarboxyaldehyde (0.60 g, 5.4 mmol). A yellow/brown solid **(32)** was obtained.

<u>Yield:</u>	1.03 g (92%).
<u>Mp:</u>	Decomposition > 180 °C.
<u>% Found:</u>	C: 59.31, H: 6.76, N: 34.84.
<u>% Calculated:</u>	C: 59.10, H: 6.45, N: 34.46 (C ₁₀ H ₁₃ N ₅ mol. wt. 203.24).
<u>¹H NMR:</u>	(ppm d ₆ -DMSO): 2.90 (t, 2H), 3.21 (t, 2H), 3.56 (s, 3H), 6.76 (s, 1H), 7.06 (s, 2H), 7.38 (s, 1H), 7.78 (s, 1H), 11.93 (s, 1H).
<u>¹³C NMR:</u>	(ppm d ₆ -DMSO): 28.1, 31.6, 50.5, 122.9, 125.1, 128.7, 133.3, 134.5, 137.5, 149.4.
<u>IR (KBr):</u>	3419, 3305, 3145, 2730, 1611, 1497, 1435, 1318, 1274, 1136, 922, 846, 807 cm ⁻¹ .
<u>Solubility:</u>	Soluble in hot water, MeOH, DMSO and hot EtOH.

2.4.5 *N*-[2-(1*H*-Imidazol-4-yl)ethyl]-*N*-[(*E*)-1*H*-imidazol-5-ylmethylidene] amine (**33**)



(33)

This solid was prepared in a similar manner to (**29**) using histamine (0.60 g, 5.4 mmol) and 4(5)-imidazolecarboxaldehyde (0.52 g, 5.4 mmol). A yellow solid (**33**) was obtained.

<u>Yield:</u>	0.81 g (80%).
<u>Mp:</u>	118-120 °C.
<u>% Found:</u>	C: 57.43, H: 6.10, N: 36.89.
<u>% Calculated:</u>	C: 57.13, H: 5.86, N: 37.01 (C ₉ H ₁₁ N ₅ mol. wt. 189.22).
<u>¹H NMR:</u>	(ppm d ₆ -DMSO): 2.87 (t, 2H), 3.80 (t, 2H), 7.36 (s, 1H), 7.58 (s, 1H), 7.75 (s, 1H), 8.20 (s, 2H), 11.86 (s, b, 2H).

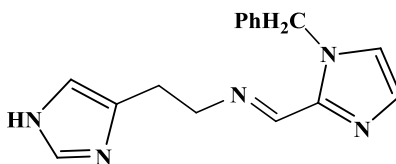
^{13}C NMR: (ppm $\text{d}_6\text{-DMSO}$): 31.5, 43.9, 55.4, 116.4, 116.5, 128.3, 131.6, 137.3, 150.5.

IR (KBr): 3387, 3101, 2892, 2610, 1611, 1573, 1459, 1374, 1354, 1292, 1260, 1119, 1091, 991, 935 cm^{-1} .

Solubility: Soluble in hot water, MeOH, DMSO and hot EtOH.

Poor solubility of the complex prevented complete ^{13}C NMR analysis.

2.4.6 (*E*)-*N*-[[(1-Benzyl-1*H*-imidazol-2-yl)methylene]-2-(1*H*-imidazol-2-yl)]ethanamine (**34**)



(34)

This solid was prepared in a similar manner to (**29**) using histamine (0.87 g, 5.4 mmol) and 1-benzylimidazole-2-carboxaldehyde (0.54 g 5.4 mmol). A yellow oil was obtained, which, on standing, the yellow/brown solid (**34**).

Yield: 1.20 g (80%).

Mp: Decomposition ≥ 200 °C.

% Calculated: C: 68.79, H: 6.13, N: 25.07 ($\text{C}_{16}\text{H}_{17}\text{N}_5$ mol. wt. 279.34).

% Found: C: 69.10, H: 6.42, N: 25.30.

^1H NMR: (ppm $\text{d}_6\text{-DMSO}$): 2.63 (t, 2H), 3.83 (t, 2H), 5.48 (s, 2H), 6.77 (s, 1H), 7.36 (m, 8H), 7.95 (s, 1H), 11.78 (s, b 1H).

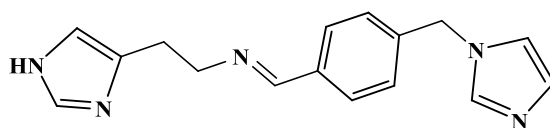
^{13}C NMR: (ppm $\text{d}_6\text{-DMSO}$): 29.7, 32.8, 49.4, 52.0, 117.3, 119.6, 122.8, 127.4, 127.6, 128.4, 128.7, 129.0, 134.5, 134.8, 136.3, 147.4.

IR (KBr): 3311, 3092, 1629, 1561, 1497, 1457, 1387, 1330, 1230, 1151, 1106, 1080, 937, 823 cm^{-1} .

Solubility: Soluble in hot water, MeOH, DMSO and hot EtOH.

Poor solubility of the complex prevented complete ^{13}C NMR analysis.

2.4.7 *N*-[2-(1*H*-Imidazol-4-yl)ethyl]-*N*-(*E*)-[4-(1*H*-imidazol-1-yl)phenyl]methylideneamine (35)



(35)

This solid was prepared in a similar manner to (29) using histamine (0.60 g, 5.4 mmol) and 4-(1*H*-imidazol-1-yl)-benzaldehyde (0.93 g, 5.4 mmol). A yellow solid (35) was obtained.

Yield: 0.89 g (76%).

Mp: 148-152 °C.

% Found: C: 68.28, H: 5.95, N: 25.20.

% Calculated: C: 68.69, H: 6.13, N: 25.07 ($\text{C}_{16}\text{H}_{17}\text{N}_5$ mol. wt. 279.34).

^1H NMR: (ppm d_6 -DMSO): 2.91 (t, 2H), 3.87 (t, 2H), 4.71 (s, 2H), 7.47 (s, 1H), 7.57 (s, 2H), 7.85 (m, 6H), 8.39 (s, 1H), 11.80 (s, b, 1H).

^{13}C NMR: (ppm d_6 -DMSO): 28.6, 57.5, 60.3, 117.8, 119.8, 128.3, 128.6, 129.7, 133.4, 133.5, 134.5, 135.4, 138.3, 159.9.

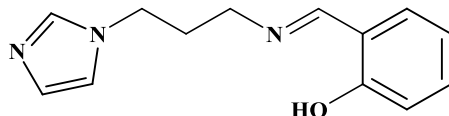
IR (KBr): 3407, 2500, 1650, 1607, 1578, 1523, 1479, 1459, 1303, 1256, 1182, 1112, 1056, 996, 960, 851, 820 cm^{-1} .

Solubility: Soluble in hot water, MeOH, DMSO and hot EtOH.

Poor solubility of the complex prevented complete ^{13}C NMR analysis.

2.5 Schiff Base Ligands Derived from Apim

2.5.1 2-([3-(1*H*-Imidazol-1-yl)propyl]aminopropyliminomethyl)phenol (36)¹⁰⁵



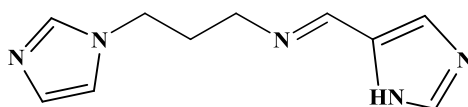
(36)

To a solution of 1-(3-aminopropyl)imidazole (Apim) (5.00 g, 43.4 mmol) in dry methanol (30 cm³) was added salicylaldehyde (5.30 g, 43.4 mmol). The resulting yellow solution was refluxed for 2 h and then stirred overnight at room temperature. The reaction was monitored by TLC (MeOH/hexane, 1:5). The solvent was removed under reduced pressure to give a yellow oil, which, on standing, yielded a yellow, crystalline solid (36). The solid was recrystallised from benzene, filtered, washed with cold, dry methanol and air-dried.

<u>Yield:</u>	9.5 g (96 %).
<u>Mp:</u>	78-80 °C.
<u>% Found:</u>	C: 68.34, H: 6.23, N: 18.66.
<u>% Calculated:</u>	C: 68.10, H: 6.59, N: 18.33 (C ₁₃ H ₁₅ N ₃ O mol. wt. 229.28).
<u>¹H NMR:</u>	(ppm d ₆ -DMSO), 2.12 (m, 2H), 3.53 (t, 2H), 4.07 (t, 2H), 6.89 (d, 2H), 7.34 (m, 3H), 7.45 (s, 1H), 7.65 (s, 1H), 8.54 (s, 1H), 13.35 (s, b, 1H).
<u>¹³C NMR:</u>	(ppm d ₆ -DMSO): 31.6, 43.8, 55.4, 115.2, 118.5, 118.7, 119.0, 128.5, 131.2, 132.0, 137.2, 160.8, 148.3.
<u>IR (KBr):</u>	3101, 1632, 1608, 1575, 1491, 1275, 1225, 1079, 808 cm ⁻¹ .
<u>Solubility:</u>	Insoluble in water and soluble in most organic solvents.

Poor solubility of the complex prevented complete ¹³C NMR analysis.

2.5.2 *N*-[(*E*)-1*H*-Imidazol-5-ylmethylidene]-*N*-[3-(1*H*-imidazol-1-yl)propyl]amine (37)

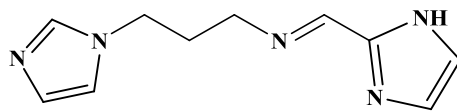


(37)

This solid was prepared in a similar manner to (36) using 4(5)-imidazolecarboxaldehyde (2.17 g, 22.5 mmol) and Apim (2.60 g, 22.5 mmol), yielding an orange powder. The solid (37) was recrystallised from benzene, filtered, washed with cold, dry ethanol and air-dried.

<u>Yield:</u>	4.1 g (97 %).
<u>MP:</u>	180-182 °C.
<u>% Found:</u>	C: 58.92, H: 6.28, N: 34.20.
<u>% Calculated:</u>	C: 59.10, H: 6.45, N: 34.46 (C ₁₀ H ₁₃ N ₅ mol. wt. 203.24).
<u>¹H NMR:</u>	(ppm d ₆ -DMSO): 2.05 (m, 2H), 3.38 (t, 2H), 3.95 (t, 2H), 6.94 (s, 1H), 7.08 (s, 1H), 7.50 (s, 1H), 7.76 (s, 1H), 8.05 (s, 1H), 9.60 (s, 1H).
<u>¹³C NMR:</u>	(ppm d ₆ -DMSO): 31.6, 43.8, 55.4, 116.4, 118.5, 128.5, 131.6, 132.3, 137.2.
<u>IR (KBr):</u>	3137, 3104, 2844, 1646, 1509, 1428, 1219, 1080, 1026, 982 cm ⁻¹ .
<u>Solubility:</u>	Insoluble in water and soluble in most organic solvents.
<u>LC/TCOF-MS:</u>	(M + H) ⁺ requires 204.12 g found 204.12 g. (M + Ag) ⁺ requires 310.98 g found 310.00 g.

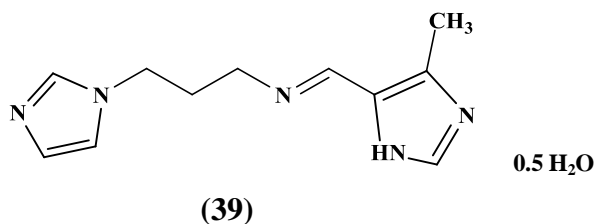
Note: ¹³C NMR incomplete.

2.5.3 *N*-[(*E*)-1*H*-Imidazol-2-ylmethylidene]-*N*-[3-(1*H*-imidazol-1-yl)propyl]amine (38)**(38)**

This solid was prepared in a similar manner to **(36)** using imidazole-2-carboxaldehyde (2.17 g, 22.5 mmol) and Apim (2.60 g, 22.5 mmol), yielding a brown oil which, on standing, solidified to give an orange/brown solid **(38)**.

<u>Yield:</u>	4.02 g (95%).
<u>Mp:</u>	45-47 °C.
<u>% Found:</u>	C: 59.07, H: 6.48, N: 34.20.
<u>% Calculated:</u>	C: 59.10, H: 6.40, N: 34.46 (C ₁₀ H ₁₃ N ₅ mol. wt. 203.24).
<u>¹H NMR:</u>	(ppm d ₆ -DMSO): 2.30 (m, 2H), 3.70 (t, 2H), 4.08 (t, 2H), 6.85 (s, 1H), 7.15 (s, 3H), 7.70 (s, 1H), 8.10 (s, 1H), 9.40 (s, b, 1H).
<u>¹³C NMR:</u>	(ppm d ₆ -DMSO): 27.8, 34.5, 54.4, 117.4, 122.0, 125.1, 126.4, 149.9.
<u>IR (KBr):</u>	3116, 1649, 1509, 1445, 1107, 1081, 762 cm ⁻¹ .
<u>Solubility:</u>	Insoluble in water and soluble in most organic solvents.

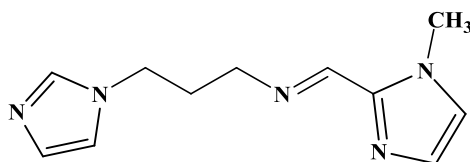
2.5.4 3-(1*H*-Imidazol-1-yl)-*N*-[(*E*)-(5-methyl-1*H*-imidazol-4-yl)methylidene]-1-propanamine (39)



This solid was prepared in a similar manner to **(36)** using 4-methyl-5-imidazolecarboxaldehyde (2.50 g, 22.5 mmol) and Apim (2.60 g, 22.5 mmol), yielding orange/yellow oil which, on standing, gave an orange/yellow solid **(39)**.

<u>Yield:</u>	3.8 g (97%).
<u>MP:</u>	95-96 °C.
<u>% Found:</u>	C: 58.20, H: 6.80, N: 30.76.
<u>% Calculated:</u>	C: 58.39, H: 7.13, N: 30.95 (C ₁₁ H ₁₆ N ₅ O _{0.5} mol. wt. 226.56).
<u>¹H NMR:</u>	(ppm d ₆ -DMSO): 2.04 (m, 2H), 3.42 (s, 3H), 3.50 (t, 2H), 4.10 (t, 2H), 6.90 (s, 1H), 7.20 (s, 1H), 7.52 (s, 1H), 7.63 (s, 1H), 8.23 (s, 1H), 12.17.
<u>¹³C NMR:</u>	(ppm d ₆ -DMSO): 28.1, 32.1, 44.0, 57.1, 119.2, 128.5, 129.8, 131.6, 137.6, 157.2.
<u>IR (KBr):</u>	3111, 2928, 1645, 1509, 1451, 1394, 1351, 1232, 1109, 1082, 1033 cm ⁻¹ .
<u>Solubility:</u>	Insoluble in water and soluble in most organic solvents.
<u>LC/TCOF-MS:</u>	(M + H) ⁺ requires 218.13 g found 218.13 g. (M + Ag) ⁺ requires 323.99 g found 324.02 g.

2.5.5 3-(1*H*-Imidazol-1-yl)-*N*-[(*E*)-(1-methyl-1*H*-imidazol-2-yl)methylidene]-1-propanamine (40)



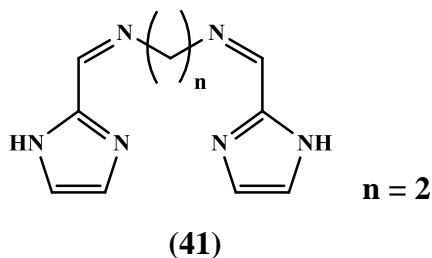
(40)

This solid was prepared in a similar manner to (36) using 1-methyl-2-imidazolecarboxaldehyde (2.50 g, 22.5 mmol) and Apim (2.60 g, 22.5 mmol). A yellow oil was obtained which, on standing, solidified to an orange/brown solid (40).

<u>Yield:</u>	3.68 g (93%).
<u>Mp:</u>	46-48 °C.
<u>% Found:</u>	C: 60.30, H: 6.55, N, 31.81.
<u>% Calculated:</u>	C: 60.81, H: 6.96, N: 32.23 (C ₁₁ H ₁₅ N ₅ mol. wt. 217.27).
<u>¹H NMR:</u>	(ppm d ₆ -DMSO): 2.30 (t, 3H), 3.45 (m, 2H), 3.90 (t, 2H), 4.1 (t, 2H), 6.85 (s, 1H), 7.0 (s, 1H), 7.2 (s, 1H), 7.3 (s, 1H), 7.60 (s, 1H), 8.72 (s, 1H).
<u>¹³C NMR:</u>	(ppm d ₆ -DMSO): 28.10, 31.56, 41.79, 55.26, 117.3, 122.9, 125.1, 125.7, 134.9, 149.8.
<u>IR (KBr):</u>	3386, 3108, 2944, 2881, 1650, 1509, 1479, 1438, 1372, 1288, 1230, 1080 cm ⁻¹ .
<u>Solubility:</u>	Insoluble in water and soluble in most organic solvents.

2.6 Schiff Base Ligands Derived from 1,2-Diaminoethane, 1,3-Diaminopropane and 1,4-Diaminobutane¹⁰⁶⁻¹¹⁸

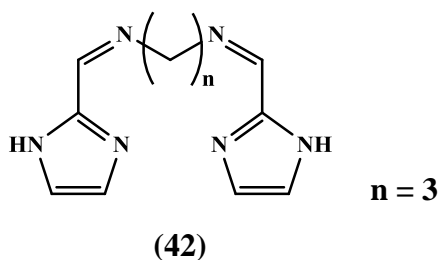
2.6.1 *N*-[(*E*)-1*H*-Imidazol-2-ylmethylidene]-*N*-(2-[(*E*)-1*H*-imidazol-2-ylmethylidene]aminoethyl)amine (**41**)



To a solution of imidazole-2-carboxaldehyde (1.60 g, 1.66 mmol) in dry methanol (30 cm³) was added molecular sieve (4A) and 1,2-diaminoethane (0.50 g, 0.83 mmol). The solution was refluxed for 4 h and then stirred overnight at room temperature. The reaction was monitored by TLC (MeOH:ethyl acetate, 1:5). The molecular sieve was filtered off and the solvent was removed under reduced pressure yielding an off-white powder. The solid (**41**) was washed with cold, dry methanol and air-dried.

<u>Yield:</u>	1.52 g (84%).
<u>Mp:</u>	Decomposition > 200 °C.
<u>% Found:</u>	C: 55.73, H: 5.59, N: 38.90.
<u>% Calculated:</u>	C: 55.54, H: 5.59, N: 38.86 (C ₁₀ H ₁₂ N ₆ mol. wt. 216.24).
<u>¹H NMR:</u>	(ppm d ₆ -DMSO); 3.92 (s, 4H), 7.13 (s, 4H), 8.21 (s, 2H), 12.67 (s, b, 2H).
<u>¹³C NMR:</u>	(ppm d ₆ -DMSO): 60.6, 119.3, 129.6, 153.3,
<u>IR (KBr):</u>	3146, 3010, 2901, 2839, 2694, 1650, 1595, 1562, 1456, 1445, 1393, 1308, 1382, 1561, 1135, 1116, 1028, cm ⁻¹ .
<u>Solubility:</u>	Hot methanol and hot DMSO.

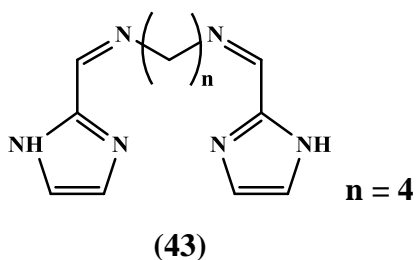
2.6.2. *N*-[(*E*)-1*H*-Imidazol-2-ylmethylidene]-*N*-(3-[(*E*)-1*H*-imidazol-2-ylmethylidene]aminopropyl)amine (42)¹¹⁵



This solid was prepared in a similar manner to **(41)** using imidazole-2-carboxaldehyde (1.30 g, 1.35 mmol) and 1,3-diaminopropane (0.50 g, 0.67 mmol). The off-white powder **(42)** was obtained.

<u>Yield:</u>	1.23 g (80%).
<u>Mp:</u>	Decomposition > 150 °C.
<u>% Found:</u>	C: 57.25, H: 6.32, N: 36.24.
<u>% Calculated:</u>	C: 57.38, H: 6.13, N: 36.50 (C ₁₁ H ₁₄ N ₆ mol. wt. 230.27).
<u>¹H NMR:</u>	(ppm d ₆ -DMSO): 2.78 (m, 2H), 3.64 (t, 4H), 6.88 (s, 2H), 7.13 (s, 2H), 8.21 (s, 2H), 11.15 (s, b, 2H).
<u>¹³C NMR:</u>	(ppm d ₆ -DMSO): 26.9, 45.1, 121.1, 144.6, 148.5, 152.3.
<u>IR (KBr):</u>	3269, 2694, 1651, 1548, 1457, 1448, 1429, 1376, 1313, 1225, 1147, 1107, 1018, 972, 880, 790, 753 cm ⁻¹ .
<u>Solubility:</u>	Hot methanol, hot ethanol and hot DMSO.

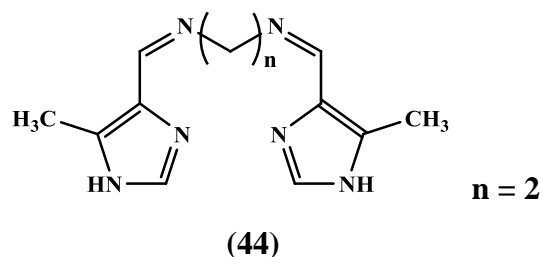
2.6.3 *N*-[(*E*)-1*H*-Imidazol-2-ylmethylidene]-*N*-(4-[(*E*)-1*H*-imidazol-2-ylmethylidene]aminobutyl)amine (43)



This solid was prepared in a similar manner to **(41)** using imidazole-2-carboxaldehyde (1.09 g, 1.14 mmol) and 1,4-diaminobutane (0.50 g, 0.57 mmol). An off-white powder **(43)** was obtained.

<u>Yield:</u>	0.98 g (72%).
<u>Mp:</u>	Decomposition > 200 °C.
<u>% Found:</u>	C: 59.19, H: 6.57, N: 34.56.
<u>% Calculated:</u>	C: 59.00, H: 6.60, N: 34.40 (C ₁₂ H ₁₆ N ₆ mol. wt. 244.30).
<u>¹H NMR:</u>	(ppm d ₆ -DMSO): 1.76 (m, 4H), 3.67 (s, 4H), 7.18 (s, 4H), 8.26 (s, 2H), 12.73 (s, b, 2H).
<u>¹³C NMR:</u>	(ppm d ₆ -DMSO): 28.3, 60.2, 130.0, 144.9, 152.4.
<u>IR (KBr):</u>	3143, 3014, 2908, 2828, 2610, 1800, 1651, 1597, 1559, 1445, 1389, 1350, 1304, 1154, 1111, 1041, 998, 910, 806, 776, 757 cm ⁻¹ .
<u>Solubility:</u>	Hot methanol and hot DMSO.

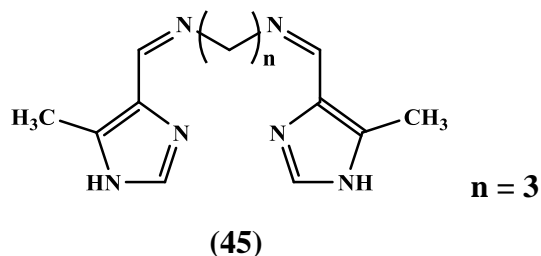
2.6.4 *N*-[(*E*)-(4-Methyl-1*H*-imidazol-5-yl)methylidene]-*N*-(2-[(*E*)-(4-methyl-1*H*-imidazol-5-yl)methylidene]aminoethyl)amine (44)¹¹⁵



This solid was prepared in a similar manner to (41) using 4-methyl-5-imidazolecarboxaldehyde (1.84 g, 1.66 mmol) and 1,2-diaminoethane (0.50 g, 0.83 mmol). A peach-coloured powder (44) was obtained.

<u>Yield:</u>	1.72 g (85%).
<u>Mp:</u>	Decomposition > 240 °C.
<u>% Found:</u>	C: 59.39, H: 6.27, N: 34.36.
<u>% Calculated:</u>	C: 59.00, H: 6.60, N: 34.40 (C ₁₂ H ₁₆ N ₆ mol. wt. 244.30).
<u>¹H NMR:</u>	(ppm d ₆ -DMSO): 2.27 (s, 6H), 3.74 (s, 4H), 7.53 (s, 2H), 8.22 (s, 2H), 12.02 (s, b, 2H).
<u>¹³C NMR:</u>	(ppm d ₆ -DMSO): 28.5, 79.1, 128.5, 136.6, 144.8, 150.8.
<u>IR (KBr):</u>	3133, 2973, 2814, 2624, 1933, 1850, 1669, 1600, 1574, 1519, 1458, 1387, 1357, 1288, 1266, 1222, 1187, 989 cm ⁻¹ .
<u>Solubility:</u>	Hot methanol and hot DMSO.

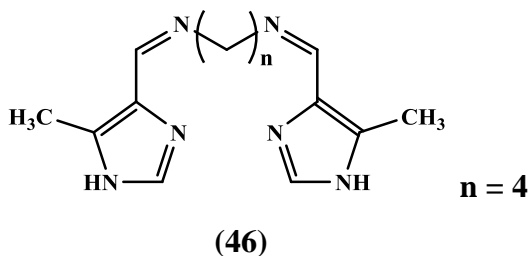
2.6.5 *N*-[(*E*)-(5-Methyl-1*H*-imidazol-4-yl)methylidene]-*N*-(3-[(*E*)-(5-methyl-1*H*-imidazol-4-yl)methylidene]aminopropyl)amine (45)¹¹⁵



This solid was prepared in a similar manner to **(41)** using 4-methyl-5-imidazolecarboxaldehyde (1.48 g, 1.35 mmol) and 1,3-diaminopropane (0.5 g, 0.67 mmol). A pink powder **(45)** was obtained.

<u>Yield:</u>	0.93 g (54%).
<u>Mp:</u>	Decomposition > 240 °C.
<u>% Found:</u>	C: 60.80, H: 6.69, N: 32.38.
<u>% Calculated:</u>	C: 60.44, H: 7.02, N: 32.53 (C ₁₃ H ₁₈ N ₆ mol. wt. 258.32)
<u>¹H NMR:</u>	(ppm d ₆ -DMSO): 1.95 (s, 6H), 3.55 (m, 2H), 3.65 (t, 4H), 7.55 (s, 2H), 8.25 (s, 2H), 12.15 (s, b, 2H).
<u>¹³C NMR:</u>	(ppm d ₆ -DMSO): 20.54, 47.7, 54.0, 132.4, 137.4, 154.8.
<u>IR (KBr):</u>	3051, 2980, 2924, 2833, 2601, 1877, 1646, 1585, 1590, 1451, 1358, 1308, 1243, 1187, 1103, 964, 844 cm ⁻¹ .
<u>Solubility:</u>	Hot methanol, hot ethanol and hot DMSO.

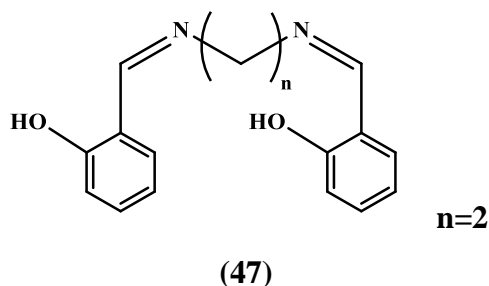
2.6.6. *N*-[(*E*)-(5-Methyl-1*H*-imidazol-4-yl)methylidene]-*N*-(4-[(*E*)-(5-methyl-1*H*-imidazol-4-yl)methylidene]aminobutyl)amine (46**)**



This solid was prepared in a similar manner to (**41**) using 4-methyl-5-imidazolecarboxaldehyde (1.26 g, 1.14 mmol) and 1,4-diaminobutane (0.50 g, 0.57 mmol). A peach-coloured powder (**46**) was obtained.

<u>Yield:</u>	1.23 g (80%).
<u>Mp:</u>	Decomposition > 240 °C.
<u>% Found:</u>	C: 61.54, H: 7.37, N: 30.81.
<u>% Calculated:</u>	C: 61.74, H: 7.40, N: 30.86 (C ₁₄ H ₂₀ N ₆ mol. wt. 272.35).
<u>¹H NMR:</u>	(ppm d ₆ -DMSO): 2.38 (m, 4H), 3.60 (s, 4H), 3.85 (s, 6H), 7.53 (s, 2H), 8.25 (s, 2H), 11.85 (s, b, 2H).
<u>¹³C NMR:</u>	(ppm d ₆ -DMSO): 26.85, 45.08, 68.48, 139.35, 144.54, 148.48, 152.3.
<u>IR (KBr):</u>	3046, 2891, 2854, 2662, 2600, 1857, 1668, 1650, 1578, 1504, 1452, 1382, 1358, 1306, 1240, 1101, 995, 963 cm ⁻¹ .
<u>Solubility:</u>	Hot methanol, sparingly in hot ethanol and hot DMSO.

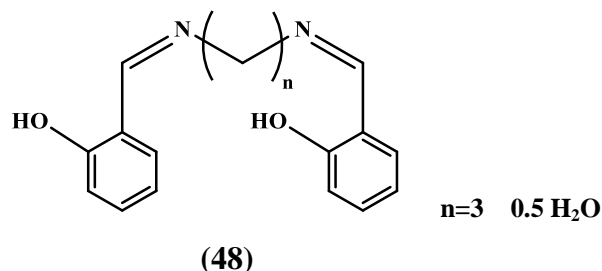
2.6.7 2-[[*(E)*-(2-Hydroxyphenyl)methylidene]aminoethyl]imino]methylphenol (47)^{106,116-118}



This solid was prepared in a similar manner to (41) using salicylaldehyde (2.03 g, 1.66 mmol) and 1,2-diaminoethane (0.50 g, 0.83 mmol). A yellow solid (47) was obtained.

<u>Yield:</u>	1.90 g (86%).
<u>Mp:</u>	112-114 °C.
<u>% Found:</u>	C: 71.52, H: 6.14, N: 10.66.
<u>% Calculated:</u>	C: 71.62, H: 6.01, N: 10.44 (C ₁₆ H ₁₆ N ₂ O ₂ mol. wt. 268.31).
<u>¹H NMR:</u>	(ppm d ₆ -DMSO): 3.90 (s, 4H), 6.87 (m, 4H), 7.32 (m, 2H), 7.45 (m, 2H), 8.59 (s, 2H), 13.34 (s, b, 2H).
<u>¹³C NMR:</u>	(ppm d ₆ -DMSO): 59.1, 116.8, 118.9, 132.0, 132.7, 160.9, 163.1, 167.3.
<u>IR (KBr):</u>	3441, 2931, 2900, 2636, 1636, 1610, 1578, 1449, 1461, 1419, 1371, 1284, 1200, 1150, 1042, 1021, 981, 858 cm ⁻¹ .
<u>Solubility:</u>	Methanol, ethanol, ethyl acetate, chloroform, DCM.

2.6.8 2-[(3-[(*E*)-(2-Hydroxyphenyl)methylidene]aminopropyl)imino]methylphenol (48)^{107,116-118}

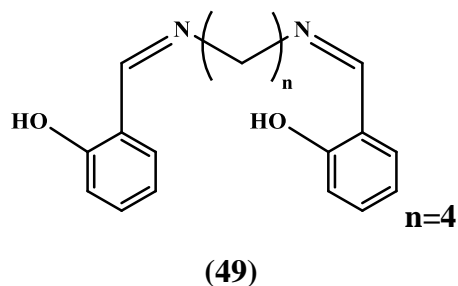


This solid was prepared in a similar manner to **(41)** using salicylaldehyde (1.64 g, 1.35 mmol) and 1,3-diaminopropane (0.5 g, 0.67 mmol). A yellow powder **(48)** was obtained.

<u>Yield:</u>	1.63 g (86%).
<u>Mp:</u>	46-48 °C.
<u>% Found:</u>	C: 70.42, H: 6.63, N: 9.90.
<u>% Calculated:</u>	C: 70.08, H: 6.55, N: 9.61 (C ₁₇ H ₁₉ N ₂ O _{2.5} mol. wt. 291.34).
<u>¹H NMR:</u>	(ppm d ₆ -DMSO): 2.08 (m, 2H), 3.75 (t, 4H), 6.90 (t, 4H), 7.75 (m, 4H), 8.55 (m, 2H), 13.50 (s, b, 2H).
<u>¹³C NMR:</u>	(ppm d ₆ -DMSO): 31.5, 55.9, 116.4, 118.5, 131.4, 131.6, 160.6.
<u>IR (KBr):</u>	3365, 2934, 1638, 1607, 1590, 1500, 1463, 1350, 1311, 1263, 1158, 1108, 1041, 820 cm ⁻¹ .
<u>Solubility:</u>	Methanol, ethanol, ethyl acetate, chloroform, DCM.

Note: incomplete ¹³C NMR data.

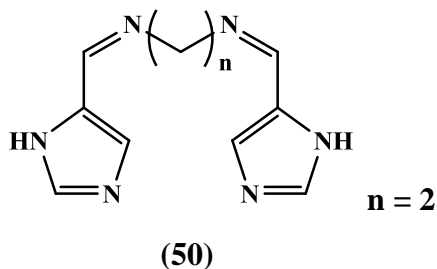
2.6.9 2-[(4-[(*E*)-(2-Hydroxyphenyl)methylidene]aminobutyl)imino]methylphenol (49)¹¹⁶⁻¹¹⁸



This solid was prepared in a similar manner to **(41)** using salicylaldehyde (1.38 g, 1.13 mmol) and 1,4-diaminobutane (0.50 g, 0.57 mmol). A yellow solid **(49)** was obtained.

<u>Yield:</u>	1.43 g (85%).
<u>Mp:</u>	84-86 °C.
<u>% Found:</u>	C: 72.81, H: 7.01, N: 9.65.
<u>% Calculated:</u>	C: 72.95, H: 6.80, N: 9.45 (C ₁₈ H ₂₀ N ₂ O ₂ mol. wt. 296.36).
<u>¹H NMR:</u>	(ppm d ₆ -DMSO): 1.78 (s, 4H), 3.65 (s, 4H), 6.82 (t 4H), 7.35 (m, 4H), 8.57 (s, 2H), 13.60 (s, b, 2H).
<u>¹³C NMR:</u>	(ppm d ₆ -DMSO): 28.4, 58.2, 116.8, 118.8, 132.6, 154.7, 155.4, 161.2.
<u>IR (KBr):</u>	3446, 2946, 2865, 1633, 1608, 1548, 1497, 1456, 1354, 1285, 1210, 1146, 1052, 1010, 878, 858, 754 cm ⁻¹ .
<u>Solubility:</u>	Methanol, ethanol, ethyl acetate, chloroform, DCM.

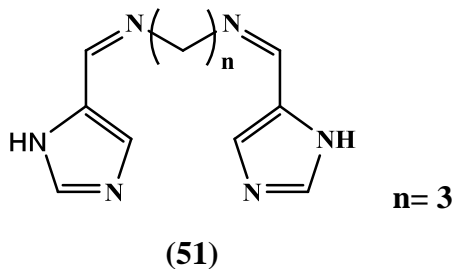
2.6.10 *N*-[(*E*)-1*H*-Imidazol-4-ylmethylidene]-*N*-(2-[(*E*)-1*H*-imidazol-4-ylmethylidene]aminoethyl)amine (50**)**



This solid was prepared in a similar manner to (**41**) using, 4(5)-imidazolecarboxaldehyde (1.59 g, 1.66 mmol) and 1,2-diaminoethane (0.50 g, 0.8 mmol). A white powder (**50**) was obtained.

<u>Yield:</u>	1.52 g (85%).
<u>Mp:</u>	Decomposition > 80 °C.
<u>% Found:</u>	C: 55.82, H: 5.65, N: 38.63.
<u>% Calculated:</u>	C: 55.54, H: 5.59, N: 38.86 (C ₁₀ H ₁₂ N ₆ mol. wt. 216.24).
<u>¹H NMR:</u>	(ppm d ₆ -DMSO): 3.75 (s, 4H), 7.34 (m, 2H), 7.70 (m, 2H), 8.19 (s, 2H), 12.47 (s, b, 2H).
<u>¹³C NMR:</u>	(ppm d ₆ -DMSO): 60.1, 122.3, 136.3, 138.0, 157.1,
<u>IR (KBr):</u>	3441, 3121, 2836, 2601, 1651, 1542, 1514, 1451, 1367, 1301, 1261, 1175, 1116, 1021, 994, 941 cm ⁻¹ .
<u>Solubility:</u>	Hot methanol, sparingly in hot ethanol and hot DMSO.

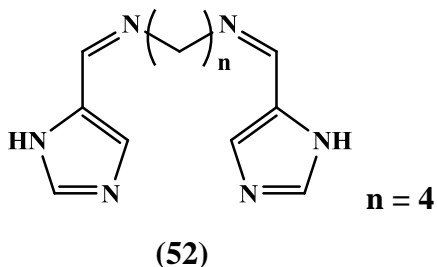
2.6.11 *N*1-[(*E*)-1*H*-Imidazol-5-ylmethylidene]-*N*-3-[(*E*)-1*H*-imidazol-5-ylmethylidene]-1,3-propanediamine (51**)**



This solid was prepared in a similar manner to (**41**) using 4(5)-imidazolecarboxaldehyde (1.30 g, 1.13 mmol) and 1,3-diaminopropane (0.5 g, 0.67 mmol). A pale peach-coloured powder (**51**) was obtained.

<u>Yield:</u>	1.28 g (83%).
<u>Mp:</u>	Decomposition > 160 °C.
<u>% Found:</u>	C: 57.10, H: 6.16, N: 36.29.
<u>% Calculated:</u>	C: 57.38, H: 6.13, N: 36.50 (C ₁₁ H ₁₄ N ₆ mol. wt. 230.27).
<u>¹H NMR:</u>	(ppm d ₆ -DMSO): 1.74 (m, 2H), 3.54 (t, 4H), 7.45 (s, 2H), 7.75 (s, 2H), 8.25 (s, 2H), 12.32 (s, b 2H).
<u>¹³C NMR:</u>	(ppm d ₆ -DMSO): 32.1, 58.34, 123.3, 136.5, 137.3, 151.7.
<u>IR (KBr):</u>	3424, 3119, 2939, 2836, 2604, 1869, 1647, 1548, 1520, 1460, 1382, 1299, 1176, 1111, 1095 cm ⁻¹ .
<u>Solubility:</u>	Hot methanol and hot DMSO.

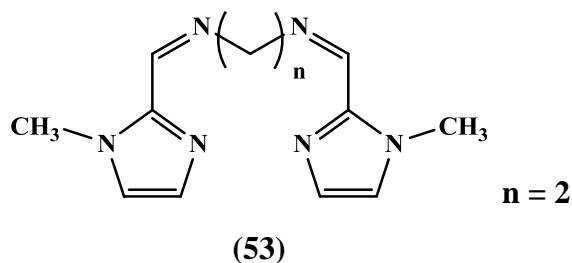
2.6.12 *N*-[(*E*)-1*H*-Imidazol-5-ylmethylidene]-5-[(*E*)-(1*H*-imidazol-5-ylmethyl)imino]-1-butylamine (52**)**



This solid was prepared in a similar manner to (**41**) using 4(5)-imidazolecarboxaldehyde (1.09 g, 1.13 mmol) and 1,4-diaminobutane (0.50 g, 0.57 mmol). A peach-coloured powder (**52**) was obtained.

<u>Yield:</u>	1.15 g (83%).
<u>Mp:</u>	Decomposition > 200 °C.
<u>% Found:</u>	C: 59.66, H: 6.19, N: 34.60.
<u>% Calculated:</u>	C: 59.00, H: 6.60, N: 34.40 (C ₁₂ H ₁₆ N ₆ mol. wt. 244.30).
<u>¹H NMR:</u>	(ppm d ₆ -DMSO): 1.61 (s, 4H), 3.56 (s, 4H), 7.39 (s, 2H), 7.69 (s, 2H), 8.19 (s, 2H), 12.39 (s, b, 2H).
<u>¹³C NMR:</u>	(ppm d ₆ -DMSO): 28.6, 69.4, 121.9, 136.4, 138.3, 163.1.
<u>IR (KBr):</u>	3423, 2861, 2596, 1898, 1651, 1566, 1513, 1458, 1377, 1327, 1289, 1220, 1096, 1062, 998, 923, 860 cm ⁻¹ .
<u>Solubility:</u>	Hot methanol and hot DMSO.

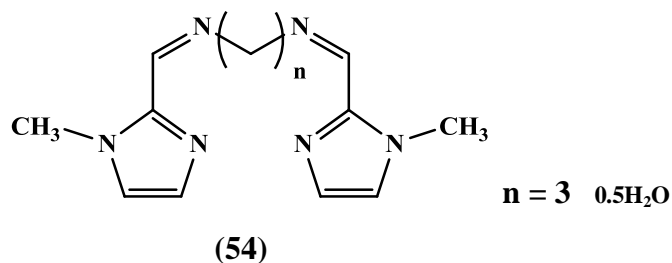
2.6.13 *N*-[(*E*)-(1-Methyl-1*H*-imidazol-2-yl)methylidene]-*N*-(2-[(*E*)-(1-methyl-1*H*-imidazol-2-yl)methylidene]aminoethyl)amine (53)^{108-109,114}



This solid was prepared in a similar manner to **(41)** using 1-methyl-2-imidazolecarboxaldehyde (1.84 g, 1.66 mmol) and 1,2-diaminoethane (0.50 g, 0.83 mmol). The pale yellow solid **(53)** was obtained.

<u>Yield:</u>	0.86 g (43%).
<u>Mp:</u>	100-104 °C.
<u>% Found:</u>	C: 58.91, H: 6.82, N: 34.29.
<u>% Calculated:</u>	C: 59.00, H: 6.60, N: 34.40 (C ₁₂ H ₁₆ N ₆ mol. wt. 244.30).
<u>¹H NMR:</u>	(ppm d ₆ -DMSO): 2.45 (s, 4H), 3.90 (s, 6H), 7.65 (s, 2H), 8.05 (s, 2H), 8.40 (s, 2H).
<u>¹³C NMR:</u>	(ppm d ₆ -DMSO): 35.2, 61.5, 125.9, 129.0, 142.7, 154.6.
<u>IR (KBr):</u>	3367, 3130, 3106, 2850, 1655, 1523, 1479, 1439, 1289, 1230, 1150, 1086, 1021, 958, 925 cm ⁻¹ .
<u>Solubility:</u>	Hot methanol and hot DMSO

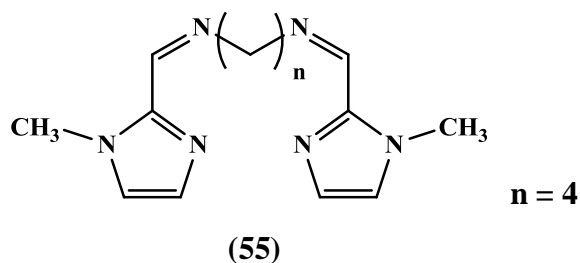
2.6.14 *N*-[(*E*)-(1-Methyl-1*H*-imidazol-2-yl)methylidene]-*N*-(3-[(*E*)-(1-methyl-1*H*-imidazol-2-yl)methylidene]aminopropyl)amine (54)^{109,114}



This solid was prepared in a similar manner to **(41)** using 1-methyl-2-imidazolecarboxaldehyde (1.45 g 1.31 mmol) and 1,3-diaminopropane (0.5 g, 0.67 mmol). A pale yellow solid **(54)** was obtained.

<u>Yield:</u>	1.12 g (65%).
<u>Mp:</u>	50-52 °C.
<u>% Found:</u>	C: 58.36, H: 6.78, N: 31.60.
<u>% Calculated:</u>	C: 58.41, H: 7.18, N: 31.43 (C ₁₃ H ₁₉ N ₆ O _{0.5} mol. wt. 267.30).
<u>¹H NMR:</u>	(ppm d ₆ -DMSO): 2.60 (m, 2H), 3.56 (t, 4H), 3.96 (s, 6H), 7.08 (s, 2H), 7.35 (s, 2H), 8.36 (s, 2H).
<u>¹³C NMR:</u>	(ppm d ₆ -DMSO): 37.6, 55.2, 58.9, 125.9, 128.9, 142.8, 153.7.
<u>IR (KBr):</u>	3440, 3262, 3122, 2920, 1652, 1525, 1484, 1443, 1370, 1293, 1230, 1157, 1094, 1060, 966, 948 cm ⁻¹ .
<u>Solubility:</u>	Hot methanol and hot DMSO.

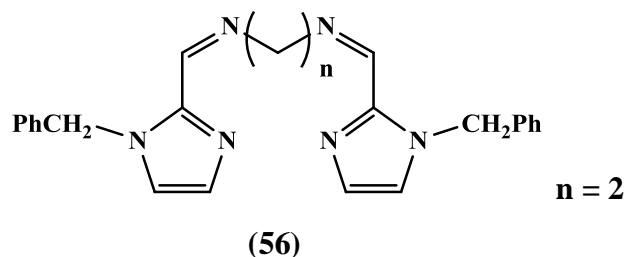
2.6.15 4-[(*E*)-2-(1-Methyl-1*H*-imidazol-2-yl)diazenyl]-*N*-[(*E*)-(1-methyl-1*H*-imidazol-2-yl)methylidene]-1-butanamine (55)



This solid was prepared in a similar manner to **(41)** using 1-methyl-2-imidazolecarboxaldehyde (1.26 g, 1.14 mmol) and 1,4-diaminobutane (0.50 g, 0.57 mmol). An off-white solid **(55)** was obtained.

<u>Yield:</u>	1.00 g (64%).
<u>Mp:</u>	74-46 °C.
<u>% Found:</u>	C: 62.00, H: 7.40, N: 30.84.
<u>% Calculated:</u>	C: 61.74, H: 7.40, N: 30.86 (C ₁₄ H ₂₀ N ₆ mol. wt. 272.35)
<u>¹H NMR:</u>	(ppm d ₆ -DMSO): 2.65 (m, 4H), 3.53 (s, 6H), 3.92 (s, 4H), 6.98 (s, 2H), 7.18 (s, 2H), 8.25 (s, 2H).
<u>¹³C NMR:</u>	(ppm d ₆ -DMSO): 28.6, 55.1, 61.0, 125.8, 128.9, 142.7, 153.4.
<u>IR (KBr):</u>	3428, 3095, 2954, 2826, 1651, 1590, 1519, 1475, 1436, 1364, 1337, 1289, 1146, 1047, 978, 920, 809 cm ⁻¹ .
<u>Solubility:</u>	Hot methanol and hot DMSO.

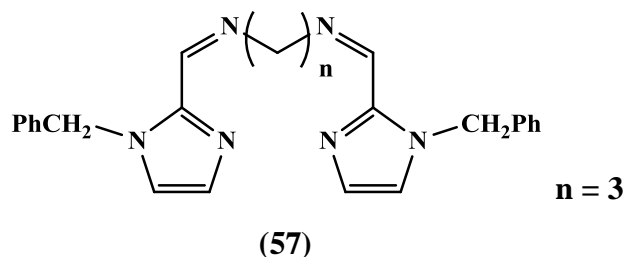
2.6.16 *N*-[(*E*)-(1-Benzyl-1*H*-imidazol-2-yl)methylidene]-*N*-(2-[(*E*)-(1-benzyl-1*H*-imidazol-2-yl)methylidene]aminoethyl)amine (56)



This solid was prepared in a similar manner to **(41)** using 1-benzylimidazole-2-carboxaldehyde (2.66 g, 1.66 mmol) and 1,2-diaminoethane (0.50 g, 0.83 mmol), yielding an oil, which, on standing, solidified to a gold-coloured solid **(56)**.

<u>Yield:</u>	2.15 g (73%).
<u>Mp:</u>	64-68 °C.
<u>% Found:</u>	C: 72.85, H: 6.35, N: 21.25.
<u>% Calculated:</u>	C: 72.70, H: 6.10, N: 21.21 (C ₂₄ H ₂₄ N ₆ mol. wt. 396.49).
<u>¹H NMR:</u>	(ppm d ₆ -DMSO): 3.78 (s, 4H), 5.62 (s, 4H), 6.82 (s, 2H), 7.15 (2H), 7.29 (m, 10H), 8.21 (s, 2H).
<u>¹³C NMR:</u>	(ppm d ₆ -DMSO): 48.6, 59.6, 118.7, 120.9, 124.7, 127.3, 127.5, 128.6, 137.8, 154.2.
<u>IR (KBr):</u>	3407, 3131, 3088, 2846, 1651, 1497, 1470, 1453, 1440, 1372, 1328, 1284, 1251, 1163, 1068, 1032, 825 cm ⁻¹ .
<u>Solubility:</u>	Methanol, ethanol, ethyl acetate, chloroform, DCM.

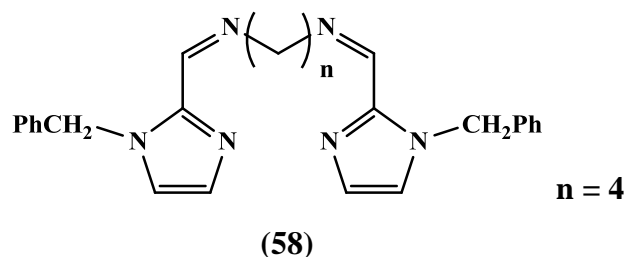
2.6.17 *N*-[(*E*)-(1-Benzyl-1*H*-imidazol-2-yl)methylidene]-*N*-(3-[(*E*)-(1-benzyl-1*H*-imidazol-2-yl)methylidene]aminopropyl)amine (57)



This solid was prepared in a similar manner to **(41)** using 1-benzylimidazole-2-carboxaldehyde (2.16 g, 1.34 mmol) and 1,3-diaminopropane (0.50 g, 0.67 mmol). This yielded a gold-coloured oil, which on standing solidified to a gold-coloured solid **(57)**.

<u>Yield:</u>	2.25 g (80%).
<u>Mp:</u>	18-20 °C.
<u>% Found:</u>	C: 73.45, H: 6.51, N: 20.69.
<u>% Calculated:</u>	C: 73.14, H: 6.38, N: 20.47 (C ₂₅ H ₂₆ N ₆ mol. wt. 410.51).
<u>¹H NMR:</u>	(ppm d ₆ -DMSO): 2.55 (d, 4H), 5.30 (d, 4H), 5.75 (s, 2H), 6.85 (s, 2H), 7.00-7.60 (m, 12H), 8.24 (s, 2H).
<u>¹³C NMR:</u>	(ppm d ₆ -DMSO): 31.6, 59.3, 62.7, 121.0, 124.8, 127.4, 128.4, 129.1, 137.5, 147.6, 153.2.
<u>IR (KBr):</u>	3394, 2850, 1651, 1497, 1471, 1455, 1360, 1272, 1157, 1112, 1030, 970 cm ⁻¹ .
<u>Solubility:</u>	Methanol, ethanol, ethyl acetate, chloroform, DCM.

2.6.18 *N*-[(*E*)-(1-Benzyl-1*H*-imidazol-2-yl)methylidene]-*N*-(4-[(*E*)-(1-benzyl-1*H*-imidazol-2-yl)methylidene]aminobutyl)amine (58)

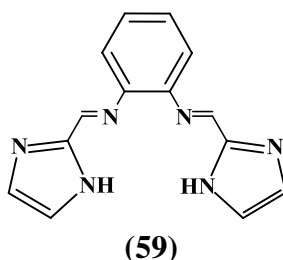


This solid was prepared in a similar manner to **(41)** using 1-benzylimidazole-2-carboxaldehyde (1.83 g, 1.14 mmol) and 1,4-diaminobutane (0.50 g, 0.57 mmol). The gold-coloured oil which, on standing solidified to a gold-coloured solid **(58)**.

<u>Yield:</u>	2.15 g (89%).
<u>Mp:</u>	78-80 °C.
<u>% Found:</u>	C: 73.20, H: 6.30, N: 20.01.
<u>% Calculated:</u>	C: 73.56, H: 6.65, N: 19.80 (C ₂₆ H ₂₈ N ₆ mol. wt. 424.54).
<u>¹H NMR:</u>	(ppm d ₆ -DMSO): 2.45 (t, 4H), 4.50 (t, 4H), 5.68 (s, 4H), 7.15 (m, 12H), 7.46 (s, 2H), 8.25 (s, 2H).
<u>¹³C NMR:</u>	(ppm d ₆ -DMSO): 38.5, 55.7, 65.5, 120.9, 126.6, 127.3, 128.3, 129.1, 137.6, 147.1, 152.9.
<u>IR (KBr):</u>	3419, 3112, 2944, 2830, 1654, 1471, 1441, 1295, 1250, 1030, 979, 920 cm ⁻¹ .
<u>Solubility:</u>	Methanol, ethanol, ethyl acetate, chloroform, DCM.

2.7 Schiff Base Ligands Derived from 1,2-Phenylenediamine, 1,3-Phenylenediamine and 1,4-Phenylenediamine¹¹⁹⁻¹²¹

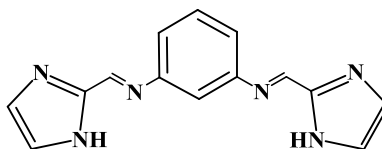
2.7.1 *N*-[(*E*)-1*H*-Imidazol-2-ylmethylidene]-*N*-(2-[(*E*)-1*H*-imidazol-2-ylmethylidene]aminophenyl)amine (**59**)



To a solution of 1,2-phenylenediamine in dry methanol (1.00 g, 0.92 mmol) was added imidazole-2-carboxaldehyde (1.77 g, 1.84 mmol) and molecular sieve (4 Å beads) as a dehydrating agent. The solution was refluxed for 4 h and then stirred overnight at room temperature. The reaction was monitored by TLC (MeOH: ethyl:acetate 1:5). The molecular sieve was filtered off and the solvent was removed under reduced pressure to yield a pale yellow/green powder. The solid (**59**) was washed with cold, dry methanol and air-dried.

<u>Yield:</u>	2.20 g (97 %).
<u>Mp:</u>	Decomposition > 210 °C.
<u>% Found:</u>	C: 63.30, H: 4.50, N: 31.45.
<u>% Calculated:</u>	C: 63.64, H: 4.58, N: 31.80 (C ₁₄ H ₁₂ N ₆ mol. wt. 264.29).
<u>¹H NMR:</u>	(ppm d ₆ -DMSO): 7.16-7.43 (m, 8H), 8.30 (s, 2H), 13.21 (s, 2H).
<u>¹³C NMR:</u>	(ppm d ₆ -DMSO): 116.3, 122.8, 126.8, 143.9, 145.3, 152.7.
<u>IR (KBr):</u>	3316, 3115, 3057, 1621, 1591, 1506, 1432, 1318, 1230, 1185, 1130 cm ⁻¹ .
<u>Solubility:</u>	Hot DMSO.

2.7.2 *N*-1-[(*E*)-1*H*-Imidazol-2-ylmethylidene]-*N*3-[(*E*)-1*H*-imidazol-2-ylmethyliden]1,3-benzenediamine (60)

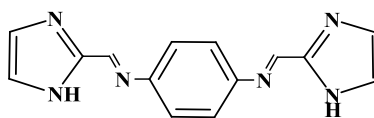


(60)

This solid was prepared in a similar manner to (41) using 1,3-phenylenediamine (1.00 g, 0.92 mmol) and imidazole-2-carboxaldehyde (1.96 g, 2.04 mmol). An off-white powder (60) was obtained.

<u>Yield:</u>	2.08 g (92 %).
<u>Mp:</u>	Decomposition > 210 °C.
<u>% Found:</u>	C: 63.43, H: 4.48, N: 31.64.
<u>% Calculated:</u>	C: 63.64, H: 4.58, N: 31.80 (C ₁₄ H ₁₂ N ₆ mol. wt. 264.29).
<u>¹H NMR:</u>	(ppm d ₆ -DMSO): 7.18 (t, 4H), 7.46 (m, 4H), 8.50 (s, 2H), 12.51 (s, 2H).
<u>¹³C NMR:</u>	(ppm d ₆ -DMSO): 113.6, 119.5, 129.6, 144.6, 147.8, 148.3, 150.9.
<u>IR (KBr):</u>	3298, 3093, 1609, 1475, 1424, 1332, 1268, 1200, 1085, 1008 cm ⁻¹ .
<u>Solubility:</u>	Sparingly in hot methanol, toluene and DMSO.

2.7.3 *N*-[(*E*)-1*H*-Imidazol-2-ylmethylidene]-*N*-(4-[(*E*)-1*H*-imidazol-2-ylmethylidene]aminophenyl)amine (61)^{120,121}

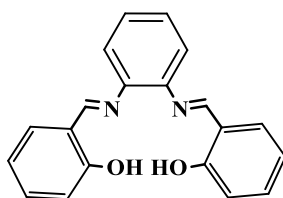


(61)

This solid was prepared in a similar manner to **(41)** using 1,4-phenylenediamine (1.10 g, 1.02 mmol) and imidazole-2-carboxaldehyde (1.96 g, 2.04 mmol). A pale yellow powder **(61)** was obtained.

<u>Yield:</u>	2.00 g (88 %).
<u>Mp:</u>	Decomposition > 220 °C.
<u>% Found:</u>	C: 63.44, H: 4.50, N: 31.45.
<u>% Calculated:</u>	C: 63.64, H: 4.58, N: 31.80 (C ₁₄ H ₁₂ N ₆ mol. wt. 264.29).
<u>¹H NMR:</u>	(ppm d ₆ -DMSO): 7.11 (s, 4H), 7.21 (s, 4H), 8.29 (s, 2H), 12.95 (s, 2H).
<u>¹³C NMR:</u>	(ppm d ₆ -DMSO): 119.4, 122.4, 145.3, 149.2, 160.3.
<u>IR (KBr):</u>	3002, 2907, 1618, 1555, 1493, 1440, 1384, 1303, 1206, 1154, 1113 cm ⁻¹ .
<u>Solubility:</u>	Sparsely in hot methanol, toluene and DMSO.

2.7.4 2-[(2-[(*E*)-(2-Hydroxyphenyl)methylidene]aminophenyl)imino] Methylphenol (**62**)



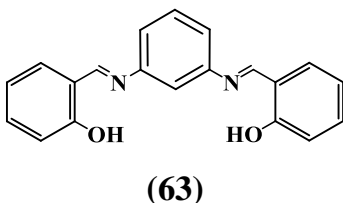
(62)

This solid was prepared in a similar manner to **(41)** using 1,2-phenylenediamine (1.00 g, 0.92 mmol) and salicylaldehyde (2.24 g, 1.84 mmol). A yellow/orange powder **(62)**^{120,121} was obtained.

<u>Yield:</u>	2.75 g (94 %).
---------------	----------------

<u>Mp:</u>	158-161 °C.
<u>% Found:</u>	C: 75.78, H: 5.05, N: 8.87.
<u>% Calculated:</u>	C: 75.93, H: 5.10, N: 8.86 (C ₂₀ H ₁₆ N ₂ O ₂ mol. wt. 316.35).
<u>¹H NMR:</u>	(ppm d ₆ -DMSO): 6.78 (m, 2H), 7.25-7.43 (m, 8H), 7.51 (d, 2H), 8.75 (s, 2H), 12.70 (s, b, 2H).
<u>¹³C NMR:</u>	(ppm d ₆ -DMSO): 117.0, 119.4, 119.8, 120.1, 128.2, 132.8, 133.8, 149.6, 160.7, 164.4.
<u>IR (KBr):</u>	3447, 3054, 1613, 1562, 1481, 1449, 1277, 1193 cm ⁻¹ .
<u>Solubility:</u>	Most organic solvents.

2.7.5 2-[(3-[(*E*)-(2-Hydroxyphenyl)methylidene]aminophenyl)imino]methylphenol (**63**)



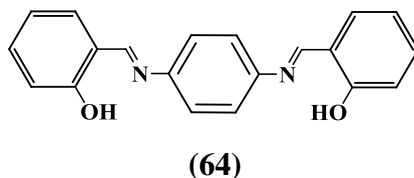
This solid was prepared in a similar manner to (**41**) using 1,3-phenylenediamine (1.00 g, 0.92 mmol) and salicylaldehyde (2.24 g, 1.84 mmol). An orange powder (**63**) was obtained.

<u>Yield:</u>	2.81 g (96 %).
<u>Mp:</u>	108-110 °C.
<u>% Found:</u>	C: 75.74, H: 5.34, N: 8.70.
<u>% Calculated:</u>	C: 75.93, H: 5.10, N: 8.86 (C ₂₀ H ₁₆ N ₂ O ₂ mol. wt. 316.35).
<u>¹H NMR:</u>	(ppm d ₆ -DMSO): 6.98 (m, 4H), 7.36 (m, 4H), 7.53 (m, 2H), 7.66 (d, 2H), 7.80 (s, 2H), 13.20 (s, b, 2H).
<u>¹³C NMR:</u>	(ppm d ₆ -DMSO): 114.2, 117.0, 119.6, 120.6, 130.7, 132.9, 133.8, 149.7, 160.7, 164.5.

IR (KBr): 3455, 2988, 1622, 1592, 1571, 1498, 1460, 1284, 1197, 1150 cm^{-1} .

Solubility: Most organic solvents

2.7.6 2-[(4-[(*E*)-(2-Hydroxyphenyl)methylidene]aminophenyl) imino] methylphenol (**64**)



This solid was prepared in a similar manner to (**41**) using 1,4-phenylenediamine (1.00 g, 0.92 mmol) and salicylaldehyde (2.24 g, 1.84 mmol). A dark orange powder (**64**) was obtained.

Yield: 2.60 g (93 %).

Mp: 210-212 °C.

% Found: C: 75.78, H: 5.08, N: 8.78.

% Calculated: C: 75.93, H: 5.10, N: 8.86 ($\text{C}_{20}\text{H}_{16}\text{N}_2\text{O}_2$ mol. wt. 316.35).

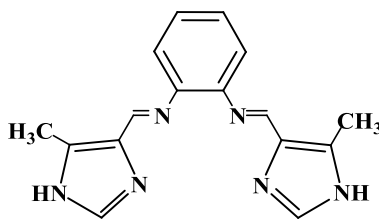
^1H NMR: (ppm d_6 -DMSO): 7.03 (t, 4H), 7.42 (m, 2H), 7.53 (m, 4H), 7.67 (d, 2H), 9.01 (s, 2H), 13.00 (s, b, 2H).

^{13}C NMR: (ppm d_6 -DMSO): 117.0, 119.5, 119.7, 122.9, 132.9, 133.7, 147.0, 160.7, 163.5.

IR (KBr): 3468, 3053, 1611, 1572, 1493, 1371, 1282, 1189 cm^{-1} .

Solubility: Most organic solvents.

2.7.7 *N*-[(*E*)-(5-Methyl-1*H*-imidazol-4-yl)methylidene]-*N*-(2-[(*E*)-(5-methyl-1*H*-imidazol-4-yl)methylidene]aminophenyl)amine (65)

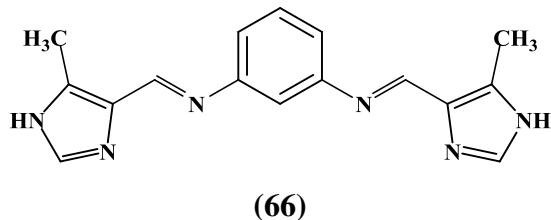


(65)

This solid was prepared in a similar manner to (41) using 1,2-phenylenediamine (1.00 g, 0.92 mmol) and 4-methyl-5-imidazolecarboxyaldehyde (2.02 g, 1.84 mmol). A pale yellow powder (65) was obtained.

<u>Yield:</u>	2.43 g (90 %).
<u>Mp:</u>	Decomposition > 260 °C.
<u>% Found:</u>	C: 65.51, H: 5.44, N: 28.27.
<u>% Calculated:</u>	C: 65.74, H: 5.52, N: 28.55 (C ₁₆ H ₁₆ N ₆ mol. wt. 292.34).
<u>¹H NMR:</u>	(ppm d ₆ -DMSO): 3.39 (s, 6H), 7.30 (s, 4H), 7.75 (s, 2H), 8.55 (s, 2H), 11.60 (s, 2H).
<u>¹³C NMR:</u>	(ppm d ₆ -DMSO): 61.7, 118.5, 120.5, 122.1, 133.8, 134.6, 147.4, 151.7.
<u>IR (KBr):</u>	3427, 3040-2654, 1875, 1621, 1577, 1490, 1457, 1393, 1340, 1252, 1210, 965, 878, 834, 764 cm ⁻¹ .
<u>Solubility:</u>	Sparingly in hot methanol, toluene and DMSO.

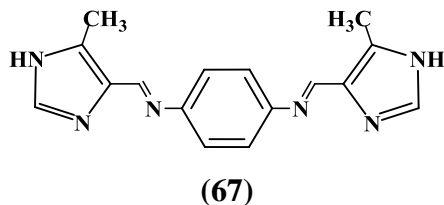
2.7.8 *N*-[(*E*)-(4-Methyl-1*H*-imidazol-5-yl)methylidene]-*N*-(3-[(*E*)-(5-methyl-1*H*-imidazol-4-yl)methylidene]aminophenyl)amine (66)



This solid was prepared in a similar manner to **(41)** using 1,3-phenylenediamine (1.00 g, 0.92 mmol) and 4-methyl-5-imidazolecarboxyaldehyde (2.03 g, 1.84 mmol). A white powder **(66)** was obtained.

<u>Yield:</u>	2.55 g (95 %).
<u>Mp:</u>	Decomposition > 250 °C.
<u>% Found:</u>	C: 65.56, H: 5.69, N: 28.47.
<u>% Calculated:</u>	C: 65.74, H: 5.52, N: 28.75 (C ₁₆ H ₁₆ N ₆ mol. wt. 292.34).
<u>¹H NMR:</u>	(ppm, d ₆ -DMSO): 3.43 (s, 6H), 7.00 (s, 3H), 7.20 (t, 1H), 7.75 (s, 2H), 8.48 (s, 2H), 11.81 (s, b, 2H).
<u>¹³C NMR:</u>	(ppm, d ₆ -DMSO): 60.7, 112.4, 119.9, 120.6, 133.5, 135.8, 143.0, 143.6, 153.8.
<u>IR (KBr):</u>	3437, 3120, 2981, 2916, 2627, 1846, 1629, 1566, 1475, 1397, 1352, 1295, 1253, 1182, 1149, 986 cm ⁻¹ .
<u>Solubility:</u>	Sparingly in hot methanol, toluene and DMSO.

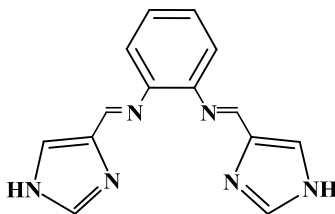
2.7.9 *N*-[(*E*)-(4-Methyl-1*H*-imidazol-5-yl)methylidene]-*N*-(4-[(*E*)-(4-methyl-1*H*-imidazol-5-yl)methylidene]aminophenyl)amine (67)



This solid was prepared in a similar manner to **(41)** using 1,4-phenylenediamine (1.00 g, 0.92 mmol) and 4-methyl-5-imidazolecarboxyaldehyde (2.02 g, 1.84 mmol). A pale yellow powder **(67)** was obtained.

<u>Yield:</u>	2.51 g (93 %).
<u>Mp:</u>	Decomposition > 250 °C.
<u>% Found:</u>	C: 65.56, H: 5.63, N: 28.40.
<u>% Calculated:</u>	C: 65.74, H: 5.52, N: 28.75 (C ₁₆ H ₁₆ N ₆ mol. wt. 292.34).
<u>¹H NMR:</u>	(ppm, d ₆ -DMSO): 3.41 (s, 6H), 7.15 (s, 2H), 7.45 (s, 2H), 7.60 (s, 2H), 7.84 (s, 2H).
<u>¹³C NMR:</u>	(ppm, d ₆ -DMSO): 65.4, 117.9, 119.8, 120.7, 135.6, 143.2, 152.5.
<u>IR (KBr):</u>	3465, 3096, 3009, 2843, 1605, 1538, 1460, 1396, 1377, 1348, 1258, 1163 cm ⁻¹ .
<u>Solubility:</u>	Sparingly in hot methanol, toluene and DMSO.

2.7.10 *N*-[(*E*)-1*H*-Imidazol-4-ylmethylidene]-*N*-(2-[(*E*)-1*H*-imidazol-5-ylmethylidene]aminophenyl)amine (68)

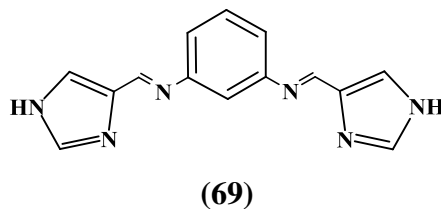


(68)

This solid was prepared in a similar manner to **(41)** using 1,2-phenylenediamine (1.00 g, 0.92 mmol) and 4(5)-imidazolecarboxyaldehyde (1.78 g, 1.84 mmol). A white powder **(68)** was obtained.

<u>Yield:</u>	2.10 g (86 %).
<u>Mp:</u>	266-268 °C.
<u>% Found:</u>	C: 63.63, H: 4.47, N: 31.62.
<u>% Calculated:</u>	C: 63.64, H: 4.58, N: 31.80 (C ₁₄ H ₁₂ N ₆ mol. wt. 264.29).
<u>¹H NMR:</u>	(ppm, d ₆ -DMSO): 6.68 (s, 2H), 7.73 (s, 2H), 7.96 (s, 2H), 7.37 (s, 2H), 8.69 (s, 2H), 11.82 (s, b, 2H).
<u>¹³C NMR:</u>	(ppm, d ₆ -DMSO): 111.3, 118.5, 122.8, 135.4, 135.9, 136.7, 163.0.
<u>IR (KBr):</u>	3120, 3061, 2973, 2815, 2624, 1850, 1612, 1574, 1519, 1398, 1357, 1288, 1266, 1222, 1188, 1085 cm ⁻¹ .
<u>Solubility:</u>	Sparingly in hot methanol, toluene and DMSO.

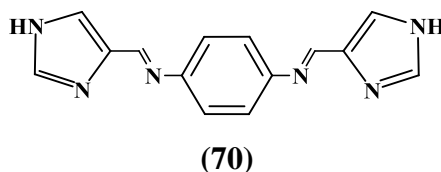
2.7.11 *N*-[(*E*)-1*H*-Imidazol-4-ylmethylidene]-*N*-(3-[(*E*)-1*H*-imidazol-4-ylmethylidene]aminophenyl)amine (69)



This solid was prepared in a similar manner to **(41)** using 1,3-phenylenediamine (1.00 g, 0.92 mmol) and 4(5)-imidazolecarboxyaldehyde (1.78 g, 1.84 mmol). A white powder **(69)**, was obtained.

<u>Yield:</u>	2.25 g (92%).
<u>Mp:</u>	Decomposition > 220 °C.
<u>% Found:</u>	C: 63.98, H: 4.48, N: 31.54.
<u>% Calculated:</u>	C: 63.62, H: 4.58, N: 31.80 (C ₁₄ H ₁₂ N ₆ mol. wt. 264.29).
<u>¹H NMR:</u>	(ppm, d ₆ -DMSO): 7.08 (m, 4H), 7.43 (s, 3H), 7.75 (s, 1H), 8.51 (s, 2H), 12.80 (s, b, 2H).
<u>¹³C NMR:</u>	(ppm, d ₆ -DMSO): 112.8, 118.5, 127.4, 128.6, 130.2, 138.7, 153.2.
<u>IR (KBr):</u>	3420, 3131, 2830, 2601, 1638, 1590, 1473, 1362, 1173, 1115, 1000 cm ⁻¹ .
<u>Solubility:</u>	Sparingly in hot methanol, toluene and DMSO.

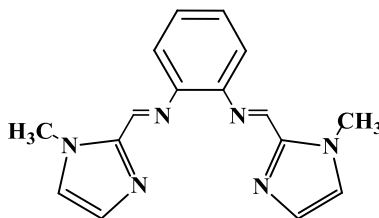
2.7.12 *N*-[(*E*)-1*H*-Imidazol-4-ylmethylidene]-*N*-(4-[(*E*)-1*H*-imidazol-4-ylmethylidene]aminophenyl)amine (70)



This solid was prepared in a similar manner to **(41)** using 1,4-phenylenediamine (1.00 g, 0.92 mmol) and 4(5)-imidazolecarboxyaldehyde (1.78 g, 1.84 mmol). A yellow powder **(70)** was obtained.

<u>Yield:</u>	2.06 g (84 %).
<u>Mp:</u>	Decomposition > 260 °C.
<u>% Found:</u>	C: 63.68, H: 4.65, N: 32.07.
<u>% Calculated:</u>	C: 63.62, H: 4.58, N: 31.80 (C ₁₄ H ₁₂ N ₆ mol. wt. 264.29).
<u>¹H NMR:</u>	(ppm, d ₆ -DMSO): 7.25 (s, 4H), 7.69 (s, 4H), 7.85 (s, 2H), 8.52 (s, 2H).
<u>¹³C NMR:</u>	(ppm, d ₆ -DMSO): 122.1, 124.2, 138.5, 138.6, 147.0, 149.6.
<u>IR (KBr):</u>	3442, 3129, 2962, 2851, 2787, 2604, 1624, 1456, 1327, 1256, 1121 cm ⁻¹ .
<u>Solubility:</u>	Sparingly in hot methanol, toluene and DMSO.

2.7.13 *N*-[(*E*)-(1-Methyl-1*H*-imidazol-2-yl)methylidene]-*N*-(2-[(*E*)-(1-methyl-1*H*-imidazol-2-yl)methylidene]aminophenyl)amine (71**)**

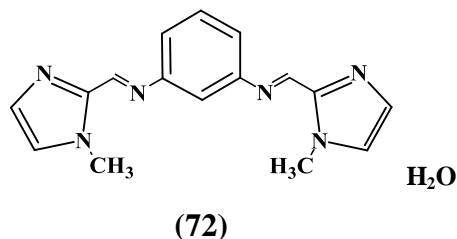


(71)

This solid was prepared in a similar way to **(41)** using 1,2-phenylenediamine (1.00 g, 0.92 mmol) and 1-methyl-2-imidazolecarboxyaldehyde (2.03 g 1.84 mmol). A green/brown powder **(71)** was obtained.

<u>Yield:</u>	2.30 g (85%).
<u>Mp:</u>	Decomposition > 120 °C.
<u>% Found:</u>	C: 65.82, H: 5.85, N: 28.80.
<u>% Calculated:</u>	C: 65.74, H: 5.52, N: 28.75 (C ₁₆ H ₁₆ N ₆ mol. wt. 292.34).
<u>¹H NMR:</u>	(ppm, d ₆ -DMSO): 4.19 (s, 6H), 6.87 (s, 2H), 7.26 (m, 4H), 7.59 (m, 2H), 8.70 (s, 2H).
<u>¹³C NMR:</u>	(ppm, d ₆ -DMSO): 66.7, 112.5, 118.8, 128.3, 128.8, 135.6, 143.9, 149.3.
<u>IR (KBr):</u>	3410, 3151, 2987, 2858, 2639, 1622, 1494, 1376, 1287, 1182, 1084, 1057 cm ⁻¹ .
<u>Solubility:</u>	Sparingly in hot methanol, toluene and DMSO.

2.7.14 *N*-[(*E*)-(1-Methyl-1*H*-imidazol-2-yl)methylidene]-*N*-(3-[(*E*)-(1-methyl-1*H*-imidazol-2-yl)methylidene]aminophenyl)amine (72)

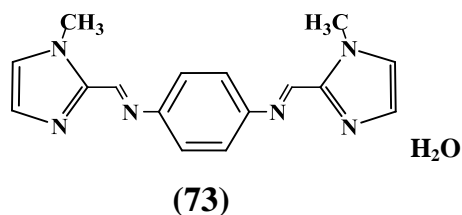


This solid was prepared in a similar manner to **(41)** using 1,3-phenylenediamine (1.00 g, 0.92 mmol) and 1-methyl-2-imidazolecarboxyaldehyde (2.03 g 1.84 mmol). The oil which was crystallised from toluene, filtered and washed with cold, dry methanol to give a white powder **(72)**.

<u>Yield:</u>	2.25 g (92%).
<u>Mp:</u>	Decomposition > 250 °C.
<u>% Found:</u>	C: 61.96, H: 5.68, N: 27.38.
<u>% Calculated:</u>	C: 61.92, H: 5.85, N: 27.08 (C ₁₆ H ₁₈ N ₆ O mol. wt. 310.35).

<u>^1H NMR:</u>	(ppm, d_6 -DMSO): 3.95 (s, 6H), 7.00 (m, 4H), 7.29 (s, 4H), 8.36 (s, 2H).
<u>^{13}C NMR:</u>	(ppm, d_6 -DMSO): 65.6, 116.9, 117.3, 128.7, 130.1, 130.3, 149.6, 152.1.
<u>IR (KBr):</u>	3360, 3111, 1630, 1584, 1520, 1482, 1434, 1369, 1292, 1157 cm^{-1} .
<u>Solubility:</u>	Sparingly in hot methanol, toluene and DMSO.

2.7.15 *N*-[(*E*)-(1-Methyl-1*H*-imidazol-2-yl)methylidene]-*N*-(4-[(*E*)-(1-methyl-1*H*-imidazol-2-yl)methylidene]aminophenyl)amine (73)



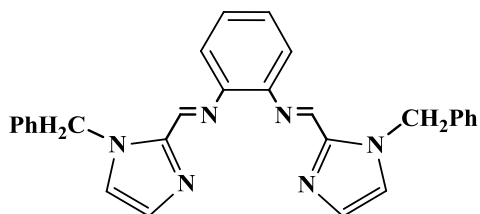
This solid was prepared in a similar manner to (**41**) using 1,4-phenylenediamine (1.00 g, 0.92 mmol) and 1-methyl-2-imidazolecarboxyaldehyde (2.03 g, 1.84 mmol), yielding a yellow/brown oil which was crystallised from toluene to give a very fine yellow/brown flaky powder (**73**), which was washed with cold dry methanol, filtered and air dried.

<u>Yield:</u>	2.25 g (92%).
<u>Mp:</u>	238-240 °C.
<u>% Found:</u>	C: 61.55, H: 5.47, N: 27.05.
<u>% Calculated:</u>	C: 61.92, H: 5.85, N: 27.08 ($\text{C}_{16}\text{H}_{18}\text{N}_6\text{O}$ mol. wt. 310.35).
<u>^1H NMR:</u>	(ppm, d_6 -DMSO): 4.13 (s, 6H), 7.23 (s, 2H), 7.44 (s, 4H), 7.51 (s, 2H), 8.60 (s, 2H).
<u>^{13}C NMR:</u>	(ppm, d_6 -DMSO): 65.6, 122.9, 126.9, 130.1, 143.1, 149.3, 151.0.

IR (KBr): 3437, 3113, 2950, 1619, 1519, 1470, 1432, 1367, 1287, 1206, 1149 cm^{-1} .

Solubility: Sparingly in hot methanol, toluene and DMSO.

2.7.16 *N*-[(*E*)-(1-Benzyl-1*H*-imidazol-2-yl)methylidene]-*N*-(2-[(*E*)-(1-benzyl-1*H*-imidazol-2-yl)methylidene]aminoethyl)amine (74)



(74)

This solid was prepared in a similar manner to **(41)** using 1,2-phenylenediamine (1.00 g, 0.92 mmol) and 1-benzyl-1*H*-imidazole-2-carboxaldehyde (2.96 g, 1.84 mmol). A gold coloured oil **(74)** was obtained.

Yield: 1.89g (46 %).

Bp: 84-86 °C.

% Found: C: 75.20, H: 5.58, N: 18.80.

% Calculated: C: 75.65, H: 5.44, N: 18.91 ($\text{C}_{28}\text{H}_{24}\text{N}_6$ mol. wt. 444.53).

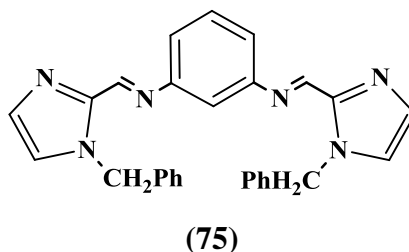
^1H NMR: (ppm, d_6 -DMSO): 4.51 (s, 4H), 6.95 (s, 2H), 7.25 (m, 12 H), 7.60 (s, 2H), 7.82 (s, 2H), 8.25 (s, 2H).

^{13}C NMR: (ppm, d_6 -DMSO): 58.4, 118.5, 120.3, 123.8, 125.1, 125.9, 127.7, 128.8, 134.5, 139.6, 149.6.

IR (KBr): 3470, 1670, 1497, 1367, 1300, 1269, 1176, 1107 cm^{-1} .

Solubility: MeOH, EtOH, chloroform, benzene, DMSO.

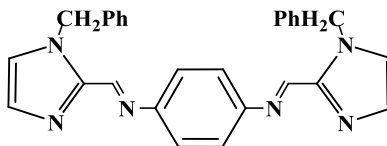
2.7.17 *N*-[(*E*)-(1-Benzyl-1*H*-imidazol-2-yl)methylidene]-*N*-(3-[(*E*)-(1-benzyl-1*H*-imidazol-2-yl)methylidene]aminophenyl)amine (75)



This solid was prepared in a similar manner to **(41)** using 1,3-phenylenediamine (1.00g, 0.92 mmol) and 1-benzyl-1*H*-imidazole-2-carboxaldehyde (2.69 g, 1.84 mmol). A green/tan powder **(75)** was obtained.

<u>Yield:</u>	2.25 g (92%).
<u>Mp:</u>	80-83 °C.
<u>% Found:</u>	C: 75.62, H: 5.51, N: 18.95.
<u>% Calculated:</u>	C: 75.65, H: 5.44, N: 18.91 (C ₂₈ H ₂₄ N ₆ mol. wt. 444.53).
<u>¹H NMR:</u>	(ppm, d ₆ -DMSO): 5.25 (m, 6H), 7.90 (m, 8H), 8.15 (m, 6H), 8.46 (s, 2H), 8.80 (s, 2H).
<u>¹³C NMR:</u>	(ppm, d ₆ -DMSO): 90.7, 117.8, 119.1, 120.2, 128.2, 130.2, 131.3, 134.3, 138.7, 139.0, 149.5, 152.2, 158.1.
<u>IR (KBr):</u>	3370, 1670, 1497, 1456, 1302, 1269, 1109, 1079 cm ⁻¹ .
<u>Solubility:</u>	MeOH, EtOH, chloroform, benzene, DMSO.

2.7.18 *N*-[(*E*)-(1-Benzyl-1*H*-imidazol-2-yl)methylidene]-*N*-(4-[(*E*)-(1-benzyl-1*H*-imidazol-2-yl)methylidene]aminophenyl)amine (76)



(76)

This solid was prepared in a similar manner to **(41)** using 1,4-phenylenediamine (1.00 g, 0.92 mmol) and 1-benzyl-1*H*-imidazole-2-carboxaldehyde (2.69 g, 1.84 mmol). A tan coloured powder **(76)** was obtained.

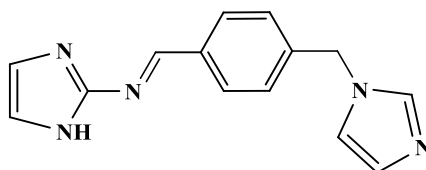
<u>Yield:</u>	1.91 g (46%).
<u>Mp:</u>	78-80 °C.
<u>% Found:</u>	C: 75.91, H: 5.58, N: 18.80.
<u>% Calculated:</u>	C: 75.65, H: 5.44, N: 18.91 (C ₂₈ H ₂₄ N ₆ mol. wt. 444.53).
<u>¹H NMR:</u>	(ppm, d ₆ -DMSO): 5.45 (s, 4H), 6.60 (s, 4H), 7.40 (m, 10H), 7.92 (s, 4H), 9.70 (s, 2H).
<u>¹³C NMR:</u>	(ppm, d ₆ -DMSO): 79.1, 111.1, 117.7, 120.2, 122.1, 128.3, 129.4, 135.6, 139.0, 149.2, 151.0.
<u>IR (KBr):</u>	3434, 3105, 1686, 1620, 1605, 1577, 1520, 1482, 1258, 1176, 1111 cm ⁻¹ .
<u>Solubility:</u>	MeOH, EtOH, chloroform, benzene, DMSO.

2.8 Experimental (part 2)
Synthesis of Ag(I) Complexes

2.8 Synthesis of Ag(I) Complexes of the Schiff Base Ligands Derived from 1*H*-imidazol-2-amine (1)

All preparations were carried out in the absence of light, and the resultant complexes stored in the dark. The reacting ratio of silver to ligand was at least 2:1 for Schiff base ligands derived from 1*H*-imidazol-2-amine (1), histamine and Apim and a ratio of 3:1 for the ligands derived from 1,2-diaminoethane, 1,3-diaminopropane and 1,4-diaminobutane and 1,2-phenylenediamine, 1,3-phenylenediamine and 1,4-phenylenediamine.

2.8.1 [Ag(22)₂]ClO₄



(22)

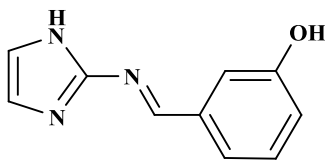
To a solution of *N*-(*E*)-[4-(1*H*-imidazol-1-yl)phenyl]methylidene-1*H*-imidazol-2-amine (22) (0.3 g, 1.19 mmol) in methanol (10 cm³) was added, drop wise, a solution of AgClO₄ (0.60 g, 2.89 mmol) in methanol (5.0 cm³). The solution was stirred for 2 h at room temperature. The solvent was reduced by approximately two thirds and the resulting suspension was then centrifuged for 10 min at 5000 rpm. The liquid was decanted off and the dark-green solid was washed with cold ethanol and suspension centrifuged again. The solid was air-dried in the dark at room temperature.

<u>Yield:</u>	0.30 g (71 %).
<u>% Found:</u>	C: 48.12, H: 3.85, N: 19.23.
<u>% Calculated:</u>	C: 47.37, H: 3.69, N: 19.73 (C ₂₈ H ₂₆ N ₁₀ O ₄ AgCl; mol. wt: 709.89).
<u>¹H NMR:</u>	(ppm, d ₆ -DMSO): 3.25 (s), 7.28 (s), 7.63 (s), 7.85 (m), 7.95-8.12 (m), 8.50 (s), 8.65 (s), 9.28 (s).

<u>^{13}C NMR:</u>	(ppm, d_6 -DMSO): 63.2, 118.4, 121.9, 126.8, 143.9, 145.3, 152.7.
<u>IR (KBr):</u>	3425, 3142, 2925, 1650, 1605, 1523, 1491, 1458, 1385, 1306, 1261, 1121, 833, 757, 624 cm^{-1} .
<u>Solubility:</u>	Hot DMSO.

Poor solubility of the complex prevented complete ^1H NMR and ^{13}C NMR analysis.

2.8.2 $[\text{Ag}(\mathbf{23})_2]\text{ClO}_4 \cdot \text{H}_2\text{O}$



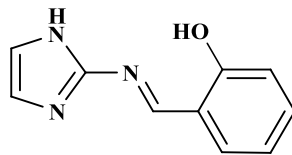
(**23**)

This brown solid was prepared in a similar manner to $[\text{Ag}(\mathbf{22})_2]\text{ClO}_4 \cdot$ using AgClO_4 (1.30 g, 6.20 mmol) and 3-[(1*H*-imidazol-2-ylimino)methyl]phenol (**23**) (0.50 g, 2.70 mmol).

<u>Yield:</u>	0.62 g (76 %).
<u>% Found:</u>	C: 41.00, H: 3.51, N: 14.59.
<u>% Calculated:</u>	C: 41.29, H: 3.12, N: 14.45 ($\text{C}_{20}\text{H}_{18}\text{O}_6\text{N}_6\text{AgCl}$; mol. wt 581.71).
<u>IR (KBr):</u>	3322 (b), 2925, 1670, 1601, 1546, 1463, 1284, 1144-1087, 941, 760, 637, 626 cm^{-1} .
<u>Solubility:</u>	Hot DMSO.

Poor solubility of the complex prevented ^1H NMR and ^{13}C NMR analysis.

2.8.3 [Ag(24)₂]ClO₄·2H₂O



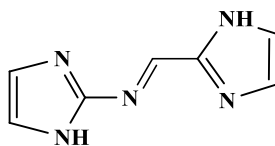
(24)

This brown solid was prepared in a similar manner to [Ag(22)₂]ClO₄ using AgClO₄ (1.24 g, 6.00 mol) and 2-[(1*H*-imidazol-2-ylimino)methyl]phenol (24) (0.5 g, 6.00 mmol).

<u>Yield:</u>	1.25 g (68 %).
<u>% Found:</u>	C: 39.51, H: 3.87, N: 13.96.
<u>% Calculated:</u>	C: 39.01, H: 3.27, N: 13.65 (C ₂₀ H ₂₀ N ₆ O ₈ ClAg; mol. wt: 615.73).
<u>IR (KBr):</u>	3425, 2924, 1605, 1524, 1385, 1306, 1261, 1121, 1088, 830, 758, 624 cm ⁻¹ .
<u>Solubility:</u>	Hot DMSO.

Poor solubility of the complex prevented ¹H NMR and ¹³C NMR analysis.

2.8.4 [Ag(25)]ClO₄



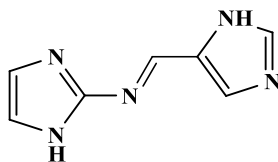
(25)

This green/brown solid was prepared in a similar manner to [Ag(**22**)₂]ClO₄ using AgClO₄ (1.30 g, 6.28 mmol) and *N*-[(*E*)-1*H*-imidazol-2-ylmethylidene]-1*H*-imidazol-2-amine (**25**) (0.50 g, 3.14 mmol).

<u>Yield:</u>	0.68 g (60 %).
<u>% Found:</u>	C: 22.52, H: 2.89, N: 18.80.
<u>% Calculated:</u>	C: 22.69, H: 2.45, N: 18.90 (C ₇ H ₉ N ₅ O ₄ ClAg; mol. wt: 370.50).
<u>¹H NMR:</u>	(ppm, d ₆ -DMSO): 6.86, 6.98 (broad), 8.99, 9.69, 11.77, 13.32.
<u>¹³C NMR:</u>	(ppm, d ₆ -DMSO): 119.0, 127.4, 136.8, 140.0, 149.2, 155.6.
<u>IR (KBr):</u>	3412 (broad), 2920, 1614, 1561, 1432, 1384, 1369, 1318, 1282, 1102, 1088, 756, 720, 668, 626, 560 cm ⁻¹ .
<u>Solubility:</u>	Hot DMSO.

Poor solubility of the complex prevented complete ¹H NMR and ¹³C NMR analysis.

2.8.5 [Ag(**26**)]ClO₄·H₂O



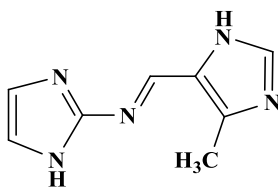
(**26**)

This green/brown solid was prepared in a similar manner to [Ag(**22**)₂]ClO₄ using AgClO₄ (1.30 g, 6.28 mmol) and *N*-[(*E*)-1*H*-imidazol-4-ylmethylidene]-1*H*-imidazol-2-amine (**26**) (0.50 g, 3.14 mmol).

<u>Yield:</u>	0.76 g (63 %).
<u>% Found:</u>	C: 21.94, H: 2.11, N: 17.42.
<u>% Calculated:</u>	C: 21.75, H: 2.35, N: 18.12 (C ₇ H ₉ N ₅ O ₅ AgCl; mol. wt: 386.5).
<u>¹H NMR:</u>	(ppm, d ₆ -DMSO): 7.42, 8.27, 8.36, 9.03, 9.80, 13.38.
<u>¹³C NMR:</u>	(ppm, d ₆ -DMSO): 119.5, 127.4, 136.8, 140.0, 149.2, 155.6.
<u>IR (KBr):</u>	3364, 2925, 1610, 1561, 1529, 1458, 1432, 1374, 1314, 1120, 1109, 861, 753, 715, 626 cm ⁻¹ .
<u>Solubility:</u>	Hot DMSO.

Poor solubility of the complex prevented complete ¹H NMR and ¹³C NMR analysis.

2.8.6 [Ag(27)]ClO₄·H₂O



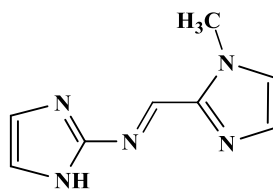
(27)

This brown solid was prepared in a similar manner to [Ag(22)₂]ClO₄ using AgClO₄ (1.18 g, 5.71 mmol) and *N*-[(*E*)-(5-methyl-1*H*-imidazol-4-yl)methylidene]-1*H*-imidazol-2-amine (27) (0.50 g, 2.85 mmol).

<u>Yield:</u>	0.58 g (51 %).
<u>% Found:</u>	C: 23.73, H: 2.30, N: 17.06.
<u>% Calculated:</u>	C: 23.99, H: 2.77, N: 17.49 (C ₈ H ₁₁ N ₅ O ₅ ClAg; mol. wt: 400.52).
<u>¹H NMR:</u>	(ppm, d ₆ -DMSO): 2.40 (s, 3H), 7.15 (s, 1H), 7.42 (s, 1H), 8.18 (s, 1H), 9.05 (s, 1H), 13.20 (s, b, 2H).

<u>^{13}C NMR:</u>	(ppm, d_6 -DMSO): 29.1, 118.3, 128.4, 131.9, 132.2, 138.9, 149.3, 154.5.
<u>IR (KBr):</u>	3270, 2923, 2047, 1610, 1576, 1520, 1477, 1462, 1331, 1368, 1360, 1258, 1090, 958, 924, 879, 754, 625 cm^{-1} .
<u>Solubility:</u>	Hot DMSO.

2.8.7 [Ag(28)]ClO₄·H₂O



(28)

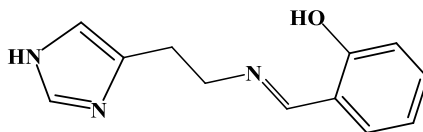
This light brown solid was prepared in a similar manner to [Ag(22)₂]ClO₄ using AgClO₄ (1.30 g, 6.28 mmol) in MeOH (5.0 cm³) and *N*-[(*E*)-1*H*-imidazol-4-ylmethylidene]-1*H*-imidazol-2-amine (28) (0.50 g, 2.85 mmol).

<u>Yield:</u>	0.62 g (67 %).
<u>% Found:</u>	C: 24.21, H: 2.10, N: 18.00.
<u>% Calculated:</u>	C: 23.99, H: 2.77, N: 17.49 (C ₈ H ₁₁ N ₅ O ₅ AgCl; mol. wt: 400.52).
<u>IR (KBr):</u>	3396, 2925, 1622, 1602, 1571, 1530, 1443, 1373, 1285, 1107, 1170, 861, 715, 617 cm^{-1} .
<u>Solubility:</u>	Hot DMSO.

Poor solubility of the complex prevented ¹H NMR and ¹³C NMR analysis.

2.9 Synthesis of Ag(I) Complexes of the Schiff Base Ligands Derived from Histamine

2.9.1 [Ag(**29**)]ClO₄·H₂O

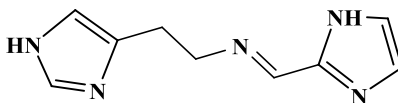


(**29**)

This yellow/brown solid was prepared in a similar manner to [Ag(**22**)₂]ClO₄ using AgClO₄ (1.00 g, 4.82 mmol) and 2-([2-(1*H*-imidazol-5-yl)ethyl]iminomethyl)phenol (**29**) (0.50 g, 2.32 mmol).

<u>Yield:</u>	0.63 g (63 %).
<u>% Found:</u>	C: 31.99, H: 2.91, N: 8.92.
<u>% Calculated:</u>	C: 32.71, H: 3.43, N: 9.54 (C ₁₂ H ₁₅ N ₃ O ₆ AgCl; mol. wt: 440.52).
<u>¹H NMR:</u>	(ppm, d ₆ -DMSO): 2.72, 3.01, 5.20, 6.49-7.37, 7.79, 8.43, 12.60 (broad), 13.28 (broad).
<u>IR (KBr):</u>	3428, 2962, 2920, 2838, 1631, 1607, 1527, 1559, 1377, 1095, 917, 820, 761, 625, 536 cm ⁻¹ .
<u>Solubility:</u>	Hot DMSO.

Poor solubility of the complex prevented complete ¹H NMR and ¹³C NMR analysis.

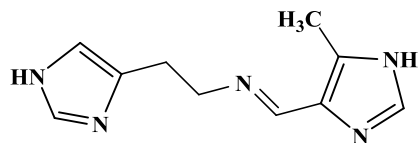
2.9.2 [Ag_{1.5}(**30**)](ClO₄)_{1.5}**(30)**

This cream coloured solid was prepared in a similar manner to [Ag(**22**)₂]ClO₄ using AgClO₄ (1.20 g, 5.79 mmol) and *N*-[2-(1*H*-imidazol-5-yl)ethyl]-*N*-[(*E*)-1*H*-imidazol-2-ylmethylidene]amine (**30**) (0.50 g, 2.64 mmol).

<u>Yield:</u>	0.95 g (72 %).
<u>% Found:</u>	C: 21.87, H: 2.29, N: 13.42.
<u>% Calculated:</u>	C: 21.61, H: 2.22, N: 13.99 C ₉ H ₁₁ N ₅ (AgClO ₄) _{1.5} , mol. wt: 500.19).
<u>¹H NMR:</u>	(ppm, d ₆ -DMSO): 2.69, 3.07, 5.33, 7.19 (broad), 7.87, 8.15, 9.63, 12.82 (broad).
<u>IR (KBr):</u>	3425, 3275, 2962, 2925, 1639, 1457, 1090, 670, 662, 625, 544 cm ⁻¹ .
<u>Solubility:</u>	Hot DMSO.

Poor solubility of the complex prevented complete ¹H NMR and ¹³C NMR analysis.

2.9.3 [Ag_{1.5}(**31**)](ClO₄)_{1.5}



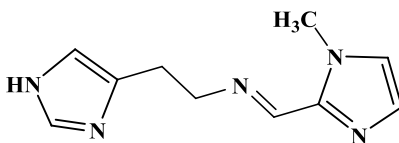
(31)

This cream coloured solid was prepared in a similar manner to [Ag(**22**)₂]ClO₄ using AgClO₄ (0.70 g, 3.38 mmol) and N-[2-(1*H*-imidazol-4-yl)ethyl]-*N*-[(*E*)-(5-methyl-1*H*-imidazol-4-yl)methylidene]amine (**31**) (0.50 g, 1.65 mmol).

<u>Yield:</u>	0.75 g (88 %).
<u>% Found:</u>	C: 22.94, H: 2.56, N: 13.05.
<u>% Calculated:</u>	C: 23.36, H: 2.55, N: 13.62 C ₁₀ H ₁₃ N ₅ (O ₄ AgCl) _{1.5} ; mol. wt: 514.22).
<u>IR (KBr):</u>	3271, 3143, 2921, 1619, 1498, 1464, 1386, 1242, 1093, 980, 821, 624 cm ⁻¹ .
<u>Solubility:</u>	Hot DMSO.

Poor solubility of the complex prevented ¹H NMR and ¹³C NMR analysis.

2.9.4 [Ag_{1.5}(**32**)](ClO₄)_{1.5}·H₂O



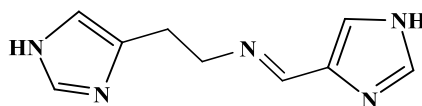
(32)

This cream coloured solid was prepared in a similar manner to [Ag(**22**)₂]ClO₄ using AgClO₄ (0.70 g, 3.38 mmol) and *N*-[2-(1*H*-imidazol-4-yl)ethyl]-*N*-[(*Z*)-(1-methyl-1*H*-imidazol-2-yl)methylidene]amine (**32**) (0.50 g, 1.65 mmol).

<u>Yield:</u>	0.69 g (81 %).
<u>% Found:</u>	C: 22.62, H: 2.48, N: 12.84.
<u>% Calculated:</u>	C: 22.56, H: 2.84, N: 13.15 (C ₁₀ H ₁₅ N ₅ O ₁ (O ₄ AgCl) _{1.5} ; mol. wt: 534.23).
<u>¹H NMR:</u>	(ppm, d ₆ -DMSO): 2.10, 3.85, 5.45, 7.10, 7.51, 7.85.
<u>¹³C NMR:</u>	(ppm, d ₆ -DMSO): 30.6, 73.1, 95.6, 117.4, 118.7, 123.0, 127.2, 137.1, 156.4.
<u>IR (KBr):</u>	3391, 3263, 1623, 1496, 1446, 1323, 1285, 1095, 952, 900, 828, 766, 711, 677, 623 cm ⁻¹ .
<u>Solubility:</u>	Hot DMSO.

Poor solubility of the complex prevented complete ¹H NMR and ¹³C NMR analysis.

2.9.5 [Ag_{1.5}(**33**)](ClO₄)_{1.5}



(**33**)

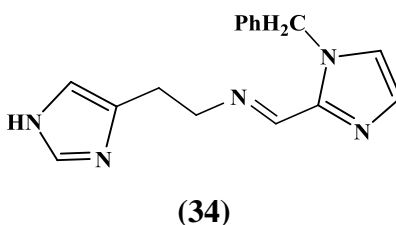
This cream coloured solid was prepared in a similar manner to [Ag(**22**)₂]ClO₄ using AgClO₄ (1.20 g, 5.79 mmol) and *N*-[2-(1*H*-imidazol-4-yl)ethyl]-*N*-[(*Z*)-1*H*-imidazol-5-ylmethylidene]amine (**33**) (0.50 g, 2.64 mmol).

<u>Yield:</u>	1.62 g (62 %).
<u>% Found:</u>	C: 21.30, H: 2.20, N: 13.31.

<u>% Calculated:</u>	C: 22.61, H: 2.22, N: 14.00 C ₉ H ₁₁ N ₅ (O ₄ AgCl) _{1.5} ; mol. wt: 500.24).
<u>IR (KBr):</u>	3533, 3349, 3275, 3145, 2922, 1623, 1497, 1463, 1440, 1385, 1351, 1323, 1247, 1216, 1092, 955, 930, 912, 849, 807, 660, 624 cm ⁻¹ .
<u>Solubility:</u>	Hot DMSO.

Poor solubility of the complex prevented ¹H NMR and ¹³C NMR analysis.

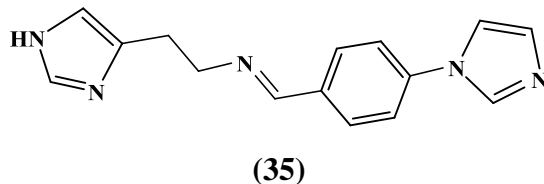
2.9.6 [Ag(34)]ClO₄·H₂O



This tan/purple solid was prepared in a similar manner to [Ag(**22**)₂]ClO₄ using AgClO₄ (1.20 g, 5.79 mmol) in MeOH (5.0 cm³) and *N*-[(*Z*)-(1-benzyl-1*H*-imidazol-2-yl)methylidene]-2-(1*H*-imidazol-4-yl)-1-ethanamine (**34**) (0.50 g, 1.78 mmol).

<u>Yield:</u>	0.64 g (72 %).
<u>% Found:</u>	C: 38.30, H: 3.20, N: 14.31.
<u>% Calculated:</u>	C: 38.08, H: 3.79, N: 13.88 (C ₁₆ H ₁₉ N ₅ O ₅ AgCl; mol. wt: 504.67).
<u>IR (KBr):</u>	3391-3287, 2925, 2886, 1588, 1492, 1446, 1385, 1327, 1261, 1218, 1109, 941, 832, 792, 723, 625 cm ⁻¹ .
<u>Solubility:</u>	Hot DMSO.

Poor solubility of the complex prevented ¹H NMR and ¹³C NMR analysis.

2.9.7 [Ag₂(35)](ClO₄)₂·H₂O

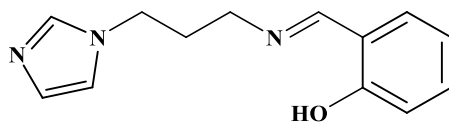
This dark cream/pink solid was prepared in a similar manner to [Ag(**22**)₂]ClO₄ using AgClO₄ (0.80 g, 3.86 mmol) and *N*-[2-(1*H*-imidazol-4-yl)ethyl]-*N*-(*Z*)-[4-(1*H*-imidazol-1-yl)phenyl]methylideneamine (**35**) (0.50 g, 1.88 mmol).

<u>Yield:</u>	0.78 g (43 %).
<u>% Found:</u>	C: 25.37, H: 2.62, N: 11.06.
<u>% Calculated:</u>	C: 25.81, H: 2.45, N: 10.03 (C ₁₅ H ₁₇ N ₅ O ₉ Ag ₂ Cl ₂ ; mol. wt: 697.95).
<u>IR (KBr):</u>	3335-3275, 2926, 1638, 1607, 1525, 1495, 1452, 1403, 1308, 1263, 1092, 932, 834, 742, 624 cm ⁻¹ .
<u>Solubility:</u>	Hot DMSO.

Poor solubility of the complex prevented ¹H NMR and ¹³C NMR analysis.

2.10. Synthesis of Ag(I) Complexes of the Schiff Base Ligands Derived From Apim

2.10.1 [Ag(36)₂]ClO₄·H₂O

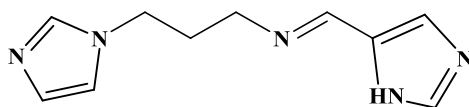


(36)

This pale yellow solid was prepared in a similar manner to [Ag(**22**)₂]ClO₄ using AgClO₄ (0.91 g, 4.40 mmol) and 2-([3-(1*H*-imidazol-1-yl)propyl]iminomethyl)phenol (**36**) (0.50 g, 2.18 mmol).

<u>Yield:</u>	1.05 g (72 %).
<u>% Found:</u>	C: 46.94, H: 3.93, N: 12.55.
<u>% Calculated:</u>	C: 45.80, H: 4.43, N: 12.32 (C ₂₆ H ₃₀ N ₆ O ₇ AgCl; mol. wt: 681.87).
<u>¹H NMR:</u>	(ppm, d ₆ -DMSO): 2.18 (t, 2H), 3.58 (t, 2H), 4.18 (s, 2H), 6.18 (m, 2H), 7.15 (s, 1H), 7.25 (m, 1H), 7.85 (m, 1H), 8.00 (s, 1H), 8.58 (s, 1H).
<u>¹³C NMR:</u>	(ppm, d ₆ -DMSO): 31.3, 54.7, 65.4, 116.4, 118.6, 120.1, 129.0, 131.6, 132.3, 138.9, 160.4, 166.4.
<u>IR (KBr):</u>	3436, 3133, 2968, 1633, 1499, 1460, 1278, 1092, 836, 768, 653, 623 cm ⁻¹ .
<u>Solubility:</u>	MeOH, EtOH, chloroform, benzene, DMSO.

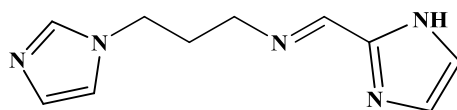


2.10.2 [Ag(37)]ClO₄

(37)

This white solid was prepared in a similar manner to [Ag(**22**)₂]ClO₄ using AgClO₄ (1.04 g, 5.01 mmol) and *N*-[(*E*)-1*H*-imidazol-5-ylmethylidene]-*N*-[3-(1*H*-imidazol-1-yl)propyl]amine (**37**) (0.50 g, 2.46 mmol).

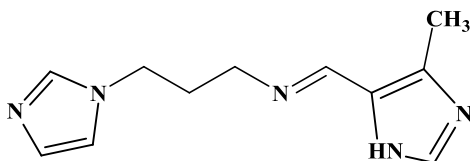
- Yield: 0.68 g (67 %).
- % Found: C: 29.53, H: 3.10, N: 16.89.
- % Calculated: C: 29.35, H: 2.19, N: 17.06 (C₁₀H₁₃N₅O₄AgCl; mol. wt: 410.56).
- ¹H NMR: (ppm, d₆-DMSO): 2.05 (t, 2H), 3.65 (t, 2H), 4.12 (t, 2H), 7.08 (s, 1H), 7.45 (s, 1H), 7.85 (s, 1H), 7.95 (s, 1H), 8.20 (s, 1H), 8.50 (s, 1H).
- ¹³C NMR: (ppm, d₆-DMSO): 32.4, 54.8, 65.5, 118.6, 120.4, 128.9, 129.2, 136.4, 138.6, 155.2.
- IR (KBr): 3262, 3138, 2916, 1646, 1516, 1482, 1441, 1381, 1288, 1233, 1144, 1110, 1089, 948, 818, 779, 663, 625 cm⁻¹.
- Solubility: DMSO.
- Note: ¹HNMR incomplete.

2.10.3 [Ag(38)]ClO₄

(38)

This white solid was prepared in a similar manner to [Ag(22)₂]ClO₄ using AgClO₄ (1.02 g, 4.90 mmol) and *N*-[(*E*)-1*H*-imidazol-2-ylmethylidene]-*N*-[3-(1*H*-imidazol-1-yl)propyl]amine (38) (0.50 g, 2.46 mmol).

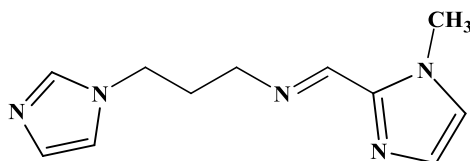
<u>Yield:</u>	0.65 g (64 %).
<u>% Found:</u>	C: 29.63, H: 3.14, N: 17.43.
<u>% Calculated:</u>	C: 29.25, H: 3.19, N: 17.06 (C ₁₀ H ₁₃ N ₅ O ₄ AgCl; mol. wt: 410.56).
<u>¹H NMR:</u>	(ppm, d ₆ -DMSO): 2.10 (t, 2H), 3.75 (t, 2H), 3.95 (s, 2H), 7.10 (s, 2H), 7.32 (s, 1H), 7.45 (s, 1H), 7.65 (s, 1H), 7.82 (s, 1H).
<u>¹³C NMR:</u>	(ppm, d ₆ -DMSO): 31.9, 52.8, 65.9, 120.5, 126.1, 129.3, 138.6, 142.8, 150.2.
<u>IR (KBr):</u>	3260, 3133, 2925, 1645, 1519, 1451, 1238, 1089, 751, 657, 623 cm ⁻¹ .
<u>Solubility:</u>	DMSO.
<u>Note:</u>	¹ HNMR incomplete.

2.10.4 [Ag(39)]ClO₄

(39)

This white solid was prepared in a similar manner to [Ag(22)₂]ClO₄ using AgClO₄ (0.95 g, 4.60 mmol) and 3-(1*H*-imidazol-1-yl)-*N*-[(*Z*)-(5-methyl-1*H*-imidazol-4-yl)methylidene]-1-propanamine (39) (0.50 g, 2.30 mmol).

<u>Yield:</u>	0.65 g (67 %).
<u>% Found:</u>	C: 31.15, H: 3.58, N: 16.50.
<u>% Calculated:</u>	C: 31.12, H: 3.56, N: 16.49 (C ₁₁ H ₁₅ N ₅ O ₄ AgCl; mol. wt: 424.59).
<u>¹H NMR:</u>	(ppm, d ₆ -DMSO): 2.10 (2H), 2.40 (3H), 3.65 (2H), 4.10 (2H), 7.10 (s, 1H), 7.40 (s, 1H), 7.92 (s, 1H), 8.05 (s, 1H), 8.60 (s, 2H).
<u>¹³C NMR:</u>	(ppm, d ₆ -DMSO): 28.6, 32.5, 54.6, 95.5, 120.1, 129.1, 132.2, 137.8, 138.6, 154.6.
<u>IR (KBr):</u>	3254, 3137, 2927, 1643, 1519, 1453, 1368, 1343, 1240, 1121, 1050, 967, 840, 804, 738, 664, 624 cm ⁻¹ .
<u>Solubility:</u>	DMSO.
Note:	¹ HNMR incomplete.

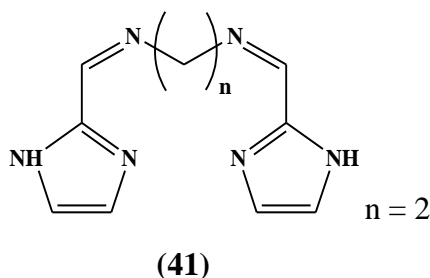
2.10.5 [Ag(**40**)]ClO₄**(40)**

This white solid was prepared in a similar manner to [Ag(**22**)₂]ClO₄, using AgClO₄ (0.95 g, 4.60 mmol) in and 3-(1*H*-imidazol-1-yl)-*N*-[(*Z*)-(1-methyl-1*H*-imidazol-2-yl)methylidene]-1-propanamine (**40**) (0.5 g, 2.30 mmol).

<u>Yield:</u>	0.75 g (73 %).
<u>% Found:</u>	C: 31.45, H: 3.52, N: 16.34.
<u>% Calculated:</u>	C: 31.12, H: 3.56, N: 16.49 (C ₁₁ H ₁₅ N ₅ O ₄ AgCl; mol. wt: 424.59).
<u>¹H NMR:</u>	(ppm, d ₆ -DMSO): 2.12 (t, 2H), 3.82 (t, 2H), 4.00 (s, 3H), 4.15 (t, 2H), 7.15 (s, 1H), 7.39 (s, 1H), 7.50 (s, 1H), 7.70 (s, 1H), 8.00 (s, 1H), 8.76 (s, 1H).
<u>¹³C NMR:</u>	(ppm, d ₆ -DMSO): 31.9, 52.9, 54.8, 56.9, 120.4, 126.1, 129.2, 129.3, 138.6, 142.8, 150.3.
<u>IR (KBr):</u>	3441, 3118, 1635, 1516, 1492, 1439, 1382, 1293, 1248, 1092, 948, 819, 780, 653, 625 cm ⁻¹ .
<u>Solubility:</u>	DMSO.
Note:	¹ HNMR incomplete.

2.11 Synthesis of Ag(I) Complexes of the Schiff Base Ligands Derived from 1,2-Diaminoethane, 1,3-Diaminopropane and 1,4-Diaminobutane

2.11.1 [Ag_{1.5}(41)](ClO₄)_{1.5}

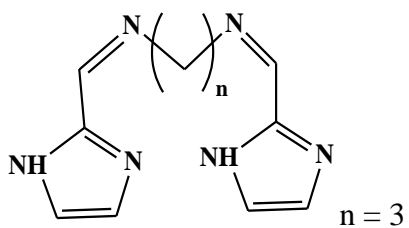


This white solid was prepared in a similar manner to [Ag(**22**)₂]ClO₄ using AgClO₄ (1.44 g, 6.94 mmol) and *N*-[(*E*)-1*H*-imidazol-2-ylmethylidene]-*N*-(2-[(*Z*)-1*H*-imidazol-2-ylmethylidene]aminoethyl)amine (**41**) (0.50 g, 2.31 mmol).

<u>Yield:</u>	0.96 g (79 %).
<u>% Found:</u>	C: 22.59, H: 2.17, N: 15.13.
<u>% Calculated:</u>	C: 22.78, H: 2.30, N: 15.93 (C ₁₀ H ₁₂ N ₆ (O ₄ AgCl) _{1.5} ; mol. wt: 526.05).
<u>¹H NMR:</u>	(ppm, d ₆ -DMSO): 4.01 (s, 4H), 7.10 (s, 2H), 7.52 (s, 2H), 8.29 (s, 2H).
<u>¹³C NMR:</u>	(ppm, d ₆ -DMSO): 59.1, 121.3, 129.6, 152.5.
<u>IR (KBr):</u>	3335, 2928, 1650, 1556, 1447, 1358, 1262, 1092, 9226, 797, 694, 625 cm ⁻¹ .

Note: ¹HNMR incomplete.

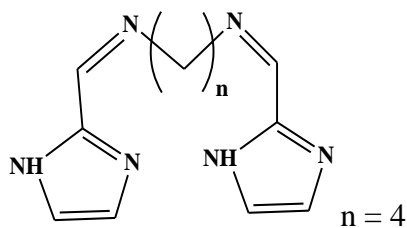
Solubility: Hot DMSO.

2.11.2 $[\text{Ag}_{1.5}(\mathbf{42})](\text{ClO}_4)_{1.5}$ **(42)**

This white solid was prepared in a similar manner to $[\text{Ag}(\mathbf{22})_2]\text{ClO}_4$ using AgClO_4 (1.35 g, 6.51 mmol) and *N*-[(*Z*)-1*H*-imidazol-2-ylmethylidene]-*N*-(3-[(*Z*)-1*H*-imidazol-2-ylmethylidene]aminopropyl)amine (**42**) (0.50 g, 2.17 mmol).

<u>Yield:</u>	0.98 g (86 %).
<u>% Found:</u>	C: 25.01, H: 2.98, N: 16.10.
<u>% Calculated:</u>	C: 24.44, H: 2.61, N: 15.52 ($\text{C}_{11}\text{H}_{14}\text{N}_6(\text{O}_4\text{AgCl})_{1.5}$; mol. wt: 541.08).
<u>IR (KBr):</u>	3473, 2926, 1635, 1439, 1361, 1313, 1091, 948, 787, 622 cm^{-1} .
<u>Solubility:</u>	Hot DMSO.

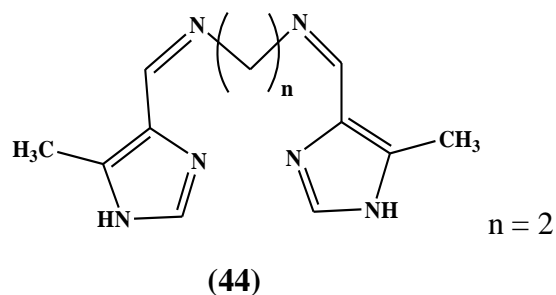
Poor solubility of the complex prevented ^1H NMR and ^{13}C NMR analysis.

2.11.3 [Ag₂(**43**)](ClO₄)₂

This white solid was prepared in a similar manner to [Ag(**22**)₂]ClO₄ using AgClO₄ (1.27 g, 6.12 mmol) and *N*-[(*E*)-1*H*-imidazol-2-ylmethylidene]-*N*-(4-[(*E*)-1*H*-imidazol-2-ylmethylidene]aminobutyl)amine (**43**) (0.5 g, 2.05 mmol).

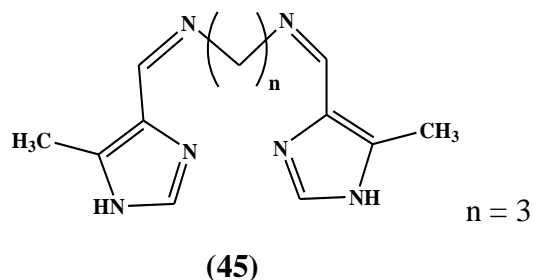
<u>Yield</u> :	1.10 g (82 %).
<u>% Found</u> :	C: 22.13, H: 2.10, N: 12.53.
<u>% Calculated</u> :	C: 21.87, H: 2.45, N: 12.75 (C ₁₂ H ₁₅ N ₆ O ₈ Ag ₂ Cl ₂ ; mol. wt: 658.92).
<u>IR (KBr)</u> :	3513, 2927, 2854, 1639, 1442, 1412, 1362, 1315, 1091, 948, 929, 791, 701, 623 cm ⁻¹ .
<u>Solubility</u> :	Hot DMSO.

Poor solubility of the complex prevented ¹H NMR and ¹³C NMR analysis.

2.11.4 [Ag₂(**44**)](ClO₄)₂

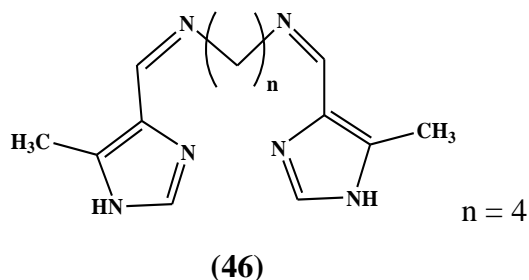
This white solid was prepared in a similar manner to [Ag(**22**)₂]ClO₄ using AgClO₄ (1.27 g, 6.12 mmol) and *N*-[(*E*)-(4-methyl-1*H*-imidazol-5-yl)methylidene]-*N*-(2-[(*Z*)-(4-methyl-1*H*-imidazol-5-yl)methylidene]aminoethyl)amine (**44**) (0.50 g, 2.05 mmol).

<u>Yield:</u>	1.12 g (83 %).
<u>% Found:</u>	C: 21.21, H: 2.68, N: 13.10.
<u>% Calculated:</u>	C: 21.87, H: 2.45, N: 12.75 (C ₁₂ H ₁₆ N ₆ O ₈ Ag ₂ Cl ₂ ; mol. wt: 658.93).
<u>¹H NMR:</u>	(ppm, d ₆ -DMSO): 2.26 (s, 6H), 3.87 (s, 4H), 7.70 (s, 2H), 8.45 (s, 2H).
<u>¹³C NMR:</u>	(ppm, d ₆ -DMSO); 28.46, 60.3, 132.2, 136.6, 155.9.
<u>IR (KBr):</u>	3491, 3276, 3134, 3018, 2920, 1638, 1584, 1513, 1441, 1357, 1248, 1143, 1116, 1106, 961, 839, 701, 627 cm ⁻¹ .
<u>Solubility:</u>	Hot DMSO.
Note:	¹ HNMR incomplete.

2.11.5 [Ag₂(45)](ClO₄)₂

This peach solid was prepared in a similar manner to [Ag(**22**)₂]ClO₄ using AgClO₄ (1.20 g, 5.81 mmol) and *N*-[(*E*)-(5-methyl-1*H*-imidazol-4-yl)methylidene]-*N*-(3-[(*Z*)-(5-methyl-1*H*-imidazol-4-yl)methylidene]aminopropyl)amine (**45**) (0.5 g, 1.94 mmol).

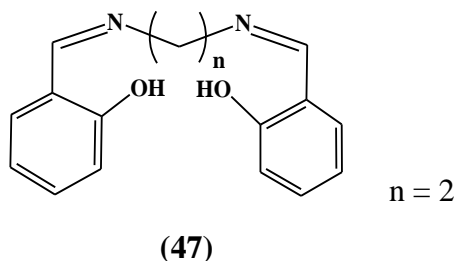
<u>Yield:</u>	1.00 g (77 %).
<u>% Found:</u>	C: 23.32, H: 2.54, N: 12.12.
<u>% Calculated:</u>	C: 23.20, H: 2.70, N: 12.49 (C ₁₃ H ₁₈ N ₆ O ₈ Ag ₂ Cl ₂ ; mol. wt: 672.96).
<u>¹H NMR:</u>	(ppm, d ₆ -DMSO): 2.00 (s, 2H), 2.33 (s, 6H), 3.55 (s, 4H), 7.88 (s, 4H), 8.45 (s, 2H).
<u>¹³C NMR:</u>	(ppm, d ₆ -DMSO): 28.6, 33.25, 58.0, 131.9, 132.4, 137.4, 154.8.
<u>IR (KBr):</u>	3525, 3249-3136, 2920, 2019, 1643, 1577, 1513, 1439, 1389, 1367, 1249, 1091, 978, 829, 758, 698, 625 cm ⁻¹ .
<u>Solubility:</u>	Hot DMSO.

2.11.6 [Ag₂(**46**)](ClO₄)₂

This peach coloured solid was prepared in a similar manner to [Ag(**22**)₂]ClO₄ using AgClO₄ (1.14 g, 5.51 mmol) and *N*-[(*E*)-(5-methyl-1*H*-imidazol-4-yl)methylidene]-*N*-(4-[(*Z*)-(5-methyl-1*H*-imidazol-4-yl)methylidene]aminobutyl)amine (**46**) (0.50 g, 1.83 mmol).

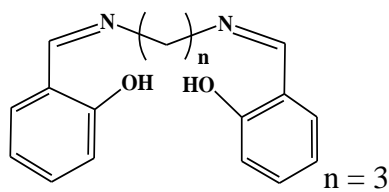
<u>Yield:</u>	1.10 g (88 %).
<u>% Found:</u>	C: 24.07, H: 2.72, N: 11.83.
<u>% Calculated:</u>	C: 24.48, H: 2.93, N: 12.23 (C ₁₄ H ₂₀ N ₆ O ₈ Ag ₂ Cl ₂ ; mol. wt: 686.99).
<u>¹H NMR:</u>	(ppm, d ₆ -DMSO): 2.25 (t, 4H), 2.33 (t, 6H), 3.75 (t, 4H), 7.70 (s, 2H), 8.45 (s, 2H), 12.75 (s, 1H).
<u>IR (KBr):</u>	3535, 3239-3136, 2926, 2854, 20.19, 1626, 1513, 1479, 1441, 1382, 1351, 1313, 1289, 1199, 1101, 975, 822, 743, 657, 624 cm ⁻¹ .
<u>Solubility:</u>	Hot DMSO.

Poor solubility of the complex prevented ¹H NMR and ¹³C NMR analysis.

2.11.7 [Ag(**47**)]ClO₄

This dark-green solid was prepared in a similar manner to [Ag(**22**)₂]ClO₄ using AgClO₄ (1.16 g, 5.60 mmol) and 2-[[[(Z)-(2-hydroxyphenyl)methylidene]aminomethyl]imino]methylphenol (**47**) (0.50 g, 1.86 mmol).

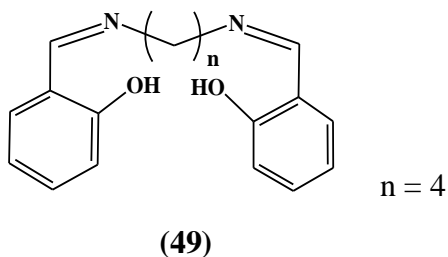
<u>Yield:</u>	0.65 g (73 %).
<u>% Found:</u>	C: 39.59, H: 3.48, N: 5.55.
<u>% Calculated:</u>	C: 40.40, H: 3.39, N: 5.89 (C ₁₆ H ₁₆ N ₂ O ₆ AgCl; mol. wt: 475.63).
<u>¹H NMR:</u>	(ppm, d ₆ -DMSO): 3.95 (s, 4H), 6.93 (m, 4H), 7.33 (t, 2H), 7.45 (d, 2H), 8.61 (s, 2H).
<u>¹³C NMR:</u>	(ppm, d ₆ -DMSO): 58.6, 78.8, 116.4, 118.6, 131.5, 132.4, 160.5, 166.8.
<u>IR (KBr):</u>	3501, 3062, 2930, 1646, 1608, 1532, 1479, 1399, 1353, 1326, 1283, 1203, 1153, 1092, 1022, 1002, 801, 864, 770, 756, 732, 622 cm ⁻¹ .
<u>Solubility:</u>	MeOH, EtOH, chloroform, benzene, DMSO.

2.11.8 [Ag(48)]ClO₄

(48)

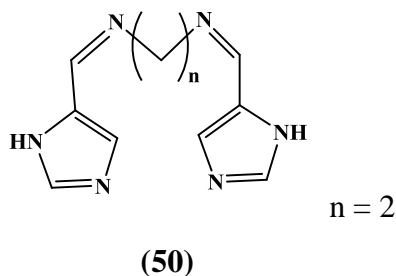
This dark-green/brown solid was prepared in a similar manner to [Ag(22)₂]ClO₄ using AgClO₄ (1.10 g, 5.31 mmol) and 2-[(3-[(*E*)-(2-Hydroxyphenyl)methylidene]aminopropyl)imino]methylphenol (**48**)^{105,110} (0.50 g, 1.77mmol).

<u>Yield:</u>	0.73 g (84 %).
<u>% Found:</u>	C: 42.33, H: 3.92, N: 5.35.
<u>% Calculated:</u>	C: 41.68, H: 3.71, N: 5.72 (C ₁₇ H ₁₈ N ₂ O ₆ AgCl; mol. wt: 489.44).
<u>¹H NMR:</u>	(ppm, d ₆ -DMSO): 1.75 (t, 2H), 3.65 (t, 4H), 6.90 (m, 4H), 7.33 (t, 2H), 7.40 (d, 2H), 8.60 (s, 2H).
<u>¹³C NMR:</u>	(ppm, d ₆ -DMSO): 31.5, 46.8, 115.7, 116.4, 118.6, 131.6, 160.6, 166.9.
<u>IR (KBr):</u>	3365, 2934, 2874, 1638, 1607, 1499, 1463, 1350, 1312, 1263, 1222, 1159, 1115, 1088, 1058, 1041, 980, 865, 820, 769, 762, 629, 618 cm ⁻¹ .
<u>Solubility:</u>	MeOH, EtOH, chloroform, benzene, DMSO.

2.11.9 [Ag₂(**49**)](ClO₄)₂

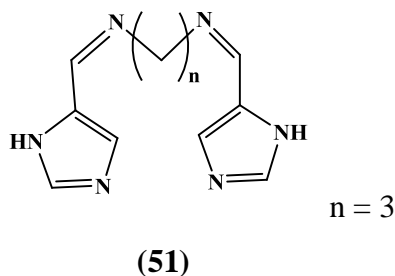
This dark-green solid was prepared in a similar manner to [Ag(**22**)₂]ClO₄ using AgClO₄ (1.05 g, 5.06 mmol) and 2-[(4-[(Z)-(2-hydroxyphenyl)methylidene]aminobutyl)imino]methylphenol (**49**) (0.50 g, 1.69 mmol).

<u>Yield:</u>	0.87 g (73 %).
<u>% Found:</u>	C: 30.01, H: 3.51, N: 4.10.
<u>% Calculated:</u>	C: 30.48, H: 2.56, N: 3.95 (C ₁₈ H ₁₈ N ₂ O ₁₀ Ag ₂ Cl ₂ ; mol. wt: 708.74).
<u>¹H NMR:</u>	(ppm, d ₆ -DMSO): 1.75 (s, 4H), 3.65 (s, 4H), 6.90 (m, 4H), 7.33 (t, 2H), 7.40 (d, 2H), 8.60 (s, 2H).
<u>¹³C NMR:</u>	(ppm, d ₆ -DMSO): 26.9, 56.7, 115.4, 117.4, 130.4, 131.1, 159.7, 164.7.
<u>IR (KBr):</u>	3316, 3115-3057, 1621, 1591, 1506, 1432, 1318, 1230, 1185, 1130, 747, 732 cm ⁻¹ .
<u>Solubility:</u>	MeOH, EtOH, chloroform, benzene, DMSO.

2.11.10 [Ag(**50**)]ClO₄

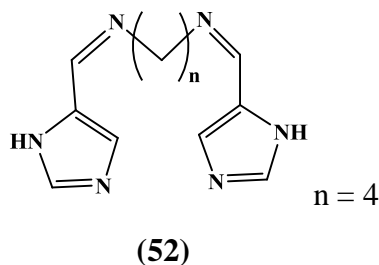
This cream solid was prepared in a similar manner to [Ag(**22**)₂]ClO₄ using AgClO₄ (1.44 g, 6.94 mmol) and *N*-[(*E*)-1*H*-imidazol-4-ylmethylidene]-*N*-(2-[(*Z*)-1*H*-imidazol-4-ylmethylidene]aminoethyl)amine (**50**) (0.50 g, 2.31 mmol).

<u>Yield:</u>	0.87 g (89 %).
<u>% Found:</u>	C: 28.24, H: 3.55, N: 19.36.
<u>% Calculated:</u>	C: 28.36, H: 2.86, N: 19.84 (C ₁₀ H ₁₂ N ₆ O ₄ AgCl, mol. wt: 423.56).
<u>¹H NMR:</u>	(ppm, d ₆ -DMSO): 3.95 (s, 4H), 7.60 (s, 2H), 7.80 (s, 2H), 8.43 (s, 2H).
<u>¹³C NMR:</u>	(ppm, d ₆ -DMSO): 60.1, 122.3, 136.3, 138.0, 157.1.
<u>IR (KBr):</u>	3360, 3144, 2923, 2859, 1644, 1507, 1437, 1345, 1303, 1261, 1230, 1092, 992, 975, 923, 863, 811, 749, 625 cm ⁻¹ .
<u>Solubility:</u>	DMSO.
<u>Note:</u>	¹ HNMR incomplete.

2.11.11 [Ag₂(**51**)](ClO₄)₂

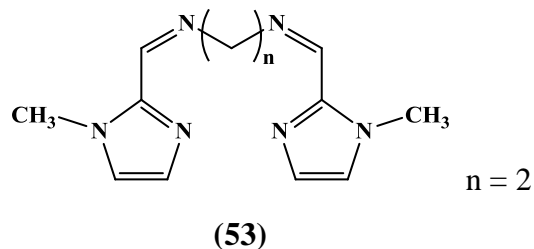
This cream solid was prepared in a similar manner to [Ag(**22**)₂]ClO₄ using AgClO₄ (1.35 g, 6.51 mmol) and *N1-[(E)-1H-imidazol-5-ylmethylidene]-N3-[(Z)-1H-imidazol-5-ylmethylidene]-1,3-propanediamine (51)* (0.50 g, 2.17 mmol).

- Yield:** 1.23 g (88 %).
- % Found:** C: 20.56, H: 2.37, N: 12.56.
- % Calculated:** C: 20.49, H: 2.19, N: 13.03 (C₁₁H₁₄N₆O₈Ag₂Cl₂; mol. wt: 644.91).
- ¹H NMR:** (ppm, d₆-DMSO): 1.95 (t, 2H), 3.74 (t, 4H), 7.75 (s, 2H), 8.05 (s, 2H), 8.40 (s, 2H).
- ¹³C NMR:** (ppm, d₆-DMSO): 33.2, 58.2, 136.38, 155.
- IR (KBr):** 3506, 3351, 3138, 2925, 2851, 2017, 1647, 1506, 1435, 1347, 1300, 1257, 1220, 1142, 1114, 1090, 940, 851, 800, 637, 626 cm⁻¹.
- Solubility:** DMSO.
- Note:** ¹HNMR incomplete.

2.11.12 [Ag₂(**52**)](ClO₄)₂

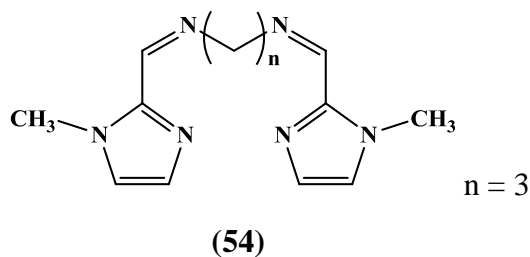
This cream solid was prepared in a similar manner to [Ag(**22**)₂]ClO₄ using AgClO₄ (1.35 g, 6.13 mmol) and *N*-[(*E*)-1*H*-imidazol-5-ylmethylidene]-5-[(1*H*-imidazol-5-ylmethyl)imino]-1-pentanamine (**52**) (0.50 g, 2.05 mmol).

<u>Yield:</u>	1.22 g (91 %).
<u>% Found:</u>	C: 21.97, H: 2.55, N: 13.55.
<u>% Calculated:</u>	C: 21.87, H: 2.45, N: 12.75 (C ₁₂ H ₁₆ N ₆ O ₈ Ag ₂ Cl ₂ ; mol. wt: 656.73).
<u>¹H NMR:</u>	(ppm, d ₆ -DMSO): 1.63. (4H), 3.50 (4H), 7.70 (s, 2H), 8.05, (s, 2H), 8.29 (s, 2H).
<u>¹³C NMR:</u>	(ppm, d ₆ -DMSO): 27.9, 58.6, 121.9, 136.4, 138.3, 155.1.
<u>IR (KBr):</u>	3333, 3143, 2927, 2855, 2016, 1647, 1551, 1506, 1434, 1385, 1343, 1301, 1220, 1114, 1142, 1090, 931, 858, 802, 725, 635, 626 cm ⁻¹ .
<u>Solubility:</u>	DMSO.
<u>Note:</u>	¹ HNMR incomplete.

2.11.13 [Ag_{1.5}(**53**)](ClO₄)_{1.5}

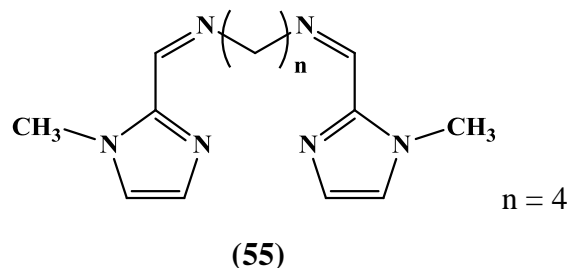
This complex was prepared using a modification of the literature method used by Yang *et al.*¹¹⁵ The white solid was prepared in a similar manner to [Ag(**22**)₂]ClO₄ using AgClO₄ (1.27 g, 6.14 mmol) and *N*-[(*E*)-(1-methyl-1*H*-imidazol-2-yl)methylidene]-*N*-(2-[(*Z*)-(1-methyl-1*H*-imidazol-2-yl)methylidene]aminoethyl)amine (**53**) (0.50 g, 2.05 mmol).

<u>Yield:</u>	1.05 g (93 %).
<u>% Found:</u>	C: 25.81, H: 2.71, N: 15.05.
<u>% Calculated:</u>	C: 25.95, H: 2.91, N: 15.13 (C ₁₂ H ₁₆ N ₆ O ₂ Ag _{1.5} Cl _{1.5} , mol. wt: 555.18).
<u>¹H NMR:</u>	(ppm, d ₆ -DMSO): 2.45 (t, 6H), 3.89 (s, 2H), 3.92 (s, 2H), 7.00 (s, 2H), 7.75 (s, 2H), 8.25 (s, 2H).
<u>¹³C NMR:</u>	(ppm, d ₆ -DMSO): 32.5, 79.8, 86.1, 128.8, 142.2, 151.9.
<u>IR (KBr):</u>	3446, 3128, 2923, 2023, 16501533, 1489, 1445, 365, 1288, 1143, 1109, 1089, 995, 920, 867, 839, 780, 703, 662, 625 cm ⁻¹ .
<u>Solubility:</u>	MeOH, EtOH, chloroform, benzene, DMSO.

2.11.14 [Ag_{1.5}(**54**)(ClO₄)_{1.5}]

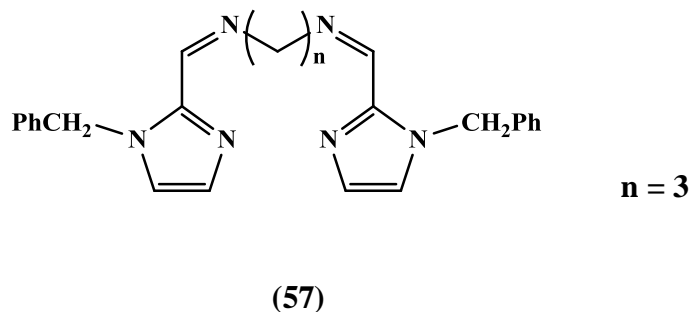
This complex was prepared using a modification of the literature method used by Yang *et al.*¹¹⁵ The white solid was prepared in a similar manner to [Ag(**22**)₂]ClO₄ using AgClO₄ (1.20 g, 5.81 mmol) and *N*-[(*E*)-(1-methyl-1*H*-imidazol-2-yl)methylidene]-*N*-(3-[(*Z*)-(1-methyl-1*H*-imidazol-2-yl)methylidene]aminopropyl)amine (**54**) (0.50 g, 1.93 mmol).

<u>Yield:</u>	0.98 g (89 %).
<u>% Found:</u>	C: 28.10, H: 2.83, N: 15.71.
<u>% Calculated:</u>	C: 27.43, H: 3.19, N: 14.76 (C ₁₃ H ₁₈ N ₆ O ₆ Ag _{1.5} Cl _{1.5} , mol. wt: 569.11).
<u>¹H NMR:</u>	(ppm, d ₆ -DMSO): 2.00 (2H), 3.80 (4H), 3.92 (6H), 7.25 (s, 2H), 7.57 (s, 2H), 8.58 (s, 2H).
<u>¹³C NMR:</u>	(ppm, d ₆ -DMSO): 32.3, 32.6, 59.5, 65.7, 129.2, 142.8, 149.2.
<u>IR (KBr):</u>	3446, 3128, 2924, 2855, 2023, 1645, 1533, 1489, 1445, 1371, 1288, 1262, 1229, 1143, 1109, 1089, 1052, 995, 959, 941, 918, 967, 838, 780, 703, 662, 636, 625 cm ⁻¹ .
<u>Solubility:</u>	MeOH, EtOH, chloroform, benzene, DMSO.

2.11.15 [Ag₂(**55**)](ClO₄)₂

This white solid was prepared in a similar manner to [Ag(**22**)₂]ClO₄ using AgClO₄ (1.14 g, 5.51 mmol) and 4-[(*E*)-2-(1-methyl-1*H*-imidazol-2-yl)diazenyl]-*N*-[(*E*)-(1-methyl-1*H*-imidazol-2-yl)methylidene]-1-butanamine (**55**) (0.50 g, 1.83 mol).

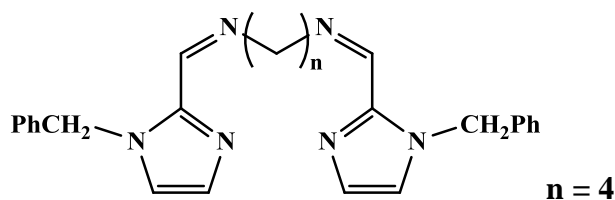
<u>Yield:</u>	0.90 g (72 %).
<u>% Found:</u>	C: 24.05, H: 2.83, N: 11.64.
<u>% Calculated:</u>	C: 24.48, H: 2.93, N: 12.23 (C ₁₄ H ₂₀ N ₆ O ₈ Ag ₂ Cl ₂ ; mol. wt: 686.99).
<u>¹H NMR:</u>	(ppm, d ₆ -DMSO): 1.72 (4H), 3.74 (4H), 3.88 (6H), 7.20 (2H), 7.58 (2H), 8.65 (2H).
<u>¹³C NMR:</u>	(ppm, d ₆ -DMSO): 26.8, 52.6, 58.0, 125.9, 129.2, 142.7, 150.2.
<u>IR (KBr):</u>	3472, 3132, 2940, 2858, 2023, 1641, 1533, 1489, 1444, 1425, 1368, 1288, 1142, 1114, 1089, 999, 965, 941, 931, 847, 777, 702, 670, 636, 625 cm ⁻¹ .
<u>Solubility:</u>	MeOH, EtOH, chloroform, benzene, DMSO.

2.11.17 [Ag₂(**57**)](ClO₄)₂

This cream solid was prepared in a similar manner to [Ag(**22**)₂]ClO₄ using AgClO₄ (0.76 g, 3.65 mmol) and *N*-[(*E*)-(1-benzyl-1*H*-imidazol-2-yl)methylidene]-*N*-(3-[(*E*)-(1-benzyl-1*H*-imidazol-2-yl)methylidene]aminopropyl)amine (**57**) (0.50 g, 1.23mmol).

<u>Yield:</u>	0.68 g (67 %).
<u>% Found:</u>	C: 37.73, H: 3.55, N: 10.98.
<u>% Calculated:</u>	C: 36.30, H: 3.41, N: 10.16 (C ₂₅ H ₂₈ N ₆ O ₈ Ag ₂ Cl ₂ ; mol. wt: 827.17).
<u>¹H NMR:</u>	(ppm, d ₆ -DMSO): 1.55 (4H), 2.08 (2H), 3.60 (2H), 5.55 (42H), 7.30 (m, 102H), 7.72 (2H), 8.72 (2H).
<u>¹³C NMR:</u>	(ppm, d ₆ -DMSO): 26.9, 30.7, 48.7, 68.2, 125.2, 127.3, 127.5, 128.1, 128.9, 129.8, 136.6, 142.3, 150.1.
<u>IR (KBr):</u>	3316, 3115-3057, 1621, 1591, 1506, 1432, 1318, 1230, 1185, 1130, 747, 732 cm ⁻¹ .
<u>Solubility:</u>	DMSO.

Poor solubility of the complex prevented complete ¹H NMR and ¹³C NMR analysis.

2.11.18 [Ag₂(**58**)](ClO₄)₂**(58)**

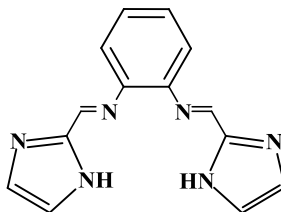
This tan solid was prepared in a similar manner to [Ag(**22**)₂]ClO₄ using AgClO₄ (0.73 g, 3.53 mmol) and *N*-[(*E*)-(1-benzyl-1*H*-imidazol-2-yl)methylidene]-*N*-(4-[(*E*)-(1-benzyl-1*H*-imidazol-2-yl)methylidene]aminobutyl)amine (**58**) (0.50 g, 1.18 mmol).

<u>Yield:</u>	0.56 g (56 %).
<u>% Found:</u>	C: 37.01, H: 3.40, N: 9.84.
<u>% Calculated:</u>	C: 37.21, H: 3.36, N: 10.01 (C ₂₆ H ₂₈ N ₆ O ₈ Ag ₂ Cl ₂ ; mol. wt: 839.18).
<u>¹H NMR:</u>	(ppm, d ₆ -DMSO): 2.10 (4H), 3.85 (2H), 5.55 (4H), 7.25 (m, 14H), 7.68 (2H), 8.65 (2H).
<u>¹³C NMR:</u>	(ppm, d ₆ -DMSO): 30.6, 62.0, 76.6, 118.7, 124.9, 127.2, 127.5, 127.6, 128.1, 128.9, 129.8, 136.2, 136.6, 142.4, 148.9.
<u>IR (KBr):</u>	3394, 3109, 3031, 2937, 2850, 1651, 1606, 1586, 1497, 1471, 1455, 1439, 1385, 1360, 1273, 1208, 1157, 1112, 1079, 1031, 969, 928, 878, 758, 740, 718, 658, 624 cm ⁻¹ .
<u>Solubility:</u>	DMSO.

Poor solubility of the complex prevented complete ¹H NMR and ¹³C NMR analysis.

2.12 Synthesis of Ag(I) Complexes of the Schiff Base Ligands Derived from 1,2-Phenylenediamine, 1,3-Phenylenediamine and 1,4-Phenylenediamine

2.12.1 [Ag_{1.5}(**59**)](ClO₄)_{1.5}

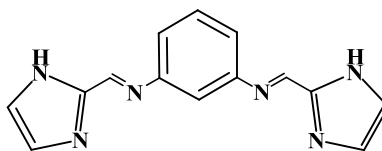


(**59**)

This yellow/green solid was prepared in a similar manner to [Ag(**22**)₂]ClO₄ using AgClO₄ (1.17 g, 5.67 mmol) and *N*-[(*E*)-1*H*-imidazol-2-ylmethylidene]-*N*-(2-[(*E*)-1*H*-imidazol-2-ylmethylidene]aminophenyl)amine (**59**) (0.50 g, 1.89 mmol).

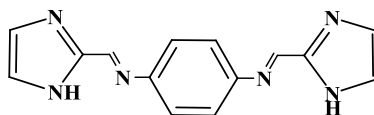
<u>Yield</u> :	0.88 g (81 %).
<u>% Found</u> :	C: 30.07, H: 1.94, N: 13.95.
<u>% Calculated</u> :	C: 29.26, H: 2.02, N: 14.62 (C ₁₄ H ₁₂ N ₆ O ₆ Ag _{1.5} Cl _{1.5} , mol. wt: 574.56).
<u>IR (KBr)</u> :	3052, 2961, 2880, 2773, 1628, 1523, 1458, 1413, 1394, 1349, 1320, 1272, 1229, 1202, 1146, 1083, 945, 747, 731, 626 cm ⁻¹ .
<u>Solubility</u> :	Hot DMSO.

Poor solubility of the complex prevented ¹H NMR and ¹³C NMR analysis.

2.12.2 [Ag(**60**)]ClO₄·2H₂O**(60)**

This yellow solid was prepared in a similar manner to [Ag(**22**)₂]ClO₄ using AgClO₄ (1.17 g, 5.67 mmol) and *N*1-[(*E*)-1*H*-imidazol-2-ylmethylidene]-*N*3-[(*Z*)-1*H*-imidazol-2-ylmethylidene]-1,3-benzenediamine (**60**) (0.50 g, 1.89 mmol).

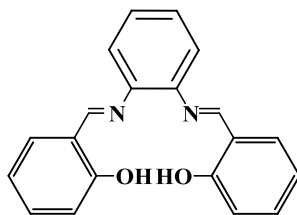
<u>Yield:</u>	0.68 g (71 %).
<u>% Found:</u>	C: 33.32, H: 2.79, N: 16.01.
<u>% Calculated:</u>	C: 33.12, H: 3.18, N: 16.56 (C ₁₄ H ₁₆ N ₆ O ₆ AgCl; mol. wt: 507.63).
<u>¹H NMR:</u>	(ppm, d ₆ -DMSO): 7.51 (s, 4H), 7.10 (m, 4H), 7.50 (m, 4H), 8.50 (s, 2H), 13.20 (s, 2H).
<u>¹³C NMR:</u>	(ppm, d ₆ -DMSO): 106.1, 108.6, 112.6, 112.9, 119.5, 129.6, 130.1, 144.7, 148.3, 149.6, 150.1, 181.2.
<u>IR (KBr):</u>	3261, 2923, 1618, 1557, 1493, 1442, 1387, 1207, 1179, 1114, 1089, 1009, 955, 866, 830, 755, 703, 627 cm ⁻¹ .
<u>Solubility:</u>	Hot DMSO.

2.12.3 [Ag(61)]ClO₄

(61)

This yellow/green solid was prepared in a similar manner to [Ag(22)₂]ClO₄ using AgClO₄ (1.17 g, 5.67 mmol) in MeOH (5.0 cm³) and *N*-[(*E*)-1*H*-imidazol-2-ylmethylidene]-*N*-(4-[(*E*)-1*H*-imidazol-2-ylmethylidene]aminophenyl)amine (61) (0.50 g, 1.89 mmol).

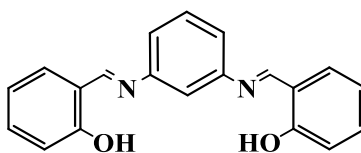
<u>Yield:</u>	0.75 g (84 %).
<u>% Found:</u>	C: 35.13, H: 2.51, N: 17.37.
<u>% Calculated:</u>	C: 35.65, H: 2.56, N: 17.82 (C ₁₄ H ₁₂ N ₆ O ₄ AgCl; mol. wt: 471.61).
<u>¹H NMR:</u>	(ppm, d ₆ -DMSO): 7.15 (s, 4H), 7.55 (s, 4H), 8.45 (s, 2H), 13.00 (s, 2H).
<u>¹³C NMR:</u>	(ppm, d ₆ -DMSO): 122.1, 144.5, 145.9, 147.8, 148.1.
<u>IR (KBr):</u>	3459, 2919, 1625, 1578, 1441, 1387, 1146, 1111, 1089, 1000, 950, 862, 756, 777, 689, 627 cm ⁻¹ .
<u>Solubility:</u>	Hot DMSO.

2.12.4 [Ag_{1.5}(**62**)](ClO₄)_{1.5}**(62)**

This tan solid was prepared in a similar manner to [Ag(**22**)₂]ClO₄ using AgClO₄ (1.00 g, 4.82 mmol) and 2-[(2-[(*E*)-(2-hydroxyphenyl)methylidene]aminophenyl)imino]methyl phenol (**62**) (0.50 g, 1.58 mmol).

<u>Yield:</u>	0.68 g (70 %).
<u>% Found:</u>	C: 38.87, H: 2.35, N: 4.36.
<u>% Calculated:</u>	C: 38.30, H: 2.57, N: 4.46 (C ₂₀ H ₁₆ N ₂ O ₈ Ag _{1.5} Cl _{1.5} , mol. wt: 627.25).
<u>IR (KBr):</u>	3332, 1611, 1571, 1492, 1371, 1282, 1188, 1148, 1109, 906, 860, 832, 759, 750, 620 cm ⁻¹ .
<u>Solubility:</u>	Hot DMSO.

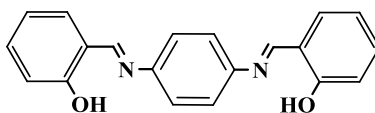
Poor solubility of the complex prevented ¹H NMR and ¹³C NMR analysis.

2.12.5 [Ag(**63**)]ClO₄**(63)**

This green/brown solid was prepared in a similar manner to [Ag(**22**)₂]ClO₄ using AgClO₄ (1.00 g, 4.82 mmol) and 2-[(3-[(*E*)-(2-hydroxyphenyl)methylidene]aminophenyl)imino]methylphenol (**63**) (0.50 g, 1.58 mmol).

<u>Yield:</u>	0.56 g (68 %).
<u>% Found:</u>	C: 36.71, H: 2.56, N: 4.15.
<u>% Calculated:</u>	C: 36.01, H: 2.71, N: 4.20 (C ₂₀ H ₁₆ N ₂ O ₆ Ag ₂ Cl ₂ ; mol. wt: 666.99).
<u>¹H NMR:</u>	(ppm, d ₆ -DMSO): 7.00 (m, 4H), 7.35-7.61 (m, 6H), 7.65 (m, 2H), 9.10 (s, 2H).
<u>¹³C NMR:</u>	(ppm, d ₆ -DMSO): 113.8, 116.5, 117.2, 119.2, 120.1, 129.7, 132.9, 133.4, 149.7, 160.3.
<u>IR (KBr):</u>	3450, 3064, 1950, 1687, 1621, 1591, 1572, 1496, 1475, 1413, 1358, 1276, 1197, 1136, 1116, 1032, 983, 955, 891, 816, 760, 697, 671, 626 cm ⁻¹ .
<u>Solubility:</u>	Hot DMSO.

2.12.6 [Ag(**64**)]ClO₄·2H₂O



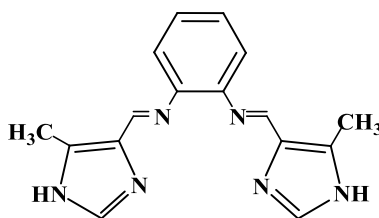
(**64**)

This yellow/brown solid was prepared in a similar manner to [Ag(**22**)₂]ClO₄ using AgClO₄ (1.00 g, 4.82 mmol) and 2-[(4-[(*E*)-(2-hydroxyphenyl)methylidene]aminophenyl)imino]methylphenol (**64**) (0.50 g, 1.58 mmol).

<u>Yield:</u>	0.67 g (76 %).
<u>% Found:</u>	C: 43.31, H: 3.63, N: 5.56.
<u>% Calculated:</u>	C: 42.92, H: 3.60, N: 5.01 (C ₂₀ H ₂₀ N ₂ O ₈ AgCl; mol. wt: 559.70).
<u>IR (KBr):</u>	3438, 1612, 1572, 1492, 1283, 1189, 1121, 833, 620 cm ⁻¹ .
<u>Solubility:</u>	Hot DMSO.

Poor solubility of the complex prevented ¹H NMR and ¹³C NMR analysis.

2.12.7 [Ag_{1.5}(**65**)](ClO₄)_{1.5}



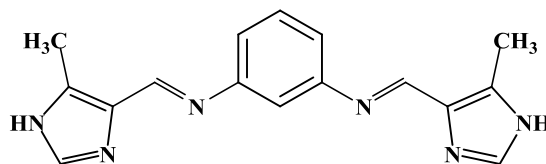
(**65**)

This dark-green solid was prepared in a similar manner to [Ag(**22**)₂]ClO₄ using AgClO₄ (1.06 g, 5.13 mmol) and *N*-[(*Z*)-(4-methyl-1*H*-imidazol-5-yl)methylidene]-*N*-(2-[(*Z*)-(4-methyl-1*H*-pyrazol-5-yl)methylidene]aminophenyl)amine (**65**) (0.50 g, 1.71 mmol).

<u>Yield:</u>	0.93 g (90 %).
<u>% Found:</u>	C: 31.75, H: 2.66, N: 13.39.
<u>% Calculated:</u>	C: 32.14, H: 2.67, N: 13.92 (C ₁₆ H ₁₆ N ₆ O ₆ Ag _{1.5} Cl _{1.5} , mol. wt: 603.24).
<u>¹H NMR:</u>	(ppm, d ₆ -DMSO): 2.30 (s, 6H), 7.08 (s, 4H), 8.15 (s, 2H), 8.75 (s, 2H), 13.00 (s, 2H).

<u>^{13}C NMR:</u>	(ppm, d_6 -DMSO): 28.84, 122.3, 133.2, 134.9, 138.4, 146.8, 150.8.
<u>IR (KBr):</u>	3349, 3139, 1619, 1577, 1492, 1440, 1481, 1343, 1248, 1210, 1108, 964, 881, 832, 771, 626 cm^{-1} .
<u>Solubility:</u>	Hot DMSO.

2.12.8 $[\text{Ag}_{1.5}(\mathbf{66})](\text{ClO}_4)_{1.5}$



(66)

This brown solid was prepared in a similar manner to $[\text{Ag}(\mathbf{22})_2]\text{ClO}_4$ using AgClO_4 (1.06 g, 5.13 mmol) and *N*-[(*E*)-(4-methyl-1*H*-imidazol-5-yl)methylidene]-*N*-(3-[(*E*)-(5-methyl-1*H*-imidazol-4-yl)methylidene]amino-2,4-cyclohexadien-1-yl)amine (**66**) (0.50 g, 1.71 mmol).

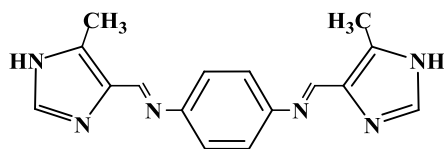
<u>Yield:</u>	0.89 g (86 %).
<u>% Found:</u>	C: 31.84, H: 2.68, N: 13.43.
<u>% Calculated:</u>	C: 32.14, H: 2.67, N: 13.92 ($\text{C}_{16}\text{H}_{16}\text{N}_6\text{O}_6\text{Ag}_{1.5}\text{Cl}_{1.5}$, mol. wt: 603.24).
<u>^1H NMR:</u>	(ppm, d_6 -DMSO): 2.45 (s), 7.10 (s), 7.10 (m), 7.25 (m), 8.15 (s), 8.70 (s).
<u>^{13}C NMR:</u>	(ppm, d_6 -DMSO): 28.9, 129.7, 132.9, 135.0, 138.3, 150.5, 152.4.

IR (KBr): 3524, 3262, 3130, 1625, 1576, 1516, 1475, 1435, 1396, 1370, 1342, 1311, 1253, 1091, 972, 949, 845, 789, 705, 691, 625 cm^{-1} .

Solubility: Hot DMSO.

Poor solubility of the complex prevented complete ^1H NMR and ^{13}C NMR analysis.

2.12.9 $[\text{Ag}_{1.5}(\mathbf{67})](\text{ClO}_4)_{1.5}$



(67)

This cream coloured solid was prepared in a similar manner to $[\text{Ag}(\mathbf{22})_2]\text{ClO}_4$ using AgClO_4 (1.06 g, 5.13 mmol) and *N*-[(*E*)-(5-methyl-1*H*-imidazol-4-yl)methylidene]-*N*-(4-[(*E*)-(5-methyl-1*H*-imidazol-4-yl)methylidene]aminophenyl)amine (**67**) (0.50 g, 1.71 mmol).

Yield: 0.75 g (73 %).

% Found: C: 31.25, H: 2.79, N: 13.49.

% Calculated: C: 32.14, H: 2.67, N: 13.92 ($\text{C}_{16}\text{H}_{16}\text{N}_6\text{O}_6\text{Ag}_{1.5}\text{Cl}_{1.5}$, mol. wt: 603.24).

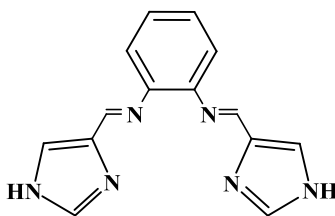
^1H NMR: (ppm, d_6 -DMSO): 2.28 (s, 6H), 5.20 (s, 2H), 7.15 (m, 2H), 7.60 (s, 2H), 8.04 (s, 2H).

^{13}C NMR: (ppm, d_6 -DMSO): 29.2, 70.3, 110.7, 118.6, 122.7, 129.6, 133.6, 135.9, 136.9, 141.1, 148.5.

IR (KBr): 3536, 3287, 3142, 1622, 1534, 1459, 1424, 1340, 1294, 1246, 1091, 978, 748, 623 cm⁻¹.

Solubility: Hot DMSO.

2.12.10 [Ag_{1.5}(**68**)](ClO₄)_{1.5}·3H₂O



(**68**)

This white solid was prepared in a similar manner to [Ag(**22**)₂]ClO₄ using AgClO₄ (1.06 g, 5.11 mmol) and *N*-[(*E*)-1*H*-imidazol-5-ylmethylidene]-*N*-(2-[(*E*)-1*H*-imidazol-5-ylmethylidene]aminophenyl)amine (**68**) (0.50 g, 1.17 mmol).

Yield: 0.86 g (84 %).

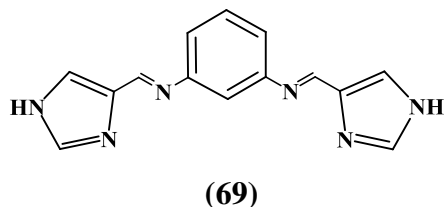
% Found: C: 27.75, H: 2.33, N: 13.94.

% Calculated: C: 26.97, H: 2.88, N: 13.97 (C₁₄H₁₈N₆O₉Ag_{1.5}Cl_{1.5}, mol. wt: 629.13).

IR (KBr): 3350, 3143, 2924, 1619, 1504, 1459, 1426, 1348, 1315, 1292, 1256, 1228, 1090, 932, 807, 750, 656, 625 cm⁻¹.

Solubility: Hot DMSO.

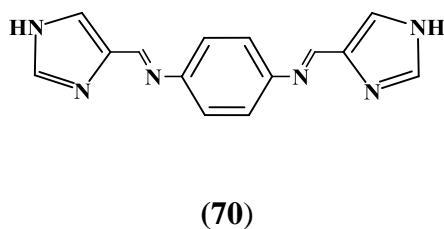
Poor solubility of the complex prevented ¹H NMR and ¹³C NMR analysis.

2.12.11 [Ag(69)]ClO₄·H₂O

This cream solid was prepared in a similar manner to [Ag(**22**)₂]ClO₄ using AgClO₄ (1.06 g, 5.11 mmol) and *N*-[(*E*)-1*H*-imidazol-4-ylmethylidene]-*N*-(3-[(*E*)-1*H*-imidazol-4-ylmethylidene]aminophenyl)amine (**69**) (0.50 g, 1.17 mmol).

<u>Yield:</u>	0.45 g (79 %).
<u>% Found:</u>	C: 34.63, H: 2.33, N: 17.30.
<u>% Calculated:</u>	C: 34.34, H: 2.88, N: 17.16 (C ₁₄ H ₁₄ N ₆ O ₅ AgCl; mol. wt: 489.62).
<u>¹H NMR:</u>	(ppm, d ₆ -DMSO): 5.75, 7.25, 7.73, 8.70.
<u>IR (KBr):</u>	3350, 3143, 1620, 1608, 1525, 1495, 1403, 1328, 1260, 1092, 933, 806, 760, 656, 625 cm ⁻¹ .
<u>Solubility:</u>	Hot DMSO.

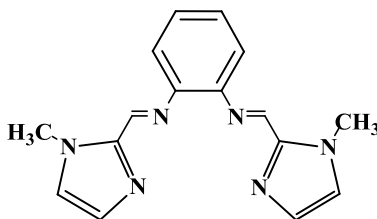
Poor solubility of the complex prevented complete ¹H NMR and ¹³C NMR analysis.

2.12.12 [Ag(70)]ClO₄·H₂O

This tan solid was prepared in a similar manner to (**77Ag**) using AgClO_4 (1.06 g, 5.11 mmol) and *N*-[(*E*)-1*H*-imidazol-4-ylmethylidene]-*N*-(4-[(*E*)-1*H*-imidazol-4-ylmethylidene]aminophenyl)amine (**70**) (0.50 g, 1.17 mmol).

<u>Yield:</u>	0.50 g (88 %).
<u>% Found:</u>	C: 34.63, H: 2.33, N: 17.30.
<u>% Calculated:</u>	C: 34.34, H: 2.88, N: 17.16 ($\text{C}_{14}\text{H}_{14}\text{N}_6\text{O}_5\text{AgCl}$; mol. wt: 488.62).
<u>^1H NMR:</u>	(ppm, d_6 -DMSO): 7.05 (s, 4H), 8.10 (s, 2H), 8.30 (s, 2H), 8.78 (s, 2H), 13.25 (s, 2H).
<u>^{13}C NMR:</u>	(ppm, d_6 -DMSO): 122.3, 124.5, 137.1, 139.5, 147.1, 152.3.
<u>IR (KBr):</u>	3339, 3138, 1622, 1493, 1435, 1418, 1355, 1327, 1305, 1256, 1205, 1121, 1092, 942, 841, 744, 625 cm^{-1} .
<u>Solubility:</u>	Hot DMSO.

2.12.13 [Ag(**71**)] $\text{ClO}_4 \cdot \text{H}_2\text{O}$



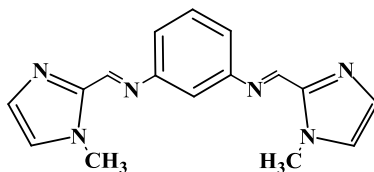
(**71**)

This tan solid was prepared in a similar manner to $[\text{Ag}(\mathbf{22})_2]\text{ClO}_4$ using AgClO_4 (1.06 g, 5.13 mmol) and *N*-[(*E*)-(1-methyl-1*H*-imidazol-2-yl)methylidene]-*N*-(2-[(*E*)-(1-methyl-1*H*-imidazol-2-yl)methylidene]aminophenyl)amine (**71**) (0.50 g, 1.71 mmol).

<u>Yield:</u>	0.78 g (88 %).
<u>% Found:</u>	C: 37.62, H: 3.21, N: 16.41.
<u>% Calculated:</u>	C: 37.12, H: 3.50, N: 16.23 (C ₁₆ H ₁₈ N ₆ O ₅ AgCl; mol. wt: 517.67).
<u>¹H NMR:</u>	(ppm, d ₆ -DMSO): 2.28 (s), 4.35 (s), 5.45 (s), 6.13 (s), 6.90 (s), 7.15 (m), 7.45 (m), 8.50 (s).
<u>¹³C NMR:</u>	(ppm, d ₆ -DMSO): 31.1, 62.0, 110.5, 111.1, 116.1, 118.7, 122.4, 122.8, 125.3, 128.2, 128.8, 132.0, 135.7, 138.5, 138.6, 142.2, 143.0, 143.2, 143.9, 144.4, 145.3, 145.6, 145.8.
<u>IR (KBr):</u>	3473, 3154, 1615, 1555, 1453, 1405, 1382, 1342, 1315, 1292, 1209, 1145, 1111, 975, 947, 929, 873, 748, 667, 625 cm ⁻¹ .
<u>Solubility:</u>	Hot DMSO.

Poor solubility of the complex prevented complete ¹H NMR and ¹³C NMR analysis.

2.12.14 [Ag(72)]ClO₄·2H₂O



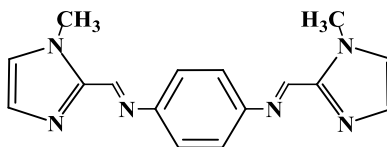
(72)

This tan solid was prepared in a similar manner to [Ag(22)₂]ClO₄ using AgClO₄ (1.06 g, 5.13 mmol) and *N*-[(*E*)-(1-methyl-1*H*-imidazol-2-yl)methylidene]-*N*-(3-[(*E*)-(1-methyl-1*H*-imidazol-2-yl)methylidene]aminophenyl)amine (72) (0.50 g, 1.71 mmol).

<u>Yield:</u>	0.87 g (95 %).
<u>% Found:</u>	C: 35.98, H: 3.07, N: 15.78.
<u>% Calculated:</u>	C: 35.87, H: 3.76, N: 15.69 (C ₁₆ H ₂₀ N ₆ O ₆ AgCl; mol. wt: 535.69).
<u>¹H NMR:</u>	(ppm, d ₆ -DMSO): 4.00 (s), 7.10 (m), 7.30 (m), 7.45(s), 7.73 (m), 8.70 (s).
<u>¹³C NMR:</u>	(ppm, d ₆ -DMSO): 33.5, 127.1, 127.4, 130.3, 143.1, 149.6.
<u>IR (KBr):</u>	34445, 3127, 1622, 1583, 1530, 1487, 1436, 1356, 1291, 1205, 1098, 960, 846, 775, 686, 624 cm ⁻¹ .
<u>Solubility:</u>	Hot DMSO.

Poor solubility of the complex prevented complete ¹H NMR analysis.

2.12.15 [Ag(**73**)]ClO₄·H₂O



(**73**)

This tan solid was prepared in a similar manner to [Ag(**22**)₂]ClO₄ using AgClO₄ (1.06 g, 5.13 mmol) and *N*-[(*E*)-(1-methyl-1*H*-imidazol-2-yl)methylidene]-*N*-(4-[(*E*)-(1-methyl-1*H*-imidazol-2-yl)methylidene]aminophenyl)amine (**73**) (0.50 g, 1.71 mmol).

<u>Yield:</u>	0.75 g (85 %).
<u>% Found:</u>	C: 37.49, H: 3.22, N: 16.22.
<u>% Calculated:</u>	C: 37.12, H: 3.50, N: 16.23 (C ₁₆ H ₁₈ N ₆ O ₅ AgCl; mol. wt: 517.67).

^1H NMR: (ppm, $\text{d}_6\text{-DMSO}$): 3.30 (s, 6H), 6.65 (s, 1H), 7.00 (t, 2H), 7.20 (m, 1H), 8.02 (s, 2H), 8.30 (s, 2H), 8.60 (s, 2H).

^{13}C NMR: (ppm, $\text{d}_6\text{-DMSO}$): 41.5, 113.7, 119.3, 124.6, 129.9, 136.9, 139.55, 150.2, 153.2.

IR (KBr): 3346, 3138, 1651, 1507, 1437, 1305, 1091, 929, 805, 624 cm^{-1} .

Solubility: Hot DMSO.

2.13 Anti-*Candida* Testing

2.13.1 Biological Preparations

2.13.2 Fungal Isolates

Candida albicans ATCC 10231 was obtained from the American Type Culture Collection (Manassas, VA, USA).

2.13.3 Sterilisation

Sterilisation was achieved by autoclaving at 121 °C and 100 kPa for 15 minutes. Alternatively, solutions that were susceptible to decomposition during autoclaving were sterilised by membrane filtration using 0.45 µm Millipore membrane filters.

2.13.4 Cell Density

Cell density was measured using an improved Neubauer haemocytometer.

2.13.5 Minimal Growth Media (MM)

MM was composed of 2% w/v glucose, 0.5% w/v yeast nitrogen base (without amino acids or ammonium sulphate) and 0.17% w/v ammonium sulphate.

2.13.6 Commercial Anti-Fungal Agents

Ketoconazole was obtained as a gift from the Biology Department, N.U.I. Maynooth.

2.13.7 Fungal Cell Culture Conditions

Cultures were grown on Sabouraud dextrose agar (SDA) plates at 37 °C and frozen for long term storage. For short-term storage, the temperature was maintained at 4 °C. Cultures were routinely sub-cultured every 3-6 weeks. Cultures were grown to the stationary phase at 37 °C and 2000 rpm in minimal medium (MM).

2.14 Susceptibility Testing Methods

2.14.1 Preparation of Complexes for Susceptibility Testing

Solutions of the test complexes were prepared by dissolving the solid complexes (0.02 g) in DMSO (1 cm³). This solution was made up to 10 cm³ with distilled H₂O, yielding a stock solution of concentration 2000 µg cm⁻³. Doubling dilutions of the stock solution were made to yield a series of test solutions ranging in concentration from 20-1.25 µg cm⁻³. Further dilutions were made when required.

Note: Solutions in DMSO: The DMSO concentration (%v/v) in the final test solutions falls well below the 3% threshold levels i.e. the point at which DMSO itself exhibits a negative effect on fungal growth.

2.14.2 Determination of Yeast Cells Minimum Inhibitory Concentrations (MIC)

The *in vitro* anti-*Candida* activity is expressed as a minimum inhibitory concentration (MIC) of drug, expressed as either µg of compound per 1 cm³ or mmol of aqueous growth medium solution required to totally inhibit the growth of the fungal cells at 37 °C. This amount of drug is deemed the MIC₁₀₀ value i.e. the amount of drug required to achieve a 100% growth inhibition of the fungal cells. Prior to MIC testing, cells were grown on SDA at 37 °C for 24 h. Cell suspensions were prepared in sterile phosphate



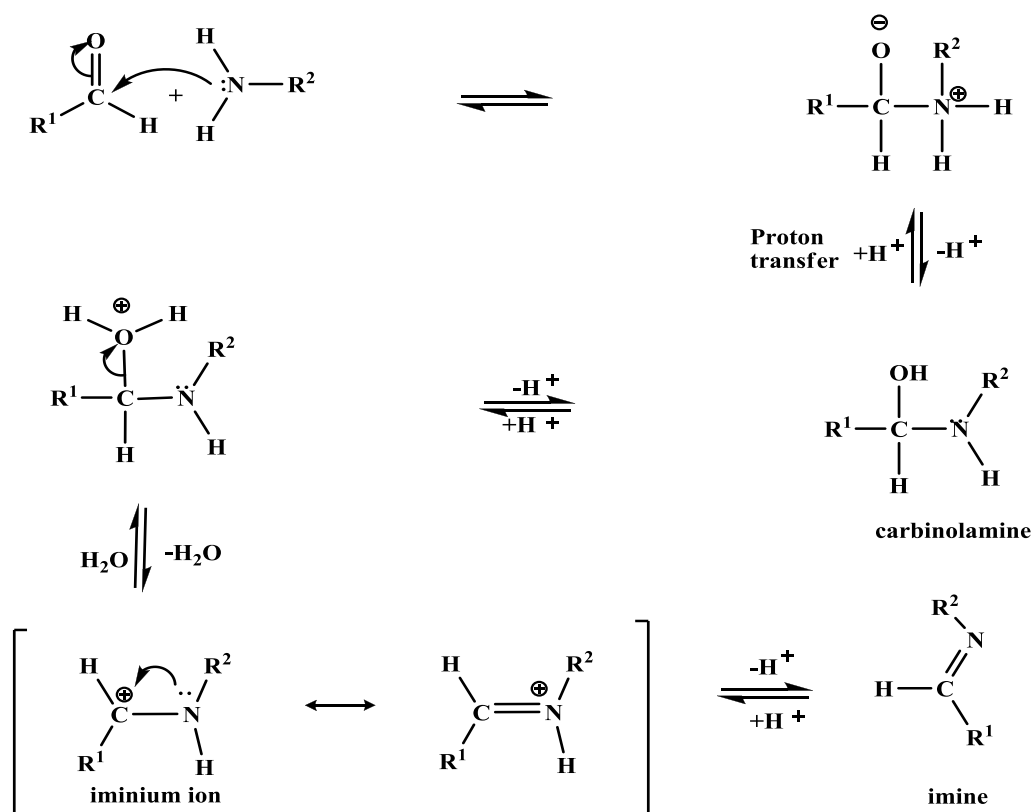
buffered saline (PBS, pH 7.2) and cells were counted microscopically following dilution with PBS. A 96 round-bottomed microtitre plate was inoculated with cells at a density of approximately 5×10^5 cells cm^{-3} . The drug/cell mixture was incubated for 24 h with continuous shaking. Each assay was performed in triplicate and included positive and negative controls. Plates were read at an absorbance of $\lambda = 549$ nm.

Results and Discussion

3.1 Schiff Base Ligands

3.1.1 The Formation of Schiff Bases

The formation of a Schiff base (Scheme 5) is an equilibrium system.^{33,94} The reaction is normally conducted under slightly acidic conditions *ca.* pH 4.5. The reaction begins with a nucleophilic attack at the carbonyl carbon of the aldehyde by the lone pair on the N atom of the incoming primary amine. A proton is moved from the positively charged nitrogen to the negatively charged oxygen producing a neutral carbinolamine. The OH group is then protonated by the acid, forming OH_2^+ , which is a better leaving group than the OH group. This dehydration step leads to the formation of an iminium ion. The next step is the deprotonation of the nitrogen of the iminium ion by water and the formation of the final product, an imine. As the formation of water is one of the driving forces of the reaction, its removal should push the reaction to the right and maximize yields.

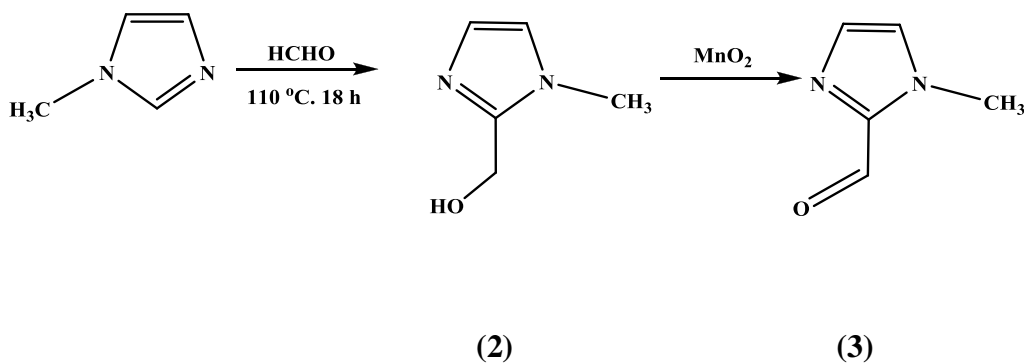


Scheme 5 Mechanism of Schiff base formation.

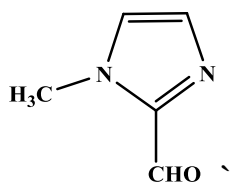
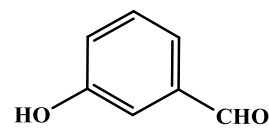
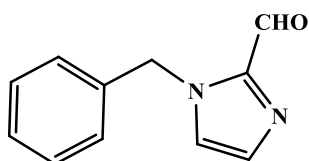
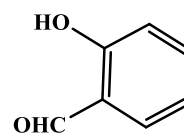
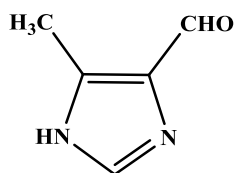
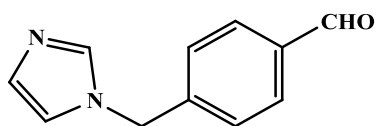
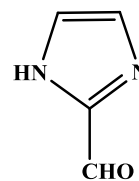
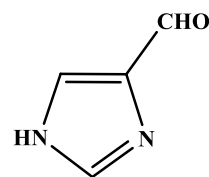
3.2 Aldehydes Used for the Synthesis of Schiff Bases

The aldehydes used in the current work are shown in Figure 30. With the exception of 1-benzyl-1*H*-imidazole-2-carboxaldehyde (**6**), all are commercially available. However, as the aldehydes 1-methyl-1*H*-imidazole-2-carboxaldehyde (**3**) and 4-methyl-1*H*-imidazole-5-carboxaldehyde (**8**) are relatively expensive, they were synthesized from inexpensive starting materials by literature procedures.^{95,96}

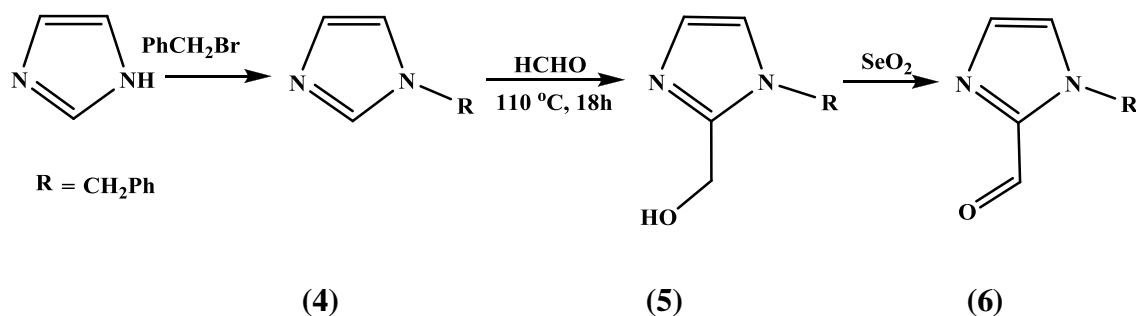
Inversen and Lund⁹⁵ synthesized 1-methyl-1*H*-imidazole-2-carboxaldehyde (**3**) by the oxidation of the corresponding hydroxymethylimidazole (**2**) using selenium dioxide. In this project, the oxidation was accomplished using manganese dioxide as outlined in Scheme 6. The use of MnO₂ in 1,4-dioxane as an oxidant reduced the reaction time to *ca.* 2.5 h compared to 11 days using selenium dioxide.⁹⁵ The reaction was carefully monitored to prevent decomposition to the starting material, 1-methylimidazole.



Scheme 6 Synthesis of 1-methyl-1*H*-imidazole-2-carboxaldehyde (**3**).

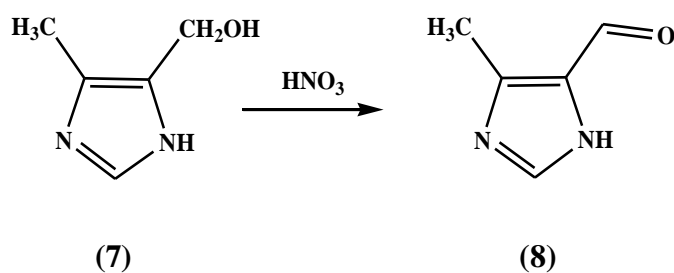
1-Methyl-1*H*-imidazole-2-carboxaldehyde (**3**)⁹⁵3-Hydroxybenzaldehyde (**10**)1-Benzyl-1*H*-imidazole-2-carboxaldehyde (**6**)⁹⁵Salicylaldehyde (**11**)4-Methyl-1*H*-imidazole-5-carboxaldehyde (**8**)⁹⁶ 1*H*-Imidazole-2-carboxaldehyde (**13**)4-(1*H*-Imidazole-1-yl)-benzaldehyde (**9**)1*H*-Imidazole-5-carboxaldehyde (**12**)**Figure 30** Aldehydes used for the synthesis of Schiff bases.

1-Benzyl-1*H*-imidazole-2-carboxaldehyde (**6**) was synthesized following the procedure of Inversen and Lund (Scheme 7).⁹⁵



Scheme 7 Synthesis of 1-benzyl-1*H*-imidazole-2-carboxaldehyde (**6**).

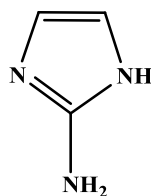
4-Methyl-1*H*-imidazole-5-carboxaldehyde (**8**) was synthesized by the oxidation of 4-methyl-5-hydroxymethylimidazole (**7**) using nitric acid⁹⁶ (Scheme 8). Carini *et al.*⁹⁷ and Weinstock *et al.*⁹⁸ used the aldehyde (**8**) in the synthesis of a number of antagiotensin II antagonists. Synthesis of the aldehydes (**3**), (**6**) and (**8**) required elevated temperature and pressure and involved autoclave procedures.



Scheme 8 Synthesis of 4-methyl-1*H*-imidazole-5-carboxaldehyde (**8**).

3.3 Schiff Base Ligands Derived from 1*H*-Imidazole-2-amine (1)

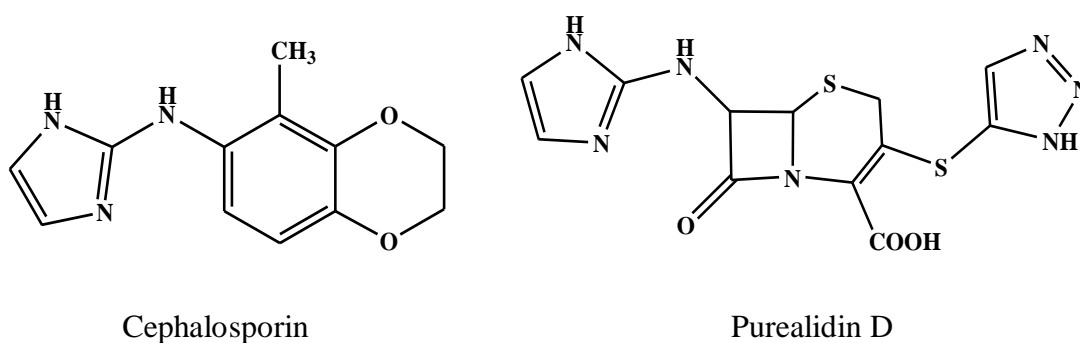
3.3.1 Synthesis of 1*H*-Imidazole-2-amine (1)⁹³



(1)

Figure 31 1*H*-Imidazole-2-amine (1).⁹³

The heterocyclic compound, 1*H*-imidazole-2-amine (1)⁹³ (Figure 31), is found as a component of many pharmacologically active compounds, e.g. the H₂-receptor antagonist, cephalosporin (Figure 32).¹¹⁰ It is also found as a component of some marine compounds, such as purealidin D (Figure 32), which is isolated from sea sponges and has been shown to have anti-cancer activity.^{111,112} 1*H*-Imidazole-2-amine (1) is also used as the starting material in the synthesis of 2-nitroimidazole, known by its trade name, Azomycin, and which is also a naturally occurring antibiotic.¹¹³

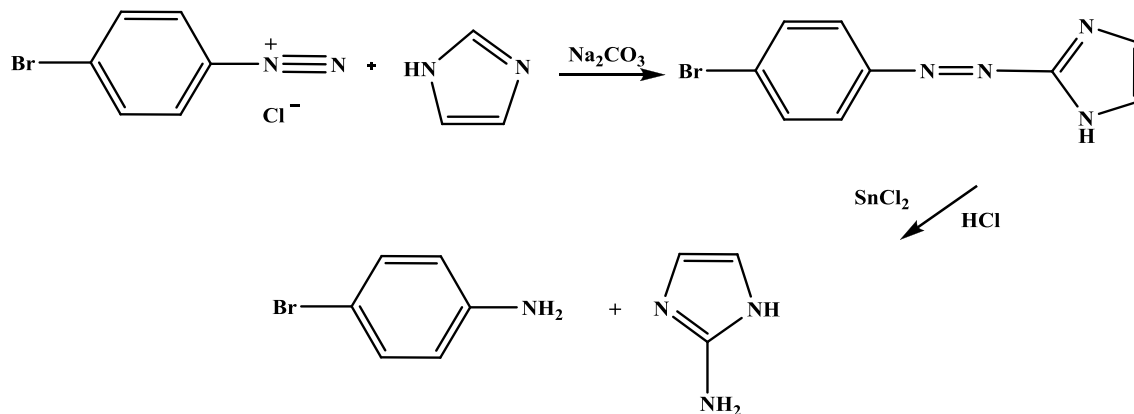


Cephalosporin

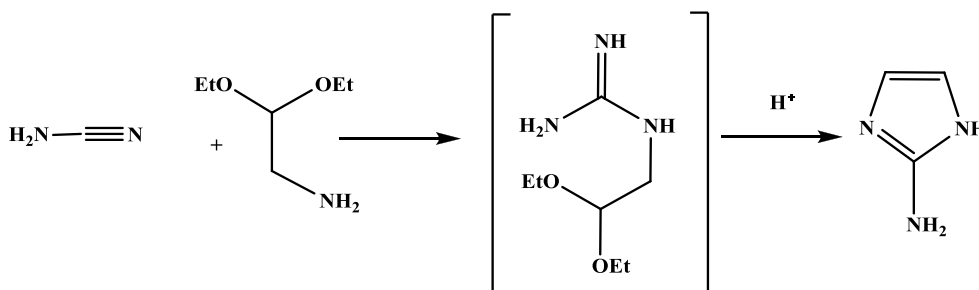
Purealidin D

Figure 32 Pharmacologically active 1*H*-imidazole-2-amine derivatives.

A number of methods have been reported for the preparation of 1*H*-imidazole-2-amine (**1**). The oldest method was described by Pyman *et al.*⁹⁶, who used the stannous chloride reduction of 2-aryldiazo-imidazole to synthesize 1*H*-imidazole-2-amine (**1**) (Scheme 9). Lawson^{99,100} used the condensation reaction of 2-aminoacetaldehyde acetal with cyanamide to prepare (**1**) (Scheme 10).

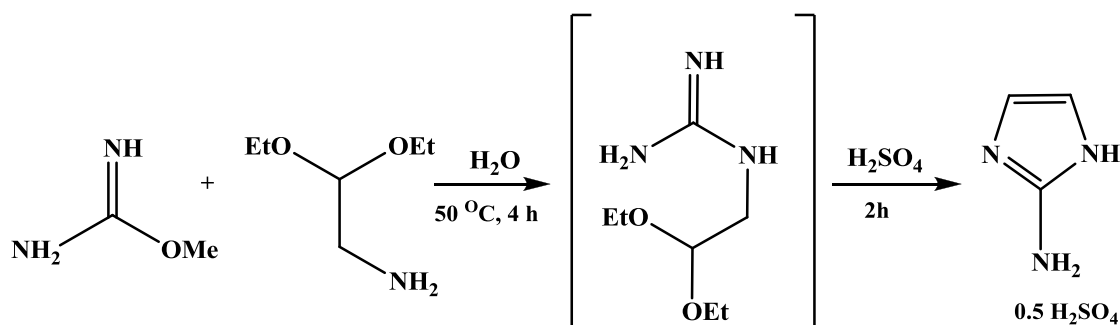


Scheme 9 Synthesis of 1*H*-imidazole-2-amine (**1**).⁹⁶



Scheme 10 Synthesis of 1*H*-imidazole-2-amine (**1**).^{99,100}

However, these two methods gave poor yields and were not suitable for the preparation of the large quantities of (**1**) required for the present study. Weinmamm *et al.*⁹³ prepared a hemisulphate salt of (**1**) in good yield using a modification of the method described by Storey *et al.*⁹⁹ and employing O-methyl-isourea in place of S-methyl-isothiourea (Scheme 11). This was the method used in the current work.

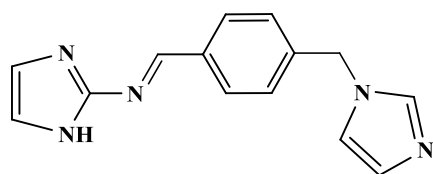


Scheme 11 Synthesis of *1H*-imidazole-2-amine (**1**).⁹³

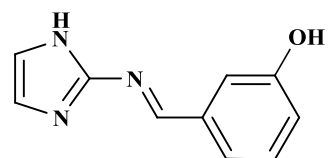
In the present study, the free amine (**1**) was released from the hemisulphate salt using barium hydroxide.

3.3.2. Synthesis of Schiff Base Ligands Derived from *1H*-Imidazole-2-amine (**1**)

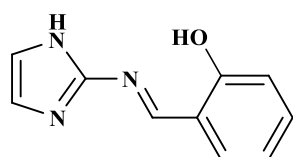
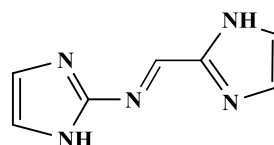
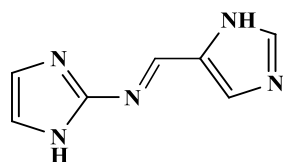
The synthesis of Schiff bases (Scheme 5) can be promoted by the removal of the by-product, water, as it is formed. However, Dean-Stark azeotropic distillation proved unsuccessful in the synthesis of Schiff bases derived from *1H*-imidazole-2-amine (**1**), due to a lack of solubility of the reactants in the solvents normally used for this technique. A solvent system, comprising a mixture of dry methanol and benzene, in conjunction with molecular sieves (4 Å beads) as a dehydrating agent, proved successful. The imine products were obtained by solvent extraction of the crude reaction residue with hot ethanol. The unreacted amine remained in the residue. On cooling, the Schiff base products precipitated. The Schiff bases did not recrystallise properly and so accurate analytical data were not obtained. However, this did not prevent the use of these compounds in the synthesis of the metal complexes where accurate analytical data were obtained. The Schiff bases derived from *1H*-imidazole-2-amine (**1**) are shown in Figure 33.



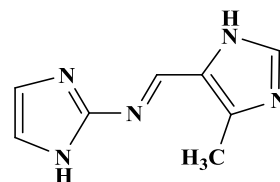
(22)



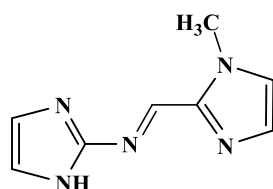
(23)

(24)³¹(25)³¹

(26)



(27)



(28)

Figure 33 Schiff base ligands derived from 1*H*-imidazole-2-amine (**1**).

As an example, the IR spectrum of the Schiff base (**22**) derived from 1*H*-imidazole-2-amine (**1**) is given in Figure 34. The spectrum shows the absence of both the strong C=O stretching band of the aldehyde at 1687 cm^{-1} and the amine (N-H bending) band at 1673 cm^{-1} , and the appearance of the new imine C=N stretching band at 1607 cm^{-1} .

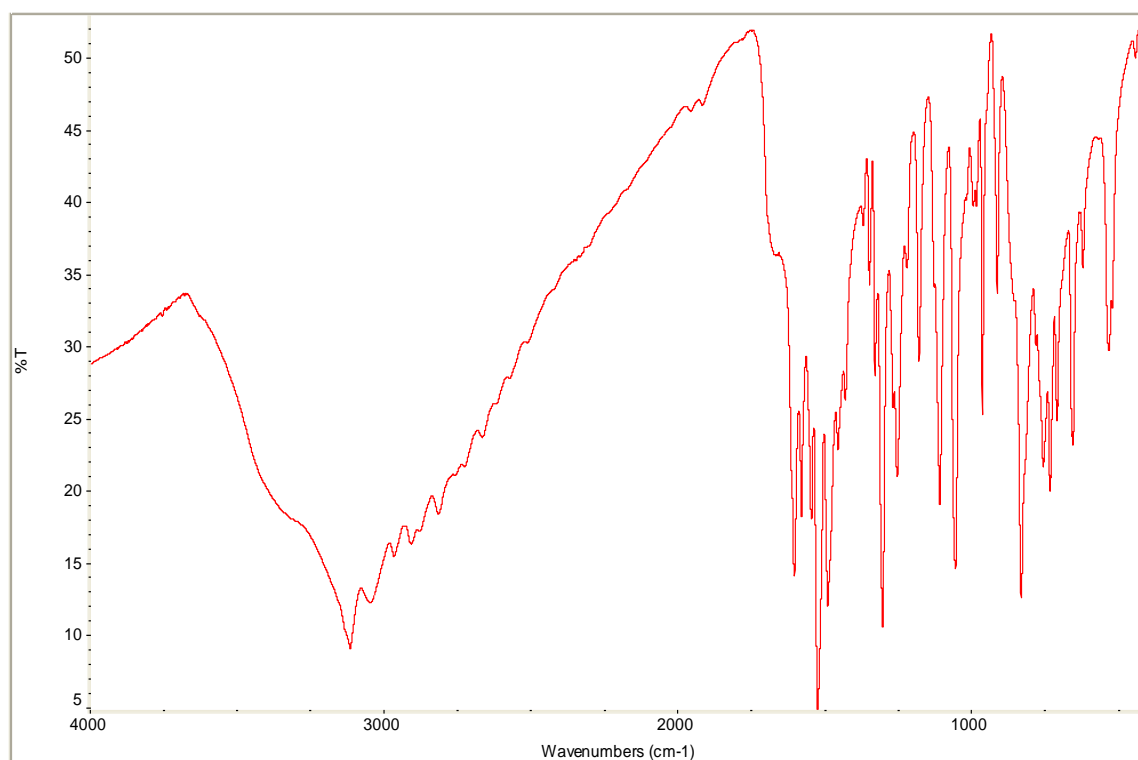


Figure 34 IR spectrum of (**22**).

Some general features of the ¹H NMR (d₆-DMSO) spectra of compounds of imidazoles are apparent in the spectra of the compounds shown in this thesis. For imidazole, a compound unsubstituted at the secondary nitrogen atom, the signal for the NH-proton occurs at *ca.* 12-13 ppm. However, this peak is often very broad and may not even be observed, and so is of little diagnostic use. The protons at the C-4 and the C-5 in an unsubstituted imidazole become equivalent through, rapid tautomerism of the hydrogen between the two nitrogens and a singlet of area two results. When the nitrogen is substituted, the 4- and 5-positions are not equivalent and separate signals are observed. However, as there is minimal coupling the resulting signals appear as singlets.

The synthesized Schiff base might result in either the *E* or *Z* form due to the stereochemistry about the carbon-nitrogen double bond. However, no evidence of more than one form is found in the NMR spectra (only one signal is seen for the imine C-H). The *E* form would be more stable on steric grounds and the X-ray crystal structures of ligands (**36**) and (**37**) (Figures 49-53) show only *E* stereochemistry.

The ^1H NMR spectra of this set of Schiff bases derived from (**1**) shows the absence of the aldehyde proton peak at *ca.* 10 ppm and the appearance of a new peak at *ca.* 9 ppm representing the imine proton. Two examples of the ^1H NMR (d_6 -DMSO) spectra obtained for this set of Schiff bases are given in Figures 35 and 36. The residual d_6 -DMSO peak is at *ca.* 2.5 ppm and the broad peak of water is *ca.* 3.2 ppm. Solubility of those compounds was problematic, hence the ^1H NMR (d_6 -DMSO) spectra of this set of ligands were run in dilute solution.

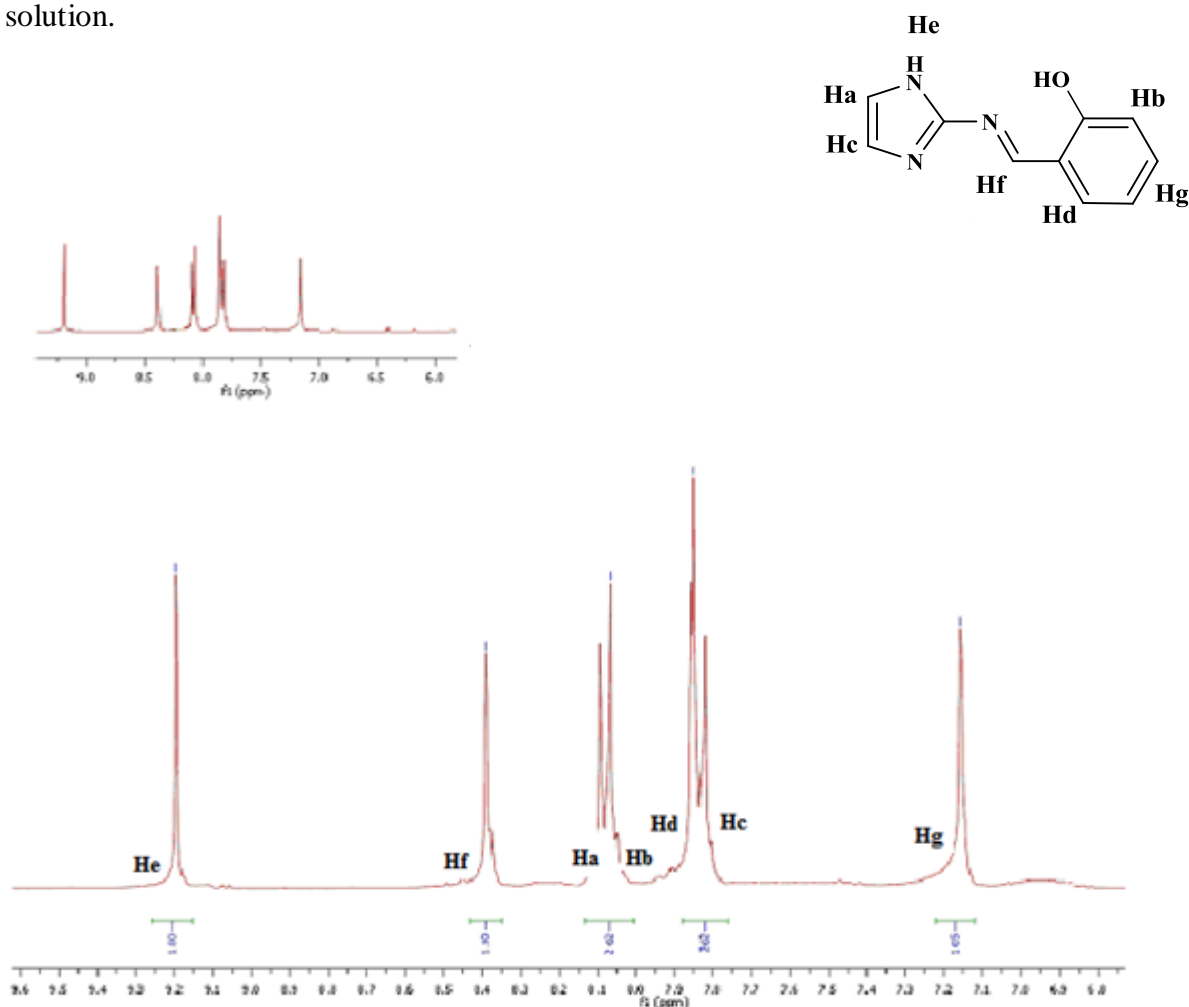


Figure 35 ^1H NMR (d_6 -DMSO) spectrum of (**24**).

The ^1H NMR (d_6 -DMSO) spectrum of compound (**24**) is shown in Figure 35. The peak at 9.19 ppm is for the imine proton (Hf), whilst the protons in the 4(5)-position of the imidazole are seen as a singlet at 7.16 ppm (Ha) and 8.39 ppm (Hc) separated by the phenol peaks at 7.86 (Hb) and 8.07 ppm (Hd). The peak representing the OH proton is not seen and may be masked by the peak for water at *ca.* 3.2 ppm or is, as suggested by Govindasamy *et al*, involved in intramolecular hydrogen bonding with the nitrogen of the imine (Figure 37).¹⁰¹

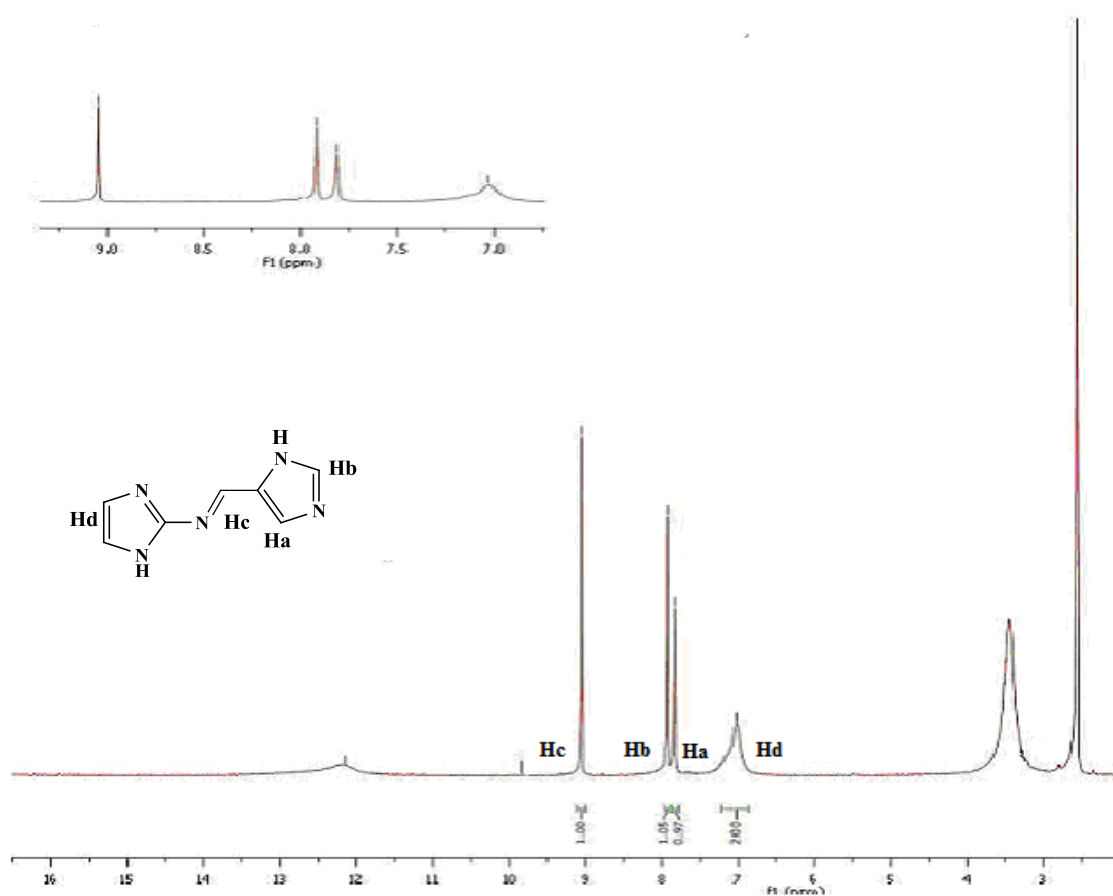


Figure 36 ^1H NMR (d_6 -DMSO) spectrum of (**26**).

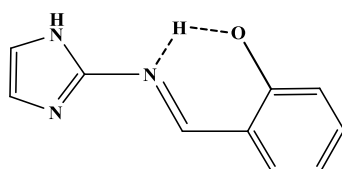


Figure 37 2-[(1*H*-Imidazol-2-ylimino)methyl]phenol (**24**).^{31,101}

The ^1H NMR (d_6 -DMSO) spectrum of (**26**) is shown in Figure 36. The imine proton signal is seen at 9.05 ppm (Hc), while the signal of the proton in the 2-position of the imidazole is seen at 7.92 ppm (Hb) and the signal at 7.81 ppm is due to the proton in the 4(5)-position (Ha). The broad peak at 7.03 ppm represents the two protons in the 4(5)-position (Hd).

Abuskhuna *et al.*³¹ synthesized compounds (**24**) and (**25**) as starting materials in their search for novel anti-*Candida* drugs. This research group further reduced compounds to the corresponding amines using sodium cyanoborohydride and subsequently complexed them to a range of metals.

3.4 Schiff Base Ligands derived from Histamine

3.4.1 Synthesis of Schiff Base Ligands Derived from Histamine

In this set of Schiff bases, the histamine molecule (Figure 38) replaced the amine, 1*H*-imidazole-2-amine (**1**). Synthesis of this set of Schiff bases (Figure 39) proved to be less

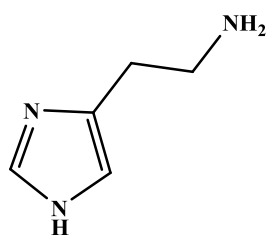


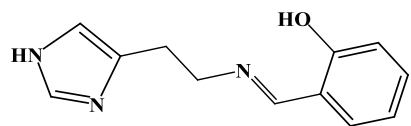
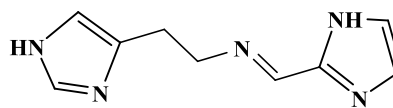
Figure 38 Histamine.

problematic than the previous set synthesized from 1*H*-imidazole-2-amine (**1**). The solvent

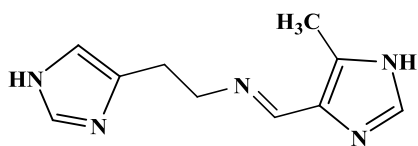
system, comprising of a mixture of dry methanol and benzene, used in conjunction with molecular sieves (4 Å beads) as a dehydrating agent was quite successful. Accurate analytical data were obtained for this set of Schiff bases and the product yields were between 75-90%.

The Schiff base (**29**), which, was synthesized from salicylaldehyde and histamine, has previously been used as a model for the study of metalloenzymes, particularly those containing iron and vanadium.¹⁰² However, in these cases the ligand itself was not isolated before complexation with the metals.^{102,103} Casella¹⁰³ synthesized and isolated (**29**) using aqueous ethanol. Scarpellini *et al.*¹⁰⁴ also synthesized and isolated compound (**32**), which was synthesized from histamine and 1-methyl-2-imidazolecarboxyaldehyde. This group¹⁰⁴ used methanol at 0 °C in the synthesis of (**32**), and a modification of this group's procedure was used in present research project.

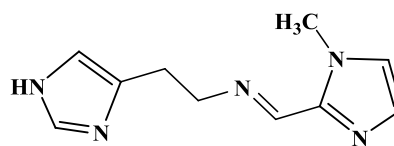
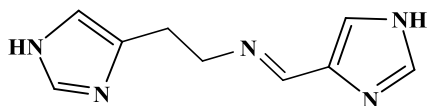
A representative example of an IR spectrum of a compound from this set of Schiff bases is shown in Figure 40. The IR spectrum of (**29**) shows the absence of the strong C=O aldehyde band at *ca.* 1666 cm⁻¹ and the strong amine band at *ca.* 3100 cm⁻¹ and the appearance of the imine band (C=N) at *ca.* 1633 cm⁻¹. The strong OH band of (**29**) is seen at 3400 cm⁻¹, as part of the broad overlapping bands of the N-H and C-H stretching vibrations appearing between 2800 cm⁻¹ and 3450 cm⁻¹.

(29)¹⁰¹⁻¹⁰³

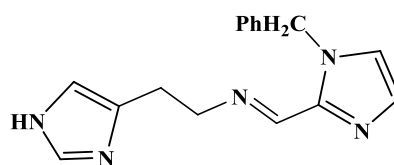
(30)



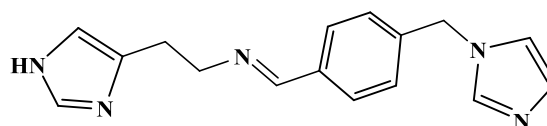
(31)

(32)¹⁰⁴

(33)



(34)



(35)

Figure 39 Schiff bases derived from histamine.

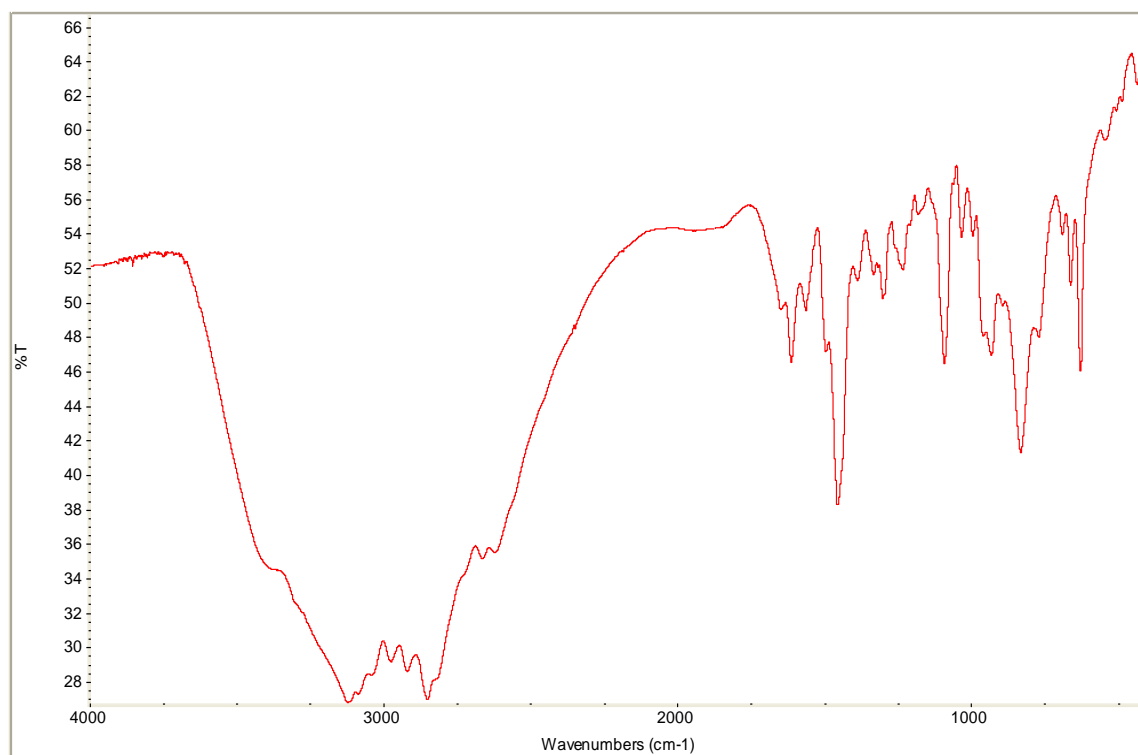


Figure 40 IR spectrum of compound of **(29)**.

The ^1H NMR ($\text{d}_6\text{-DMSO}$) spectra obtained for this set of Schiff bases shows the absence of the aldehyde proton peak at *ca.* 10 ppm and the appearance of a peak at *ca.* 8.5 ppm corresponding to the proton of the imine. Two examples of ^1H NMR spectra obtained for this set of Schiff bases are given in Figures 41 and 42. The ^1H NMR ($\text{d}_6\text{-DMSO}$) spectrum of **(31)** is shown in Figure 41. The imine proton (Hc) is seen at 8.21 ppm. The two peaks at 7.57 ppm (Hg) and 7.52 ppm (Hb) are the protons in the 2-positions of the imidazoles. The peak at 6.76 ppm is the proton in the 4(5)-position of the imidazole (Hf). The protons of the methyl group are seen at 2.29 ppm (Ha) and the two methylenes of the histamine moiety appear as triplets at 2.8 ppm (He) and 3.72 ppm (Hd), respectively.

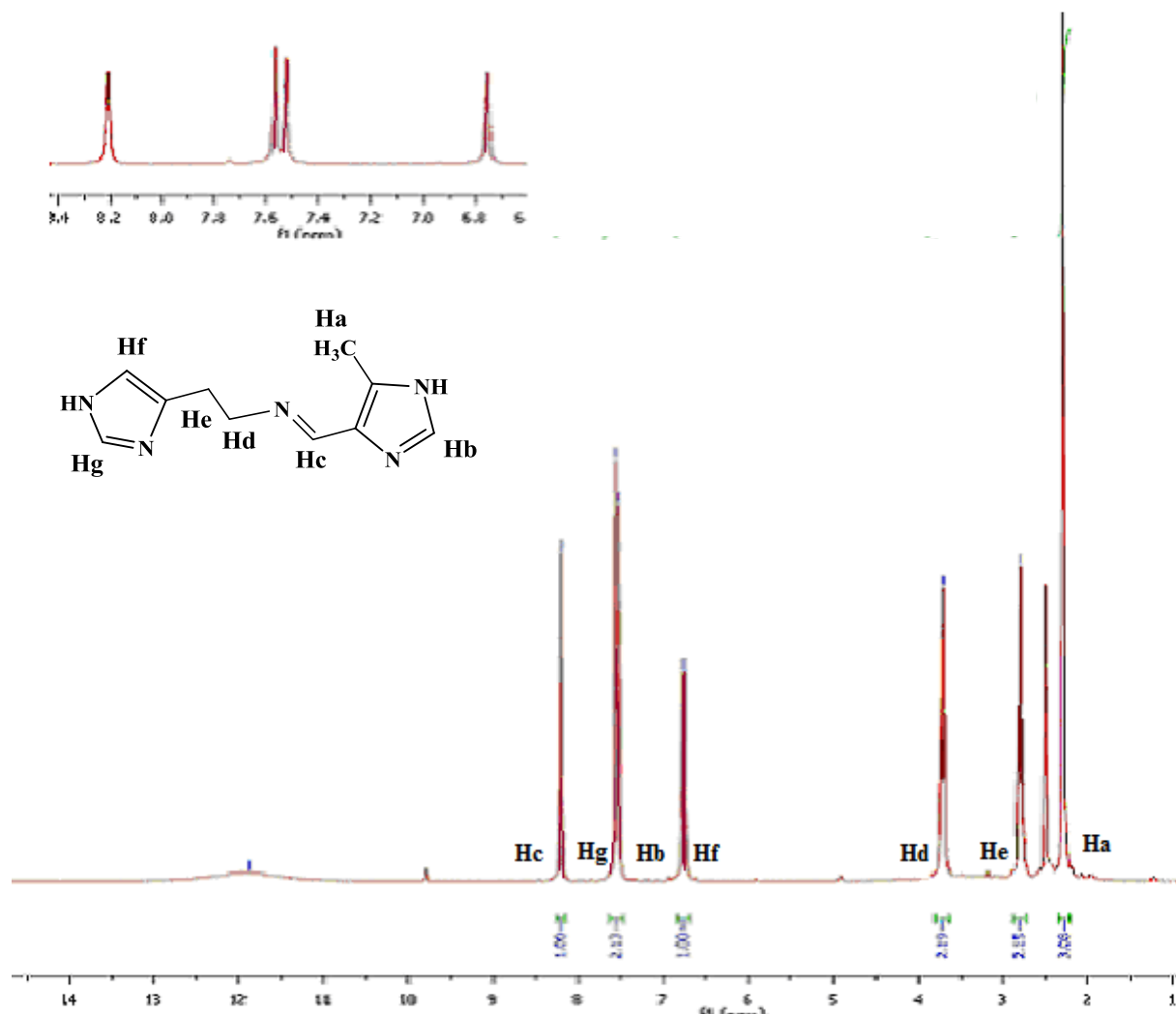


Figure 41 ^1H NMR (d_6 -DMSO) spectrum of (31).

The ^1H NMR (d_6 -DMSO) spectrum of compound (30) is shown in Figure 42. The imine peak (Hc) is seen at 8.20 ppm, while the peak at 7.56 ppm (Hf) and 6.76 ppm (Hg) are the protons in the 2-position and the 4(5)-position of the histamine moiety. The peaks at 7.36 ppm and 7.51 ppm represent the two protons (Ha) and (Hb) in the 4(5)-position. The methylenes of the histamine moiety are seen as triplets at 3.55 ppm (Hd) and 2.70 ppm (He).

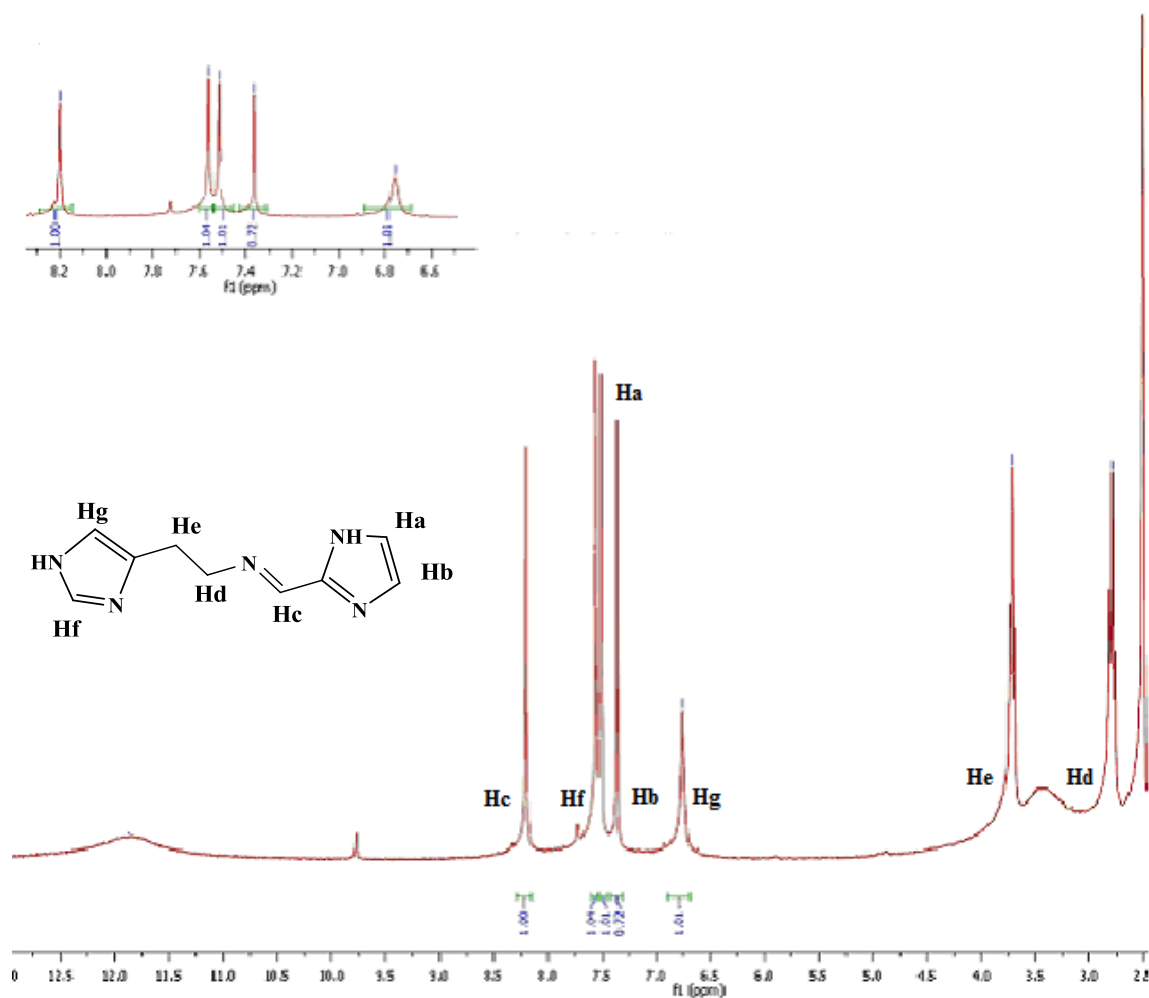


Figure 42 ^1H NMR ($\text{d}_6\text{-DMSO}$) spectrum of (30).

Attempts to obtain a single crystal suitable for X-ray crystallographic analysis for this group of ligands or their metal complexes proved unsuccessful. Scarpellini *et al.*¹⁰⁴ obtained the crystal structure of a copper(II) analogue of ligand (32). This copper complex gives an indication of the structural characteristics of this ligand group and possible silver coordination patterns (discussed later in the thesis).

3.5 Synthesis of Schiff Base Ligands Derived from 1-(3-Aminopropyl)imidazole (Apim)

This set of Schiff bases were synthesized from the amine, Apim (Figure 43). The Schiff base products consist of either two imidazoles or a salicylaldehyde linked by a 5-atom spacer chain (Figure 44). The preparation of this set of Schiff bases also proved to be less problematic than the set synthesized from 1*H*-imidazole-2-amine (**1**). The solvent used was dry methanol, in conjunction with molecular sieves (4 Å beads) as a dehydrating agent. Accurate analytical data were obtained and product yields were *ca.* 90%.

Ouadi *et al.*, in their search for task specific ionic liquids, synthesized (**36**) using Schlenk-tube techniques.¹⁰⁵ A modification of their synthetic procedure was used in the present study.

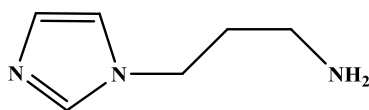
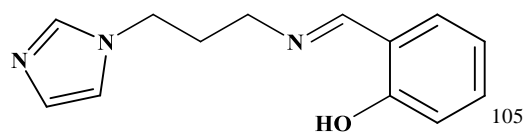
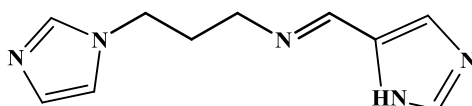
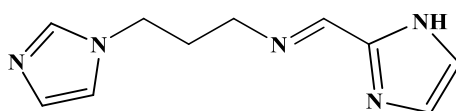


Figure 43 1-(3-Aminopropyl)imidazole (Apim).

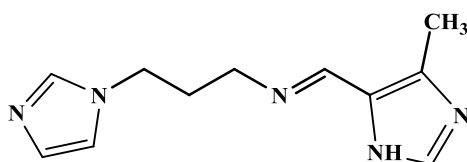
The IR spectra of this set of ligands shows the absence of the strong aldehyde C=O band at *ca.* 1666 cm^{-1} , the strong amine band at *ca.* 3100 cm^{-1} and *ca.* 1600 cm^{-1} (N-H bending) and the appearance of the imine band (C=N) at *ca.* 1650 cm^{-1} . The IR spectrum of compound (**36**) (Figure 45) shows the strong OH band at 3183 cm^{-1} , as part of a broad band comprising the N-H and C-H stretching vibrations at between *ca.* 2800 cm^{-1} and *ca.* 3083 cm^{-1} . The width of this band is due to intramolecular and intermolecular H-bonding. The imine band (C=N) is seen at 1649 cm^{-1} .

(36)¹⁰⁵

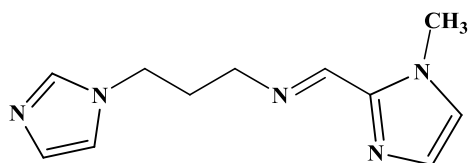
(37)



(38)



(39)



(40)

Figure 44 Schiff bases derived from Apim.

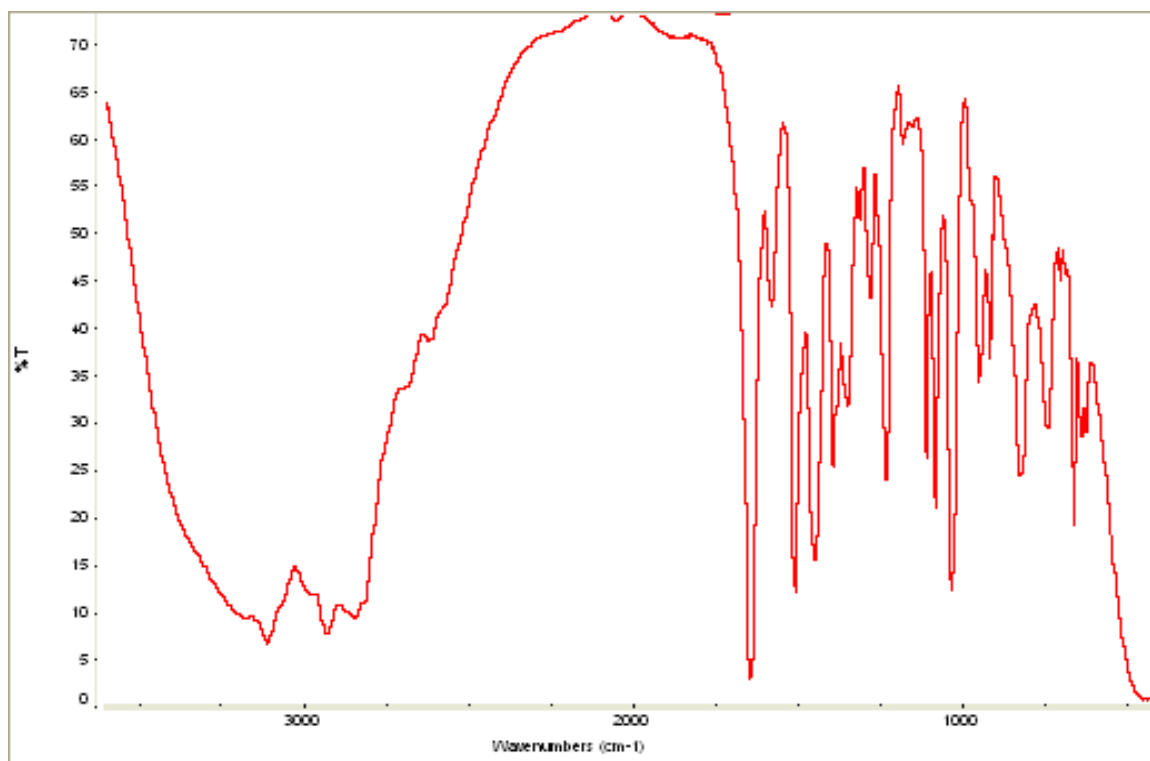


Figure 45 IR spectrum of **(36)**.¹⁰⁵

The ¹H NMR (d₆-DMSO) spectrum of **(39)** is shown in Figure 46. The imine peak (Hc) is seen at 8.22 ppm, while the peaks at 7.58 ppm (Hb) and 7.63 ppm (Hj) arise from the protons in the 2-positions of the imidazoles. The protons in the 4(5)-position of the Apim moiety are seen at 7.19 ppm (Hg) and 6.90 ppm (Hi), respectively. The methylenes of the spacer chain are seen as triplets at 2.01 ppm (He), 3.42 ppm (Hf) and 4.06 ppm (Hd). The protons of the methyl group are seen as a singlet at 2.27 ppm (Ha).

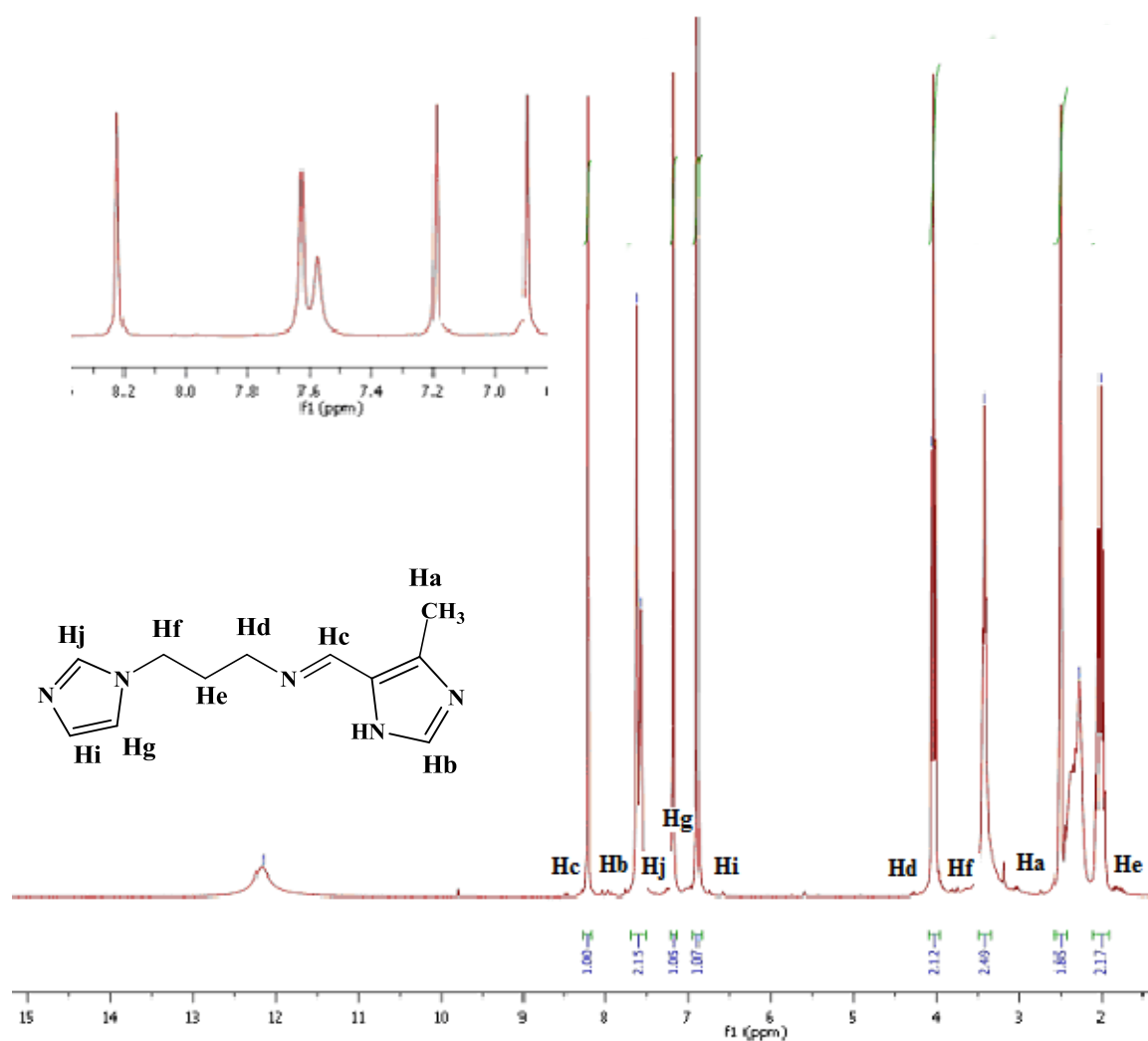


Figure 46 ^1H NMR (d_6 -DMSO) spectrum of (39).

The ^1H NMR (d_6 -DMSO) spectrum of compound (40) is shown in Figure 47. The imine peak (Hd) is seen at 8.25 ppm, while the peak at 7.64 ppm (Hj) represents the proton in the 2-position of the imidazole. The peaks at 7.20 and 7.31 ppm represent the protons in the 4(5)-position of the aldehyde moiety, (Hb) and (Hc). The peaks representing the proton in the 4- and 5-positions of the Apim moiety are seen at 7.04 ppm (Hi) and 6.90 ppm (Hh), respectively. The peak at 3.92 ppm represents the methyl group. The methylenes of the spacer chain are seen as triplets at 4.05 ppm (He), 3.52 ppm (Hg) and 2.08 ppm (Hf).

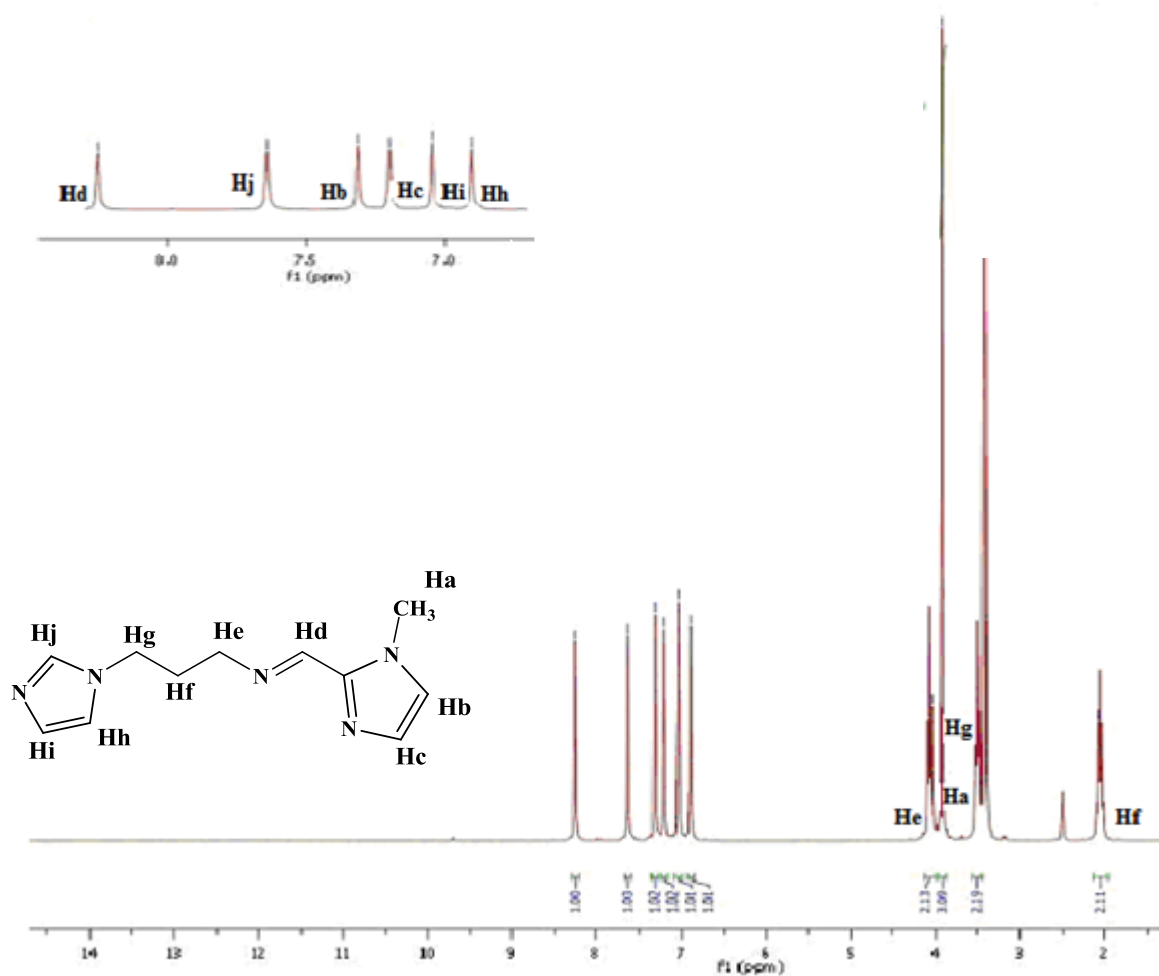


Figure 47 ^1H NMR (d_6 -DMSO) spectrum of (40).

The X-ray crystal structures of (36)¹⁰⁵ (Figures 48-50) and (37) were obtained (Figures 51-53). X-ray crystal data tables are given in Appendix 1 and 2. In compound (36) there is intermolecular hydrogen bonding between the phenolic protons and the imine nitrogen (N3) (Figure 48).¹⁰¹ A distance of 2.689-3.397 Å separates the imidazole rings of neighbouring molecules. There is intramolecular hydrogen bonding between the centroid of each imidazole ring and a hydrogen of the C4 methylene group of the spacer chain of the imidazole. This gives an angle of approximately 90° so that the imidazole ring and the phenol ring are almost perpendicular. The packing arrangement for (36) is shown in Figure 50. The intermolecular hydrogen bonding between the imidazole rings holds the lattice shape. There is no π - π stacking, although there is hydrogen bonding between neighbouring imidazole rings. This

angle (between the centroid of each imidazole ring and a hydrogen of the C4 methylene group of the spacer chain of the imidazole), of approximately 90° , has also been found in similar structures containing the imidazole moiety.³¹

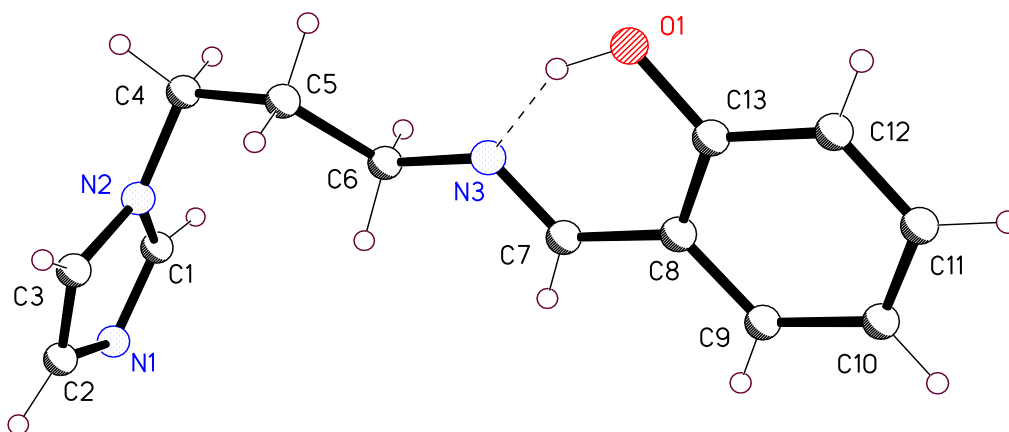


Figure 48 The X-ray crystal structure of **(36)**.



Figure 49 The X-ray crystal structure of **(36)** showing the intermolecular hydrogen bonding.

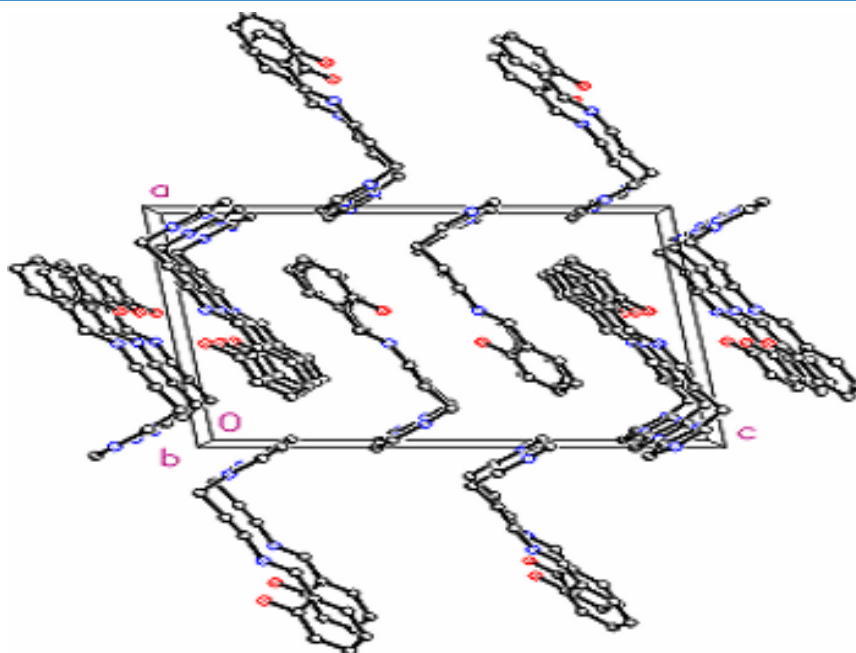


Figure 50 Packing diagram for **(36)**.

The X-ray crystal structure for ligand **(37)** is shown in Figure 51. There is intermolecular hydrogen bonding between the centroid of each imidazole ring and a hydrogen of the C6 methylene group of spacer chain of imidazole. Again this gives an angle of approximately 90° at the C4- and C5-positions on the chain, so that the imidazole rings are almost perpendicular to each other. Hydrogen bonding is also seen between the imine of one ligand and the hydrogen on the nitrogen of the imidazole ring of an adjacent ligand. There are also hydrogen-bonding interactions between the hydrogen on carbon in the 2-position of the imidazole ring and the nitrogen of the imidazole ring of another adjacent ligand (Figure 53). Hydrogen bonding interactions are also seen between the hydrogen on N4 of the imidazole ring of one ligand and the imine, (N3) and N5 of the imidazole of an adjacent ligand, leading to a very regular zigzag pattern (Figure 53).

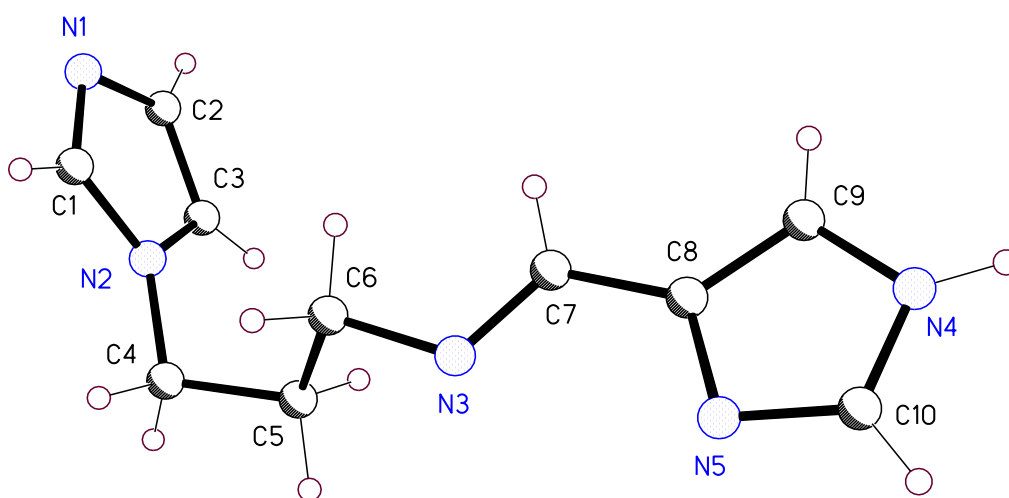


Figure 51 The X-ray crystal structure of (37).

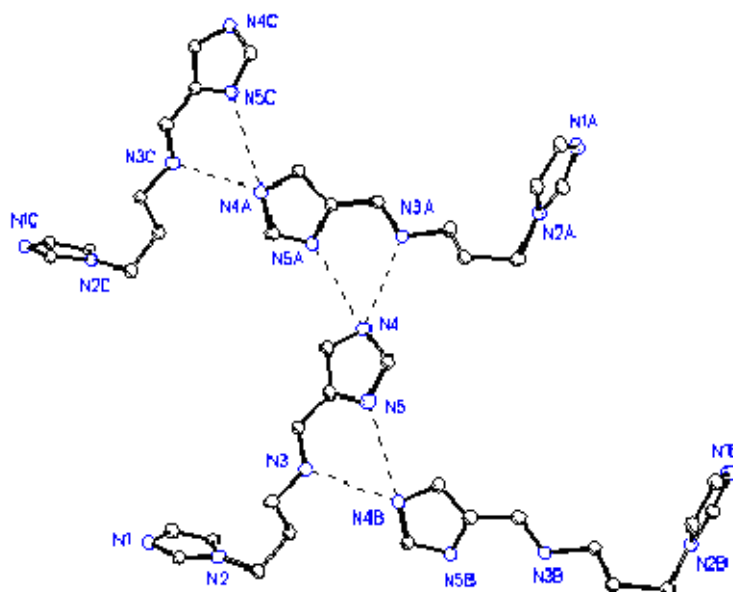


Figure 52 Intermolecular hydrogen bonding in (37).

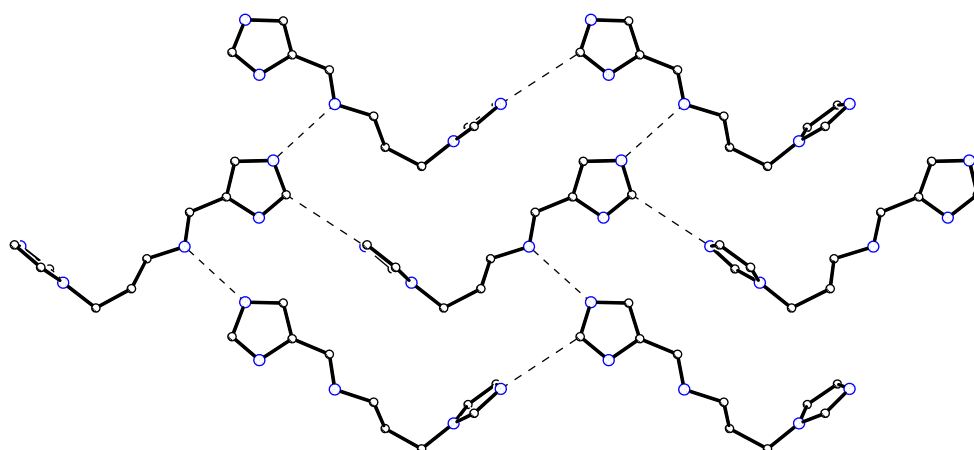


Figure 53 Intermolecular hydrogen bonding in (37) and the resultant characteristic zigzag pattern.

3.6 Synthesis of Schiff Base Ligands Derived from 1,2-Diaminoethane, 1,3-Diaminopropane and 1,4-Diaminobutane

For this set of Schiff bases the diamines, 1,2-diaminoethane, 1,3-diaminopropane and 1,4-diaminobutane (Figure 54), were used with the selected aldehydes. This provides carbon-nitrogen spacer chain lengths of 6-8 atoms. The Schiff base products are shown in Figure 55. A number of these Schiff base ligands have been previously studied in some depth, because of their potential as supramolecular, polydentate building blocks that will self-assemble in specific networks.¹¹⁴ These compounds have possible applications in microelectronics and nonlinear optics. They also have potential as gas storage material because of their porous nature.¹⁰⁶ This set of Schiff bases were synthesized using dry methanol and molecular sieves (4Å beads) as a dehydrating agent. Accurate analytical data were obtained and product yields were *ca.* 80%.

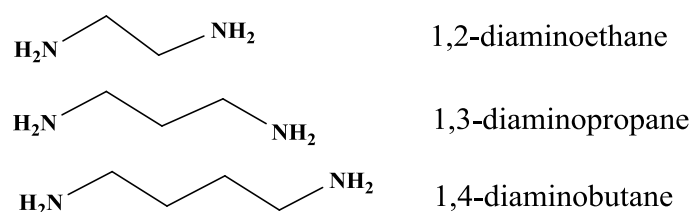


Figure 54 1,2-Diaminoethane, 1,3-diaminopropane and 1,4-diaminobutane.

Raghu *et. al* synthesized **(47)** in dry ethanol, as part of their study of thermoplastic polyurethanes.¹⁰⁶ Ibrahim and Etaiw synthesized **(48)** in their study of supramolecular silver structures,¹⁰⁷ and LaRonde and Brook¹⁰⁸ prepared **(53)** in their study of extra-coordinate silicon with C_2 -symmetric ligands. While they were unsuccessful in their attempt to get a crystal structure of the silicon complexes, they were able to obtain a crystal structure of a copper complex.¹⁰⁸ Brook *et. al*¹⁰⁹ also synthesized ligand **(54)** and reduced it to the corresponding amine using sodium cyanoborohydride and subsequently prepared a copper(II) complex.¹⁰⁹ Yang *et. al*¹¹⁴ also synthesized the Schiff bases **(53)** and **(54)** and then complexed them to silver. Dominguez-Vera *et. al*¹¹⁵ synthesized **(42)** during their study of possible new materials. This research group also synthesized compounds **(44)** and **(45)**. Nathan *et. al*¹¹⁶ used the salicylaldehyde compounds **(47)**, **(48)** and **(49)** to study the geometry of copper(II) complexes with ligands of varying chain lengths. Taylor *et al*¹¹⁷ also synthesized the same three compounds (**(47)**, **(48)**, **(49)**) in their research on the ability of ligands to alter the geometry at metal centers during the course of chemical reactions. Cai *et al*¹¹⁸ also synthesized compounds **(47)**, **(48)** and **(49)** in their search for novel ionic liquids. The broad diversity of the research interest hints at the potential of these Schiff bases.

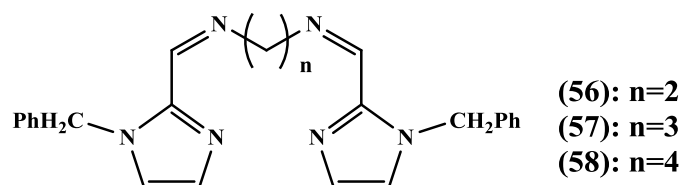
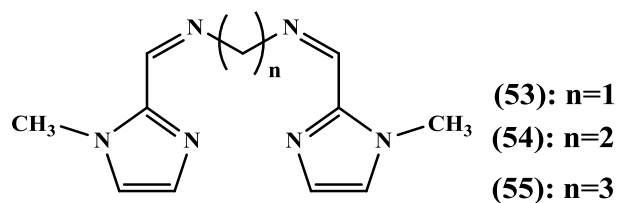
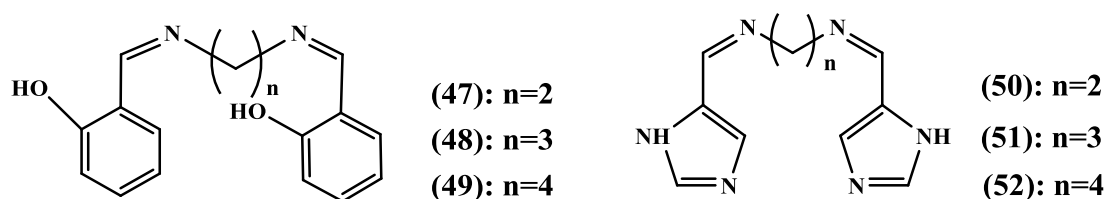
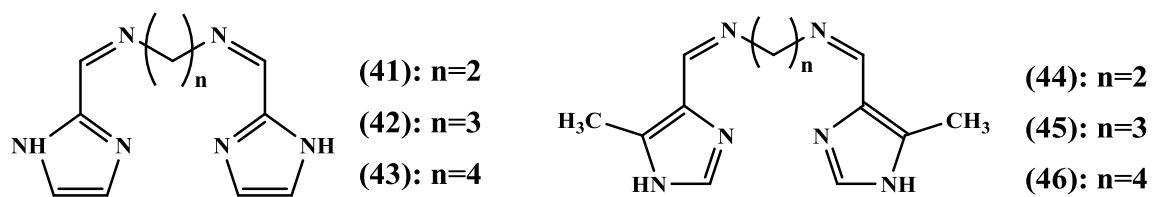


Figure 55 Schiff bases derived from 1,2-diaminoethane, 1,3-diaminopropane and 1,4-diaminobutane.

The IR spectra obtained for this set of Schiff bases shows the absence of the strong C=O aldehyde band at *ca.* 1654 cm^{-1} , the strong amine band at *ca.* 3100 cm^{-1} and *ca.* 1600 cm^{-1} (N-H bending) and the appearance of the imine band (C=N) at *ca.* 1650 cm^{-1} . An example of an IR spectrum for this set of Schiff bases (**41**) is shown in Figure 56. The spectrum shows the overlapping bands of the N-H and C-H stretching vibrations between 2839 cm^{-1} and 3146 cm^{-1} , respectively. The imine (C=N) band is seen at 1651 cm^{-1} .

The ^1H NMR (d_6 -DMSO) spectra for this set of Schiff bases shows the absence of the aldehyde proton peak at *ca.* 10 ppm and the appearance of a peak at *ca.* 8.2 ppm corresponding to the imine proton. Two examples of ^1H NMR (d_6 -DMSO) spectra for this set of Schiff bases are given in Figures 57 and 58.

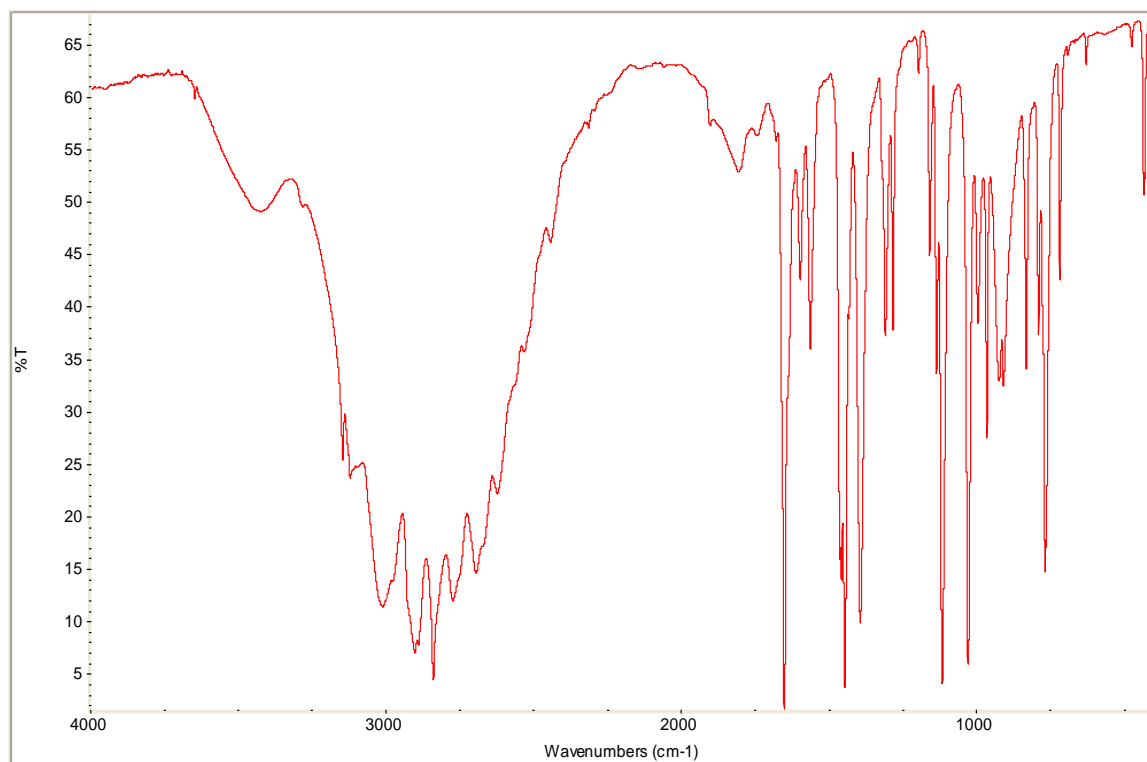


Figure 56 IR spectrum of (**41**).

The ^1H NMR (d_6 -DMSO) spectrum of (**49**)¹¹⁶⁻¹¹⁸ is shown in Figure 57. The peak for the imine proton (Ha) is seen at 8.58 ppm. The multiplets at 7.41 ppm, 7.32 ppm and 6.86 ppm

represent the aromatic protons of the phenyl moiety. The methylene groups within the chain are seen as triplets at 3.65 ppm (Hf) and 1.72 ppm (He). The peak at 13.62 ppm represents the OH protons (Hg).

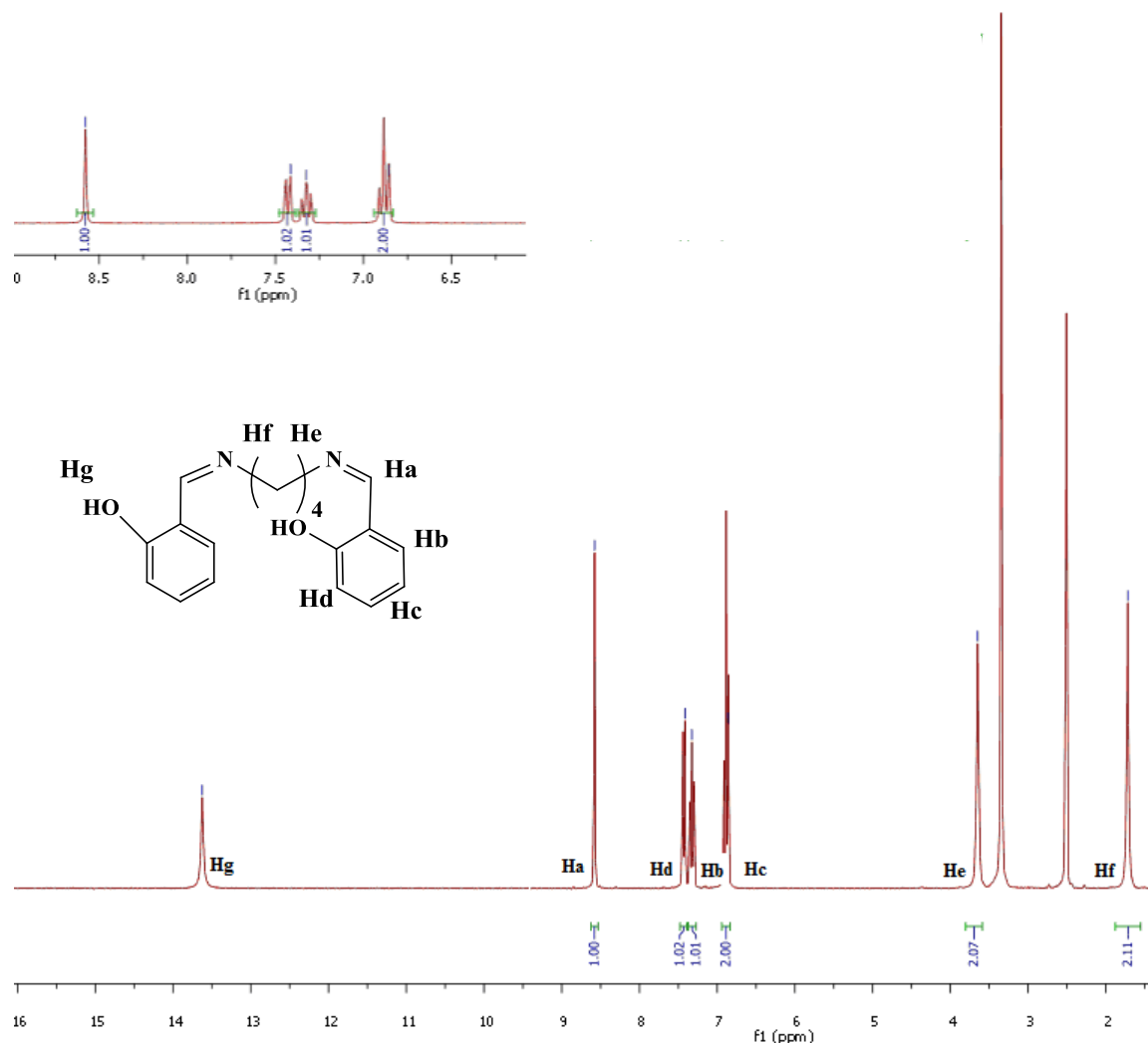


Figure 57 ^1H NMR (d_6 -DMSO) spectrum of (49).

The ^1H NMR (d_6 -DMSO) spectrum of (44)¹¹⁵ is shown in Figure 58. The imine peak (Ha) is seen at 8.22 ppm. The peak at 7.53 ppm represents the proton in the 2-position (Hc). The methylene groups of the spacer chain are seen as a triplet at 3.74 ppm (Hd), and the singlet at 2.26 ppm (Hb) represents the methyl group in the 4(5)-position of the imidazole.

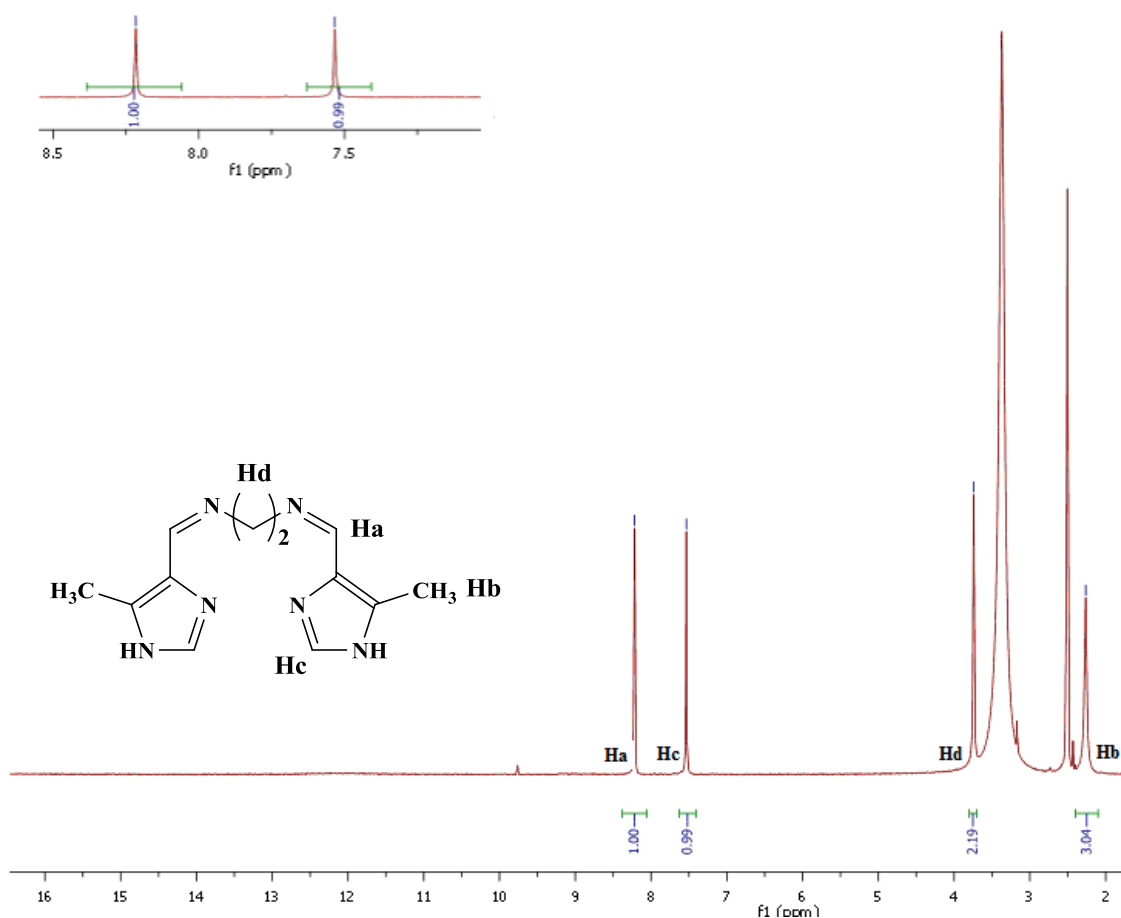
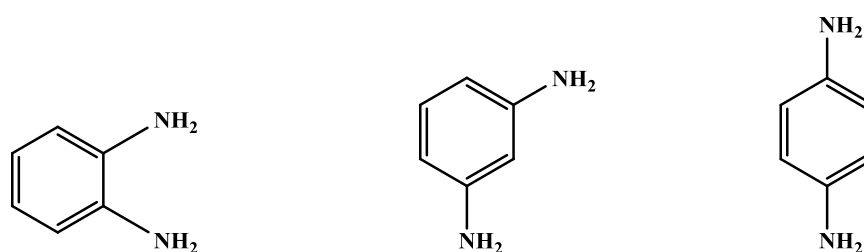


Figure 58 ^1H NMR (d_6 -DMSO) spectrum of (44).

3.7 Synthesis of Schiff Base Ligands Derived from 1,2-Phenylenediamine, 1,3-Phenylenediamine and 1,4-Phenylenediamine

For this set of Schiff bases the diamines, 1,2-phenylenediamine, 1,3-phenylenediamine and 1,4-phenylenediamine (Figure 59) were used. The solvent of dry methanol, in conjunction with molecular sieves (4 Å beads) as a dehydrating agent was successful. Accurate analytical data were obtained for this set of Schiff base products (Figure 60) and product yields were *ca.* 90%. Phenylenediamines are used in the in the manufacture of photographic developers and

dyestuffs.¹¹⁹ The presence of the phenyl group increases the level of aromaticity and π -electron donating capacity in the resulting Schiff base ligands. There are also two imine moieties in this set of Schiff base ligands. Mucha *et al*¹²⁰ and Singh *et al*.¹²¹ synthesized compound (**62**) in their work on hexa-coordinated silicon.



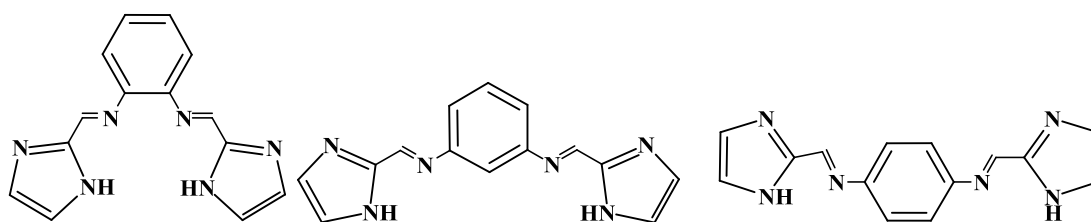
1,2-phenylenediamine

1,3-phenylenediamine

1,4-phenylenediamine

Figure 59 1,2-Phenylenediamine, 1,3-phenylenediamine and 1,4-phenylenediamine.

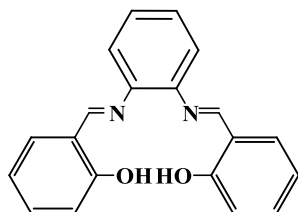
An example of an IR spectrum obtained for this set of Schiff bases (**66**) is shown in Figure 61. It shows the absence of the strong C=O aldehyde band at *ca.* 1667 cm^{-1} , the strong amine band at *ca.* 3100 cm^{-1} and *ca.* 1633 cm^{-1} (N-H bending) and the appearance of the imine band (N=C) at *ca.* 1629 cm^{-1} . The very broad peak at *ca.* 3000 cm^{-1} is due to intramolecular H-bonding.



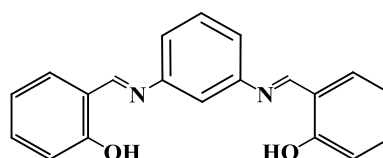
(59)

(60)

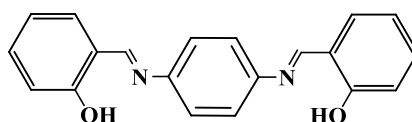
(61)



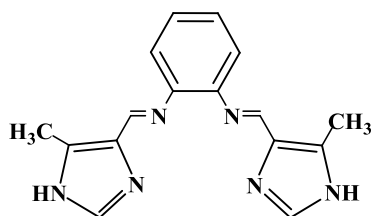
(62)



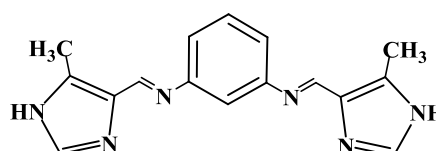
(63)



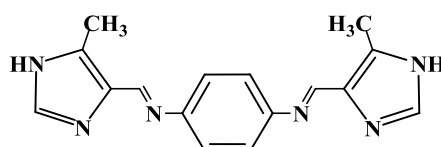
(64)



(65)

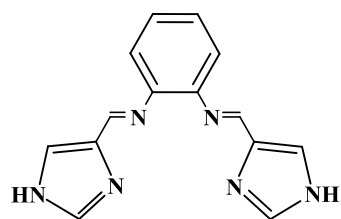


(66)

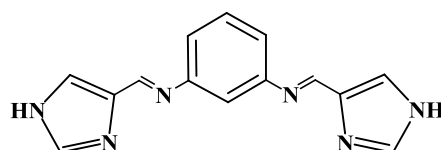


(67)

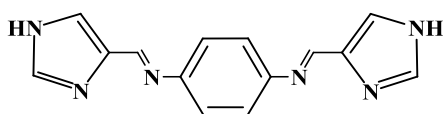
Figure 60 Schiff base ligands derived from 1,2-, 1,3- and 1,4-phenylenediamine.



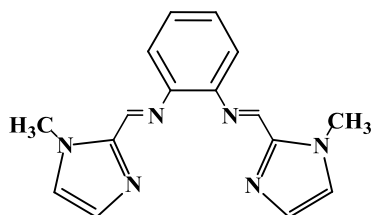
(68)



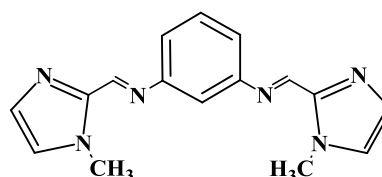
(69)



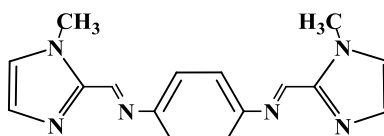
(70)



(71)



(72)



(73)

Figure 60 (contd.) Schiff base ligands derived from 1,2-, 1,3- and 1,4-phenylenediamine.

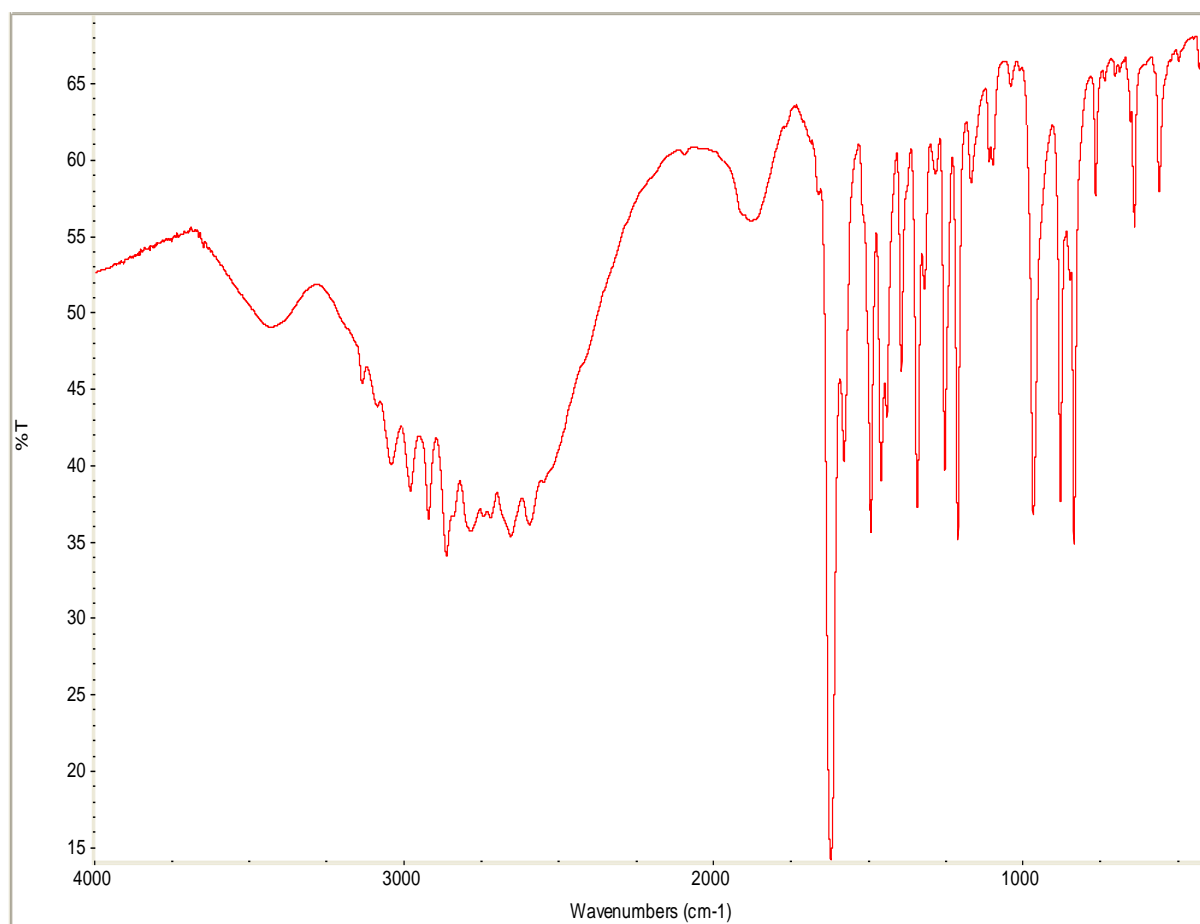


Figure 61 IR spectrum of **(66)**.

The ^1H NMR (d_6 -DMSO) spectrum of **(63)** is shown in Figure 62. The peak for the imine proton is seen at 9.05 ppm (Ha). The peak representing the protons of the two OH groups is seen at 13.01 ppm (He), while the peaks of the phenyl rings are seen at 6.96 ppm, 7.39 ppm, 7.51 ppm and 7.69 ppm.

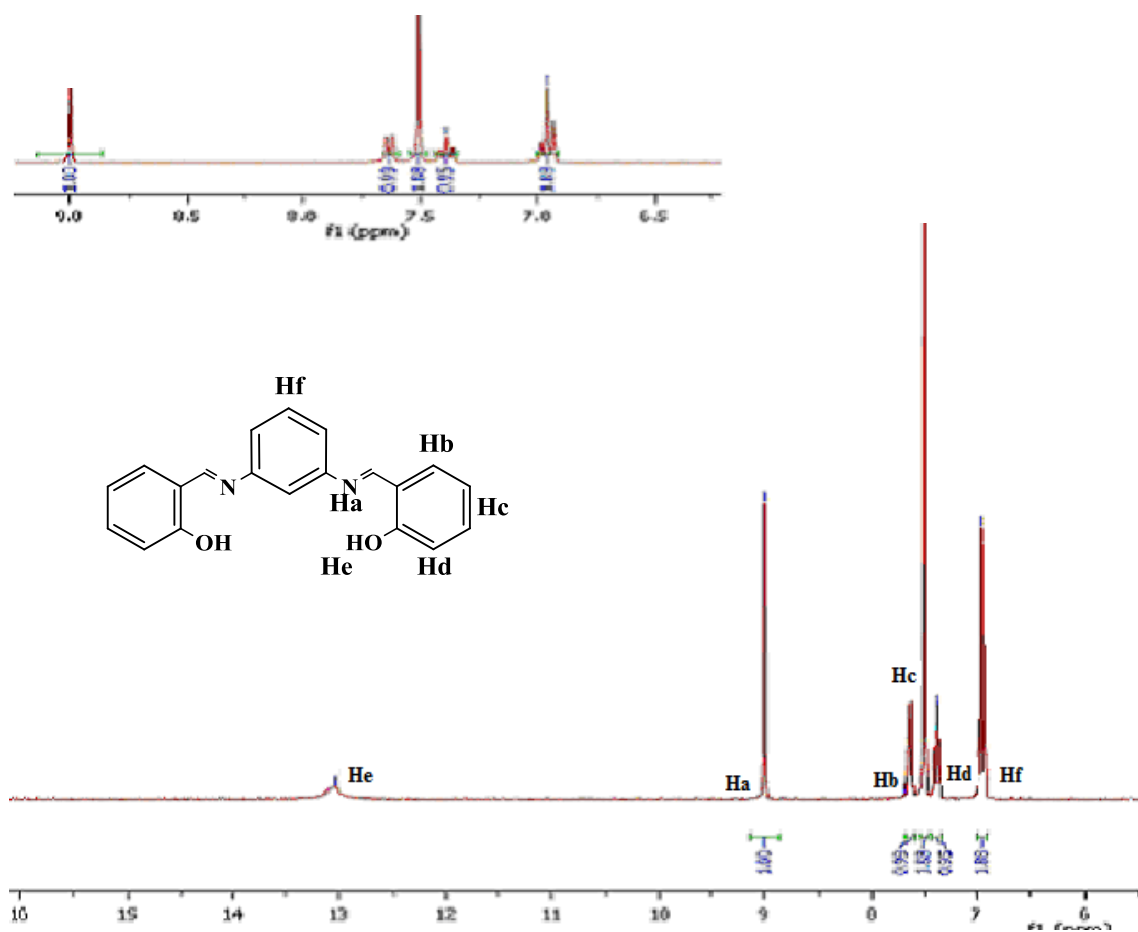


Figure 62 ^1H NMR (d_6 -DMSO) spectrum of (63).

The ^1H NMR (d_6 -DMSO) spectrum of (66) is shown in Figure 63. The imine peak is seen at 8.51 ppm (Hc), while the protons in the 2-position (Hb) are seen at 7.70 ppm. The peaks at 7.40 ppm and 7.03 ppm represent the protons of the aromatic rings. The latter peak at 7.03 ppm comprises two concurrent peaks, giving an area of 3. The singlet for the methyl group is seen at 2.43 ppm.

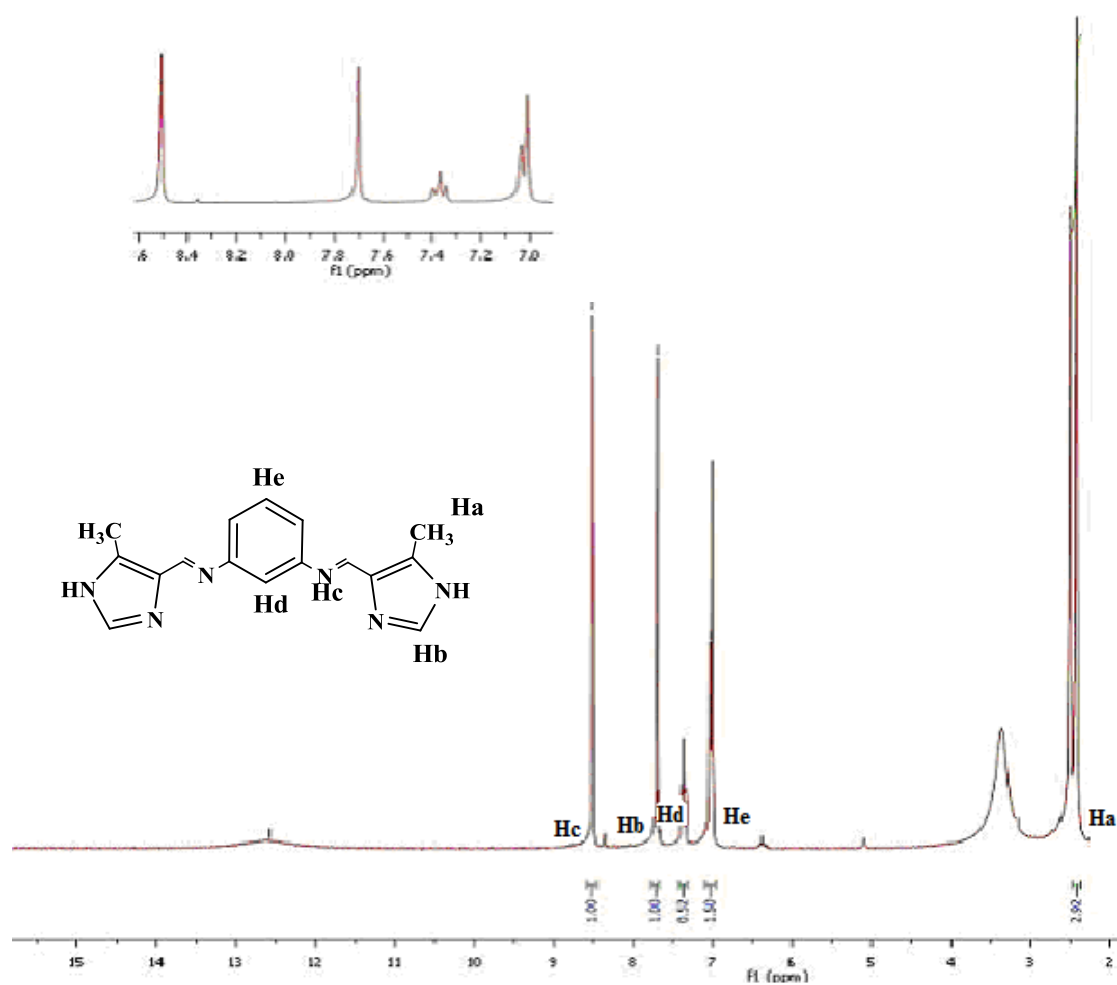


Figure 63 ^1H NMR ($\text{d}_6\text{-DMSO}$) spectrum of (**66**).

3.8 Synthesis of Ag(I) Complexes

Currently, there is renewed interest in the creation of new functional materials and, from this, stems an interest in organic-inorganic materials with coordination bonds between metal centers and ligand donor atoms. This metal-ligand interaction can provide interesting assembly motifs that may be utilized in the creation of novel supramolecular materials. By appropriate ligand design and careful choice of the metal center it is possible to exert control

over the course of a reaction with a reasonable expectation of the outcome of the material in terms of dimensionality and functionality.¹²² Constable *et al.*^{122a} in their study of silver coordinating polymers, used silver(I) because of its variable coordinating numbers and geometries. The flexible bonding interactions of silver, such as silver-donor, silver-silver and silver-hydrogen, as well as its possible photophysical, electronic and biomedical applications, make silver an ideal metal for research.¹²² Papaefstathiou *et al.* used silver in their studies of metal-organic frameworks (MOF) and their possible use as storage facilities because of their porous nature, and if functionalized, possible biological/environmental roles.¹²³

In the absence of X-ray crystal structural data, the Ag(I) complexes presented in this thesis were characterized by microanalysis, IR and, where possible, by NMR spectroscopy. In addition, the structural information from a number of known and related imidazole complexes was used in deciphering the structures of the present Ag(I) complexes.^{31,32,118,124-127}

The Schiff base ligands presented in this study provide good nitrogen donors and their flexible nature, due to the C-N spacer chain, should allow the ligand to bend and rotate when coordinating to the metal, so as to conform to the coordinating geometry demands of the metal.

Abuskhuna *et al.*³¹ reported the X-ray crystal structure of the Ag(I)-2-BIM complex, $[\text{Ag}_2(2\text{-BIM})_2](\text{ClO}_4)_2$ (Figure 64), where the 2-BIM ligand has some similarity to ligand (**25**). The complex is centrosymmetric, containing two $\text{Ag}(2\text{-BIM})^+$ units. The Ag(I) ions are two-coordinate and have identical atoms in the plane of the chelating ligands. Using the two imine N atoms, each 2-BIM ligand bridges a pair of Ag(I) ions. All four N atoms are coplanar and the two imidazole groups in each 2-BIM ligand have an angle of $75.52(8)^\circ$. The two Ag(I) ions are only weakly interacting, the distance separating them being $3.2612(4) \text{ \AA}$.

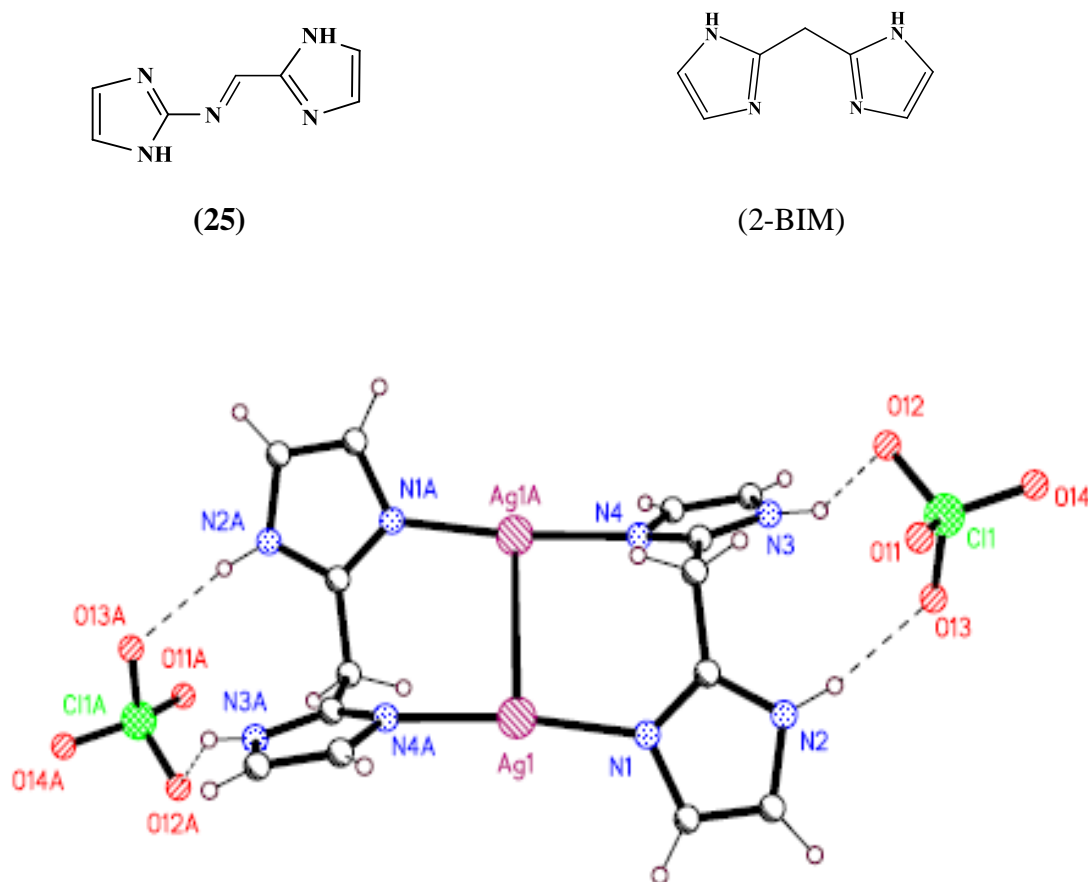


Figure 64 The X-ray crystal structure of $[\text{Ag}_2(2\text{-BIM})_2](\text{ClO}_4)_2$ (showing ligand **(25)** and the structurally related $(2\text{-BIM})^{31}$ ligand).

Jin *et al.*¹²⁴ obtained X-ray crystal structures of Ag(I) complexes of bis(imidazole-1-yl), (BIM) and bis(2-methylimidazole-1-yl)methane, (2-mBIM), (Figure 65). This group used AgNO_2 to synthesise $\{[\text{Ag}(2\text{-m-BIM})_2](\text{NO}_2)_2\}_n$ (Figure 66) and $\text{Ag}(\text{SO}_3\text{CF}_3)$ to synthesise $\{[\text{Ag}(\text{BIM})\text{SO}_3\text{CF}_3]\}_n$ (Figure 67). The X-ray crystal structure of $\{[\text{Ag}(2\text{-m-BIM})_2](\text{NO}_2)_2\}_n$ shows that Ag(I) is coordinated to two imidazoles ligands *via* the imine nitrogens and also to an oxygen of the NO_2^- ion to give a zigzag chain. The N1-Ag(I)-N5 bond distances are 2.123(8) Å and 2.108(8) Å, respectively. There are also weak Ag-Ag interactions which cross-link the chains. The X-ray crystal structure of $\{[\text{Ag}(\text{BIM})\text{SO}_3\text{CF}_3]\}_n$ shows a similar pattern, i.e. the Ag(I) is coordinated to two imidazoles ligands *via* imine nitrogens in a distorted linear geometry. There are also weak Ag-Ag interactions which, again, cross-link

the chains. The overall effect is a one-under one-over 3-D super structure that Jin *et al* called a warp-and-woof network (Figure 67).¹²⁴



Figure 65 (BIM)¹²⁴ and (2-m-BIM).¹²⁴

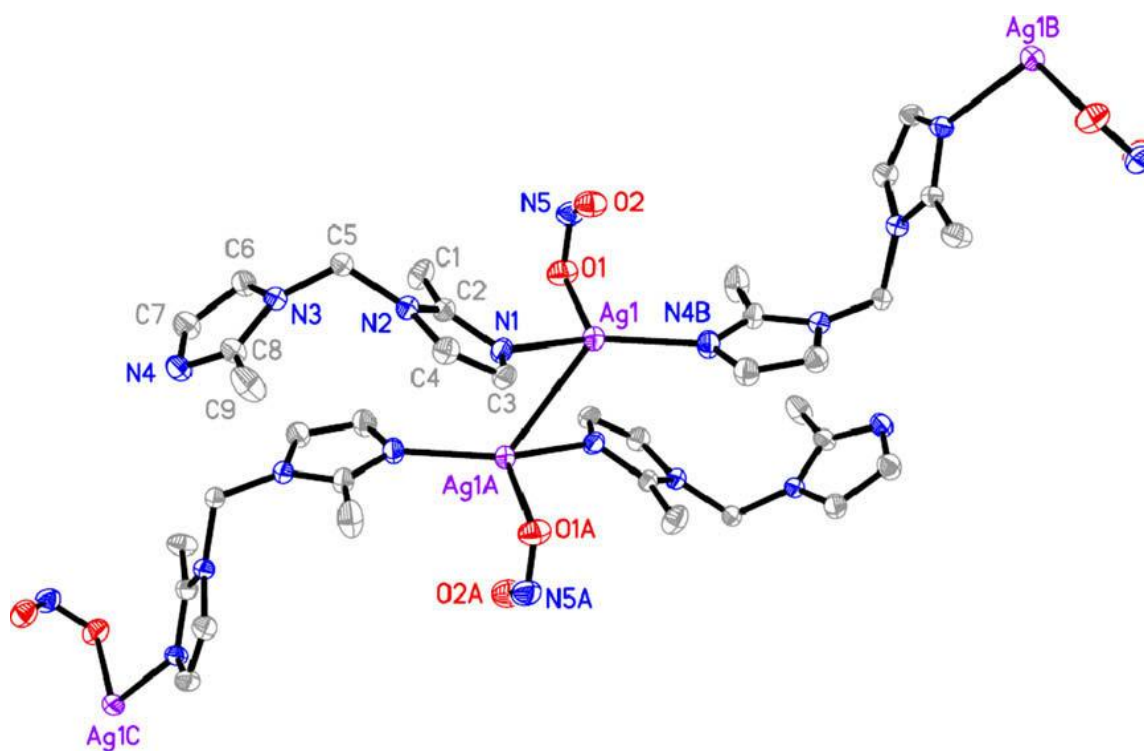


Figure 66 X-ray crystal structure of [Ag(2-m-BIM)₂(NO₂)]_n¹²⁴ showing the Ag-N and Ag-Ag interactions.

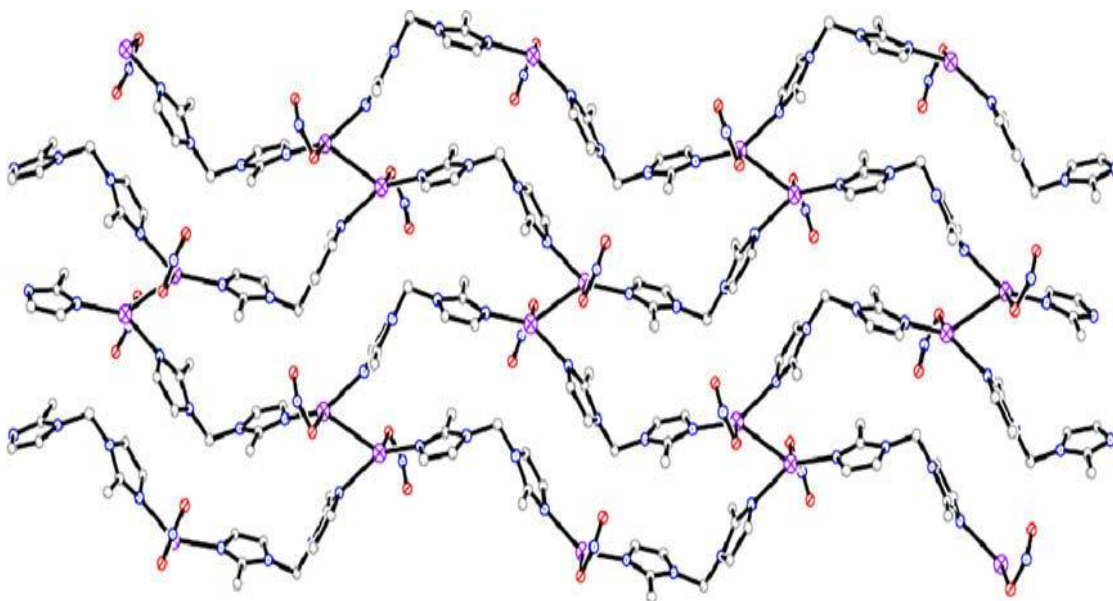


Figure 67 X-ray crystal structure of $\{[\text{Ag}(2\text{-m-BIM})\text{SO}_3\text{CF}_3]_n\}^{124}$ showing the Ag-Ag interactions and the cross-linking of the imidazole chains in the complex.

In earlier work by our research group on simple Ag(I)-imidazole complexes¹²⁵ (Figures 68, 70), we obtained an X-ray crystal structure of the Ag(I)-nitroimidazole complex, $[\text{Ag}(\text{NO}_2\text{imi})_2]\text{ClO}_4 \cdot \text{H}_2\text{O}$ (Figure 68) and the Ag(I)-Apim complex, $[\text{Ag}(\text{Apim})_2]\text{ClO}_4$ (Figure 69). The X-ray analysis of $[\text{Ag}(\text{NO}_2\text{imi})_2]\text{ClO}_4 \cdot \text{H}_2\text{O}$ shows that the Ag(I) ion lies on a center of symmetry and the perchlorate anion lies on a mirror plane, thus the asymmetric unit comprises half the cation, half the anion and one water molecule. The cations are linked into two-dimensional sheets via long Ag-O-N-O-Ag interactions, and these are linked by hydrogen-bonding through the water solvate, through intervening layers containing the perchlorate anion and water molecule. This gives a zigzag shape similar to that found by Jin *et al* for $\{[\text{Ag}(2\text{-m-BIM})\text{SO}_3\text{CF}_3]_n\}$ (Figure 66).¹²⁴

The X-ray structure of $[\text{Ag}(\text{Apim})_2]\text{ClO}_4$ ¹²⁵ (Figure 69) shows the Ag(I) to be coordinated to two imidazoles units *via* the imine nitrogen and the pendent amine nitrogen and also to the oxygen of the ClO_4^- ion in a head-to-tail formation to give a zigzag chain which was also similar to that found by Jin *et al*¹²⁴ (Figures 66 and 67). A similar zigzag pattern was also found for the Ag(I) complex of 2-methyl-4(5)-nitroimidazole, $([\text{Ag}(\text{NO}_2\text{-Me-IMI})_2]\text{ClO}_4 \cdot \text{H}_2\text{O})$, and $[\text{Ag}(\text{Apim})](\text{ClO}_4)$ (Figures 68 and 69).¹²⁵ In $[\text{Ag}(\text{NO}_2\text{-Me-imi})_2]$

$\text{ClO}_4 \cdot \text{H}_2\text{O}$ the metal is coordinated head-to-tail *via* the nitrogens of the imidazoles and also to one of the oxygen's of the NO_2 and to two oxygen of the NO_2 of an adjacent imidazole, thus linking the chains *via* the oxygens. There are also some N-O interactions, between the nitrogen of the imidazole and the ClO_4^- ions. However, there are no Ag-Ag interactions (Figure 69).^{124,125}

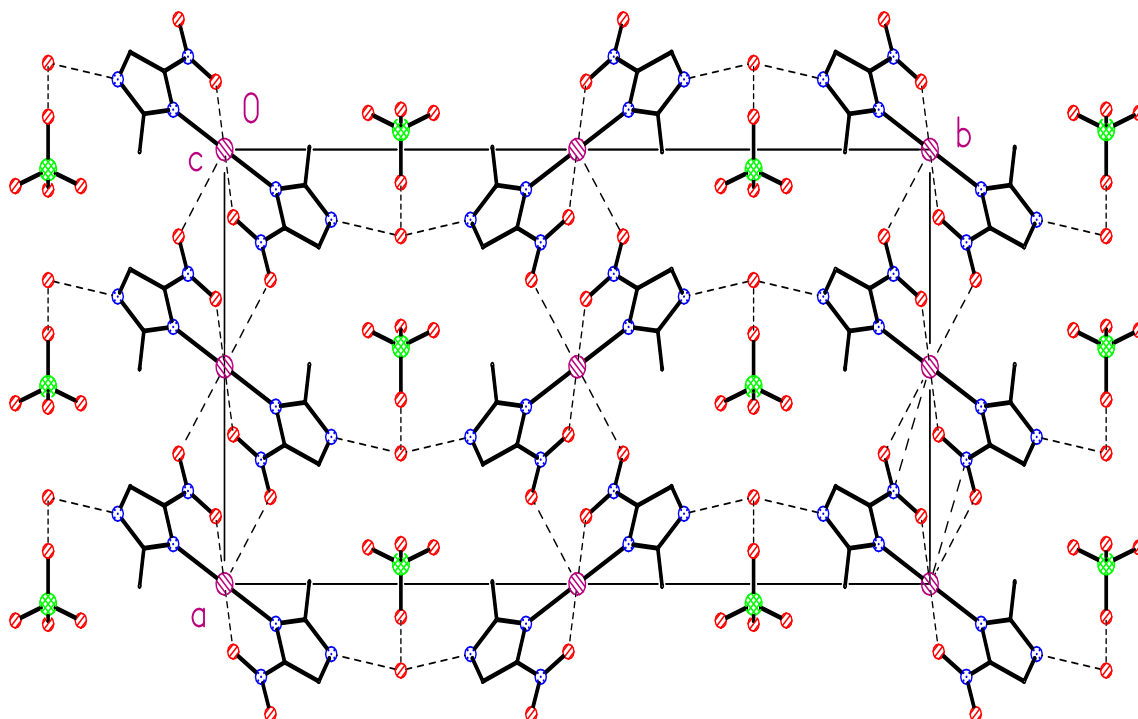


Figure 68 X-ray crystal structure of $[\text{Ag}(\text{NO}_2\text{-2-Me-IMI})_2]\text{ClO}_4 \cdot \text{H}_2\text{O}$ showing the lattice ClO_4^- interactions to give the zigzag shape.¹²⁵

Cui *et al*¹²⁶ found a similar zigzag structural geometry in their study of the Ag(I) complex of bis(1*H*-imidazol-1-yl)methane (1-Bimi), (Figures 70, 71). The X-ray crystal structure of the polymeric Ag(I) complex of $\{[\text{Ag}(1\text{-Bimi})_2](\text{ClO}_4)^+\}_n$, shows that Ag(I) is coordinated to two imidazoles units *via* the imine nitrogens, again, giving a zigzag chain (Figure 71a). In this case there are no Ag-Ag interactions.¹²⁴ However, there are interactions between the Ag(I) ion of one chain and the nitrogens of the adjacent chain which act to cross-link the chains.¹²⁶ In order to achieve these cross-linking interactions the chains are off-set relative to

each other so that each Ag(I) is coordinate to the two nitrogens of opposite imidazoles, making each Ag(I) ion six-coordinate. The ClO_4^- anions are not coordinated. The complex has a highly ordered, cationic, polymeric superstructure (Figure 71b).

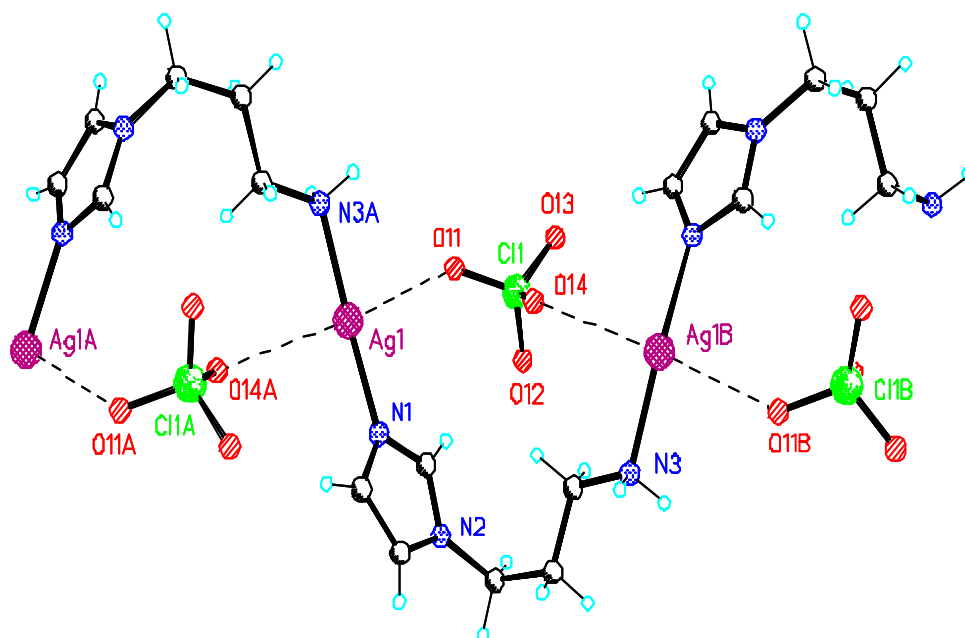


Figure 69 X-ray crystal structure of $[\text{Ag}(\text{Apim})]\text{ClO}_4$.¹²⁵

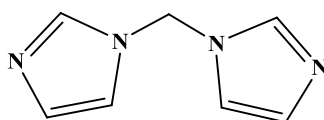


Figure 70 Bis(1*H*-imidazol-1-yl)methane (1-Bimi)¹²⁶

A zigzag structural geometry was also seen in the X-ray crystal structure of the metal-free ligands (36) and (37) (Figures 50 and 53). This suggests that this may be the energetically or the sterically preferred geometry of this type of ligand and possibly its silver complex in the solid state. Ibrahim and Etaiw *et al*¹⁰⁷ suggested that the bonding of the ligand to Ag(I) is controlled by the chain length, and that a short or a very long spacer chain may inhibit the

formation of a supramolecular architecture. These researchers also suggested that the imine group may activate the phenol group (also a future of the present research ligands) through intermolecular hydrogen bonding. The activated phenol group can then be used in forming self-assembled, helicate-type supramolecular complexes,¹⁰⁶ which is in keeping with the X-ray crystal structure obtained by Abuskhuna *et al.*³¹

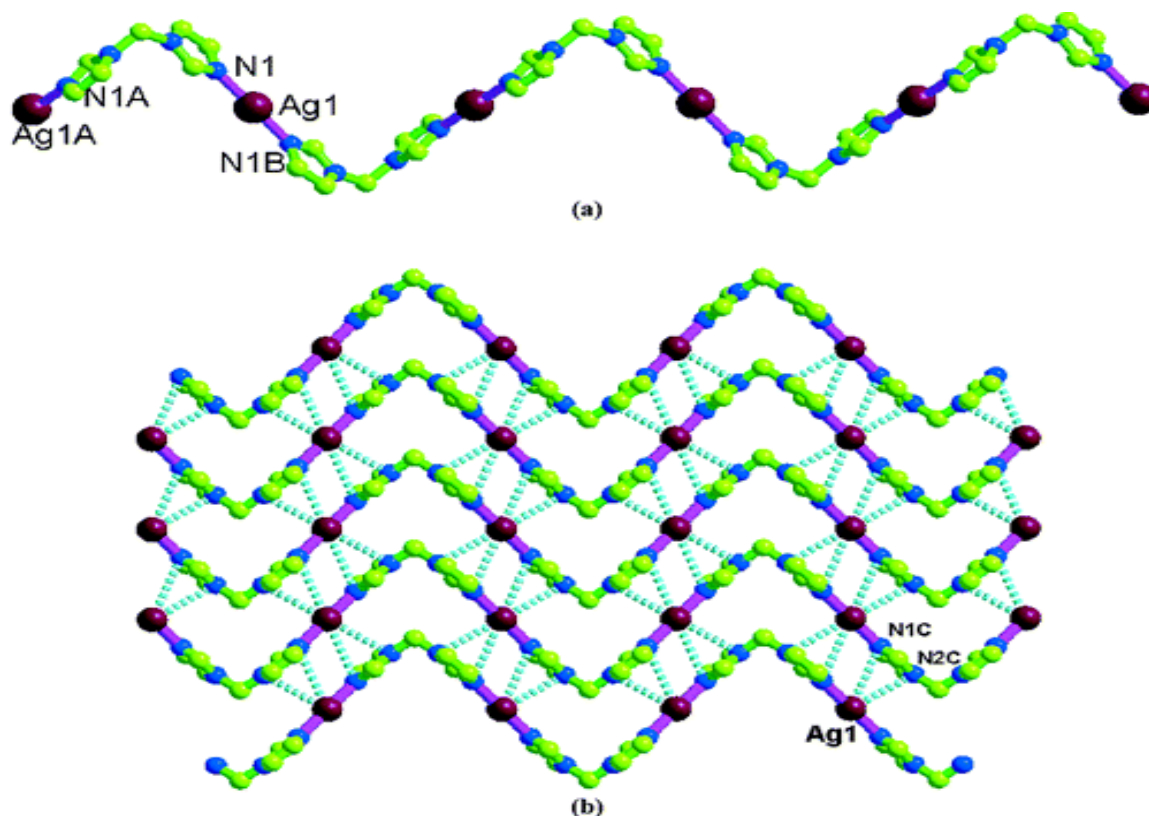


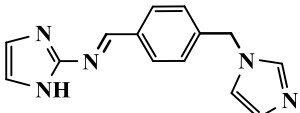
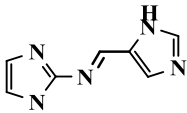
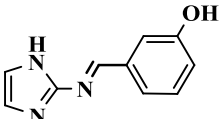
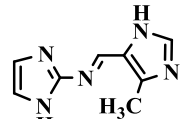
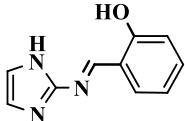
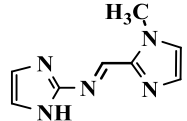
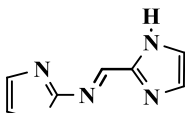
Figure 71 The X-ray crystal structure of $\{[Ag(1-Bimi)_2](ClO_4)]^+\}_n$ showing (a) the Ag-N coordination and (b) Ag(I) cross-linking between the chains.¹²⁶

These examples go some way to demonstrate the variable coordination numbers and geometries that are possible for silver-imidazole complexes. Given the structural similarity of these examples to the ligands presented in this thesis, it is thought that the Ag(I) complexes of these ligands may have similar geometries.

3.9 Synthesis of the Ag(I) Complexes of the Schiff Base Ligands Derived from 1*H*-Imidazole-2-amine (1)

The seven Schiff base ligands ((22)-(28)) were each reacted with an excess of AgClO₄ at room temperature to give the respective Ag(I) complexes (Table 1) in moderate yields. The complexes were only soluble in hot DMSO and attempts to grow crystals suitable for X-ray crystal structure analysis were unsuccessful. Empirical formulae are proposed mainly on the basis of microanalytical, IR and NMR spectroscopic data. While three of the complexes were

Table 1 Ligand structures and empirical formulae of the Ag(I) complexes of Schiff bases derived from 1*H*-Imidazole-2-amine (1).

Ligand	Empirical formula	Ligand	Empirical formula
 (22)	[Ag(22) ₂]ClO ₄	 (26)	[Ag(26)]ClO ₄
 (23)	[Ag(23) ₂]ClO ₄	 (27)	[Ag(27)]ClO ₄
 (24)	[Ag(24) ₂]ClO ₄	 (28)	[Ag(28)]ClO ₄
 (25)	[Ag(25)]ClO ₄		

formulated on the bases of a 1:2 Ag:ligand ratio, the remainder had a 1:1 Ag:ligand ratio. The IR spectra of all the metal complexes show characteristic bands at *ca.* 1100 and 625 cm^{-1} associated with the $\nu_{\text{asym}}\text{ClO}_4$ and $\nu_{\text{sym}}\text{ClO}_4$ stretching frequencies, respectively, of the perchlorate anion.³¹ In addition, the C=N stretching band for the imine functionalities of the metal-free Schiff base ligands shift from *ca.* 1650 cm^{-1} to *ca.* 1600 cm^{-1} upon complexation to the Ag(I) centre. In these spectra, it was impossible to distinguish between the imidazole C=N band and the C=N band of the imine function of the spacer chain. Representative IR spectra for the metal-free ligand (**24**) and its Ag(I) complex are shown in Figure 78.

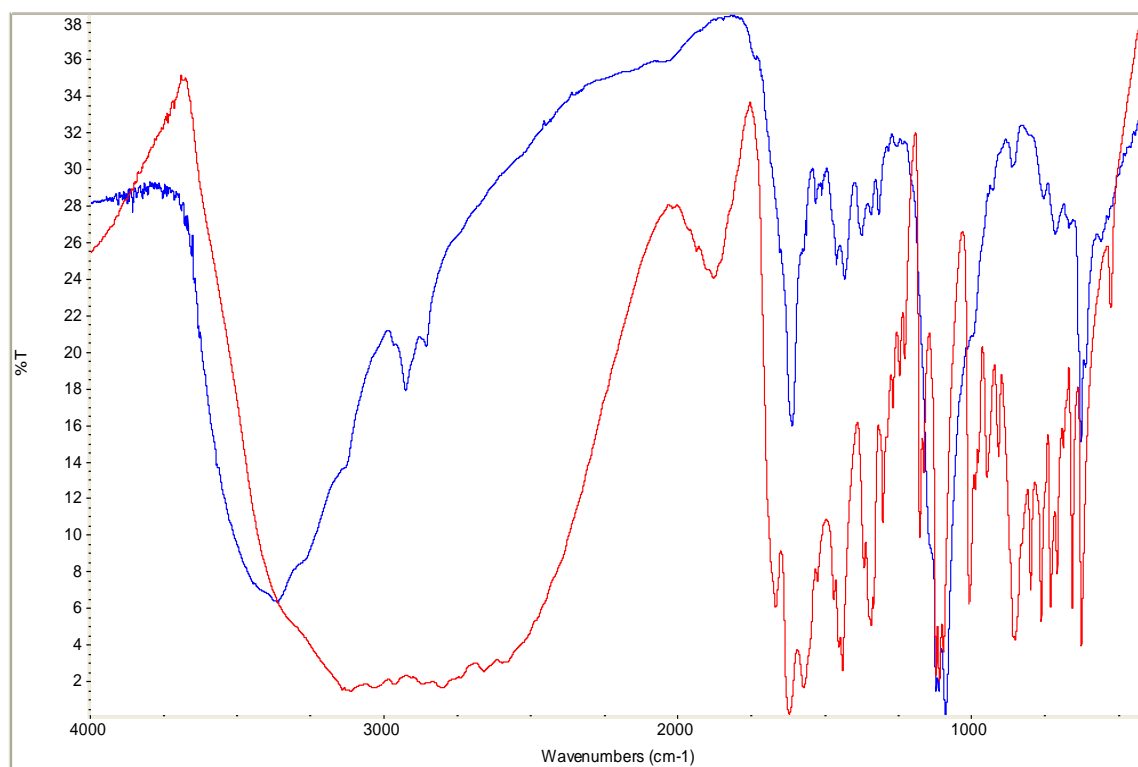


Figure 78 IR spectra of ligand (**24**) (red) and $[\text{Ag}(\mathbf{24})_2]\text{ClO}_4$ (blue).

The only Ag(I) complexes which were sufficiently soluble in d_6 -DMSO to allow full NMR spectral analysis were $[\text{Ag}(\mathbf{22})_2]\text{ClO}_4$, $[\text{Ag}(\mathbf{25})]\text{ClO}_4$, $[\text{Ag}(\mathbf{26})]\text{ClO}_4$ and $[\text{Ag}(\mathbf{27})]\text{ClO}_4$. The highly insoluble nature of the Ag(I) complexes suggest that they may have a polymeric structure. A comparison of the ^1H NMR spectra of ligand (**26**) and its Ag(I) complex, $[\text{Ag}(\mathbf{26})]\text{ClO}_4$ (Figure 79), shows that there is no significant shift for the imine proton of the spacer chain of the metal-free ligand (9.00 ppm) compared to the same proton in the Ag(I) complex (9.10 ppm). This suggests that the imine N atom in the spacer chain is not involved

in coordination to the silver ion. In contrast, a large shift is observed in the positions of the signals of the 4(5) protons adjacent to the imine N atoms of the two imidazole rings (7.09 and 7.81 ppm) upon complexation to the metal ion (7.15 ppm and 7.45 ppm, respectively). This downfield shift is indicative of coordination of the imidazole rings to metal centres.^{31,125,126} The N-H peak of the imidazole, which is barely distinguishable in the spectrum of the metal-free ligand, is very clearly observed in the spectrum (*ca.* 13 ppm) of the Ag(I) complex, indicating possible coordination of the imidazole ring (via the imine N atom of the ring).

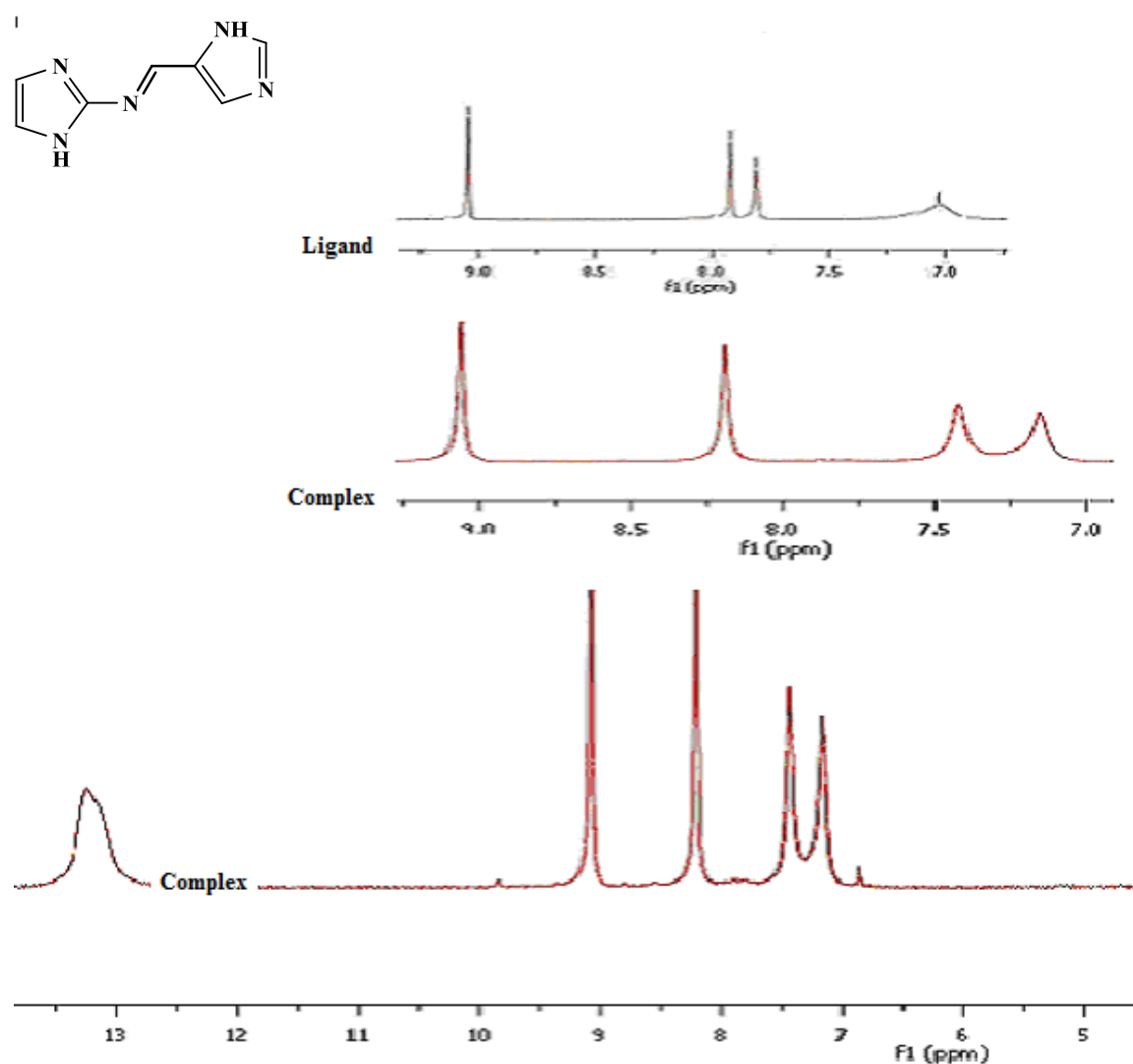


Figure 79 ^1H NMR (d_6 -DMSO) spectra for ligand (26) and the Ag(I) complex $[\text{Ag}(26)]\text{ClO}_4$.

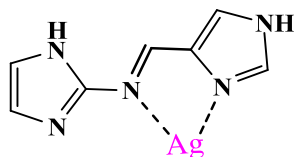


Figure 80 A possible metal-ligand chelating interaction for complexes $[\text{Ag}(\mathbf{25})]\text{ClO}_4$.

In the case of $[\text{Ag}(\mathbf{26})]\text{ClO}_4$ the ligands could possibly chelate to the metal centre using the imine N-atom in the linker chain and the imine N of one of the imidazoles rings as shown in Figure 80. However, this possible structure can be ruled out on the basis of the ^1H NMR spectral data, which shows that there is no change in the position of the proton on the imine carbon atom of the spacer chain (9.20 ppm for both the metal-free ligand and for the complex). The relative insolubility of the complex suggests that it may have a polymeric structure, as outlined in Figure 81. In this structure, the Ag(I) ions are ligated by imidazole imine N atoms on the adjacent ligands. The poor solubility of $[\text{Ag}(\mathbf{25})]\text{ClO}_4$ in d_6 -DMSO prevented complete resolution of its ^1H NMR spectrum (broad signals at the positions quoted in the experimental section). It is anticipated that the structure of $[\text{Ag}(\mathbf{25})]\text{ClO}_4$ is similar to that shown for $[\text{Ag}(\mathbf{26})]\text{ClO}_4$ (Figure 81).

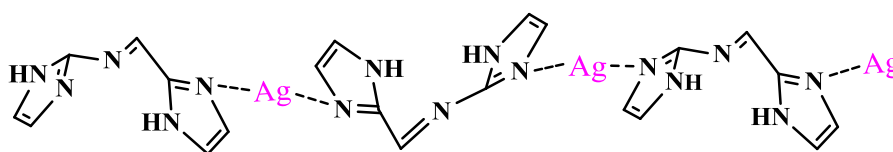


Figure 81 Possible polymeric structure for $[\text{Ag}(\mathbf{26})]\text{ClO}_4$ (ClO_4^- ion omitted for clarity).

In the case of ligands (**23**) and (**24**), which contain phenolic moieties, the phenols do not seem to deprotonate upon coordination to the Ag(I) centre as a ClO_4^- ion is present in the formulation of the respective 1:2 Ag:ligand complexes, $[\text{Ag}(\mathbf{23})_2]\text{ClO}_4$ and $[\text{Ag}(\mathbf{24})_2]\text{ClO}_4$. A

plausible polymeric structure for $[\text{Ag}(\mathbf{23})_2]\text{ClO}_4$ is shown in Figure 82. This proposed structure is very similar to that reported for the closely related, highly insoluble and structurally characterised Ag(I) complex, $[\text{Ag}(\text{sal-imi})_2]\text{ClO}_4 \cdot 2\text{H}_2\text{O}$ (Figures 83, 84).^{31b} The sal-imi Schiff base ligand is an isomer of ligands **(23)** and **(24)**.

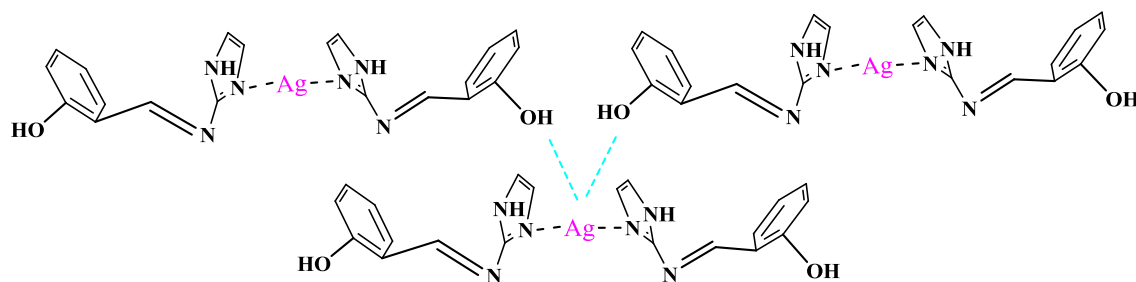


Figure 82 Possible polymeric structure for $[\text{Ag}(\mathbf{23})_2]\text{ClO}_4$.

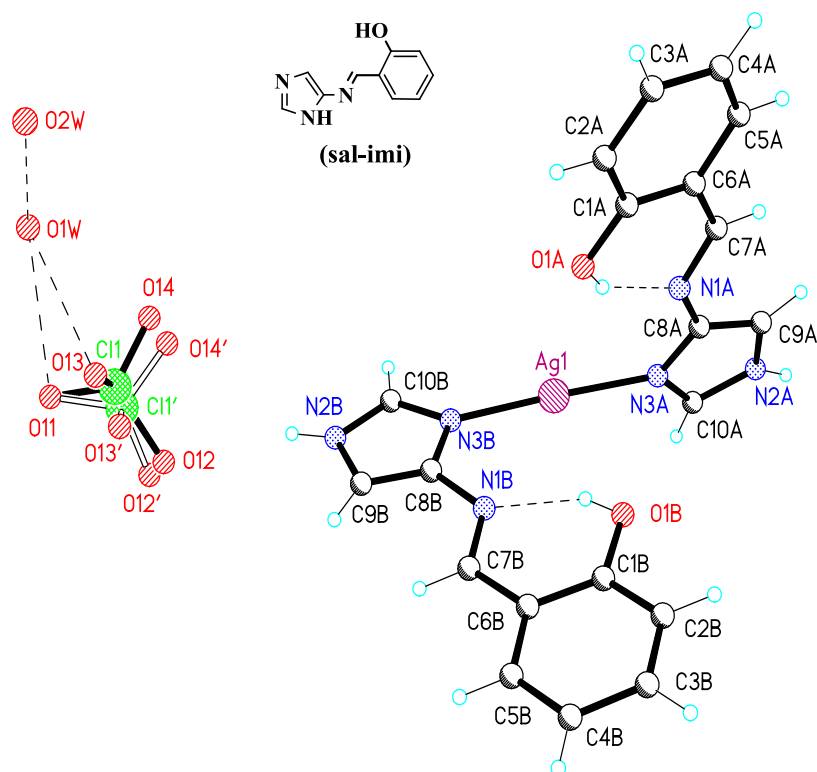


Figure 83 X-ray crystal structure of $[\text{Ag}(\text{sal-imi})_2]\text{ClO}_4 \cdot 2\text{H}_2\text{O}$.^{31(b)}

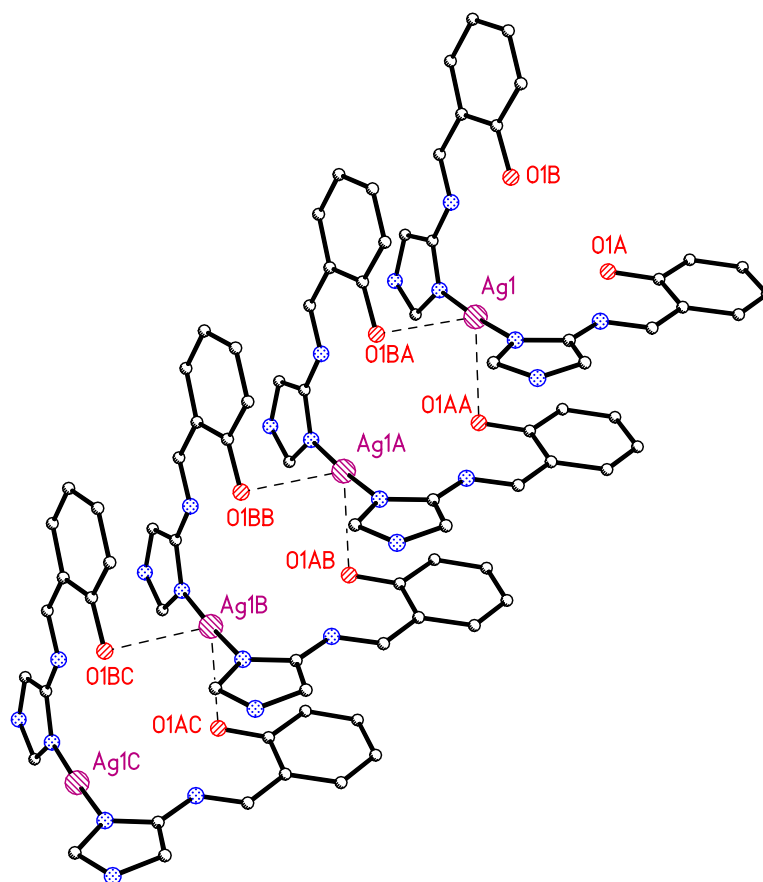


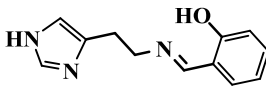
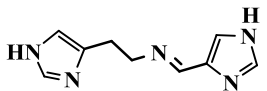
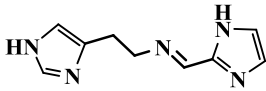
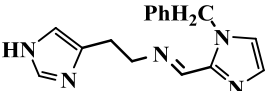
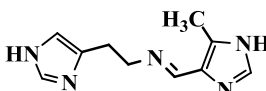
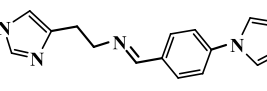
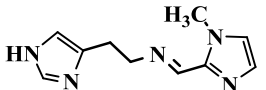
Figure 84 Packing diagram for $[\text{Ag}(\text{sal-imi})_2]\text{ClO}_4 \cdot 2\text{H}_2\text{O}$ (ClO_4^- omitted for clarity).³¹

3.10 Synthesis of the Ag(I) Complexes of the Schiff Base Ligands Derived from Histamine

The Schiff base ligands containing the histamine moiety, ((29)-(35)), were reacted with an excess of AgClO_4 at room temperature to give the respective Ag(I) complexes (Table 2) in moderate to good yield. Again, these complexes were only soluble in hot DMSO. Three of the complexes formulated with a 1:1 Ag:ligand ratio, three had a 1.5:1 ratio and one had a 2:1

ratio. IR spectral bands associated with the perchlorate anion and the imine functionalities were clearly visible. Representative IR spectra of the metal-free ligand (**29**) and its Ag(I) complex, $[\text{Ag}(\mathbf{29})]\text{ClO}_4$, are illustrated in Figure 85. Extremely poor solubility in DMSO prevented the capture of good quality ^1H NMR spectra. The insolubility of these complexes, coupled with the close structural similarities between these histamine-based Schiff base ligands and those derived from imidazole-2-amine, suggests that they are essentially isostructural with the polymeric Ag(I) complexes formed by the 1*H*-imidazole-2-amine (**1**) ligand set.

Table 2 Ligand structures and empirical formulae of the Ag(I) complexes of Schiff bases derived from histamine.

Ligand structure	Empirical formula	Ligand structure	Empirical formula
 (29)	$[\text{Ag}(\mathbf{29})]\text{ClO}_4$	 (33)	$[\text{Ag}_{1.5}(\mathbf{33})](\text{ClO}_4)_{1.5}$
 (30)	$[\text{Ag}_{1.5}(\mathbf{30})](\text{ClO}_4)_{1.5}$	 (34)	$[\text{Ag}(\mathbf{34})]\text{ClO}_4$
 (31)	$[\text{Ag}_{1.5}(\mathbf{31})](\text{ClO}_4)_{1.5}$	 (35)	$[\text{Ag}_2(\mathbf{35})](\text{ClO}_4)_2$
 (32)	$[\text{Ag}_{1.5}(\mathbf{32})](\text{ClO}_4)_{1.5}$		

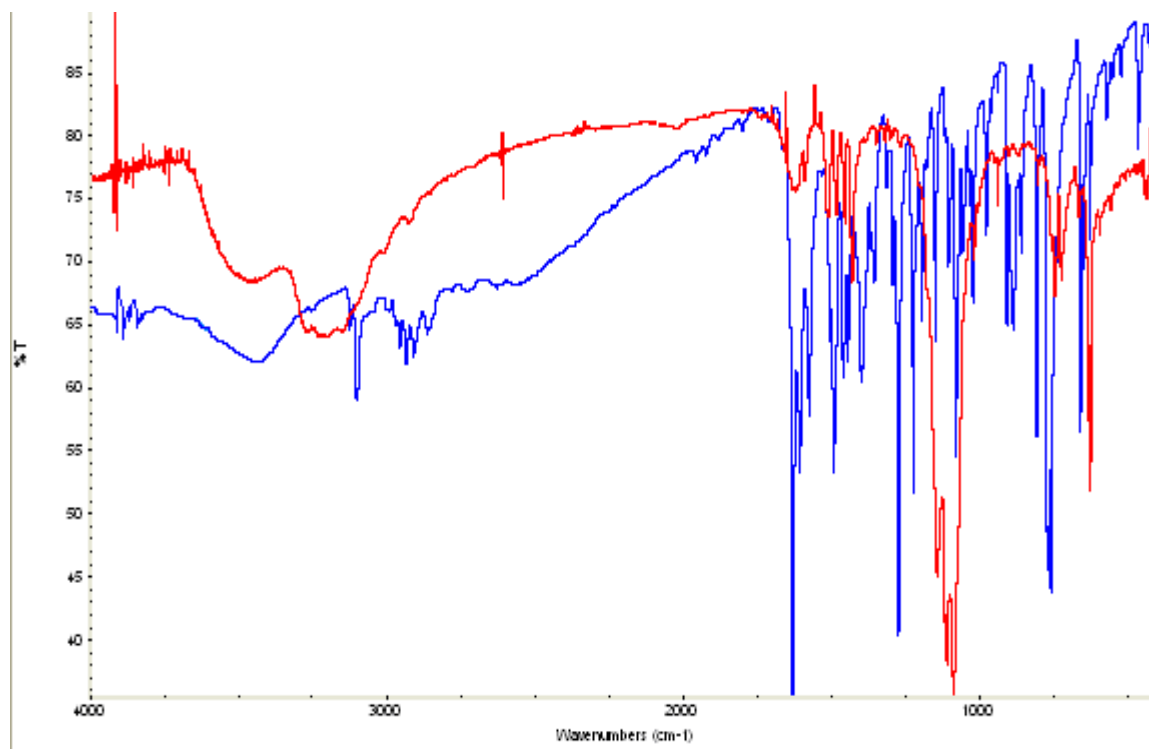
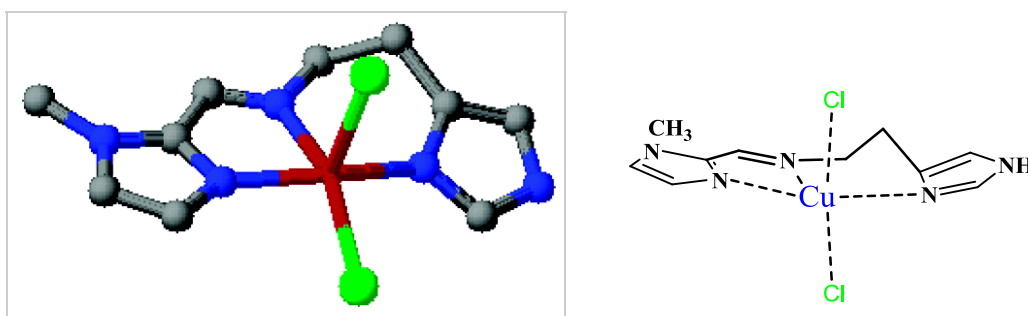
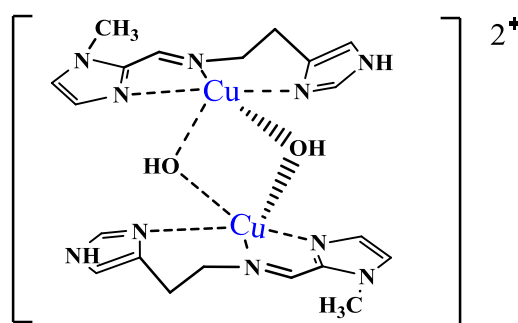
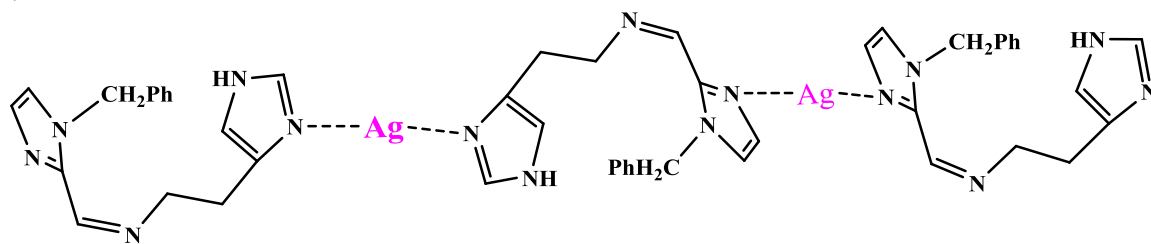


Figure 85 IR spectra of ligand **(29)** (blue) and its Ag(I) complex, [Ag**(29)**]ClO₄ (red).

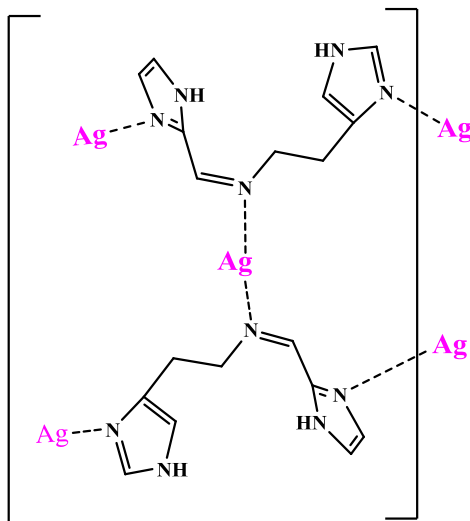
Scarpellini *et al.*¹⁰⁴ reported the X-ray crystal structures of mononuclear and binuclear Cu(II) complexes of the Schiff base, **(32)**. The complexes formulated as [Cu**(32)**Cl₂] and [Cu₂(b(32)₂(OH)₂)(ClO₄)₂·2H₂O and their structures are shown in Figure 86. In both complexes, the three imine N atoms (two from the imidazole rings and one from the spacer chain) are chelated to the metals and the five-coordinate geometry is completed by two chloro or hydroxo ligands. Although these two Cu(II) structures clearly illustrate the flexibility of ligand **(32)** and its ability to chelate to a single metal centre it is not thought that it adopts this coordination mode in the Ag(I) complex, [Ag_{1.5}(b(32))](ClO₄)_{1.5}.

[Cu(**32**)Cl₂][Cu₂(**32**)₂(OH)₂](ClO₄)₂·2H₂O.**Figure 86** Structures of [Cu(**32**)Cl₂] and [Cu₂(**32**)₂(OH)₂](ClO₄)₂·2H₂O.¹⁰⁴

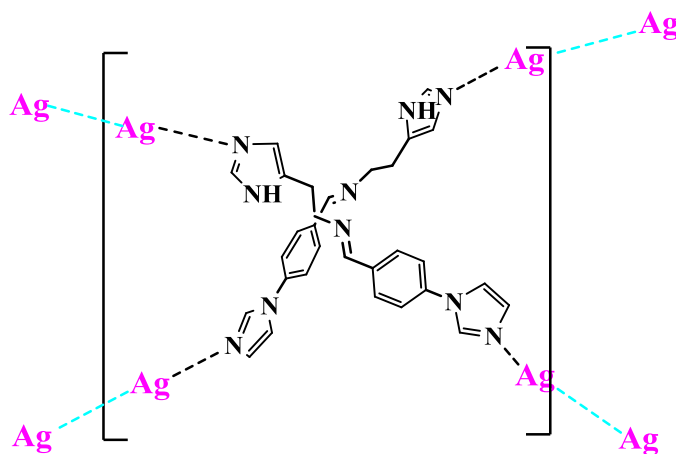
Shown in Figure 87 are some possible structures for the set of Ag(I) complexes containing Schiff base ligands derived from histamine. These structures take into account the polymeric nature of the complexes and the various metal:ligand ratios (1:1, 1.5:1 and 2:1). The structure for the 1:1 Ag(I):ligand complex, [Ag(**34**)]ClO₄ (Figure 87 (a)), is similar to that given for [Ag(2-m-BIM)SO₃CF₃]_n (Figure 67)¹²⁴ and {[Ag(1-Bimi)₂](ClO₄)⁺]_n¹²⁶ (Figure 71). The proposed structure for the 1.5:1 Ag(I):ligand complex [Ag_{1.5}(**30**)](ClO₄)_{1.5} is shown in Figure 87 (b). The proposed structure for the 2:1 Ag(I):ligand complex, [Ag₂(**35**)](ClO₄)₂ (Figure 87 (c)), is in accordance with the interwoven “warp-and-woof” type 2D sheet network found for polymeric [Ag(2-m-BIM)SO₃CF₃]_n¹²⁴ (Figure 88). The latter polymer is also cross linked through interchain Ag–Ag interactions.



(a) Possible structure of the 1:1 Ag:ligand complex $[\text{Ag}(\mathbf{34})]\text{ClO}_4$ (ClO_4^- not shown).



(b) Possible structure of the 1.5:1 Ag:ligand complex $[\text{Ag}_{1.5}(\mathbf{30})](\text{ClO}_4)_{1.5}$ (ClO_4^- not shown).



(c) Possible structure of the 2:1 Ag:ligand complex $[\text{Ag}_2(\mathbf{35})](\text{ClO}_4)_2$ (ClO_4^- not shown).

Figure 87. Possible polymeric structures for (a) 1:1 Ag:ligand complex $[\text{Ag}(\mathbf{34})]\text{ClO}_4$, (b) 1.5:1 Ag:ligand complex $[\text{Ag}_{1.5}(\mathbf{30})](\text{ClO}_4)_{1.5}$ and (c) 2:1 Ag:ligand complex $[\text{Ag}_2(\mathbf{35})](\text{ClO}_4)_2$.

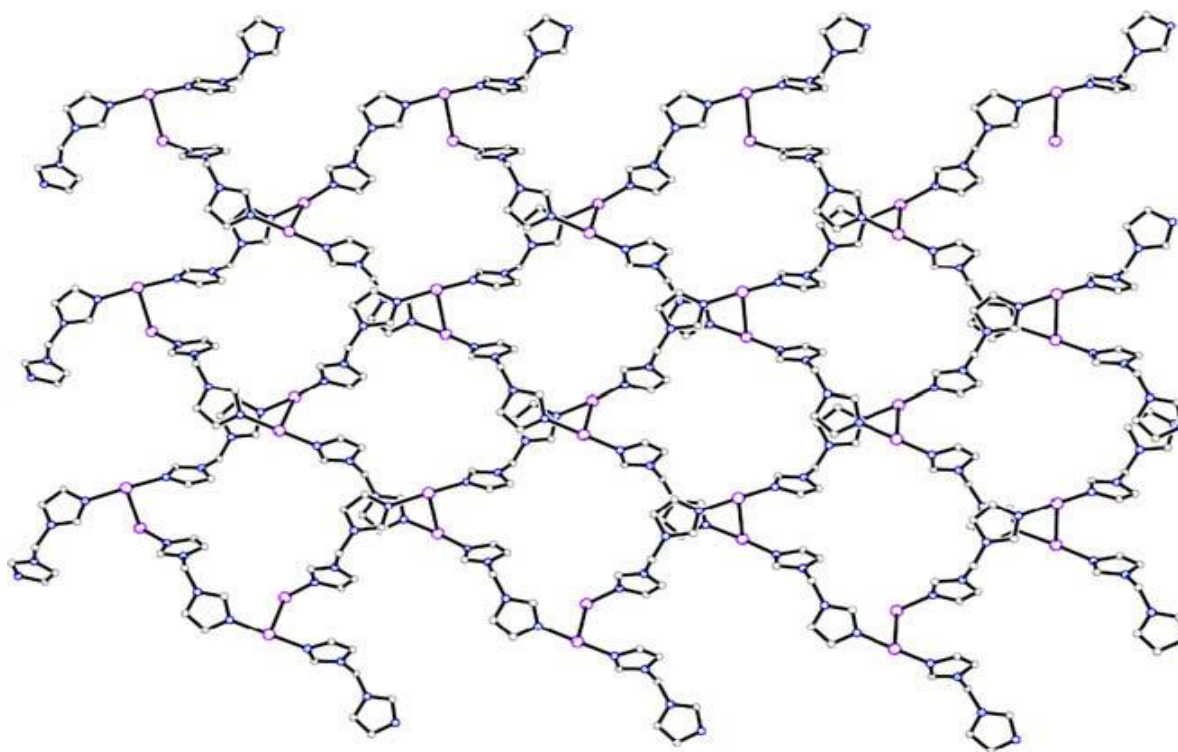
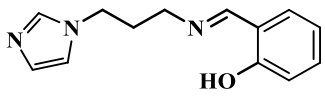
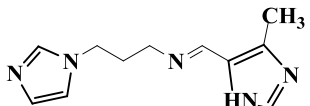
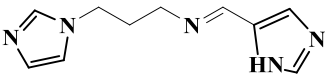
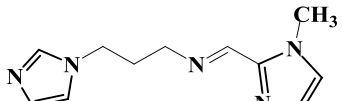
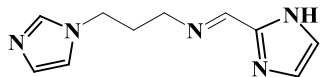


Figure 88 A view of $\{[\text{Ag}(2\text{-m-BIM})\text{SO}_3\text{CF}_3]\}_n$ showing the interwoven ‘warp-and-woof’ like 2D sheet network and inter-chain Ag–Ag interactions.¹²⁴

3.11 Synthesis of the Ag(I) Complexes of the Schiff Base Ligands Derived from Apim

The Schiff base ligands containing the Apim moiety ((**36**)-(40)) were reacted with an excess of AgClO_4 at room temperature to give the respective Ag(I) complexes (Table 3) in high yield. Unlike the Ag(I) complexes of the ligands derived from 1*H*-imidazole-2-amine (**1**) and histamine, the five Ag(I) complexes with ligands based on the Apim moiety were reasonably soluble in DMSO. Four of the complexes formulated with a 1:1 Ag:ligand ratio and the remaining complex, $[\text{Ag}(\mathbf{36})_2]\text{ClO}_4$, had a 1:2 ratio.

Table 3 Ligand structures and empirical formulae of the Ag(I) complexes derived from Apim.

Ligand structure	Empirical formula	Ligand structure	Empirical formula
 <p style="text-align: center;">(36)</p>	[Ag (36)] ₂ ClO ₄	 <p style="text-align: center;">(39)</p>	[Ag (39)]ClO ₄
 <p style="text-align: center;">(37)</p>	[Ag (37)]ClO ₄	 <p style="text-align: center;">(40)</p>	[Ag (40)]ClO ₄
 <p style="text-align: center;">(38)</p>	[Ag (38)]ClO ₄		

IR spectral bands associated with the perchlorate anion (*ca.* 1100 and 625 cm⁻¹) and the imine (*ca.* 3100 cm⁻¹) functionalities were clearly visible. The IR spectra of the metal-free ligand **(40)** and its Ag(I) complex [Ag**(40)**]ClO₄ are shown in Figure 89.

The ¹H NMR (d₆-DMSO) spectra of ligand **(39)** and its Ag(I) complex, [Ag**(39)**]ClO₄, are shown in Figure 90. The imine peak in the spacer chain of the metal-free ligand is seen at 8.20 ppm, and is significantly moved in the corresponding Ag(I) complex (8.58 ppm). The two coalescing peaks representing the protons in the 2-position of the imidazoles of the metal-free ligand, at 7.50 ppm and 7.60 ppm, are shifted downfield and become two sharp peaks at 7.80 ppm and 8.20 ppm in the Ag(I) complex. This downfield shift is also seen for the two peaks of the protons in the 4(5)-position which are shifted from 6.90 ppm and 7.20 ppm to 7.10 ppm and 7.40 ppm, respectively. Again, the N-H peak at 13 ppm in the Ag(I) complex is sharper and is shifted downfield compared to that of the metal-free ligand (12.20 ppm).

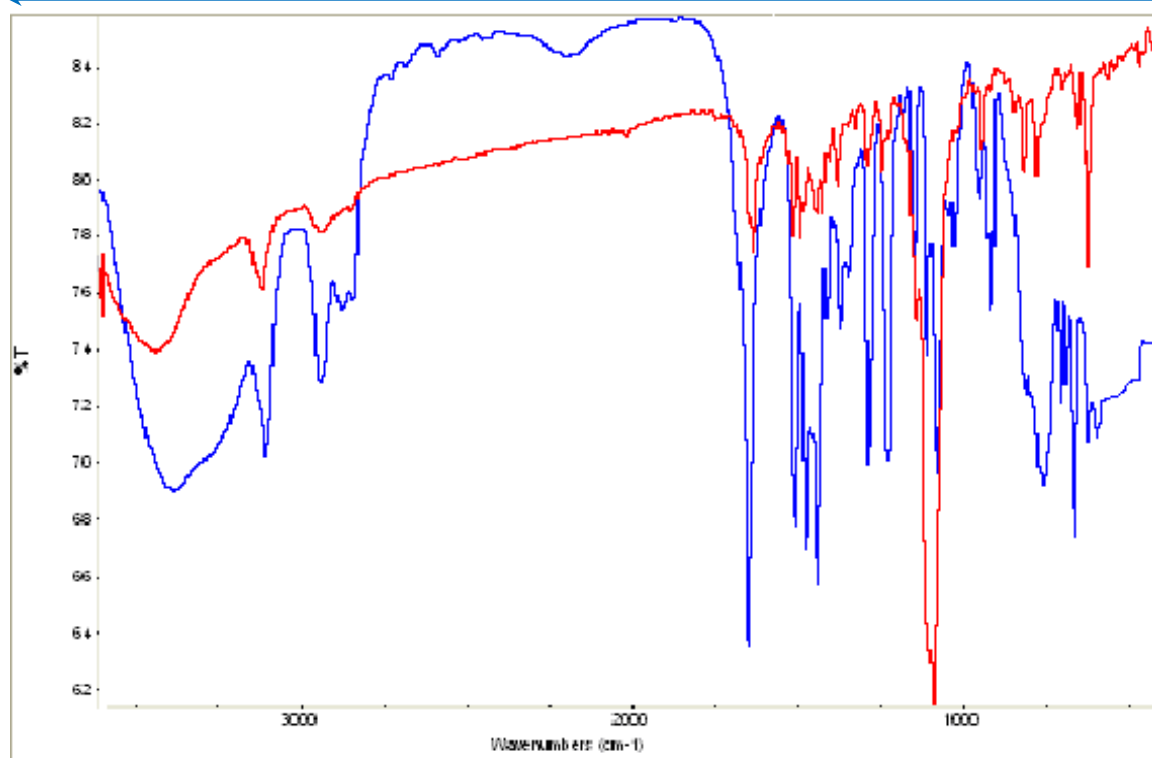


Figure 89 IR spectra of ligand (40) (blue) and its Ag(I) complex, [Ag(40)]ClO₄, (red).

These ¹H NMR spectra suggests that Ag(I) coordination is at the N atom of the imine of the imidazoles, not at the imine N atom of the spacer chain. Such a coordination mode is consistent with that found by Jin *et al.*¹²⁴ and Cui *et al.*¹²⁶ A possible polymeric structure for the representative Ag(I) complex, [Ag(37)]ClO₄, is given in Figure 91.

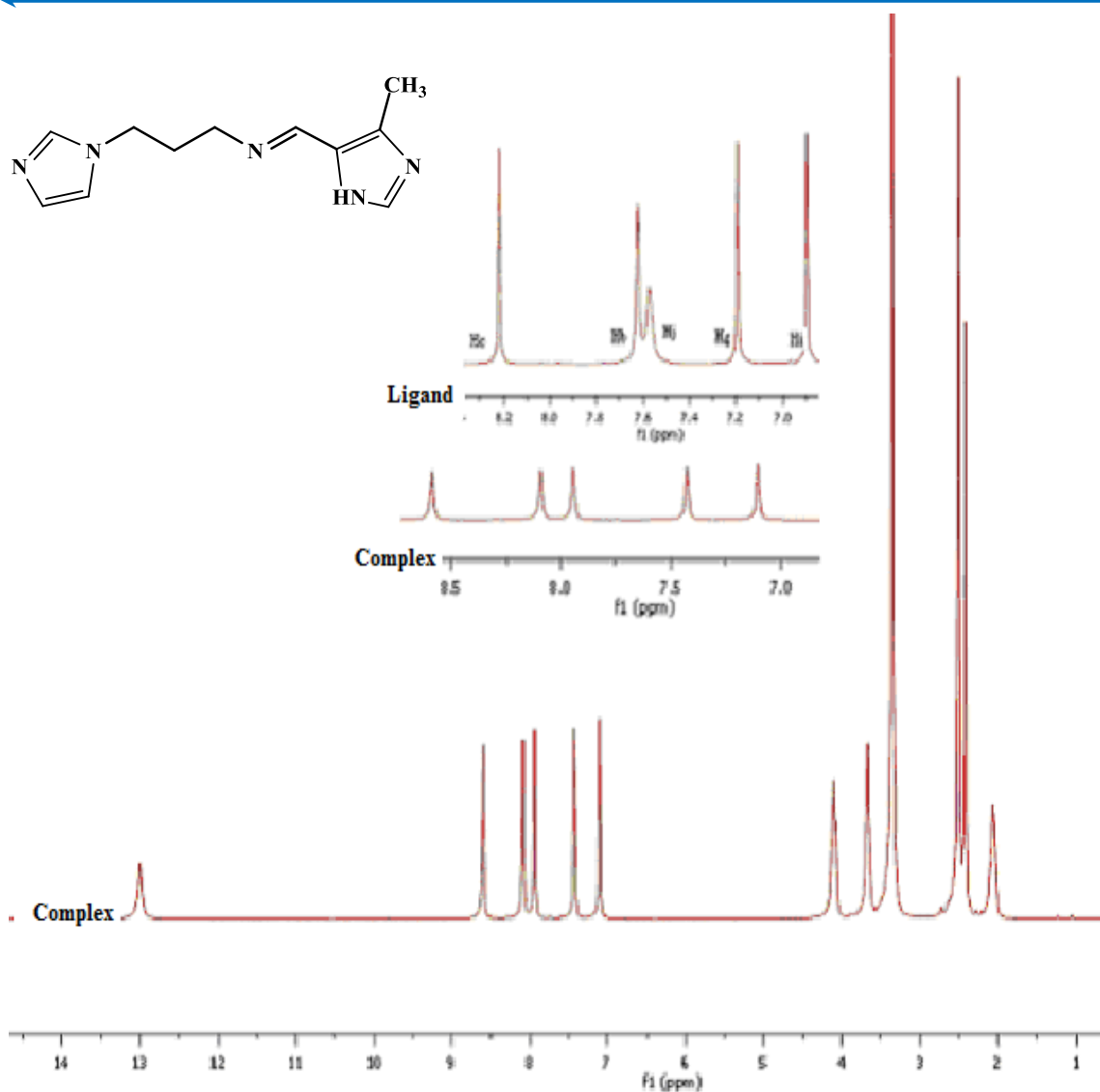


Figure 90 ^1H NMR (d_6 -DMSO) spectra of **(39)** and its Ag(I) complex, $[\text{Ag}(\mathbf{39})]\text{ClO}_4$.

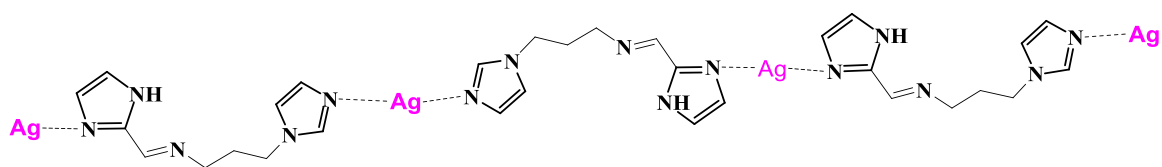
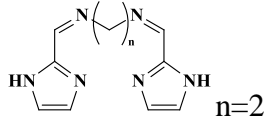
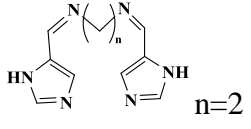
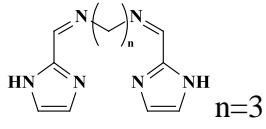
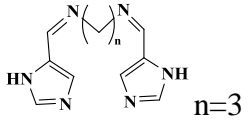
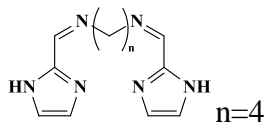
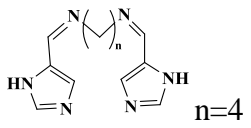


Figure 91 Proposed polymeric structure of $([\text{Ag}(\mathbf{37})]\text{ClO}_4)$.

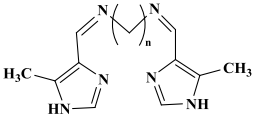
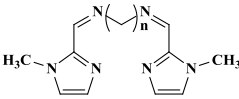
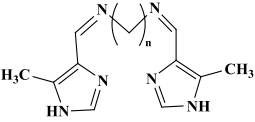
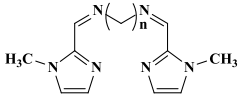
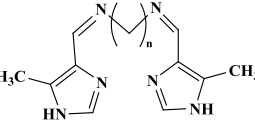
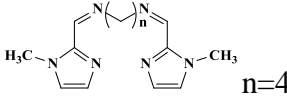
2.11.6 [3.12 Synthesis of the Ag(I) Complexes of Schiff Base Ligands Derived from 1,2-Diaminoethane, 1,3-Diaminopropane and 1,4-Diaminobutane

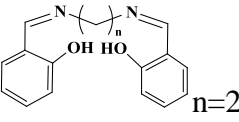
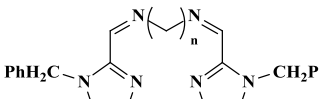
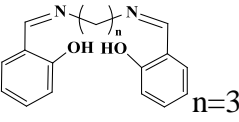
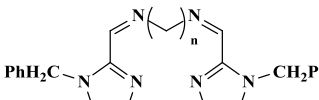
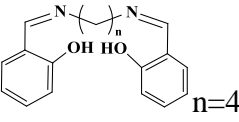
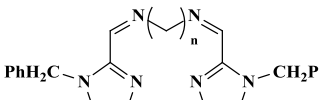
The Schiff base ligands, **(41)**-**(58)**, derived from 1,2-diaminoethane, 1,3-diaminopropane and 1,4-diaminobutane, were reacted with an excess of AgClO_4 at room temperature to give the respective Ag(I) complexes (Table 4) in moderate to good yields. The microanalytical data for this set of Ag(I) Schiff base complexes implied a 1:1 Ag(I):ligand ratio for three complexes, five others had a 1.5:1 ratio and the remainder formulated with a 2:1 ratio. There was no distinctive metal:ligand ratio pattern observed amongst the various di-Schiff base ligand subsets.

Table 4 Ligand structures and empirical formulae of the Ag(I) Schiff base complexes derived from 1,2-diaminoethane, 1,3-diaminopropane and 1,4-diaminobutane.

Ligand structure	Emp. Formula	Ligand structure	Emp. Formula
 <p>(41) n=2</p>	$[\text{Ag}_{1.5}(\mathbf{41})](\text{ClO}_4)_{1.5}$	 <p>(50) n=2</p>	$[\text{Ag}(\mathbf{50})]\text{ClO}_4$
 <p>(42) n=3</p>	$[\text{Ag}_{1.5}(\mathbf{42})](\text{ClO}_4)_{1.5}$	 <p>(51) n=3</p>	$[\text{Ag}_2(\mathbf{51})](\text{ClO}_4)_2$
 <p>(43) n=4</p>	$[\text{Ag}_2(\mathbf{43})](\text{ClO}_4)_2$	 <p>(52) n=4</p>	$[\text{Ag}_2(\mathbf{52})](\text{ClO}_4)_2$

Contd.

 <p>n=2 (44)</p>	[Ag ₂ (44)](ClO ₄) ₂	 <p>n=2 (53)</p>	[Ag _{1.5} (53)](ClO ₄) _{1.5}
 <p>n=3 (45)</p>	[Ag ₂ (45)](ClO ₄) ₂	 <p>n=3 (54)</p>	[Ag _{1.5} (54)](ClO ₄) _{1.5}
 <p>n=4 (46)</p>	[Ag ₂ (46)](ClO ₄) ₂	 <p>n=4 (55)</p>	[Ag ₂ (55)](ClO ₄) ₂

 <p>n=2 (47)</p>	[Ag(47)]ClO ₄	 <p>n=2 (56)</p>	[Ag _{1.5} (56)](ClO ₄) _{1.5}
 <p>n=3 (48)</p>	[Ag(48)]ClO ₄	 <p>n=3 (57)</p>	[Ag ₂ (57)](ClO ₄) ₂
 <p>n=4 (49)</p>	[Ag ₂ (49)](ClO ₄) ₂	 <p>n=4 (58)</p>	[Ag ₂ (58)](ClO ₄) ₂

The X-ray crystal structures of a number of oligomeric and polymeric Ag(I) helical complexes of ligands (**53**) and (**54**) have previously been reported.¹¹⁴ The complexes formulated as $[\text{Ag}_6(\mathbf{53})_5(\text{MeCN})](\text{CF}_3\text{SO}_3)_6 \cdot \text{H}_2\text{O}$, $[\text{Ag}_7(\mathbf{53})_6](\text{ClO}_4)_7\text{MeCN}$, $[\text{Ag}_2(\mathbf{53})_2](\text{NO}_3)_2 \cdot 0.5\text{H}_2\text{O}$, $[\text{Ag}_3(\mathbf{54})_2](\text{CF}_3\text{SO}_3)_3$ and $\{[\text{Ag}_3(\mathbf{54})_2](\text{NO}_3)_3\}_n$, and their structures are shown in Figures 92-97, respectively. The authors suggested that the metal:ligand ratio and subsequent structural motif was dependent upon the type of silver(I) salt employed as a starting material (AgCF_3SO_3 , AgClO_4 or AgNO_3) and also upon the reaction solvent. In complex $[\text{Ag}_6(\mathbf{54})_5(\text{MeCN})](\text{CF}_3\text{SO}_3)_6 \cdot \text{H}_2\text{O}$ (Figure 92), the Ag(I):Schiff base ligand ratio is 6:5 and the coordination environments around the metals are depicted in Figure 93(a) and (b).

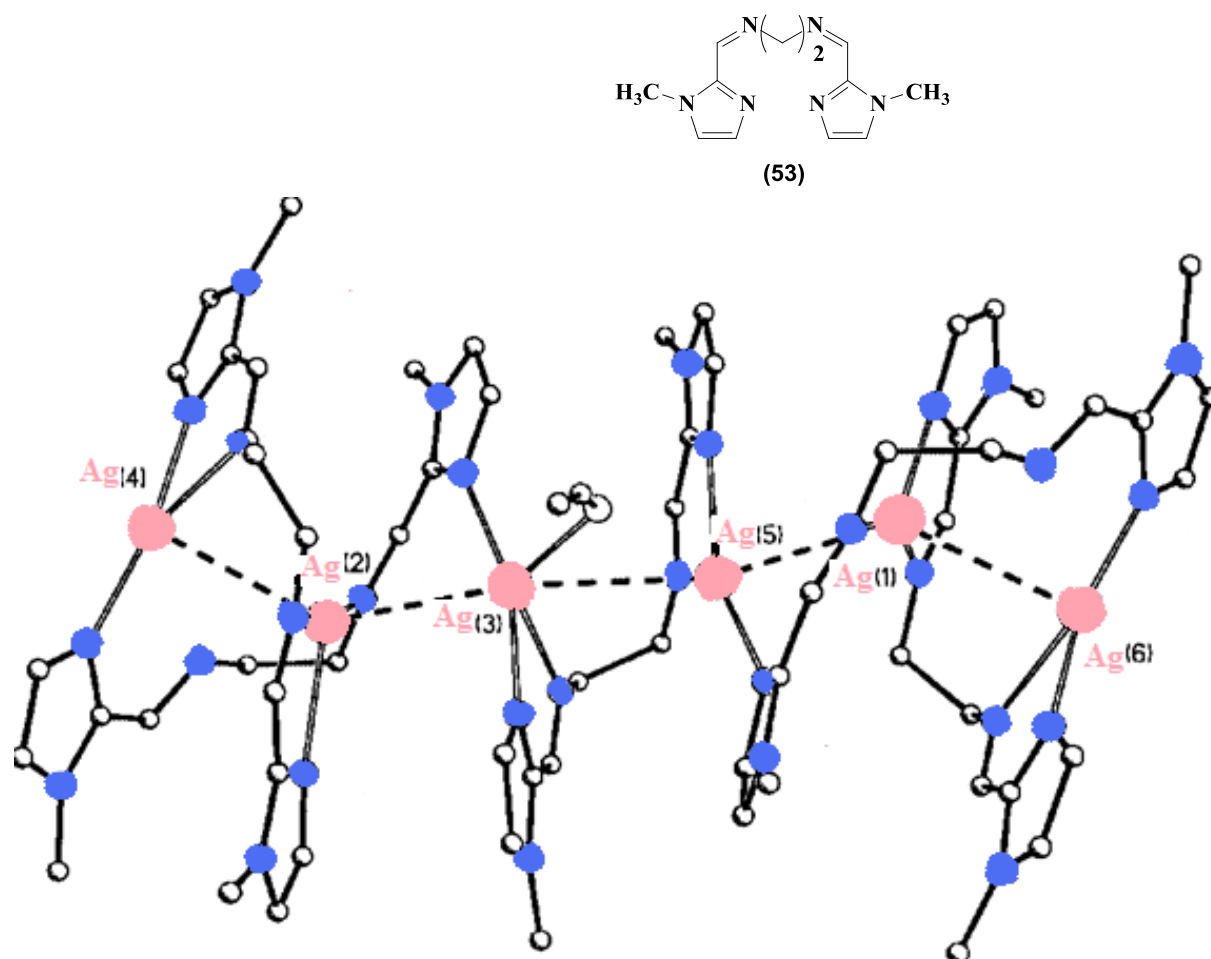


Figure 92 Polymeric, hexanuclear helical structure of $[\text{Ag}_6(\mathbf{53})_5(\text{MeCN})](\text{CF}_3\text{SO}_3)_6 \cdot \text{H}_2\text{O}$ (CF_3SO_3^- and H_2O not shown).¹¹⁵

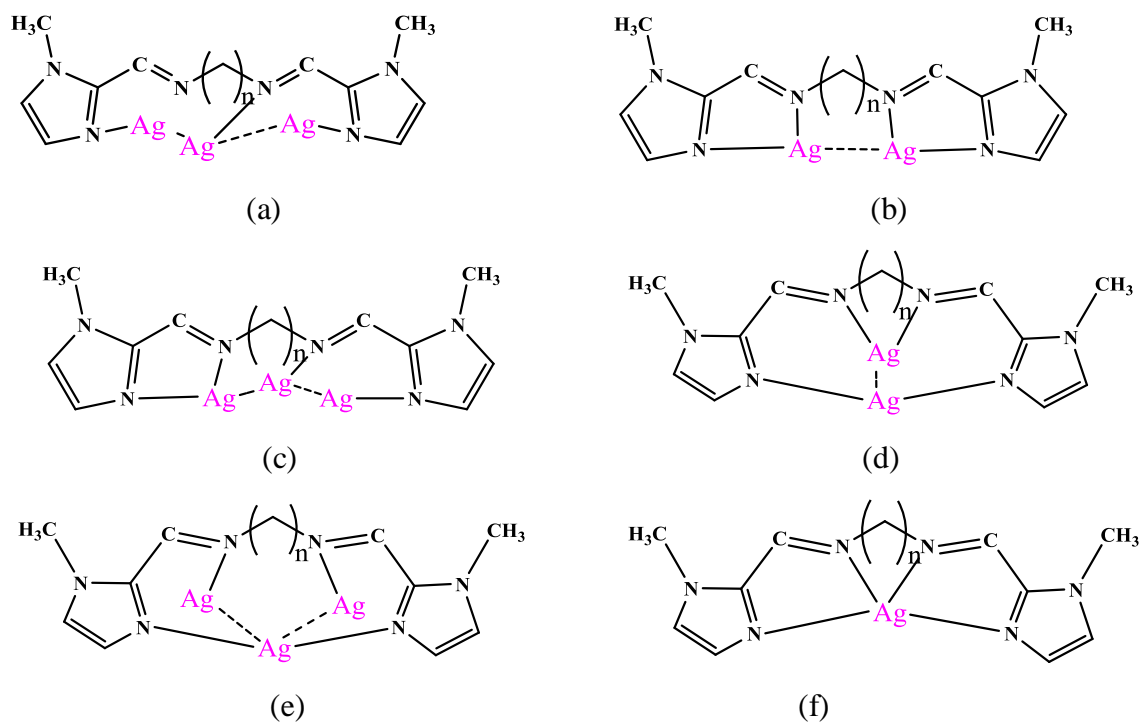


Figure 93 Structural motifs identified in the Ag(I) complexes of ligands (**53**) and (**54**).¹¹⁵

In complex $[\text{Ag}_7(\mathbf{53})_6](\text{ClO}_4)_7 \cdot \text{MeCN}$ (Figure 94), the Ag(I):ligand ratio is 7:6 and the coordination environments around the metals are depicted in Figure 93(b) and (c).

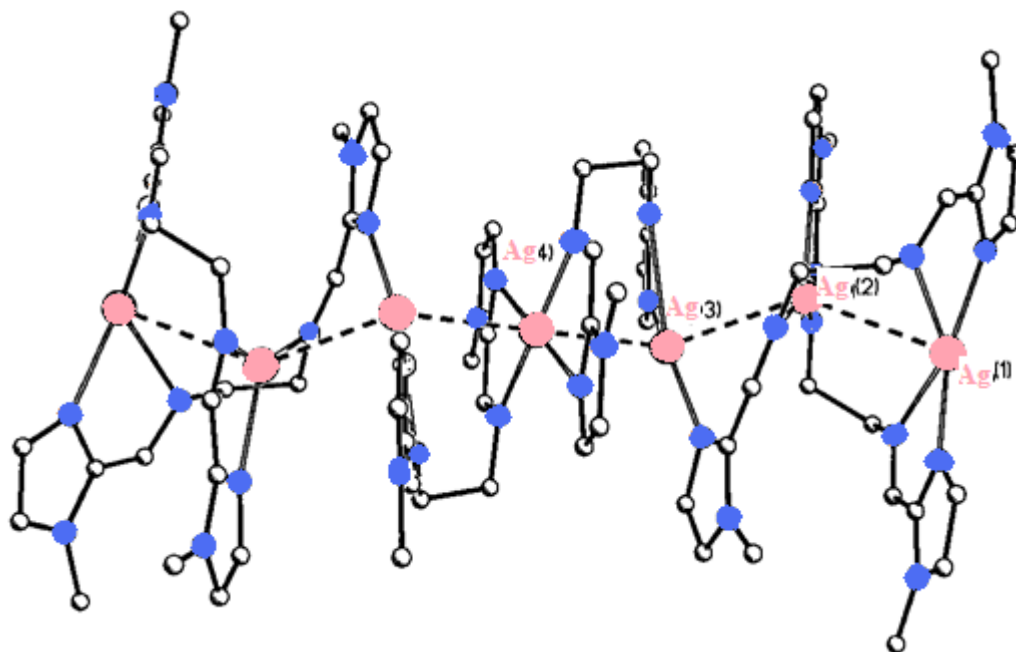


Figure 94 X-ray crystal structure showing the perspective view of the heptanuclear complex of (**53**), $[\text{Ag}_7(\mathbf{53})_6](\text{ClO}_4)_7 \cdot \text{MeCN}$ (MeCN and ClO_4^- not shown).¹¹⁵

For $[\text{Ag}_2(\mathbf{53})_2](\text{NO}_3)_2 \cdot 0.5\text{H}_2\text{O}$ (Figure 95), the Ag(I):Schiff base ligand ratio is 2:2 and the coordination environments around the metals are depicted in Figure 93(b). The double helical structure is achieved by intramolecular twisting of the two ligands. In addition, there are strong π - π interactions between a pair of imidazole rings from different ligands in the helix. Complex $[\text{Ag}_3(\mathbf{54})_2](\text{CF}_3\text{SO}_3)_3$ (Figure 96) has a Ag(I):ligand ratio of 3:2 and the metal coordination spheres are as shown in Figure 93(d). The two ligands are almost planar and are more or less parallel to each other. Again, there are strong π - π interactions between a pair of imidazole rings from different ligands in the double helix.

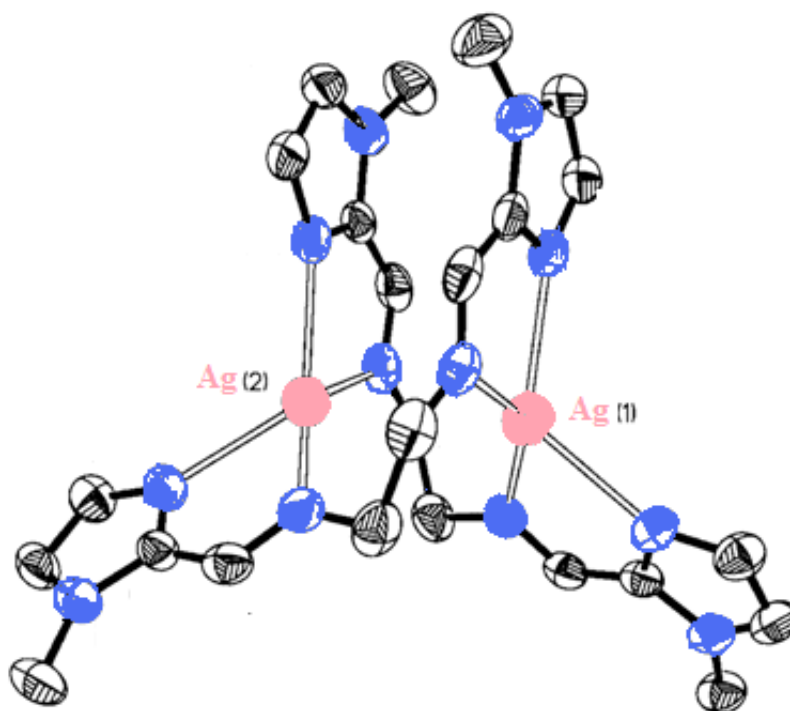


Figure 95 X-ray crystal structure of the double helicate complex, $[\text{Ag}_2(\mathbf{53})_2](\text{NO}_3)_2 \cdot 0.5\text{H}_2\text{O}$ (H_2O and NO_3^- not shown).¹¹⁵

Complex $\{[\text{Ag}_3(\mathbf{54})_2](\text{NO}_3)_3\}_n$ (Figure 97) also has a Ag(I):ligand ratio of 3:2 and the metal coordination spheres are shown in Figure 93(d). The metals are arranged in a zigzag fashion and are extended into infinite chains through the bridging coordination. The imidazole rings in the chain are also arranged in a staggered fashion and there are no π - π interactions between the rings.

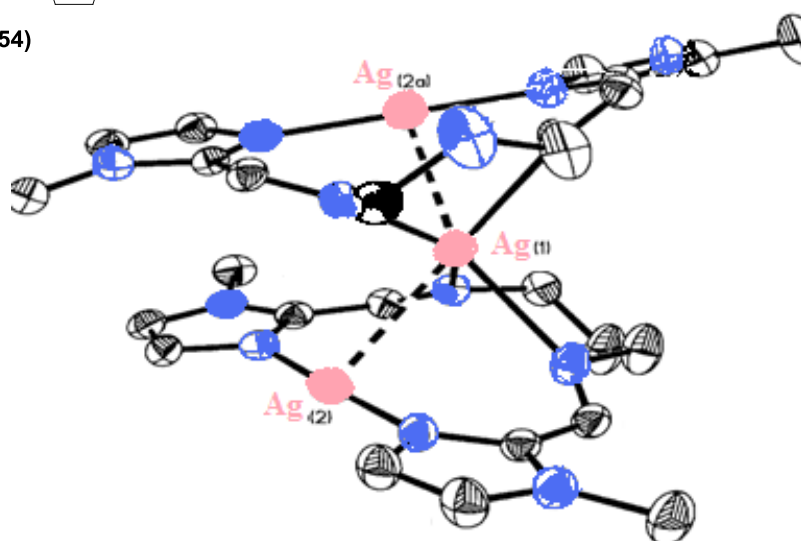
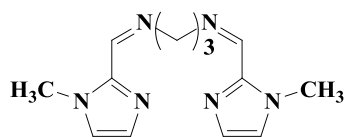


Figure 96 X-ray crystal structure of $[\text{Ag}_3(\mathbf{54})_2](\text{CF}_3\text{SO}_3)_3$ (CF_3SO_3^- not shown).¹¹⁵

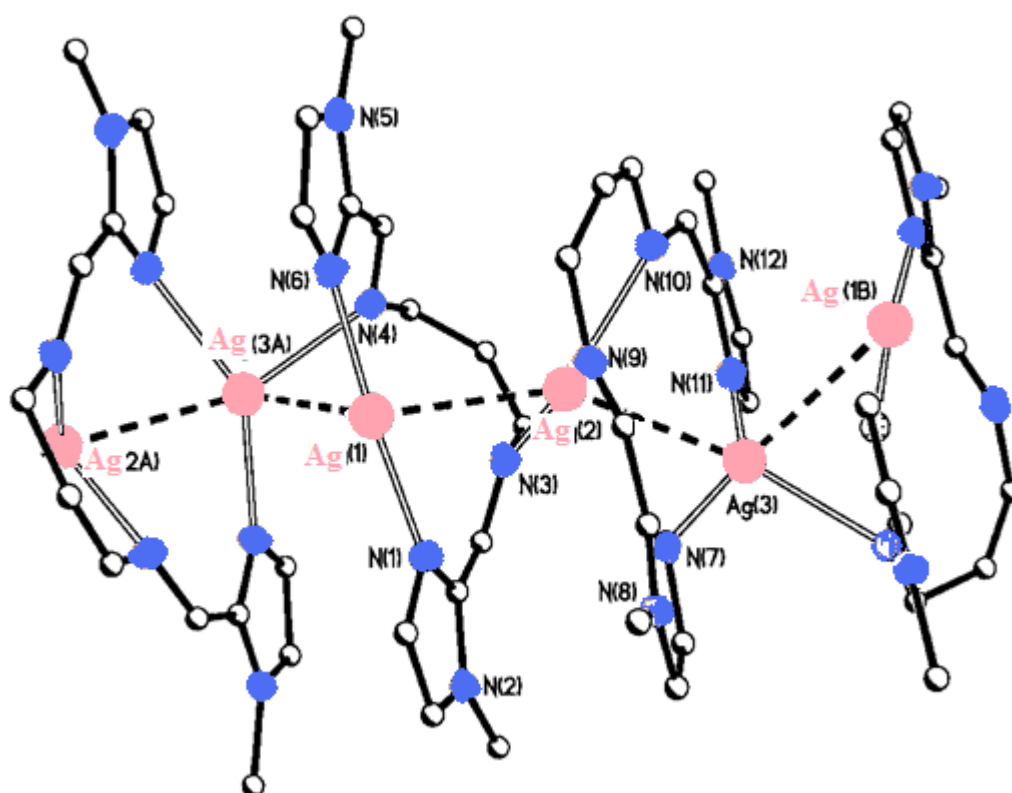


Figure 97 X-ray crystal structure of $\{[\text{Ag}_3(\mathbf{54})_2](\text{NO}_3)_3\}_n$, (NO_3^- not shown).¹¹⁵

Representative IR spectra for the present alkyldiamino set of Ag(I) complexes are shown in Figures 98 and 99. Spectral bands associated with the perchlorate anions (*ca.* 1100 and 625 cm^{-1}) and the imine functionalities (*ca.* 1600-1650 cm^{-1}) were clearly visible in all of the spectra of the metal complexes. The presence of the perchlorate bands in the spectra of the Ag(I) complexes of the phenol containing ligands, (**47-49**), would seem to indicate that the phenyl moieties of the ligands are not deprotonated. These latter three complexes are thought to have a polymeric structure similar to those discussed previously (e.g. $[\text{Ag}(\mathbf{23})_2]\text{ClO}_4$ and $[\text{Ag}(\mathbf{24})_2]\text{ClO}_4$, see Figure 82). The IR spectra of the metal-free, Schiff base ligand (**46**) and its Ag(I) complex, $[\text{Ag}_2(\mathbf{46})](\text{ClO}_4)_2$, and the Schiff base ligand (**47**) and its Ag(I) complex, $[\text{Ag}(\mathbf{47})]\text{ClO}_4$, are shown in Figures 98 and 99, respectively.

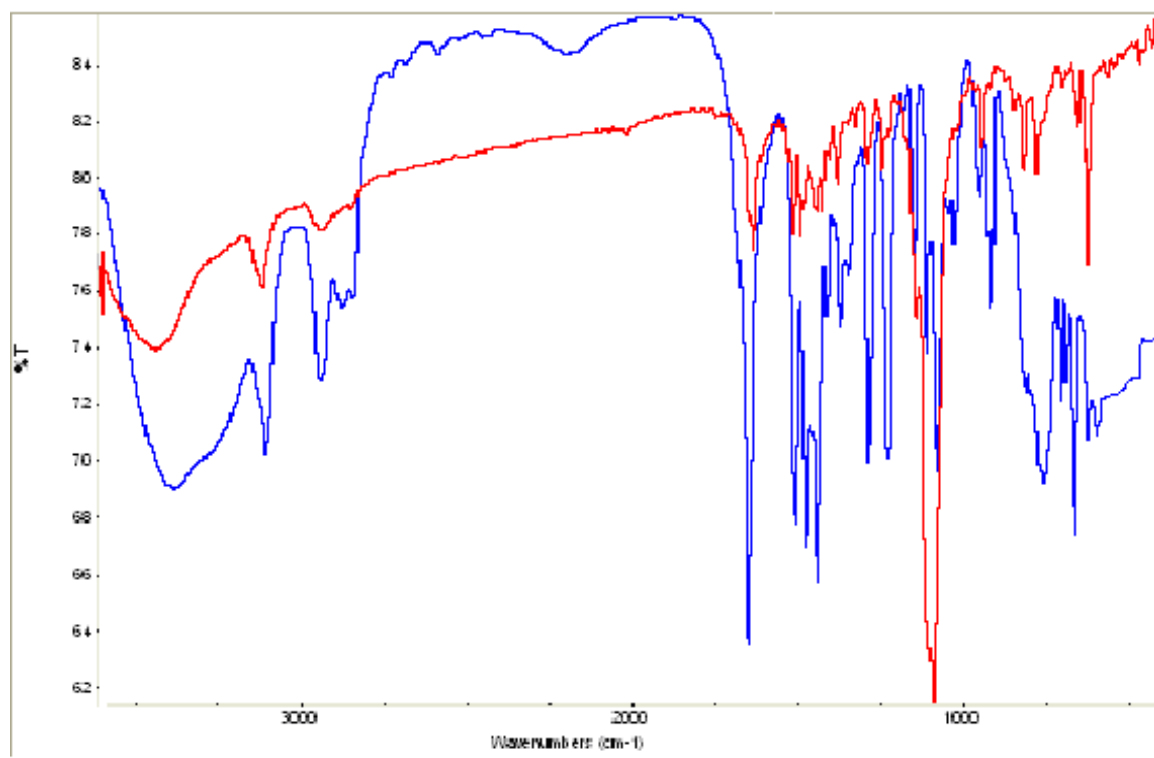


Figure 98 IR spectra of the metal-free ligand (**46**) (blue) and its Ag(I) complex, $[\text{Ag}_2(\mathbf{46})](\text{ClO}_4)_2$ (red).

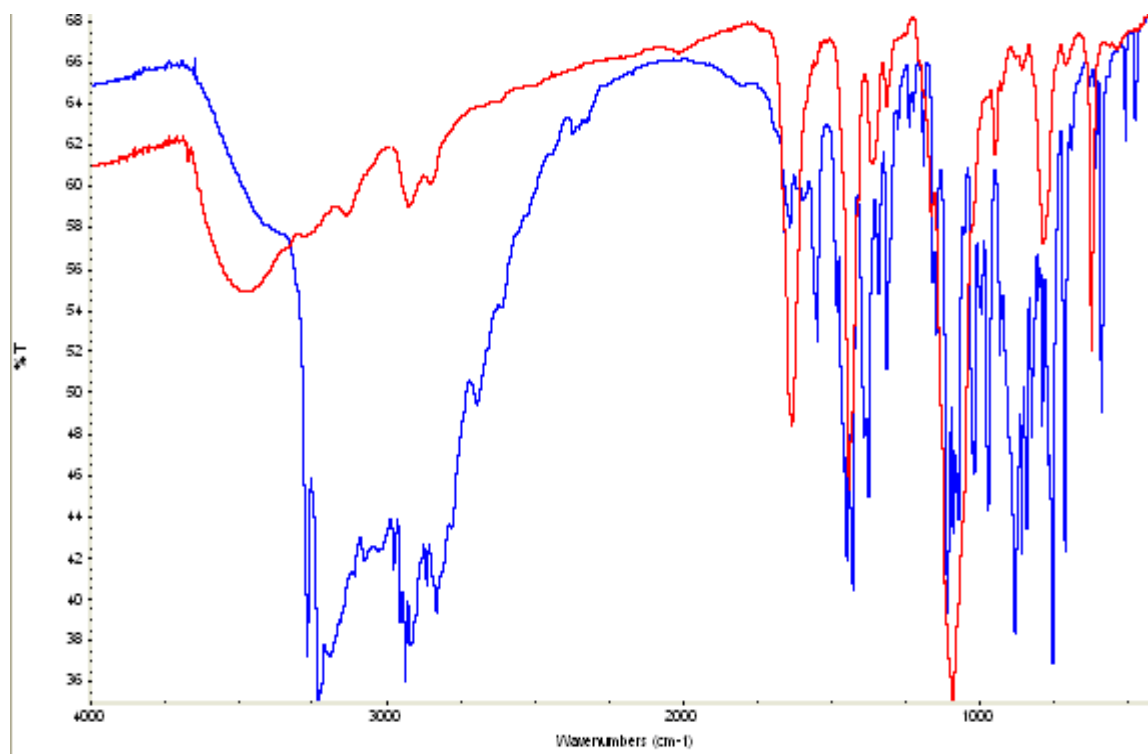


Figure 99 The IR spectra of the metal-free ligand (**47**) (blue) and its Ag(I) complex, [Ag(**47**)]ClO₄ (red).

Representative ¹H NMR (d₆-DMSO) spectra for this set of alkyldiamino Ag(I) complexes are shown in Figures 100-102. For ligand (**46**) and its Ag(I) complex [Ag₂(**46**)](ClO₄)₂ (Figure 100) the imine peak of the spacer chain in the metal-free ligand (8.25 ppm) is shifted downfield (8.45 ppm) upon complexation to the metal. The peak representing the protons in the 2-position of the imidazole rings (7.75 ppm) also experience a very small upfield shift (7.70 ppm) upon complexation.

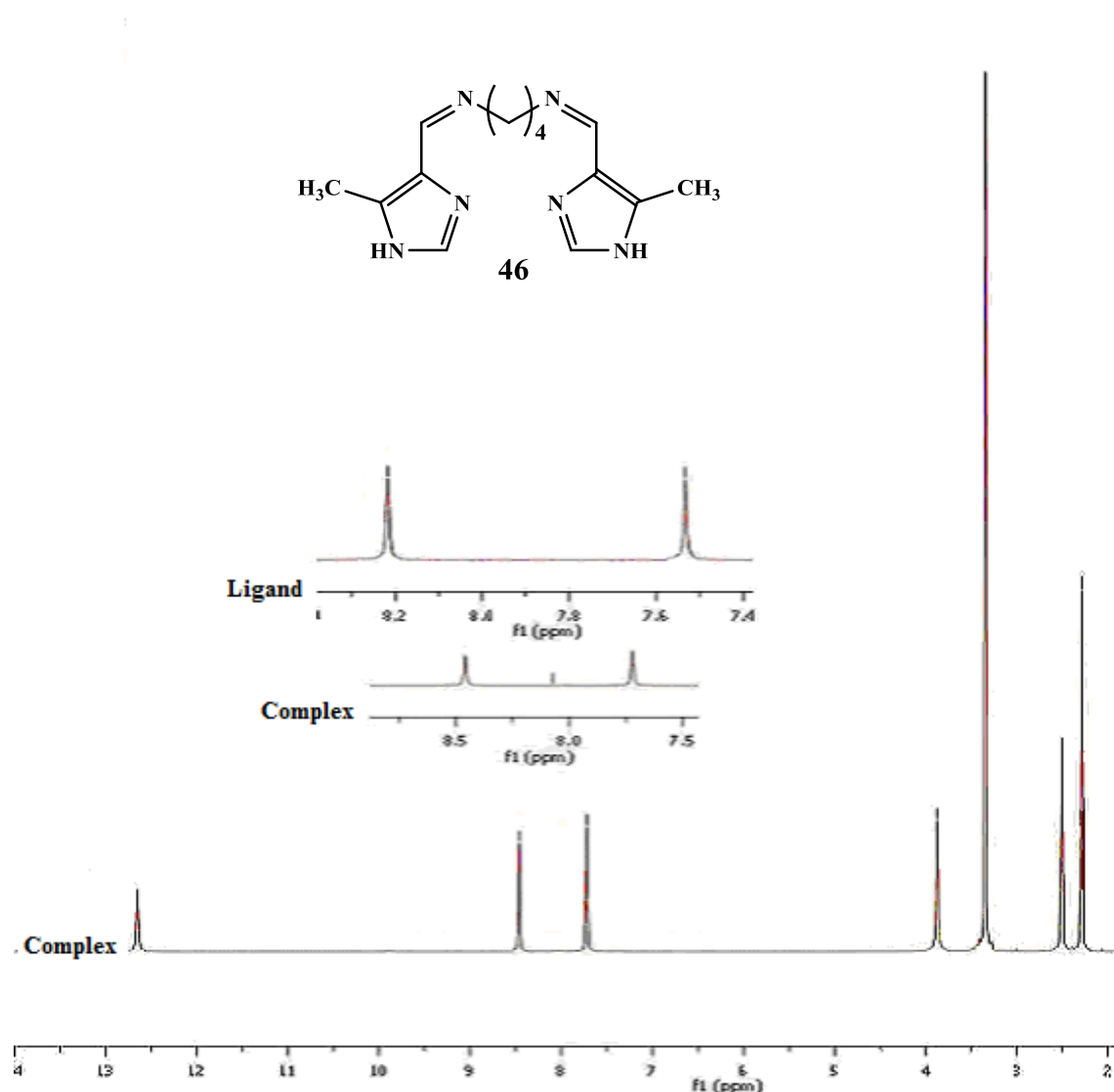


Figure 100 ^1H NMR (d_6 -DMSO) spectra of ligand (**46**) and its the Ag(I) complex, $[\text{Ag}_2(\mathbf{46})](\text{ClO}_4)_2$.

The ^1H NMR (d_6 -DMSO) spectra of ligand (**53**) and its the Ag(I) complex, $[\text{Ag}_{1.5}(\mathbf{53})](\text{ClO}_4)_{1.5}$, are shown in Figure 101. The imine peak of the imidazole ring of the ligand (8.35 ppm) is shifted downfield to (8.58 ppm) in the spectrum of the Ag(I) complex. The peaks representing the protons in the 4(5)-position of the ligand are shifted downfield from 7.00 ppm and 7.27 ppm of the ligand to 7.75 ppm and 8.25 ppm, in the Ag(I) complex. The N- CH_3 peak of the complex (3.96 ppm) is shifted downfield from that of the free ligand (3.90 ppm). The N- CH_2 peak of the complex (at 2.45 ppm) is also shifted downfield compared to the metal-free ligand (2.00 ppm).

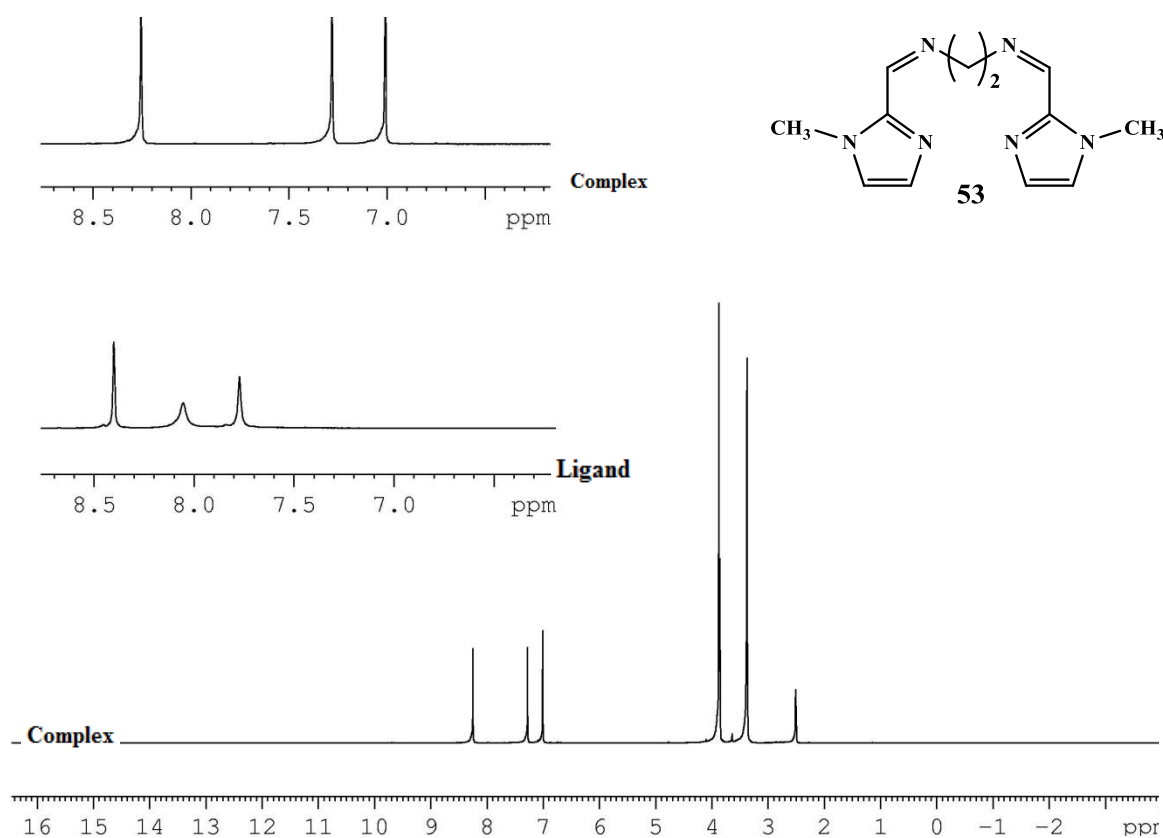


Figure 101 ^1H NMR (d_6 -DMSO) spectra of ligand (**53**) and its Ag(I) complex, $[\text{Ag}_{1.5}(\mathbf{53})](\text{ClO}_4)_{1.5}$.

The ^1H NMR (d_6 -DMSO) spectra of ligand (**54**) and its the Ag(I) complex, $[\text{Ag}_{1.5}(\mathbf{54})](\text{ClO}_4)_{1.5}$, are shown in Figure 102. The imine peak of the imidazole ring at 8.36 ppm of the metal-free ligand is shifted downfield to 8.58 ppm in the Ag(I) complex. The peaks representing the protons in the 4(5)-position of the metal-free ligand (7.08, 7.35 ppm) are shifted downfield in the Ag(I) complex (7.25 ppm and 7.55 ppm). The N-CH₃ peak (at 2.04 ppm) is shifted downfield in the complex compared to that of the free ligand (2.00 ppm). The N-CH₂ peaks of the ligand (2.00 and 3.80 ppm) are shifted downfield in the complex (2.04 and 3.96 ppm).

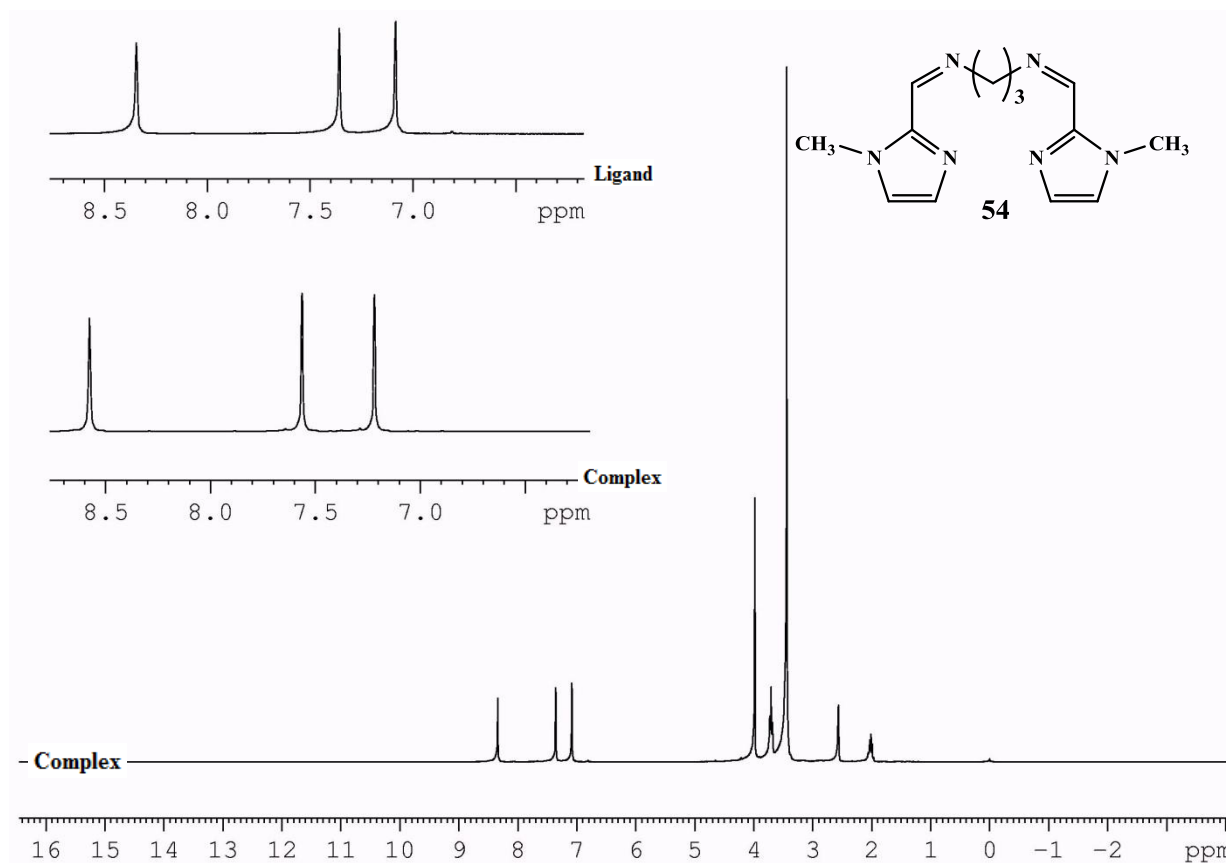


Figure 102 ^1H NMR (d_6 -DMSO) spectra of ligand (**54**) and its Ag(I) complex, $[\text{Ag}_{1.5}(\mathbf{54})](\text{ClO}_4)_{1.5}$

The ^1H NMR data (ppm) obtained for ligand (**53**) and its Ag(I) complexes, $[\text{Ag}_6(\mathbf{53})_5(\text{MeCN})](\text{CF}_3\text{SO}_3)_6 \cdot \text{H}_2\text{O}^{115}$ (a), $[\text{Ag}_7(\mathbf{53})_6](\text{ClO}_4)_7 \text{MeCN}^{115}$ (b), $[\text{Ag}_2(\mathbf{53})_2](\text{NO}_3)_2 \cdot 0.5 \text{H}_2\text{O}^{115}$ (c) and $[\text{Ag}_{1.5}(\mathbf{53})](\text{ClO}_4)_{1.5}$ (d) (present work) are shown in Table 5. The literature complexes, (a), (b) and (c), and the metal-free ligand were run as solutions in CD_3CN . Complex (d) and the metal-free ligand (both from the present study) were run as solutions in d_6 -DMSO. The ^1H NMR data (ppm) obtained for ligand (**54**) and its Ag(I) complexes, $[\text{Ag}_3(\mathbf{54})_2](\text{CF}_3\text{SO}_3)_3^{115}$ (a), $\{[\text{Ag}_3(\mathbf{54})_2](\text{NO}_3)_3\}_n^{115}$ (b) and $[\text{Ag}_{1.5}(\mathbf{54})](\text{ClO}_4)_{1.5}$ (c) are shown in Table 6.

Table 5 ^1H NMR data (ppm) for ligand (**53**) and its Ag(I) complexes, $[\text{Ag}_6(\mathbf{53})_5(\text{MeCN})](\text{CF}_3\text{SO}_3)_6 \cdot \text{H}_2\text{O}^{115}$ (a), $[\text{Ag}_7(\mathbf{53})_6](\text{ClO}_4)_7\text{MeCN}^{115}$ (b), $[\text{Ag}_2(\mathbf{53})_2](\text{NO}_3)_2 \cdot 0.5 \text{H}_2\text{O}^{115}$ (c) and $[\text{Ag}_{1.5}(\mathbf{53})](\text{ClO}_4)_{1.5}$ (d) (present work).

Proton	Ligand (53) ¹¹⁵	Ag(I) complexes ¹¹⁵ (a), (b), (c)	Ligand (53)	Ag(I) complex (d)
N-CH₃	3.89	(a) 3.75 (b) 3.75 (c) 3.76	3.90	(d) 4.00
4,5 H	6.98, 7.04	(a) 6.96, 7.21 (b) 6.95, 7.21 (c) 6.96, 7.20,	7.27, 8.25	(d) 7.75, 8.10
N=C-H (imine of the chain)	8.23	(a) 8.44 (b) 8.44 (c) 8.44	8.25	(d) 8.40
N-CH₂ (chain)	3.88	(a) 4.01 (b) 3.99 (c) 3.95	3.90	(d) 4.00

Table 6 ^1H NMR data (ppm) for ligand **(54)** and its Ag(I) complexes, $[\text{Ag}_3(\mathbf{54})_2](\text{CF}_3\text{SO}_3)_3$ ¹¹⁵ (a), $\{[\text{Ag}_3(\mathbf{54})_2](\text{NO}_3)_3\}_n$ ¹¹⁵ (b) and $[\text{Ag}_{1.5}(\mathbf{54})](\text{ClO}_4)_{1.5}$ (c) (present work).

Proton	Ligand (54) ¹¹⁵	Ag(I) complexes ¹¹⁵ (a), (b)	Ligand (54)	Ag(I) complex (c)
N-CH₃	3.95	(a) 3.82 (b) 3.82	3.96	(c) 3.92
4,5 H	7.00, 7.29	(a) 7.11, 7.28 (b) 7.12, 7.26	7.10, 7.39	(c) 7.25, 7.57
N=C-H (imine of the chain)	8.27	(a) 8.40 (b) 8.41	8.35	(c) 8.58
N-CH₂ (chain)	2.01, 3.68	(a) 2.06, 3.90 (b) 2.08, 3.93	2.00, 3.59	(c) 2.00, 3.80

The ^1H NMR spectral data shown in Tables 5 and 6 show that when the Schiff base ligands **(53)** and **(54)** complex to the metal centres a slight, but consistent, shift (*ca.* 0.13 ppm) in the position of the imidazole ring N-CH₃ protons is observed. From the X-ray crystallographic data of the Ag(I) complexes¹¹⁵ it is evident that the tertiary N atom of the imidazole ring (N-CH₃) moiety is not coordinated to a metal centre in the solid state. In the present study, similar small shifts in the N-CH₃ proton signals are also observed in the

spectra of the metal complexes. Likewise, a small shift is seen in the position of the spacer chain imine proton (N=CH) signal (*ca.* 0.11-0.13 ppm¹¹⁵ and *ca.* 0.22-0.32 ppm for the present study) upon coordination of the Schiff base ligand to the Ag(I) ion. Therefore, it appears that essentially all protons on the ligand undergo shifts upon coordination to the metal centre. Thus, even protons which are relatively remote from ligand donor atoms are influenced by the presence of the Ag(I) ion.

The myriad of structural geometries observed for the previously reported Ag(I) complexes described above¹¹⁵ clearly illustrate both the wide range of coordination possibilities and the flexibility of the di-Schiff base ligands.

3.13 Synthesis of the Ag(I) Complexes of Schiff Base Ligands Derived from 1,2-Phenylenediamine, 1,3-Phenylenediamine and 1,4-Phenylenediamine

Schiff base ligands derived from 1,2-, 1,3- and 1,4-phenylenediamine ((**59**)-(**73**)) were reacted with an excess of AgClO₄ at room temperature to give the respective Ag(I) complexes (Table 7) in moderate to good yield. These complexes were also only soluble in hot DMSO. Based on the microanalytical data, complexes containing the 1,2-phenylenediamine moiety formulated with a 1.5:1 Ag(I):ligand ratio, except in the case of ligand (**71**) (1:1 ratio). Complexes containing either 1,3- or 1,4-phenylenediamine moieties had a 1:1 Ag(I):ligand ratio, except in the cases of ligands (**66**) and (**67**) (1.5:1 ratio).

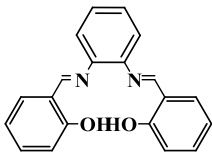
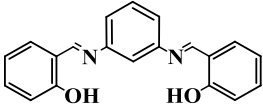
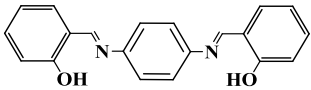
Representative examples of IR and ¹H NMR spectra for this phenylenediamino set of Ag(I) complexes are shown in Figure 105 and Figures 106-108, respectively. The ¹H NMR (d₆-DMSO) spectra of the metal-free ligand (**60**) and its Ag(I) complex, [Ag(**60**)]ClO₄, are shown in Figure 106.

Table 7 Ligand structures and empirical formulae of the Ag(I) complexes derived from 1,2, 1,3- and 1,4-phenylenediamine.

Ligand structure	Emp. formula	Ligand structure	Emp. Formula
 (59)	$[\text{Ag}_{1.5}(\mathbf{59})](\text{ClO}_4)_{1.5}$	 (68)	$[\text{Ag}_{1.5}(\mathbf{68})](\text{ClO}_4)_{1.5}$
 (60)	$[\text{Ag}(\mathbf{60})]\text{ClO}_4$	 (69)	$[\text{Ag}(\mathbf{69})]\text{ClO}_4$
 (61)	$[\text{Ag}(\mathbf{61})]\text{ClO}_4$	 (70)	$[\text{Ag}(\mathbf{70})]\text{ClO}_4$
 (65)	$[\text{Ag}_{1.5}(\mathbf{65})](\text{ClO}_4)_{1.5}$	 (71)	$[\text{Ag}(\mathbf{71})]\text{ClO}_4$
 (66)	$[\text{Ag}_{1.5}(\mathbf{66})](\text{ClO}_4)_{1.5}$	 (72)	$[\text{Ag}(\mathbf{72})]\text{ClO}_4$
 (67)	$[\text{Ag}_{1.5}(\mathbf{67})](\text{ClO}_4)_{1.5}$	 (73)	$[\text{Ag}(\mathbf{73})]\text{ClO}_4$

Contd

Table 7 (contd.)

 <p>(53)</p>	$[\text{Ag}_{1.5}(\mathbf{62})](\text{ClO}_4)_{1.5}$
 <p>(63)</p>	$[\text{Ag}(\mathbf{63})]\text{ClO}_4$
 <p>(64)</p>	$[\text{Ag}(\mathbf{64})]\text{ClO}_4$

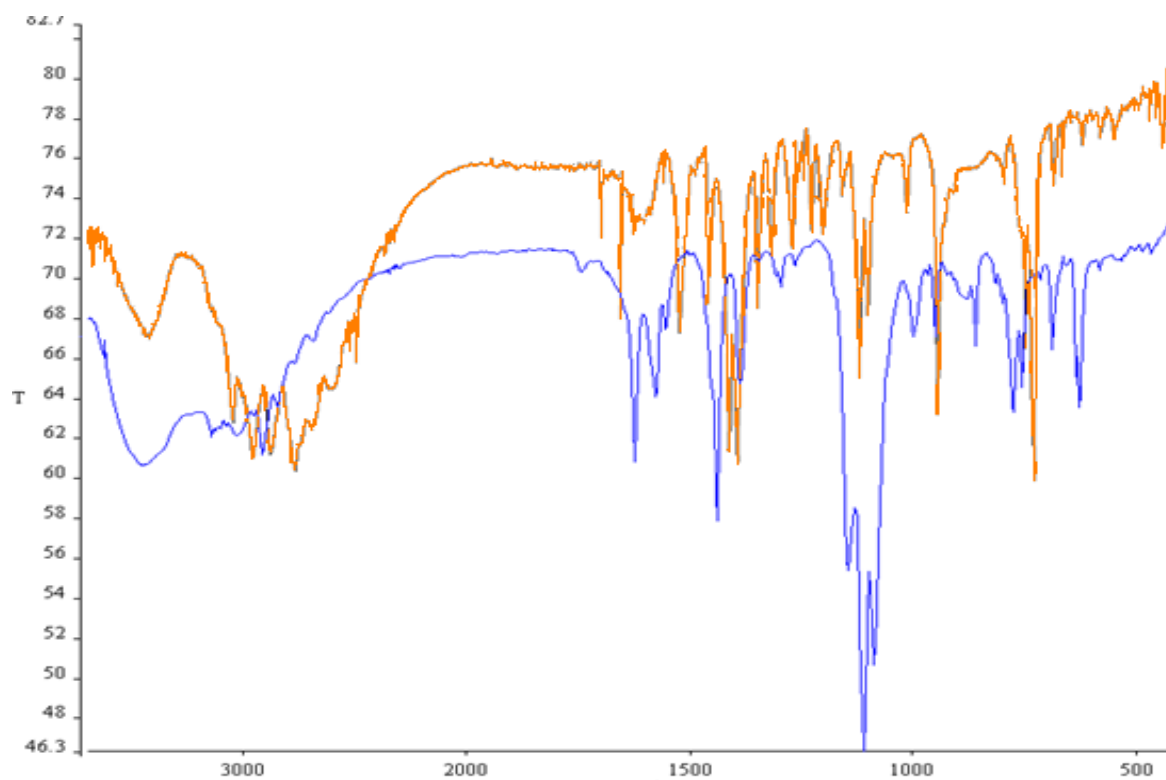


Figure 105 The IR spectra of the metal-free ligand (**60**) (orange) and its Ag(I) complex, $[\text{Ag}(\mathbf{60})]\text{ClO}_4$ (blue).

The imine peak of the ligands spacer-chain, which is seen at 8.50 ppm, undergoes a small shift upfield to 8.45 ppm for the Ag(I) complex. The peak representing the protons in the 4(5) positions, which is seen at 7.46 ppm in the metal-free ligand, is shifted to 7.51 ppm for the Ag(I) complex. The N-H peak of the imidazole, barely distinguishable in the spectrum of the metal-free ligand (*ca.* 12.5 ppm), is very sharp and shifted downfield to 13.2 ppm in the Ag(I) complex, indicating possible coordination of the imine N of the imidazole.

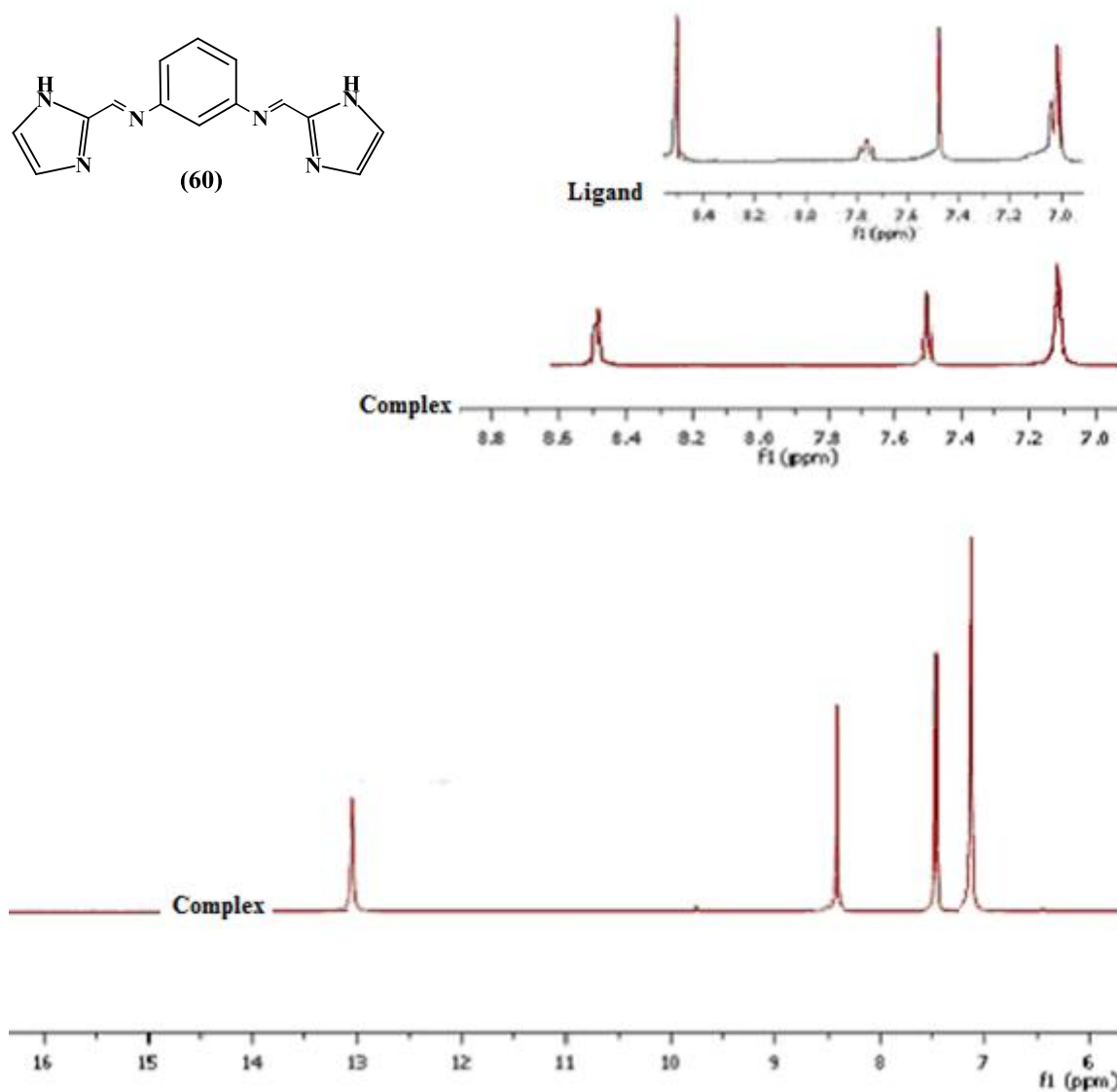


Figure 106 ^1H NMR (d_6 -DMSO) spectra of the metal-free ligand (60) and its Ag(I) complex, $[\text{Ag}(\mathbf{60})]\text{ClO}_4$.

The ^1H NMR (d_6 -DMSO) spectra of the metal-free ligand (**65**) and the Ag(I) complex, $[\text{Ag}_{1.5}(\mathbf{65})](\text{ClO}_4)_{1.5}$, are shown in Figure 107. The imine peak of the imidazole in the metal-free ligand is seen at 8.55 ppm, is shifted downfield to 8.75 ppm in the Ag(I) complex. The peak for the protons in the 4(5)-position for the metal-free ligand is seen at 7.75 ppm, while the corresponding peak of the Ag(I) complex is shifted downfield to 8.10 ppm. The phenyl peak of the metal-free ligand appears at 7.30 ppm, while in the Ag(I) complex it is shifted upfield to 7.10 ppm. The N-H peak of the imidazole is barely distinguishable in the spectrum of the metal-free ligand (12.6 ppm). However, the corresponding peak in the Ag(I) complex is very sharp and shifted downfield to 13.0 ppm, again indicating possible coordination at the imine N of the imidazole.

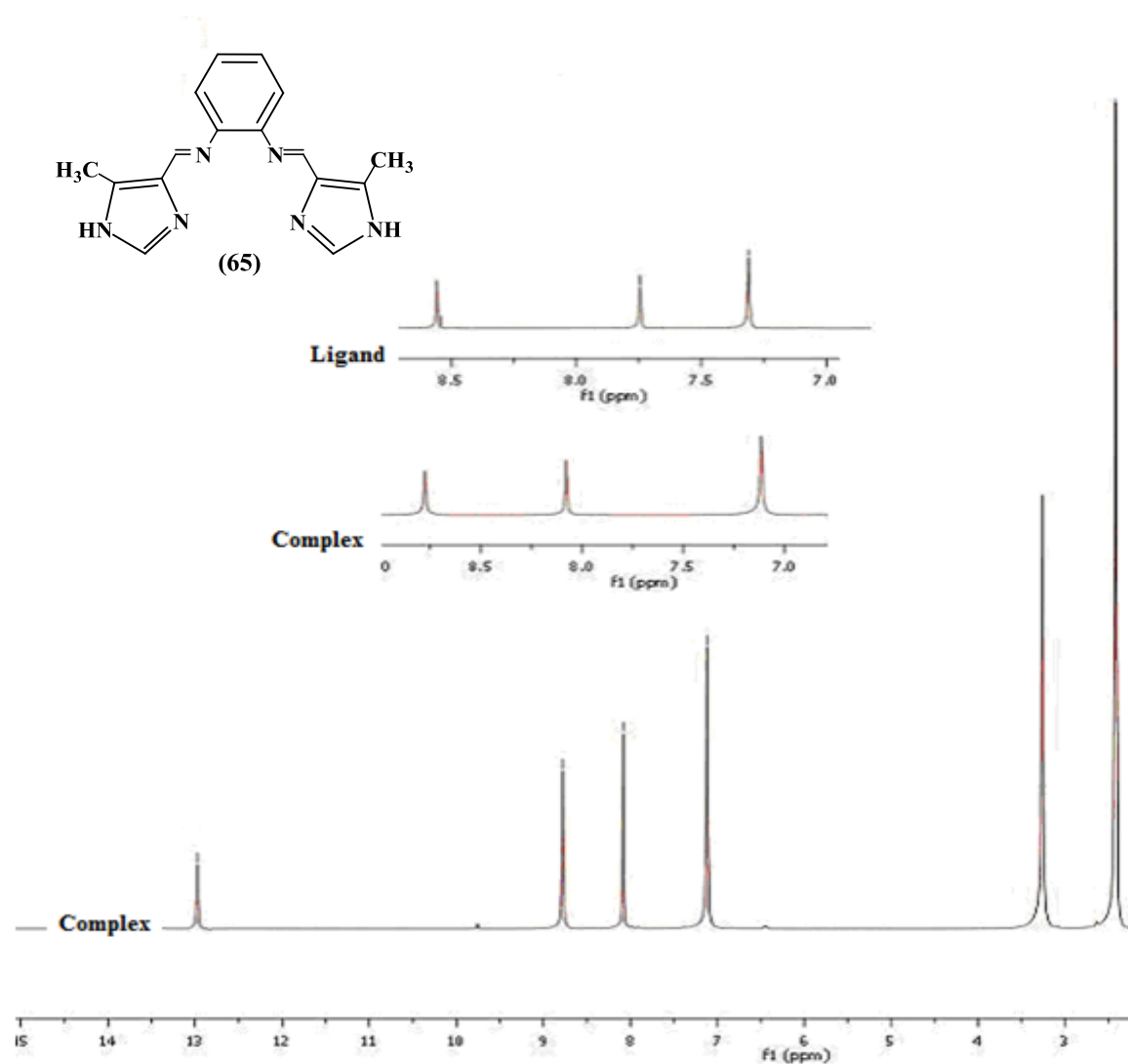


Figure 107 ^1H NMR (d_6 -DMSO) spectra of the metal-free ligand (**65**) and its Ag(I) complex, $[\text{Ag}_{1.5}(\mathbf{65})](\text{ClO}_4)_{1.5}$.

The ^1H NMR ($\text{d}_6\text{-DMSO}$) spectra of the metal-free ligand (**70**) and its Ag(I) complex, $[\text{Ag}(\mathbf{70})]\text{ClO}_4$, are shown in Figure 108. The imine peak of the metal-free ligand is seen at 8.52 ppm, while that of the Ag(I) complex is seen at 8.78 ppm. The peak for the protons in the 2-position is seen at 7.85 ppm in the metal-free ligand, while the corresponding peak for the Ag(I) complex is shifted upfield to 8.30 ppm. The protons in the 4(5)-position of the imidazole ring are observed at 7.69 ppm in the metal-free ligand and 8.10 ppm in the Ag(I) complex. The phenyl protons of the free ligand appear at 7.25 ppm and at 7.05 ppm in the Ag(I) complex. The imidazole N-H peak of the metal-free ligand is not seen in the spectrum of the free ligand, but appears at 13.25 ppm in the spectrum of the Ag(I) complex.

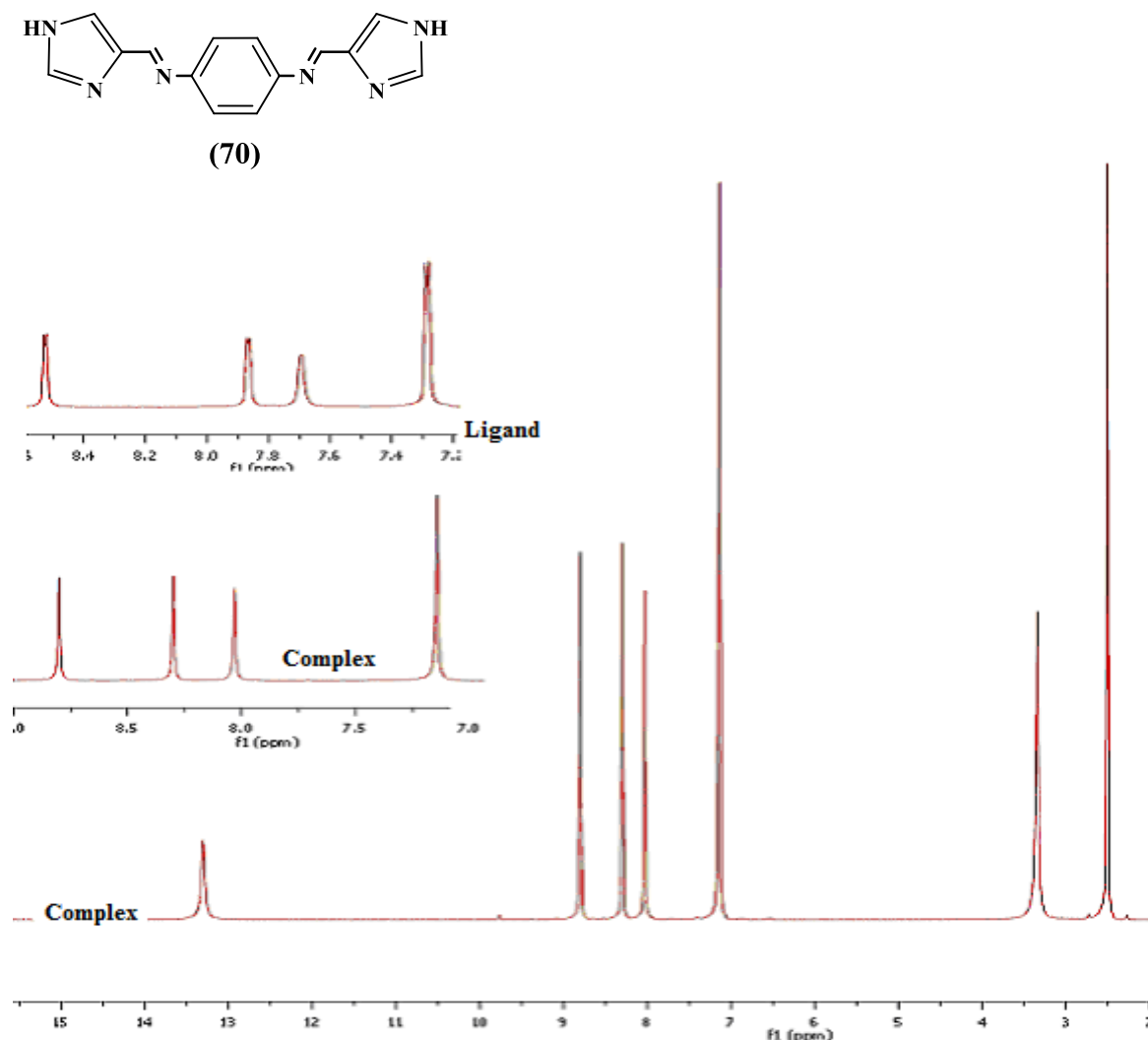


Figure 108 The ^1H NMR ($\text{d}_6\text{-DMSO}$) spectra of the metal-free ligand (**70**) and its Ag(I) complex, $[\text{Ag}(\mathbf{70})]\text{ClO}_4$.

From a survey of the literature, this group of phenylenediamine-based Schiff base ligands appears to be unique. The closest structural analogue of ligand (**60**) is the 1,3-bis(4,5-dihydro-1H-imidazole-2-yl)benzene (bib) ligand, reported by Ren *et al.*¹²⁷ (Figure 109). The major structural differences between (**60**) and the bib ligand are that the latter does not contain any imine moieties in the spacer chain and that the alkene unit of the imidazole ring has been reduced. The X-ray crystal structures of two Ag(I) complexes of the bib ligand have been reported.¹²⁷ The [2+2] metallocyclic complex, $\{[\text{Ag}(\text{bib})](\text{NO}_3)\cdot\text{H}_2\text{O}\}_n$, adopts a *cis* configuration, leading to a 1D polymeric chain (Figure 110). Complex $\{[\text{Ag}_2(\text{bib})_2(\text{NO}_2)](\text{NO}_2)\cdot 19/8\text{H}_2\text{O}\}_n$ adopts a *trans* configuration, resulting in a single strand, polymeric helix (Figure 111).

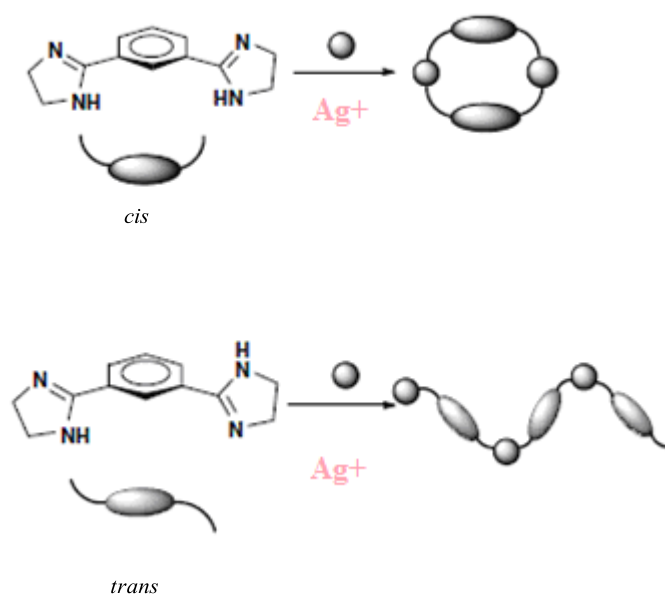


Figure 109 *Cis* and *trans* conformations of $\{[\text{Ag}(\text{bib})](\text{NO}_3)\cdot\text{H}_2\text{O}\}_n$, (top) and $\{[\text{Ag}_2(\text{bib})_2(\text{NO}_2)](\text{NO}_2)\cdot 19/8\text{H}_2\text{O}\}_n$ (bottom).¹²⁷



Figure 110 X-ray crystal structure of $\{[\text{Ag}(\text{bib})](\text{NO}_3)\cdot\text{H}_2\text{O}\}_n$.¹²⁷

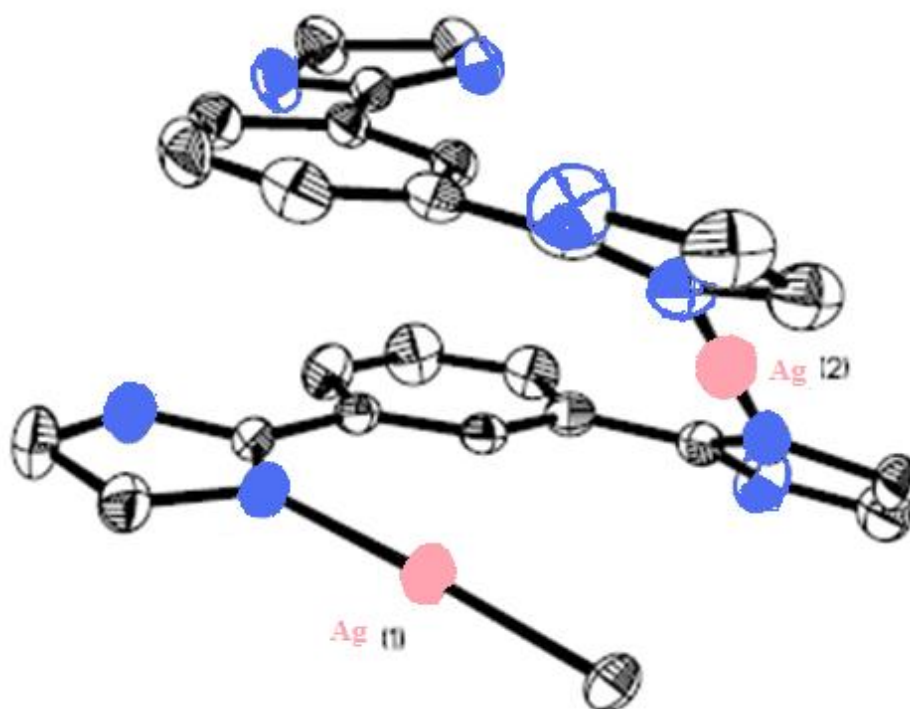


Figure 111 X-ray crystal structure of $\{[\text{Ag}_2(\text{bib})_2(\text{NO}_2)](\text{NO}_2)\cdot 19/8\text{H}_2\text{O}\}_n$.¹²⁷

Although there are obvious structural differences between the present Schiff base ligands and the bib ligand, it is reasonable to assume that there are configurational similarities in the structures of their Ag(I) complexes. On this premise, possible polymeric *cis* and *trans* geometries for the representative complex, [Ag(60)]ClO₄, are shown in Figures 112 and

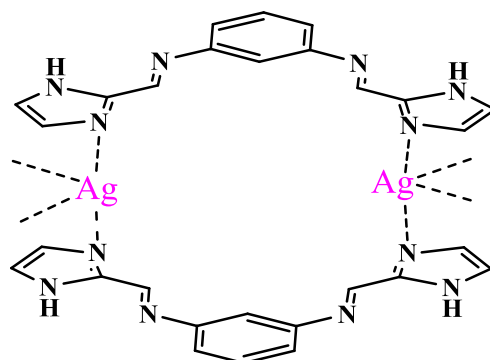


Figure 112 Possible polymeric, *cis* structure for the Ag(I) complex, [Ag(60)]ClO₄.

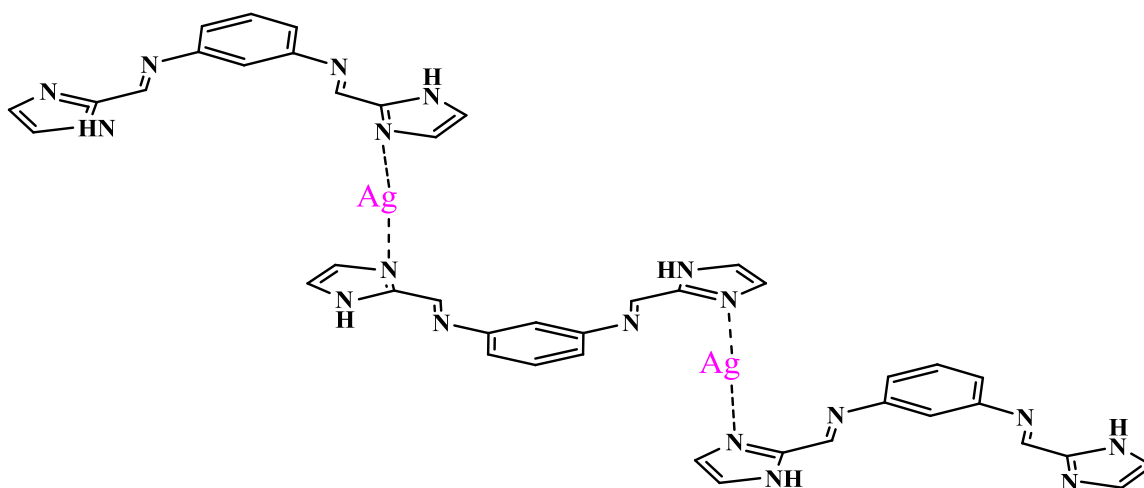


Figure 113 Possible polymeric, *trans* structure for the Ag(I) complex, [Ag(60)]ClO₄.

113, respectively. Microanalytical, IR and NMR data for the Ag(I) complexes of Schiff base ligands derived from salicylaldehyde, (62)-(64), indicate that the phenol moieties in these ligands are not deprotonated. Thus, the behaviour of these ligands appears to be somewhat different to that of the common “salen-type” ligands, as the latter typically

deprotonate at the two phenol moieties and have N_2O_2 coordination.¹²⁸ The highly insoluble nature of $[Ag_{1.5}(\mathbf{62})](ClO_4)_{1.5}$, $[Ag(\mathbf{63})]ClO_4$ and $[Ag(\mathbf{64})]ClO_4$ would again imply that they have a polymeric structure. Possible structures for the 1:1 Ag:ligand complexes, $[Ag(\mathbf{63})]ClO_4$ and $[Ag(\mathbf{64})]ClO_4$, are shown in Figures 114 and 115, respectively. There does not appear to be an obvious structure that can be drawn which conforms to the 1.5:1 Ag:ligand complex, $[Ag_{1.5}(\mathbf{62})](ClO_4)_{1.5}$.

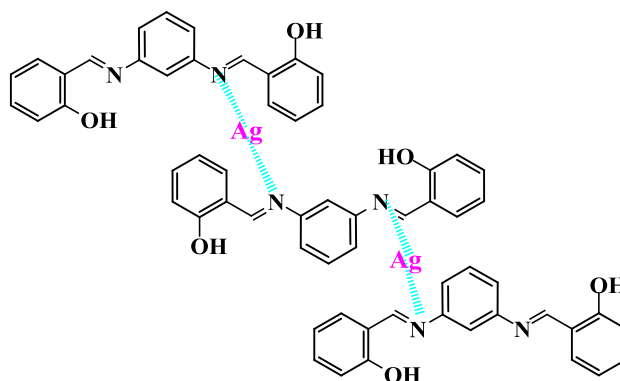


Figure 114 Possible polymeric structure for the Ag(I) Complex, $[Ag(\mathbf{63})]ClO_4$

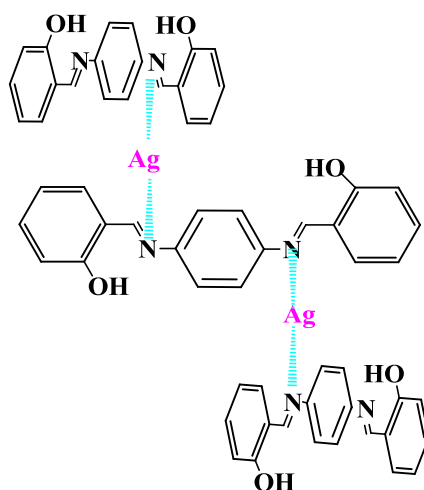


Figure 115 Possible polymeric structure for the Ag(I) complex, $[Ag(\mathbf{64})]ClO_4$.

3.14 Biological Activity

3.14.1 The Fungal Growth Curve

The growth cycle (Figure 116) of the yeast *Candida albicans* can be divided into four phases. The lag phase, which is where the cells are acclimatizing to the new environmental conditions and there is no significant increase in cell numbers with time. The exponential phase is where maximum population growth occurs as the cells double in number every twenty minutes. The stationary phase is where there is no further increase in population size (population growth is static) as the available nutrients become limited. Finally, the death phase (not shown), where the cell population rapidly diminishes as the nutrients are completely exhausted.

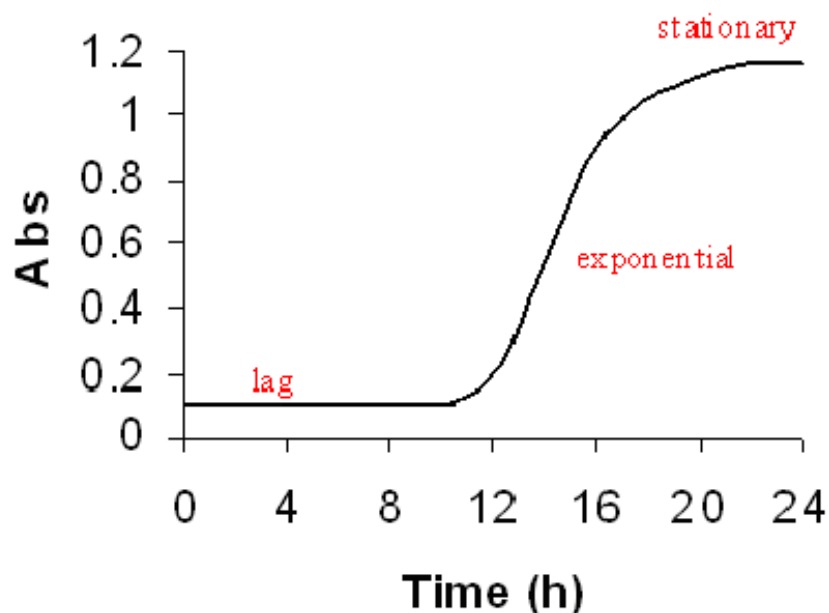


Figure 116 Growth curve (absorbance at $\lambda = 540$ nm) for *C. albicans* (death phase not included) in the absence of drug (control).

3.14.2 Anti-*Candida* Activity of Imidazole Ligands and their Metal-Complexes

All of the metal-free ligands and their Ag(I) complexes were tested for their anti-*Candida* activity in minimal medium (MM). As the metal-free ligands and the Ag(I) complexes are essentially insoluble in water, all activity tests were conducted as a suspension using a solvent mixture of DMSO and water. While there may be varying degrees of solubility for the different sets of complexes, it is difficult to quantify this because of the extremely small quantities of samples that were used in this study. In all cases, the activity of the complexes was compared to that of a drug-free, positive control, where the fungal cells replicated rapidly (maximum growth potential) under the test conditions employed. A blank, or negative control (no fungal cells or drugs), was also included in each test run. All activity tests were done in triplicate over three consecutive days (a total of nine readings). In addition, the anti-fungal prescription drug, Ketoconazole, the topical cream, SSD, and a selected number of simple Ag(I) salts and previously reported Ag(I) complexes were also screened.

The *in vitro*, anti-*Candida* activity of the test compounds is expressed as a minimum inhibitory concentration (MIC_{100}) of drug, specified as both μg of compound per 1 cm^3 of medium and as an approximated μM concentration, required to totally inhibit the growth of the fungal cells at $37\text{ }^\circ\text{C}$. MIC_{50} is the minimum drug concentration for 50% inhibition of fungal cell growth. In general, the MIC_{100} is the reference standard quoted in this study. The fungal cell growth profiles are shown in Figure 117. Cell growth was monitored over a 24 h period at $37\text{ }^\circ\text{C}$. Cells subjected to a drug concentration that inhibits all growth (MIC_{100}) will exhibit the growth profile illustrated by the blue line. Cells subjected to a drug concentration which cause a 50% reduction in cell growth (MIC_{50}) will exhibit the growth profile illustrated by the red line. Cells unaffected by the administered drug will have the 100% growth profile (black line).

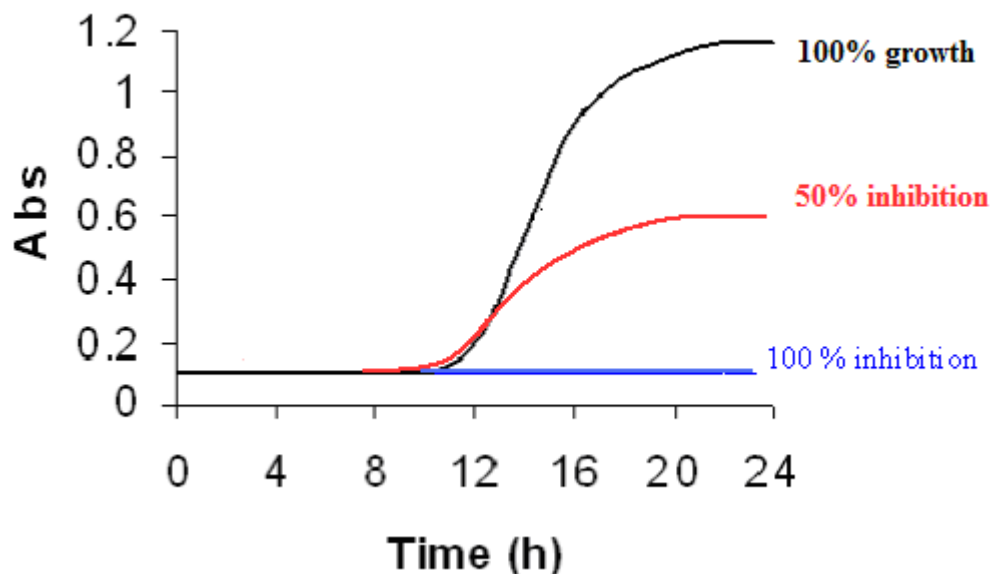


Figure 117 Growth profiles (absorbance at $\lambda = 540$ nm) for *C. albicans* showing the expected curve when there is 100% growth (black), 100% inhibition (blue) and 50% inhibition (red).

All of the metal-free ligands synthesised in the present work were found to be essentially inactive at a concentration of $\leq 50 \mu\text{g cm}^{-3}$. The cut-off test concentration of $50 \mu\text{g cm}^{-3}$ was chosen because above this concentration the drug dose required to maintain therapeutic levels would be unrealistically high and would significantly increase the likelihood of adverse side-effects.

The anti-*Candida* activities of some simple Ag(I) salts, selected Ag(I) complexes, SSD and Ketoconazole are given in Table 8. The Ag(I) complexes used in this reference table, $[\text{Ag}(\text{NO}_2\text{imi})]^{125}$, $[\text{Ag}_2(\text{SalH})_2]^{28,29}$ and $[\text{Ag}(\text{Apim})]\text{ClO}_4^{125}$ were chosen as representative examples of previous relevant work from within our research group.

Table 8 Anti-*Candida* activity of simple Ag(I) salts, selected Ag(I) complexes, SSD and ketoconazole.

Ag(I) salt/complex/drug	MIC ₁₀₀ ($\mu\text{g cm}^{-3}$)	MIC ₁₀₀ (μM)
AgNO ₃ ¹²⁵	0.31	1.82
AgClO ₄ ¹²⁵	0.31	1.49
[Ag(NO ₂ imi)] ¹²⁵	0.62	1.93
[Ag ₂ (SalH) ₂] ^{28,29}	0.31	1.35
[Ag(Apim)]ClO ₄ ¹²⁵	0.62	1.80
SSD	1.25	3.18
Ketoconazole	12.5*	23.57

NO₂imiH = 4(5)-nitroimidazole

SalH₂ = salicylic acid

SSD = silver sulfadiazine

Apim = 1-(3-aminopropyl)imidazole

*MIC₅₀ = 3.12 $\mu\text{g cm}^{-3}$

The simple Ag(I) salt, AgNO₃, is rarely used clinically today in the developed world. When used therapeutically, it is administered at extremely low concentrations because of its corrosive nature and the cosmetically undesirable side-effect of a long-lasting, dark brown stain on the skin when it is exposed to light.

The anti-*Candida* activities of the Ag(I) complexes shown in Table 8 are not significantly different from the results obtained for the simple Ag(I) salts. However, the MIC₁₀₀ value for Ketoconazole is relatively high compared to that of the simple Ag(I) salts and the Ag(I) complexes. Although it is known that the activity of Ketoconazole is superior *in vivo* than *in vitro*,^{3,4,9,10,12,28,29,125} the compound also exhibits a "tailing effect" *in vitro* i.e. it continues to have an inhibitory effect on cell growth even at very low concentrations (e.g. it was found to have a MIC₅₀ value of 3.12 µg cm⁻³ under the present test conditions). It is suggested that this tailing effect may be due to either the insolubility of Ketoconazole, which allows for the slow release of the drug, or there may be secondary activity due to the compounds metabolites.^{3,4,9,10,12} SSD also exhibits a similar tailing effect.^{19,43,64,65,68-70} In the case of SSD, the insolubility of the complex may allow for a slow release of the Ag(I) ions, thus prolonging the therapeutic effect.^{19,68-70}

3.14.3 Anti-*Candida* Activity of the Ag(I) Complexes of the Schiff Base

Ligands Derived from 1*H*-imidazole-2-amine (1)

Figure 118 shows the general structural formula for the set of Schiff base ligands derived from 1*H*-imidazole-2-amine (1).

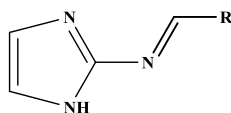
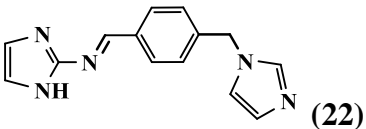
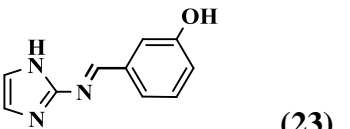
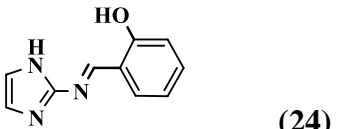
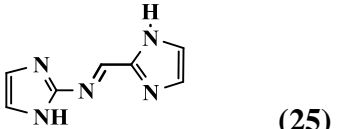
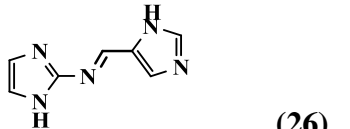
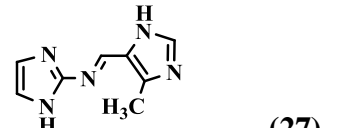
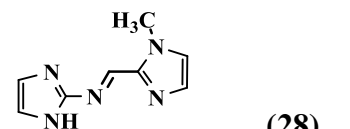


Figure 118 General structural formula for the Schiff base ligands derived from 1*H*-imidazole-2-amine (1).

The results of the anti-*Candida* activity for the Ag(I) complexes of the ligands derived from 1*H*-imidazole-2-amine (**1**) are shown in Table 9. Although each of the seven Ag(I) complexes are more active than Ketoconazole ($\text{MIC}_{100} = 23.57 \mu\text{M}$), only $[\text{Ag}(\mathbf{22})_2]\text{ClO}_4$ ($\text{MIC}_{100} = 2.22 \mu\text{M}$) had superior activity to SSD ($\text{MIC}_{100} = 3.18 \mu\text{M}$). None of the complexes had activity exceeding that of the simple Ag(I) salts, AgNO_3 and AgClO_4 ($\text{MIC}_{100} = 1.82$ and $1.49 \mu\text{M}$, respectively). The variation in antifungal activity within the group of Ag(I) complexes is also of interest. The activity of $[\text{Ag}(\mathbf{22})_2]\text{ClO}_4$, which contains a phenylene moiety within the spacer chain between the two imidazole rings, is *ca.* 2-4 times greater than that of any of the other Ag(I) complexes listed in Table 9. It is reasonable to assume that the phenol group renders the complex more lipophilic, thus making the passage through the fungal membrane easier. With the exception of complexes $[\text{Ag}(\mathbf{22})_2]\text{ClO}_4$ and $[\text{Ag}(\mathbf{28})]\text{ClO}_4$, complexes having two imidazole moieties in the Schiff base ligands (e.g. $[\text{Ag}(\mathbf{26})]\text{ClO}_4$) were marginally less active than those containing one imidazole and one phenol moiety (e.g. $[\text{Ag}(\mathbf{23})_2]\text{ClO}_4$). It is interesting to note that complexes $[\text{Ag}(\mathbf{27})]\text{ClO}_4$ and $[\text{Ag}(\mathbf{28})]\text{ClO}_4$, which contain isomeric Schiff base ligands, had quite different activities. Complex $[\text{Ag}(\mathbf{28})]\text{ClO}_4$, which has a methyl substituent on the imidazole nitrogen (1-position), was twice as potent as $[\text{Ag}(\mathbf{27})]\text{ClO}_4$, which has the methyl substituent on the 4(5)-carbon atom of the imidazole ring. Assuming that it is the complex, as a whole, that is bioactive, then it is hard to explain the activity difference between the isomers $[\text{Ag}(\mathbf{27})]\text{ClO}_4$ and $[\text{Ag}(\mathbf{28})]\text{ClO}_4$, particularly as the amine nitrogen is generally regarded as a spectator atom (non-coordinating). In contrast to the difference in activity observed between the isomeric pair, $[\text{Ag}(\mathbf{27})]\text{ClO}_4$ and $[\text{Ag}(\mathbf{28})]\text{ClO}_4$, isomers $[\text{Ag}(\mathbf{23})_2]\text{ClO}_4$ and $[\text{Ag}(\mathbf{24})_2]\text{ClO}_4$ displayed similar activities. The activities of isomers $[\text{Ag}(\mathbf{25})]\text{ClO}_4$ and $[\text{Ag}(\mathbf{26})]\text{ClO}_4$ were also the same.

The bis-imidazole ligand, 2-BIM³¹ (Figure 22), which contains a single methylene group in the spacer chain (no imine moiety), is structurally related to the bis-imidazole Schiff base ligand in the Ag(I) complex, $[\text{Ag}(\mathbf{25})]\text{ClO}_4$. It has been previously reported³¹ that the silver(I) complex of 2-BIM, $[\text{Ag}_2(2\text{-BIM})_2](\text{ClO}_4)_2$ (Figures 64, 65), has a MIC_{100} value of $5\text{-}10 \mu\text{g cm}^{-3}$. The lower MIC_{100} value obtained for $[\text{Ag}(\mathbf{25})]\text{ClO}_4$ ($3.12 \mu\text{g cm}^{-3}$) would suggest that the inclusion of an imine moiety in the spacer chain of the ligand, though it must be noted that the former contains two Ag(I) ions against the one Ag(I) ion for the present complexes.

Table 9 Anti-*Candida* activity of Ag(I) complexes of the Schiff base ligands derived from 1*H*-imidazole-2-amine (**1**).

Ligand structure	Emp. formula	MIC ₁₀₀ ($\mu\text{g cm}^{-3}$)	MIC ₁₀₀ (μM)
 (22)	[Ag(22) ₂]ClO ₄	1.56	2.22
 (23)	[Ag(23) ₂]ClO ₄	3.12	5.36
 (24)	[Ag(24) ₂]ClO ₄	3.12	5.36
 (25)	[Ag(25)]ClO ₄	3.12	8.47
 (26)	[Ag(26)]ClO ₄	3.12	8.16
 (27)	[Ag(27)]ClO ₄	3.12	7.81
 (28)	[Ag(28)]ClO ₄	1.56	4.07

enhances the antifungal properties of the resulting Ag(I) complex. The improved activity of the phenylene-containing complex, [Ag(**22**)₂]ClO₄, is consistent with the findings of Coyle *et al.*²⁵ who suggested that extending the aromaticity of their ligands enhanced lipophilicity and improved the antifungal activity. It was also noted that the present set of Ag(I) complexes (with Schiff base ligands derived from 1*H*-imidazole-2-amine) exhibited a tailing effect, with some level of inhibition down to a concentration of 1.56 μg cm⁻³ ([Ag(**23**)₂]ClO₄, [Ag(**24**)₂]ClO₄, [Ag(**25**)]ClO₄, [Ag(**26**)]ClO₄, and [Ag(**27**)]ClO₄). This would suggest that either solubility or secondary activity due to the drugs metabolites might also be factor in the anti-*Candida* activity.

3.14.4 Anti-*Candida* Activity of the Ag(I) Complexes of the Schiff Base Ligands Derived from Histamine

The general formula for the set of Schiff base ligands derived from histamine is shown in Figure 119, and the anti-*Candida* activities are given in Table 10. The complexes are

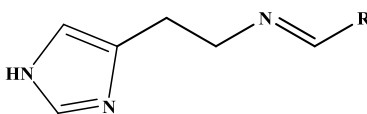
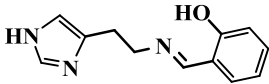
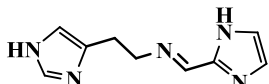
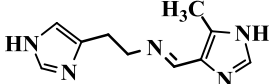
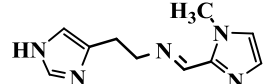
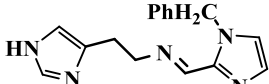
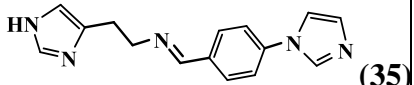


Figure 119 General structural formula for the Schiff base ligands derived from histamine.

4-31 times more active than the previous set whose ligands were derived from 1*H*-imidazole-2-amine (**1**). The most active Ag(I) complex, [Ag₂(**35**)](ClO₄)₂, was 84 times more active than Ketoconazole, 6 times more active than SSD and 11 times more active than [Ag(Apim)]ClO₄.

Table 10 The anti-*Candida* activities for the Ag(I) complexes of the Schiff base ligands derived from histamine.

Ligand structure	Emp. formula	MIC ₁₀₀ (μg cm ⁻³)	MIC ₁₀₀ (μM)
 <p>(29)</p>	[Ag(29)]ClO ₄	0.78	1.85
 <p>(30)</p>	[Ag _{1.5} (30)](ClO ₄) _{1.5}	0.78	1.56
 <p>(33)</p>	[Ag _{1.5} (33)](ClO ₄) _{1.5}	0.35	0.71
 <p>(31)</p>	[Ag _{1.5} (31)](ClO ₄) _{1.5}	0.78	1.51
 <p>(32)</p>	[Ag _{1.5} (32)](ClO ₄) _{1.5}	0.78	1.56
 <p>(34)</p>	[Ag(34)]ClO ₄	0.19	0.39
 <p>(35)</p>	[Ag ₂ (35)](ClO ₄) ₂	0.19	0.28

Although [Ag(**29**)]ClO₄ was the least active of this set it was still 13 times more active than Ketoconazole. Complexes [Ag_{1.5}(**33**)](ClO₄)_{1.5}, [Ag(**34**)]ClO₄ and [Ag₂(**35**)](ClO₄)₂ were more active than the simple Ag(I) salts (Table 8). The improved activity of this set of complexes, compared to the 1*H*-imidazole-2-amine (**1**) complexes, may be attributed to the difference in the structures of the Schiff base ligands and the formulation of some of the complexes. The ligands derived from histamine have two additional methylene units in the spacer chain compared to those originating from 1*H*-imidazole-2-amine (**1**). Also, the spacer chain is attached to a different carbon atom of the imidazole ring in the histamine residues (C-4(5)) and 1*H*-imidazole-2-amine (**1**) (C-2) of the respective Schiff base ligands. Furthermore, some of the Ag(I) complexes incorporating the histamine residue have more silver content (e.g. [Ag_{1.5}(**30**)](ClO₄)_{1.5}, MIC₁₀₀ = 1.56 μM) compared to the equivalent complex with the 1*H*-imidazole-2-amine (**1**) residue (e.g. [Ag(**25**)]ClO₄, MIC₁₀₀ = 8.47 μM). The increase in the length of the spacer chain of the complexes, due to the extra methylenes, may increase the flexibility of the complexes, possibly enhancing their ability to penetrate into the fungal cell and may also facilitate interactions within the fungal cell itself.

The variation in the antifungal activity within this histamine set of Ag(I) complexes is also of interest. Again, the most potent Ag(I) complex was the one containing a phenylene moiety in the spacer chain ([Ag₂(**35**)](ClO₄)₂ MIC₁₀₀ = 0.28 μM). The isomeric pair, [Ag_{1.5}(**31**)](ClO₄)_{1.5} and [Ag_{1.5}(**32**)](ClO₄)_{1.5}, both of which contain a methyl group on the imidazole ring, are equally active. This is in contrast to the findings for the corresponding isomeric pair, [Ag(**27**)]ClO₄ and [Ag(**28**)]ClO₄, in the previous 1*H*-imidazole-2-amine (**1**) set of complexes (Table 9). The isomeric pair [Ag_{1.5}(**30**)](ClO₄)_{1.5} and [Ag_{1.5}(**33**)](ClO₄)_{1.5} show a significant difference in activity (1.56 μM and 0.71 μM, respectively). Again, this is contrary to the findings for the corresponding isomeric pair, [Ag(**25**)]ClO₄ and [Ag(**26**)]ClO₄, from the 1*H*-imidazole-2-amine (**1**) set where no real difference in activity was found. Whilst [Ag_{1.5}(**30**)](ClO₄)_{1.5} and [Ag_{1.5}(**33**)](ClO₄)_{1.5} have the same Ag:ligand ratio (1.5:1), the only difference between the complexes lies in the position of the attachment of the spacer chain to the imidazole ring. The spacer chain is linked to the imidazole carbon at the 2-position in the ligand in [Ag_{1.5}(**30**)](ClO₄)_{1.5} while

it is joined in the 4(5)-position at the ligand of the more potent complex, $[\text{Ag}_{1.5}(\mathbf{33})](\text{ClO}_4)_{1.5}$.

3.14.5 Anti-*Candida* Activity of the Ag(I) Complexes of the Schiff Base Ligands Derived from Apim

The general structural formula for the set of Schiff base ligands derived from Apim is shown in Figure 120 and the anti-*Candida* activities for the Ag(I) complexes are given in Table 11.

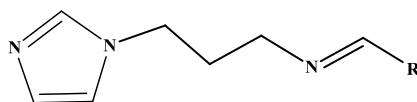
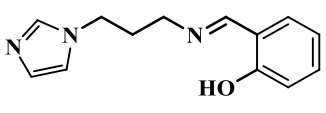
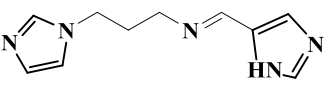
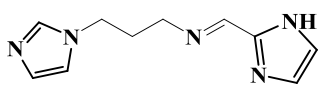
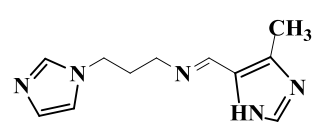
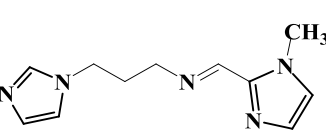


Figure 120 The general structural formula for the set of Schiff base ligands derived from Apim.

Complex $[\text{Ag}(\mathbf{36})_2]\text{ClO}_4$, which contains only one imidazole residue in its Schiff base ligands, was the least active of this set. Whilst the ratio of Ag(I):ligand for $[\text{Ag}(\mathbf{36})_2]\text{ClO}_4$ is 1:2, the rest of the complexes have a 1:1 Ag(I):ligand ratio. Thus, it may be that it is the higher amount of the Ag(I) ion in the latter complexes that is responsible for the improved antifungal activity. With the exception of $[\text{Ag}(\mathbf{36})_2]\text{ClO}_4$, the anti-*Candida* activity of this set of Ag(I) complexes was greatly superior to the two previous sets (i.e. the Ag(I) complexes of Schiff base ligands derived from 1*H*-imidazole-2-amine (**1**) and those derived from histamine). The present set of complexes were also significantly more potent than the simple Ag(I) salts, the Ag(I) complexes and SSD (Table 8). In addition,

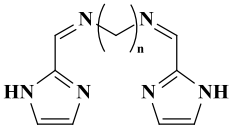
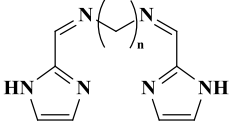
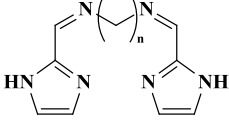
Table 11 The anti-*Candida* activities for the Ag(I) complexes of the Schiff base ligands derived from Apim.

Ligand structure	Emp. formula	MIC ₁₀₀ ($\mu\text{g cm}^{-3}$)	MIC ₁₀₀ (μM)
 <p>(36)</p>	[Ag(36) ₂]ClO ₄	0.31	0.45
 <p>(37)</p>	[Ag(37)]ClO ₄	0.03	0.07
 <p>(38)</p>	[Ag(38)]ClO ₄	0.03	0.07
 <p>(39)</p>	[Ag(39)]ClO ₄	0.03	0.07
 <p>(40)</p>	[Ag(40)]ClO ₄	0.03	0.07

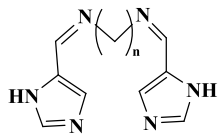
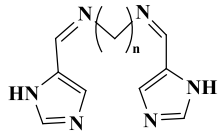
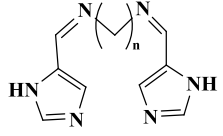
the complexes were up to 340 times more potent than Ketoconazole. The two sets of isomers, [Ag(37)]ClO₄, [Ag(38)]ClO₄ and [Ag(39)]ClO₄, [Ag(40)]ClO₄, were found to have the same anti-*Candida* activity. The activity of this set of Ag(I) complexes containing Schiff base ligands derived from Apim might have been expected to be

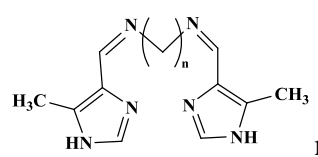
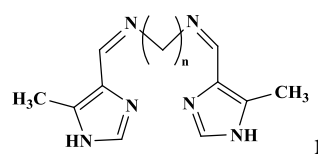
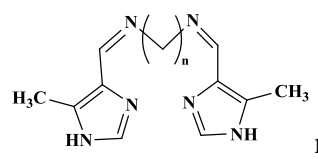
This set of complexes is divided into sub-sets in accordance with the substituted imidazolecarboxaldehydes or the salicylaldehyde which were reacted with the diamines. With the exception of $[\text{Ag}_2(\mathbf{51})](\text{ClO}_4)_2$ and $[\text{Ag}_2(\mathbf{52})](\text{ClO}_4)_2$ this set of complexes showed a significant reduction in activity (2-3 times less active) compared to the Apim set (Table 9). It would seem that incorporating a second imine moiety in the spacer chain of the ligand is, at least, partially responsible for this decrease in activity. The most active complexes were $[\text{Ag}_2(\mathbf{51})](\text{ClO}_4)_2$ and $[\text{Ag}_2(\mathbf{52})](\text{ClO}_4)_2$, and the least active were in the sub-set comprising $[\text{Ag}_{1.5}(\mathbf{56})](\text{ClO}_4)_{1.5}$, $[\text{Ag}_2(\mathbf{57})](\text{ClO}_4)_2$ and $[\text{Ag}_2(\mathbf{58})](\text{ClO}_4)_2$. The major structural difference between the most active and the least active complexes in the set is the presence of the phenyl substituents on the periphery of the Schiff base ligand in the latter sub-set.

Table 12 The anti-*Candida* activities of the Ag(I) complexes of the Schiff base ligands derived from 1,2-diaminoethane, 1,3-diaminopropane and 1,4-diaminobutane.

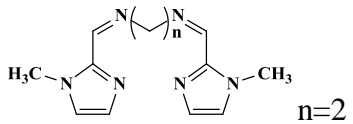
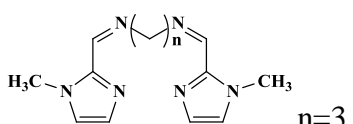
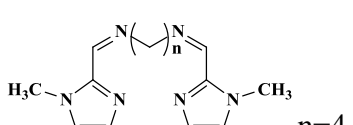
Ligand structure	Emp. formula	MIC ₁₀₀ ($\mu\text{g cm}^{-3}$)	MIC ₁₀₀ (μM)
 n=2 (41)	$[\text{Ag}_{1.5}(\mathbf{41})](\text{ClO}_4)_{1.5}$	0.15	0.28
 n=3 (42)	$[\text{Ag}_{1.5}(\mathbf{42})](\text{ClO}_4)_{1.5}$	0.15	0.28
 n=4 (43)	$[\text{Ag}_2(\mathbf{43})](\text{ClO}_4)_2$	0.15	0.23

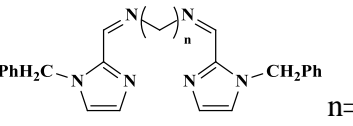
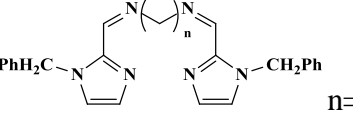
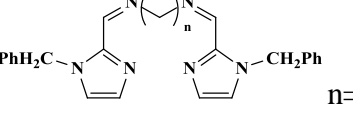
Contd.

 $n=2$ (50)	$[\text{Ag}(\mathbf{50})]\text{ClO}_4$	0.19	0.45
 $n=3$ (51)	$[\text{Ag}_2(\mathbf{51})](\text{ClO}_4)_2$	0.10	0.16
 $n=4$ (52)	$[\text{Ag}_2(\mathbf{52})](\text{ClO}_4)_2$	0.10	0.15

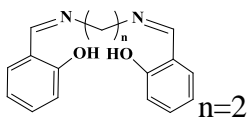
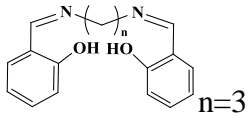
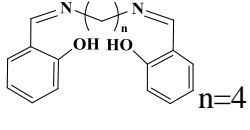
 $n=2$ (44)	$[\text{Ag}_2(\mathbf{44})](\text{ClO}_4)_2$	0.39	0.59
 $n=3$ (45)	$[\text{Ag}_2(\mathbf{45})](\text{ClO}_4)_2$	0.39	0.58
 $n=4$ (46)	$[\text{Ag}_2(\mathbf{46})](\text{ClO}_4)_2$	0.39	0.57

Contd.

 <p style="text-align: center;">(53)</p>	$[\text{Ag}_{1.5}(\mathbf{53})](\text{ClO}_4)_{1.5}$	0.19	0.34
 <p style="text-align: center;">(54)</p>	$[\text{Ag}_{1.5}(\mathbf{54})](\text{ClO}_4)_{1.5}$	0.19	0.33
 <p style="text-align: center;">(55)</p>	$[\text{Ag}_2(\mathbf{55})](\text{ClO}_4)_2$	0.19	0.28

 <p style="text-align: center;">(56)</p>	$[\text{Ag}_{1.5}(\mathbf{56})](\text{ClO}_4)_{1.5}$	0.78	1.10
 <p style="text-align: center;">(57)</p>	$[\text{Ag}_2(\mathbf{57})](\text{ClO}_4)_2$	0.78	0.95
 <p style="text-align: center;">(58)</p>	$[\text{Ag}_2(\mathbf{58})](\text{ClO}_4)_2$	0.78	1.36

Contd.

 <p style="text-align: center;">(47)</p>	[Ag (47)] ClO_4	0.19	0.40
 <p style="text-align: center;">(48)</p>	[Ag (48)] ClO_4	0.19	0.39
 <p style="text-align: center;">(49)</p>	[Ag ₂ (49)](ClO_4) ₂	0.19	0.27

Within the sub-set comprising complexes [Ag**(50)**] ClO_4 , [Ag₂**(51)**](ClO_4)₂ and [Ag₂**(52)**](ClO_4)₂, complex [Ag**(50)**] ClO_4 is approximately three times less active than [Ag₂**(51)**](ClO_4)₂ and [Ag₂**(52)**](ClO_4)₂. The major difference between these three complexes is that [Ag**(50)**] ClO_4 is formulated as a 1:1 Ag:ligand complex, while [Ag₂**(51)**](ClO_4)₂ and [Ag₂**(52)**](ClO_4)₂ are 2:1 Ag:ligand complexes. It is plausible that it may be the reduced Ag(I) content that is responsible for the corresponding reduction in activity. Kamenecka *et al.*,¹²⁸ in their work on amidines as possible cancer drugs, investigated the effect of the imine moiety on the activity of their organic compounds. While the imine moiety was clearly needed for potency, it was suggested that its role was to provide the appropriate local $\text{p}K_a$ for the drugs affinity. This would suggest that the presence of two imines in the current set of Ag(I) complexes might increase the basicity of the complex above the critical physiological level, thus having a negative effect on their anti-*Candida* activity. Thus, any positive effects on activity due to the variation in the spacer chain length are mitigated by the negative effect of the increase in ligand basicity.

3.14.7 Anti-*Candida* Activity of the Ag(I) Complexes of the Schiff Base Ligands Derived from 1,2-, 1,3- and 1,4-Phenylenediamine

The general structural formulae for the set of Schiff base ligands derived from 1,2-, 1,3- and 1,4-phenylenediamine are shown in Figure 122 and the anti-*Candida* activities for the Ag(I) complexes are given in Table 13. In general, this set of Ag(I) complexes were

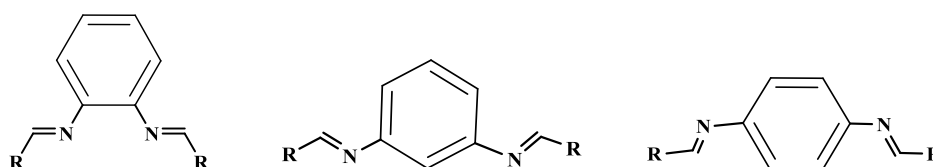
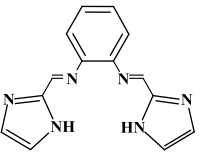
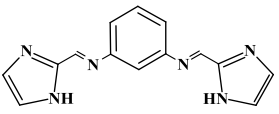
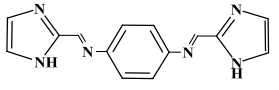
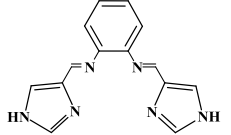
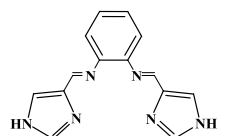
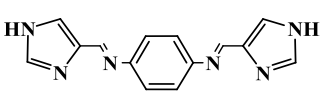
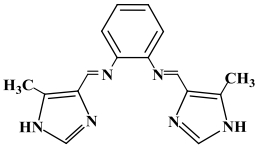
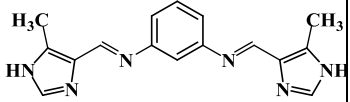
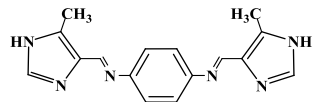


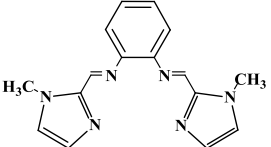
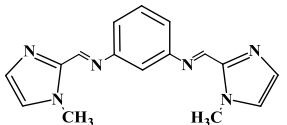
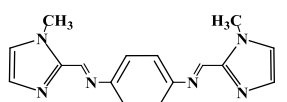
Figure 122 The general structural formula for the set of Schiff base ligands derived from 1,2- 1,3- and 1,4-phenylenediamine.

not as active as those originating from histamine, Apim or those derived from 1,2-diaminoethane, 1,3-diaminopropane and 1,4-diaminobutane. The introduction of an aromatic phenylene moiety into the spacer chain, instead of the aliphatic methylenes that were used in the previous ligand set, resulted in a general decrease in antifungal activity. In addition, it is evident that the structural differences within the spacer chain of this set of ligands (1,2-, 1,3- and 1,4-phenylenediamine) does not impact on the antifungal activity. Furthermore, activity is unaffected when imidazole end groups are replaced by a phenol moiety.

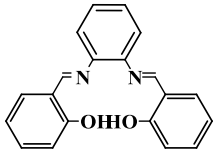
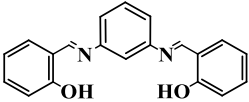
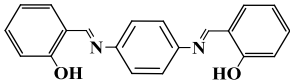
Table 13 The anti-*Candida* activity for the Ag(I) complexes of the Schiff base ligands derived from 1,2-, 1,3- and 1,4-phenylenediamine.

Ligand structure	Emp. formula	MIC ₁₀₀ ($\mu\text{g cm}^{-3}$)	MIC ₁₀₀ (μM)
 <p style="text-align: center;">(59)</p>	[Ag _{1.5} (59)](ClO ₄) _{1.5}	0.78	1.35
 <p style="text-align: center;">(60)</p>	[Ag(60)]ClO ₄	0.78	1.54
 <p style="text-align: center;">(61)</p>	[Ag(61)]ClO ₄	0.78	1.66
 <p style="text-align: center;">(68)</p>	[Ag _{1.5} (68)](ClO ₄) _{1.5}	0.78	1.30
 <p style="text-align: center;">(69)</p>	[Ag(69)]ClO ₄	0.78	1.60
 <p style="text-align: center;">(70)</p>	[Ag(70)]ClO ₄	0.78	1.60

 <p style="text-align: center;">(65)</p>	$[\text{Ag}_{1.5}(\mathbf{65})](\text{ClO}_4)_{1.5}$	0.78	1.29
 <p style="text-align: center;">(66)</p>	$[\text{Ag}_{1.5}(\mathbf{66})](\text{ClO}_4)_{1.5}$	0.78	1.29
 <p style="text-align: center;">(67)</p>	$[\text{Ag}_{1.5}(\mathbf{67})](\text{ClO}_4)_{1.5}$	0.78	1.29

 <p style="text-align: center;">(71)</p>	$[\text{Ag}(\mathbf{71})]\text{ClO}_4$	0.78	1.51
 <p style="text-align: center;">(72)</p>	$[\text{Ag}(\mathbf{72})]\text{ClO}_4$	0.78	1.46
 <p style="text-align: center;">(73)</p>	$[\text{Ag}(\mathbf{73})]\text{ClO}_4$	0.78	1.51

Contd.

 <p style="text-align: center;">(62)</p>	$[\text{Ag}_{1.5}(\mathbf{62})](\text{ClO}_4)_{1.5}$	0.78	1.28
 <p style="text-align: center;">(63)</p>	$[\text{Ag}(\mathbf{63})]\text{ClO}_4$	0.78	1.50
 <p style="text-align: center;">(64)</p>	$[\text{Ag}(\mathbf{64})]\text{ClO}_4$	0.78	1.39

3.15 Summary of Anti-*Candida* Activity

Of the five sets of Ag(I) complexes screened, the most active was the set containing the Schiff base ligands derived from Apim (Table 9). With an average MIC₁₀₀ value of 0.07 μM this set of Ag(I) complexes ($[\text{Ag}(\mathbf{37})]\text{ClO}_4$, $[\text{Ag}(\mathbf{38})]\text{ClO}_4$, $[\text{Ag}(\mathbf{39})]\text{ClO}_4$ and $[\text{Ag}(\mathbf{40})]\text{ClO}_4$) displayed the highest anti-*Candida* activity of any of the metal complexes reported to date in the literature. It is obvious from these studies that a positive synergism exists between the metal and the ligand in the antimicrobial action of the complexes. However, detailed mechanistic investigations will be necessary to establish the mode(s) of action of the complexes.



Conclusions



According to Cohen *et al.*¹²⁹ "the challenges in developing the most effective drugs are, "to find the appropriate group, the correct substituents and the correct substitution positions in the target molecule". To meet these challenges and to design an effective antifungal drug, or family of drugs, the previous knowledge and experience of imidazole chemistry within this research group was utilized.^{31,55} Four objectives were set. The ideal drug should incorporate (i) a hydrophobic functionality, (ii) a hydrophilic functionality, (iii) a metal binding site and (iv) a degree of flexibility. In order to fulfil these requirements, a set of imidazolecarboxaldehydes were chosen and reacted with selected amines, to give five sets of Schiff base ligand. The position and length of the spacer chain linking the two imidazoles moieties or phenol groups was varied, as was the position and the substituents on the imidazole ring. The Schiff base ligands were then complexed to Ag(I) ions. The resulting complexes contained a hydrophilic group (the imidazole) and a flexible hydrophobic linker chain. The Ag(I) metal binding site was provided by the N atom of the imine groups on the imidazoles and possibly also the imine N atom of the spacer chain. The electron-donating imine group also provided an extra reactive functionality (e.g. drug-target site H-bonding). The presence of the imidazole N-H amine group is also thought to enhance bioactivity due to its H-bonding abilities and the provision of the physiologically appropriate pK_a .¹²⁹ The hydrophobic moiety should facilitate entry of the drug into the fungal cell by providing greater lipophilicity, which may also play an important part in maintaining the drugs at therapeutic dosage levels. The linker chain may allow the degree of flexibility needed for the fluid nature of protein-drug interactions.¹³⁰

While the synthesis of some of the Schiff base ligands in the present work was problematic (due largely to their insolubility) this did not prevent them from complexing to Ag(I) ions. The ligands were characterized using standard IR and NMR spectroscopic methods, microanalysis and, in some instances, by X-ray crystallography.

The synthesized Schiff base ligands might result in either the *E* or *Z* forms due to stereochemistry about the carbon-nitrogen double bond. However, evidence for more than one form was not found in the ^1H NMR spectra since only one signal is seen for the imine $\text{N}=\text{C}-\text{H}$. The *E* form would be expected to be more stable on steric grounds. Poor solubility did not yield X-ray quality crystals for four of the five ligand sets or for any of the $\text{Ag}(\text{I})$ complexes. However, X-ray crystal structures were obtained for two of the Schiff base ligands derived from the Apim set, confirming the *E* stereochemistry, and consistent with the NMR data. Compared to the synthesis of the ligands, the preparation of the $\text{Ag}(\text{I})$ complexes was relatively simple and the products were isolated in moderate to good yields. The complexes were characterized using standard IR and NMR spectroscopic methods, microanalysis and, in two cases, by mass spectrometry.

All of the Schiff base ligands and their corresponding $\text{Ag}(\text{I})$ complexes were tested for their anti-*Candida* activity. While all the metal-free ligands were essentially inactive the $\text{Ag}(\text{I})$ complexes showed excellent antifungal activity. The set of $\text{Ag}(\text{I})$ complexes based on the Apim Schiff base ligands were the most potent. A progressive improvement in activity of the $\text{Ag}(\text{I})$ complexes was seen on going from ligands derived from 1*H*-imidazole-2-amine (**1**), to histamine to Apim, corresponding to the increase in spacer-chain length of the respective ligand sets. However, this pattern was not found in the case of the set of $\text{Ag}(\text{I})$ complexes of di-Schiff base ligands derived from 1,2-diaminoethane, 1,3-diaminopropane and 1,4-diaminobutane. A notable reduction in activity was observed despite increasing the spacer chain length. It is possible that the extra imine group in the spacer chain may have had a negative impact on activity and negated any positive effect due to the progressive increase in spacer chain length.

The set of $\text{Ag}(\text{I})$ complexes containing di-Schiff base ligands derived from 1,2-, 1,3- and 1,4-phenylenediamine had similar activity to those complexes with ligands derived from 1,2-diaminoethane, 1,3-diaminopropane and 1,4-diaminobutane. In this instance, the resulting increase in the level of aromaticity and presumably lipophilicity, does not appear to influence the anti-*Candida* activity.

Bibliography

- 1 Murray, P., Rosenthal, K.S., Kobayashi, G.S., Pfaller, M.A., *Medical Microbiology*, 4th edn., 2002, Mosby, Inc. St. Louis.
- 2 (a) Brown, M., *Medical Microbiology*, 3rd edn., 1998, Mosby, Inc. St. Louis; (b) Rang, H.P., Dale, M.M., Ritter, J.M., *Pharmacology*, 4th edn., 1999, Churchill, Livingstone.
- 3 O'Rourke, Canon, J., *The History of the Great Irish Famine of 1847*, 3rd edn., 1902, Reprint, 1989, Veritas.
- 4 (a) Centre for Disease Control and Prevention, (CDC) C.R., Atlanta, GA 30333, USA; (b) National Centre for Zoonotic, 2008, Vector-Borne and Enteric Diseases (ZVED); (c) Van Tyle, JH., *Pharmacotherapy*, 1984, **6**, 343-373.
- 5 (a) Lipski, E., *Leaky Gut Syndrome*, 1998, McGraw-Hill, USA; (b) Gow, N., *Mycologist*, 2002, **16**, Cambridge University Press, U.K.
- 6 Stone, E.A., Harold, H.F., Kirshenbaum, L. *Clinical Therapeutics*, 2002, **24**, 3-12, and references therein.
- 7 (a) Onishi, J., Meinz, M., Thompson, J., *J. Antimicrob. Agent, Chemo.*, 2000, **44**, 368-377; (b) Georgopapadakou, N.H., *Microb.*, 1995, **3**, 98-104.
- 8 Hazen, E., Brown, R., *Science*, 1950, **112**, 423-423.
- 9 (a) The US, National Library of Medicine & The National Institute of Health, *Chemical Compounds*, 2008; (b) Odds, F., *Mycologist*, 2003, **17**, 51-55. (c) Andriole, V., *Int. J. Antimicrob. Agents*, 2000, **16**, 317-321.
- 10 Ghannoum, M.A., Rice, L.B., *Clinical Microb. Rev.*, 1999, 501-517.
- 11 De Kruijff, B.D., Demel, R.A., *Biochim. Biophys. Acta*, 1974, **339**, 57-70.
- 12 Ruge, E., Korting, H.C., Borelli, C., *Antimicrob. Agents*, 2005, **26**, 427-441.
- 13 Munayyer, H., Shaw, R.S., Hare, B., Salisbury, L., Heimark, B., Pramanik, K. Greene, J.R., 36th Interscience Conference on *Antimicrob. Agents and Chemotherapy*, 1996, and references therein; (b) Hector, R.F., *Clin. Tec. Small Anim. Prac.*, 2005, **20**, 240-249.

- 14 Basilio, A., Collado, J., Diez, M. T., Guan, Z., Harris, G.H., Justice, M.C., Nielsen-kahn, J., Shastry, M. S., Merck and Co. INC (P O BOX 2000 Rahway, NJ, U.S., 0706509071971, **51**, 119-120.), 2004 patent (IPC1-7): A61K031/522; A61K031/7076; C07D493/12; A61K031/7072.
- 15 (a) NIH (U.S. National Institute of Health) *Metals in Medicine: Conference Target, Diagnostics and Therapeutics*, 2000; (b) Stemmler, A.J., Burrows, C., *J. Am. Chem. Soc.*, 1999, **29**, 6956–6957; (c) Redox Pharmaceuticals Corp., Greenvale, New York, USA, WO Patent WO/2008/070,317, 2008 IPC: A61K 31/70 (2006.01), A61K 31/7088 (2006.01); (d) Zhang, Z., Nair, S.A., McMurry, T.J., *Current Med. Chem.*, 2000, **12**, 751-778, (e) Kato, H., Kanazawa, Y., Okumura, M., Taninaka, A., Yokawa, T., Shinohara, H., *J. Am. Chem. Soc.*, 2003, **14**, 4391–4394.
- 16 Chopra. I., *J. Antimicrob. Chem.*, 2007, **59**, 587-590.
- 17 (a) Ebers G.M., Stern. L., *Papyrus Ebers*. Facsimile with a partial translation 2 volumes, 1875; (b) Arab, S.M., *Medicine in Ancient Egypt*, Arab World Books, part 3 of 3, 1998-2000; (c) Merry, W.W., Riddell, J., Monro, D.B., *Commentary on the Odyssey*, Oxford, Clarendon Press, 1886, (Homer's Odyssey Books I-XII. 2nd ed.); (d) Raulin. J., *Ann. Sci. Nat. Botan.*, 1869, **11**, 293-299.
- 18 Moyer, C.A., Brentano, L., Gravens, D.L., Margraf, H.W., Monafó, W.W., *Arch. Surg.*, 1965, **90**, 812-867; (b) Klasen, H.J., *Burns*, 2000, **26**, 131-138.
- 19 (a) Fox, C.L., *Arch. Surg.*, 1968, **96**, 184-188; (b) Johnson & Johnson SILVERCEL ® Antimicrobial Alginate Dressing.
- 20 McHugh G.L., Moellering, R.C., Hopkins, C.C., Swartz, M.N., *Lancet*, 1975, **1**, 235-240; (b) Fung MC, Bowen DL., F.D.A, Rockville, Maryland, USA., *J Toxicol Clin Toxicol.*, 1996, **34**,119-126.
- 21 (a) Powderly, W.G., *Resistant Candidiasis*, AIDS Research and Human Retroviruses, Mary Ann Liebert, Inc., USA, Publishers, 1994, 10; (b) Melhus, A., *Expert Opinion, Informa. Pharm. Sci.*, 2005, 1-4, (in collaboration with the Swedish Doctors for the Environment (LfM)).

- 22 (a) Gupta, A., Phung L.T., Taylor D.E, Silver, S., *Microbiol.*, 2001, **147**, 3393-3402; (b) Gupta, A., Matsui, K., Lo, J.F., *Nat. Med.*, 1999, **5**, 183-188; (c) Ip, M., Lui, S.L., Chau, S.S.L., Lung, I., Burd, A., *J. Hosp. Infect.*, 2006, **63**, 342-357; (d) Li, XZ., Nikaido, H., Willams, K.E., *J. Bacteriol.*, 1997, **179**, 6127-6132.
- 23 (a) Gielen, M., Tiekink, E.R.T., *Metallotherapeutic Drugs and Metal-Based Diagnostic Agents: The Use of Metals in Medicine*, Wiley & Son Ltd., Chichester, UK., 2005; (b) Database on Metallopharmaceuticals, URDIP (Unit for Research and Development of Information Products), Jopasana 85/1, Paud Rd., Kothrud, Pune, India; (c) Sakurai, H., *The Chem. Record*, 2002, **2**, 237-248; (d) Thompson, K.H., McNeill, J.H., Orvig, C., *Chem. Rev.*, 1999, **99**, 2561-2571; (e) Aguilar, F., Boskou, D., Gott, D., Grilli, S., Grunow, W., Hulshof, K., Larsen, J. Leblanc, J.-C., Leclercq, C., Mortensen, A., Parent-Massin, D., Pratt, I., Rietjens, I., Speijers, G., Tobback, P., Toldrá, F., Scientific Opinion of the Panel on Food Additives, Flavourings, Processing Aids and Materials in Contact with Food, The European Food Safety Authority, Commission Directive 2001/15/EC of 15th, February 2001, *J. EFSA* 2008, **634**, 1-15.
- 24 Top, S., Dauer, B., Vaissermann, J., Jaouen, G., *J. Organometal. Chem.*, 1997, **541**, 355-361; (b) Kreidenwiss, A., Kremsner, P.G., Dietz, K., Mordmuller, B., *Am. J. Trop. Med. Hyg.*, 2006, **75**, 1178-1181.
- 25 (a) Geraghty, M., McCann, M., Devereux, M., Cronin, J.F., Curran, M., McKee V., *Metal-Based Drugs*, 1999, **6**, 41-48; (b) Geraghty, M., Sheridan, V., McCann, M., Devereux, M., McKee V., *Polyhedron*, 1999, **18**, 2931-2939.
- 26 Geraghty, M., McCann, M., Devereux, M., McKee, V.; *Inorg. Chim. Acta*, 1999, **293**, 160-166.
- 27 (a) Devereux, M., McCann, M., Leon, V., Geraghty, M., McKee V., Wikaira, J., *Polyhedron*, 2000, **19**, 1205-1211; (b) McCann, M., Geraghty, M., Devereux, M., O' Shea, D., Mason, J., O' Sullivan, L., McKee, V., *Metal-Based Drugs*, 2000, **7**, 185-193; (c) Devereux, M., McCann, M., Leon, V., Geraghty, M., McKee V., Wikaira, J. *Metal-Based Drugs*, 2000, **7**, 275-289.

- 28 McCann, M., Coyle, B., McKay, S., McCormack, P., Kavanagh, K., Devereux, M., McKee, V., Kinsella, P., O'Connor, R., Clynes, M., *BioMetals*, 2004, **17**, 635-645.
- 29 Coyle, B., McCann, M., Kavanagh, K., Devereux, M., McKee, V., Kayal, N., Egan, D., Deegan, C., Finn, G.J., *J. Inorg. Biochem.*, 2004, **98**, 1361-1366.
- 30 Joseph, M., Leigh, T., Swain, M.L., *Synthesis*, 1977, **7**, 459-461.
- 31 (a) Abuskhuna, S., Briody, J., McCann, M., Devereux, M., Kavanagh, K., Barreira-Fontecha, J., McKee, V., *Polyhedron*, 2004, **23**, 1249-1255, (b) Abuskhuna, S., M.Sc. Thesis, 2004, The National University of Ireland, Maynooth, Co. Kildare, Ireland.
- 32 (a) Cotton, F.A., Wilkinson, G.K., *Advanced Inorganic Chemistry*, 6th edn., 1999, Wiley, New York; (b) Shrivvers, D.F., & Atkins, P.W., *Inorganic Chemistry*, 3rd edn., 1999, Oxford University Press.
- 33 (a) Bruice, P.Y., *Organic Chemistry*, 5th edn., 2007, Pearson Education Inc.; (b) Thomas, C.W., Mak, Xiao-Li, Z., *Encyclopedia of Inorganic Chemistry*, 2nd edn., 2006, Wiley, New York.
- 34 (a) Van Wüllen, W., Vensky, S., Hoffbauer, L., Jensen, M., *Solid State Sci.*, 2005, **7**, 920-924; (b) Link, C., Jansen, M., *Inorg. Chem.*, 1994, **33**, 2614-2616. (c) Decken, A., Knapp, C., Nikiforov, G., Passmore, J., Rautiainen, M., Wang, X., Zeng, X., *J. Euro. Chem.*, 2009, **15**, 6504-6517.
- 35 (a) Weibel, J-M., Blanc, A., Pale, P., *Chem. Rev.*, 2008, **8**, 3149-3173; (b) Halbes-Letinois, U., Weibel, J-M., Pale, P., *Chem. Soc. Rev.*, 2007, **36**, 759-769.
- 36 Ratte, H.T., *Envi. Toxi. Chem.*, 1999, **18**, 89-108.
- 37 Kozin, A.K., Bogdanova, A.K., *Teor. Eksp. Khimi.*, 2001, **37**, 251-255.
- 38 Wells, T.N.C., Scully, P., Paravicini, G., Proudfoot, A.E.I., Payton, M.A., *Biochem.*, 1995, **34**, 7896-7903.
- 39 Gliemeroth, G., Mader, K.H., *Angew. Chem. Int. Ed.*, 1970, **9**, 434-445.
- 40 Kestner, M.O., Allred, A.L., *J. Am. Chem. Soc.*, 1972, **94**, 7189-7190.
- 41 Stillman, M.J., Presta, A., Gui, Z., Jiang, D-T, *Metal-Based Drugs*, 1994, **1**, 375-394.

- 42 Ahmad, S., Isab, A.A., Ali, S., Rahman, A-A., *Polyhedron*, 2006, **25**, 1633-1645.
- 43 (a) Nomiya, K., Kondoh, Y., Nagano, H., Oda, M., Sakuma, S., *J. Inorg. Biochem.*, 1995, **60**, 289-290; (b) Nomiya, K., Onoue, K-I., Kondoh, Y., Kasuga, N C., Nagano, H., Oda, M., Sakuma, S., *Polyhedron*, 1995, **10**, 1359-1367; (c) Nomiya, K., Yoshizawa, A., Tsukagoshi K., Kasuga NC., Hirakawa S., Watanabe J.K., *J. Inorg. Biochem.*, 2004, **98**, 46-60.
- 44 Thruman, R.B., Gerba, C.P., *CRC Crit. Rev. Env. Control*, 1989, **18**, 295-315.
- 45 Dias, H.V.R., Browning, R.G., Polach, S.A., Diyabalanage, H.V.K., Lovely, C.J., *J. Am. Chem. Soc.*, 2003, **125**, 9270-9271.
- 46 (a) Claus, P., Hofmeister, H., *J. Phys. Chem. B.*, 1999, **103**, 2766-2772; (b) Grunert, P., Brucker, A., Hofmeister, H., *J. Phys. Chem. B.*, 2004, **108**, 5709-5717; (c) Sundberg R.J., Martin, R., *Chem. Rev.*, 1974, **4**, 471-475.
- 47 (a) Kestenbaum, H., Lang de Oliveria. A., Schmidt, W., Schuth, F., Ehrfeld, K. Gebauer, H. Löwe, T. Richter, D. Lebiez, Untiedt, I., Züchner, H., *Ind. Eng. Chem. Res.*, 2002, **41**, 710-719; (b) Breen, J.P., Burch, R., Hardacre, C., Hill, C. J., *J. Phys. Chem. B.*, 2005, **109**, 4805-4810; (c) Iliopoulou, E.F., Efthimiadis, E.A., Vasalos, I.A., *Ind. Eng. Chem. Res.*, 2004, **43**, 1388-1394.
- 48 Cho, G.Y., Bolm, C., *Org. Lett.*, 2005, **7**, 4983-4985.
- 49 Kakuta, N., Goto, N., Ohkita, H., Mizushima, T., *J. Phys. Chem. B.*, 1999, **103**, 5917-5919.
- 50 Nakatsuji, H., Hu, Z.M., Nakai, H., *Int. J. Quantum Chem.*, 1997, **65**, 839-855.
- 51 Yang, Z., Li, J., Yang, X., Xie, X., Wua, Y., *J. of Mol. Catalysis*, 2005, **241**, 15-22.
- 52 (a) Lansdown, A.B.G., *Crit. Rev. Toxicol.*, 1995, **25**, 397-462; (b) Lansdown, A.B.G., *J. Wound Care*, 2002, **11**, 173-177.
- 53 Wan, A.T., Conyers, R.A.L., Coombs, C.J., Mastertons, J.P., *Clin. Chem.*, 1991, **37**, 1683-1687.
- 54 Lansdown, A.B.G., *Crit. Rev. Toxicol.*, 2007, **37**, 237-250.
- 55 Simpkins, C.O., *Cell Mol. Biol.*, 2000, **46**, 465-488.

- 56 Lansdown, A.B.G., Sampson, B., Rowe, A.M., *Wound Rep. Regen.*, 1999, **8**, 306-346.
- 57 Molinero, A., Carrasco, J., Hernandez, J., Hidalgo, J., *Neurochem. Int.*, 1998, **33**, 559-566.
- 58 Lansdown, A.B.G., Williams, A., *J. Wound Care*, 2004, **13**, 131-140.
- 59 Zheng, W., *Microsc. Res. Tech.*, 2001, **52**, 89-103; (b) Zheng, W., Aschner, M., Ghersi-Egea, J.F., *Toxicol. Appl. Pharm.*, 2003, **192**, 1-11.
- 60 Chua, A.C.G., Stonell, L.M., Savigine, D.L., Morgan, E.H., *J. Physiol.*, 1996, **99**, 493-505.
- 61 Gunshin, H., MacKenzie, U.V., Gunshin, Y., Romero, M., Boron, W.F., *Nature*, 1997, **388**, 482-488.
- 62 Castellan, G.W., *Physical Chemistry*, 2nd edn., 1964, Addison-Wesley Publishing Company, Reading, MA, USA.
- 63 Jones, S.K., Riley, P.A., *Cell Biochem. Funct.*, 1991 **9**, 245-253.
- 64 (a) Nomiya, K., Tsuda, K., Sudoh, T., Oda, M., *J. Inorg. Biochem.*, 1997, **68**, 39-44; (b) Sereemaspum, A., Hongpiticharoen, P., Rojanathanes, R., Maneewattanapinyo, P., Ekgasit, S., Warisnoicharoen, W., *Int. J. Pharm.*, 2008, **4**, 492-495.
- 65 (a) Hanukoglu, I., *Adv. Mol. Cell. Bio.*, 1996, **14**, 29-55; (b) Narasimhulu, A., *Rev. Biochem. Biophysio. Acta*, 2007, **1770**, 360-375.
- 66 (a) Hornsby, P.J., *Free Radicals in Biology and Medicine*, 2nd edn., 1989, Clarendon Press, Oxford, UK; (b) Hanukoglu, I., Rapoport, R., Weiner, L., Sklan, D., *Arch. Biochem. Biophys.*, 1993, **305**, 489-498; (c) Hirsch, L.R., Stafford, R.J., Bankson, J.A., Sershen, SR., Rivera, B., Price, R.E., Hazle, J.D., Halas, N.J., West, J.L., *PNAS*, 2003, **100**, 13549-13554.
- 67 Batarseh, K.I., *J. Antimicro. Chemotherapy*, 2004, **54**, 546-548.
- 68 Modal, S.M.F., Fox, C.L., *Biochem. Pharm.*, 1972, **22**, 2391-2398.
- 69 Jain, R.K., Abeleff, M., Armtage, J., Kastan, M., *Clinical Oncology*, 3rd edn., 2005, Elsevier, Philadelphia, USA.

- 70 Fox, C.L., Modak, S.M.F., *Antimicro. Agent. Chemotherapy*, 1994, **5**, 582-588.
- 71 Hobbs, S.K., Monsky, W.L., Yuan, F., Roberts, G.W., Griffith, L., Torchin, V.P., *Proc. Natl. Sci. USA.*, 1998, **95**, 4607-4612.
- 72 Nomiya, K., Onoue, K., Kondoh, Y., Kasuga, N.C., Nagano, H., Oda, M., *Polyhedron*, 1995, **14**, 1359-1367.
- 73 Loginova, N.V., Chernyavskaya, A.A., Polozov, G.I., Koval'Chuk, R.V., Zheldakova, V.T., Osipovich, R.A., Glushonok, N.P., Polozov, G.K., Sorokin, H.I., leg, V.L O., Shadyro, O.I., *Polyhedron*, 2005, **24**, 611-618.
- 74 (a) Silver, S., Gupta, A., Matsui, K., Lo, J-F., *Metal Based-Drugs*, 1999, **6**, 315-320; (b) Grewal, J.S., Tiwari, R.P., *Cytobios.*, 1999, **98**, 113-123.
- 75 (a) Fan, B., Grass, G., Rensing, C., Rosen, B., *Biochem. Biophys. Res. Commun.*, 2001, **286**, 414-418; (b) Silver, S., Phung, L.T., *Ann. Rev. Microbiol.*, 1996, **50**, 753-789.
- 76 Pedersen, P., Carafoli, E., *Trends Biochem. Sci.*, 1989, **12**, 146-150.
- 77 Gatti, D., Mitra, B., Rosen, B., *J. Biol. Chem.*, 2000, **275**, 34009-34012.
- 78 Gupta, A., Matsui, K., Lo, J-F., Silver, S., *Nat. Med.*, 1999, **5**, 183-188.
- 79 DiDonato, M., Hsu, H., Narindrasorasak, S., Que, L., Jr., Sarkar, B., *Biochem.*, 2000, **39**, 1890-1896.
- 80 Tsivkovskii, R., MacArthur, B., Lutsenko, S., *J. Biol. Chem.*, 2001, **276**, 2234-2242.
- 81 O'Halloran, T., Culotta, V., *J. Biol. Chem.*, 2000, **275**, 25057-25060.
- 82 Schellhammer, C.W.S., Offen, F.G., *Chem. Abstr.*, 1988, **108**, 1124-1167.
- 83 Iddon, B., Ngoochindo, R.I., *Heterocycles*, 1994, **38**, 2487-2490.
- 84 Lindell, S. D., Turner, R.M., *J. Org. Chem.*, 1991, **56**, 5739-5740.
- 85 Debus, H., *Leigibs. Ann. Chem.*, 1985, **107**, 199-204.
- 86 Bu, X.R., Gunner, P., *Tet. Lett.*, 2001, **42**, 805-810.
- 87 Usyatinsky, A., Khmelnitsky, Y., *Tet. Lett.*, 2000, **41**, 5031-5037.
- 88 Campbell, N.A., Reece, J.B., Mitchell, L.G., *Biology*, 5th edn. 1999, Benjamin-Cummings Pub. Co., Menlo Park, California, USA.

- 89 Handy, S.T., *J. Eur. Chem.*, 2003, **9**, 2938-2942.
- 90 Earle, M.J., Seddon, R.K., *Pure. Appl. Chem.*, 2000, **72**, 1391–1398.
- 91 (a) Bass, F. Ph.D. Thesis, 2001, The National University of Ireland, Maynooth, (b) Briody, J., The National University of Ireland, Maynooth, Personal communication; (c) Sedgwick, N.V., Miller, I.T., Springall, H.D., *Sedgwick's Organic Chemistry of Nitrogen*, 3rd edn., 1966, Clarendon Press, Oxford University, Oxford, England.
- 92 Balbuena. P., Blocker, W., Dudek, R., Cabrales-Navarro, F., Hirunsit. P., *J. Phys. Chem. A*, 2008, **41**, 10210–10219.
- 93 Weinmann, H., Harre, M., Koenig, K., Merten E., Tilstam, U., *Tet. Lett.*, 2002, **43**, 593-595.
- 94 Schiff, H., *Ann. Chem.*, 1859, **131**, 1-59; (b) Layer, W., *Chem. Rev.*, 1963, **63**, 489–510.
- 95 Iversen, P.E., Lund, H., *Acta. Chem. Scand.*, 1966, **20**, 2649-2652.
- 96 Pyman, F.L., *J. Chem. Soc.*, 1916, **106**, 186-202.
- 97 Carini, D.J. Duncia, J.V. Aldrich, P.E. Chiu, A.T., *J. Med. Chem.*, 1991, **34**, 2525-2567.
- 98 Weinstock, J., Keenan, R.M., Samamen J.J., *J. Med. Chem.*, 1991, **34**, 1514-1524.
- 99 Storey, T.B., Sullivan, W.W., Moyer, L.C., *J. Org. Chem.*, 1964, **29**, 3118-3125.
- 100 Lawson, A., *J. Chem. Soc.*, 1956. 307-310.
- 101 Govindasamy, L., Velmurugan, D., Rajendran, T., *Acta Cryst.*, 1999, **55**, 1368-1369.
- 102 (a) Casella, L., Gullotti, M., *J. Am. Chem. Soc.*, 1981, **103**, 6338-6347; (b) Hartung, J., Drees, S., Greb, A., Schmidt, P., Svoboda, I., Fuess, H., Murso, A., Stalker, D., *Eur. J. Org. Chem.*, 2003, **13**, 2388-2408.
- 103 (a) Casella, L., Gullotti, M., Pintar, A., Messori, L., Rockenbauer, A., Gyor, M., *Inorg. Chem.*, 1987, **26**, 1031-1038; (b) Cornman, C., Kampf, J., Soo Lah, M., Pecoraro, V., *Inorg. Chem.*, 1992, **31**, 2035-2043.

- 104 Scarpellini, M., Neves, A., Hrner, R., Bortoluzzi, A., Szpoganicz, B., Zucco, C., Nome Silva, R., Drago, V., Mangrich, A., Ortiz, W., Passos, A., de Oliveira, C., Terenzi, H., *Inorg. Chem.*, 2003, **42**, 8353-8365.
- 105 (a) Quadi, A., Gadenne, B., Hessemann, P., Moreau, J., Billard, I., Gaillard, C., Mekki, S., Moutiers, G., *J. Eur. Chem.*, 2006, **12**, 3074-3081; (b) Davis, J., ACS Symposium Series, 2002, **818**, 247-258.
- 106 Raghu, A., Gadaginamath, G., Jawalkar, S., Halligudi, S., Aminabhavi, T., *J. Polym. Sci.*, 2006, **44**, 6032-6046.
- 107 Ibrahim, M., Etaiw, S., *Synth. React. Inorg. Metal-Org. Chem.*, 2004, **34**, 629-639.
- 108 (a) LaRonde, F., Brook, M., *Inorg. Chim. Acta.*, 1999, **296**, 208-221; (b) LaRonde, F., Brook, M., *Tet. Lett.*, 1999, **40**, 3507-3510.
- 109 Brook, M., *Silicon in Organic, Organometallic and Polymer Chemistry*, 2000, Wiley, New York.
- 110 Widmer, A.F., *Clin. Inf. Dis.*, 2008, **46**, 656-658.
- 111 Sepčić K., *Toxin. Rev.*, 2000, **19**, 139-160.
- 112 Lancini, G.C., Lazzari, E., Arioli, V., Bellani, P., *J. Med. Chem.*, 1969, **12**, 775-780.
- 113 Kumar, P., Emami, S., Kresolek, Z., Yang, J., McEwan, A.J., Wiebe, L.I., *Med. Chem.*, 2009, **2**, 118-129.
- 114 Yang, S-P., Chem, X-M., Ji, L-N., *J. Chem. Soc.*, 2000, 2337-2343.
- 115 (a) Dominguez-Vera, J., Camara, F., Moreno, J., Isaac-Garcia, J., Colacio, E., *Inorg. Chim. Acta*, 2000, **306**, 137-141; (b) Dominguez-Vera, J., Camara, F., Moreno, J., Isaac-Garcia, J., Colacio, E., Stoeckli-Evens, H., *Inorg. Chim. Acta*, 1998, **37**, 3046-3050.
- 116 Nathan, L., Kehone, J., Gilmore, J., Hannibal, K., Dewhirst, W., Mai, T., *Polyhedron*, 2003, **22**, 887-894.

- 117 (a) Taylor, M., Reglinski, J., Berlouisa, L., Kennedy, A., *Inorg. Chim. Acta*, 2006, **359**, 2455-2464; (b) Reglinski, J., Taylor, M., Kennedy, A., *Inorg. Chem. Commun.*, 2006, **9**, 736-739.
- 118 Cai, Q-H., Wang, H., Jin, C., Wu, F., Shan, Y-K., *Chinese J. Chem.*, 2005, **23**, 990-992.
- 119 Gubelmann, I., EI du Pont de Nemours & Company, Inc. Wilmirigton, Delaware, USA, *Ind. Eng.*, 1935, **6**, 618-626.
- 120 Mucha, F., Boehme, U., Roewer, G., *J. Chem. Soc., Chem. Commun.*, 1998, **8**, 1289-1290.
- 121 (a) Singh, M., Singh, P., *Synth. React. Inorg. Chem.*, 2003, **33**, 271-280; (b) Huiyong, C. Archer, R., *Inorg. Chem.*, 1994, **33**, 5195-5202.
- 122 (a) Constable, E., *Aust. J. Chem.*, 2006, **59**, 1-2; (b) Aakeroy, C., Beatty, A., *Crystal Eng.*, 1998, **1**, 39-49.
- 123 Papaefstathiou, G., MacGillivray, L., *Coord. Chem. Rev.*, 2003, **246**, 169-184.
- 124 Jin, C-M., Chen, Z-F., Mei, H-F., Shi, X-K., *J. Mol. Struct.*, 2009, **921**, 58-62.
- 125 Rowan, R., Tallon, T., Sheahan, A., Curran, R., McCann, M., Kavanagh, K., Devereux, M., McKee, V., *Polyhedron*, 2005, **25**, 1171-1778.
- 126 Cui, G-H., Li, J-R., Tian, J-L., Bu, X-H., Batten, S., *Cryst. Growth Des.*, 2005, **5**, 1775-1780.
- 127 (a) Ren, C-X., Cheng, L., Ye, B-H., Chen, X-M., Park, Y-J., Lin, L.S., de Laszlo, S.M., McCauley, E.D., Van Riper, G., Egger, L., Kidambi, U., Mumford, R.A., Tong, S., Tang, W., Colletti, A., Teffera, Y., Stearns, R., MacCoss, M., Schmidt, J.A., Hagmann, W.K., *Inorg. Chim. Acta*, 2007, **360**, 3741-3747. (b) Tan, H-Y., Zhang, H-A., Ou, H-D., Kang, B-S., *Inorg. Chim. Acta*, 2004, **357**, 869-874.
- 128 Cunningham, D., McGinley, J., *J. Chem. Soc. Dalton Trans.* 1992, 1387-1391.
- 129 (a) Cohen, M.C., Sisco, M., Prophete, C., Chen, L-C., Zelikoff, JT., Ghio, AJ., Stonehuerner, J.D., Smee, J.J., Holder, A., Crans, D.C., *J. Immunotoxicology*, 2007, **4**, 49-60; (b) Cohen, M.C., Prophete, C., Sisco, M., Chen, L-C., Zelikoff, J., Smee, J., Holder, A., Crans, D., *J. Immunotoxicology*, 2006, **3**, 69-81.

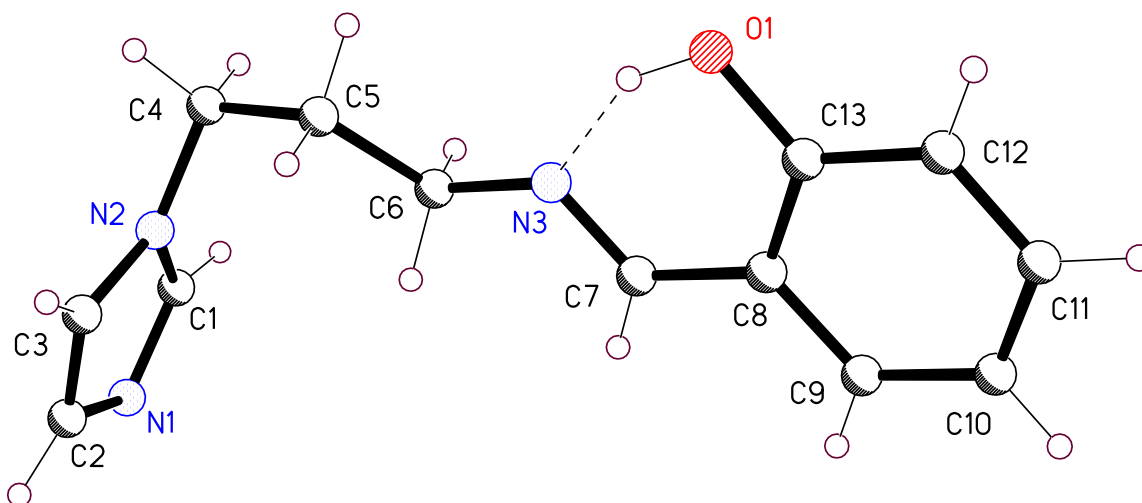
- 130 Kamenecka, T.M., Park, Y.J., Lin, L.S., de Laszlo, S., *Bioorg. & Med. Chem. Lett.*, 2004, **14**, 2323-2326.
- 131 Cozzini, P., Kellogg, G., Spyraakis, F., Abraham, D., Costantino, G., Emerson, A., Fanelli, F., Gohlke, F., Kuhn, L., Morris, G., Orozco, M., Pertinhez, T., Rizzi, M., Sottriffe, C., *J. Med. Chem.* 2008, **51**, 6237-6255.



Appendix 1



X-ray crystal data for ligand (**36**).



Data were collected at 150(2)K on a Bruker SMART 1000 CCD diffractometer. The structure was solved by direct methods and refined on F^2 using all the reflections*. All the non-hydrogen atoms were refined using anisotropic atomic displacement parameters and hydrogen atoms bonded to carbon were inserted at calculated positions using a riding model. The hydrogen bonded to O1 was located from difference maps and refined with a fixed isotropic atomic displacement parameter. Parameters for data collection and refinement are summarised in Table 1.

There is no sign of any obvious π - π stacking, though there are some interactions between neighbouring imidazole rings. These don't look very strong but may be responsible for the observation that the imidazole ring and phenol ring are almost perpendicular.

* G.M. Sheldrick, SHELXTL Version 6.12, Bruker AXS, Madison WI, 2001.

Table 1. Crystal data and structure refinement for **(36)**.

Identification code	(36)	
Empirical formula	C ₁₃ H ₁₅ N ₃ O	
Formula weight	229.28	
Temperature	150(2) K	
Wavelength	0.71073 Å	
Crystal system	Monoclinic	
Space group	P2(1)/c	
Unit cell dimensions	a = 12.3194(11) Å	$\alpha = 90^\circ$.
	b = 5.8438(5) Å	$\beta = 97.963(2)^\circ$.
	c = 16.3752(15) Å	$\gamma = 90^\circ$.
Volume	1167.52(18) Å ³	
Z	4	
Density (calculated)	1.304 Mg/m ³	
Absorption coefficient	0.086 mm ⁻¹	
F(000)	488	
Crystal size	0.33 x 0.22 x 0.10 mm ³	
Crystal description	colourless block	
Theta range for data collection	1.67 to 28.78°.	
Index ranges	-16 ≤ h ≤ 15, -7 ≤ k ≤ 7, -21 ≤ l ≤ 21	
Reflections collected	9584	
Independent reflections	2753 [R(int) = 0.0260]	
Completeness to theta = 26.00°	100.0 %	
Absorption correction	Semi-empirical from equivalents	
Max. and min. transmission	1.00000 and 0.844722	
Refinement method	Full-matrix least-squares on F ²	
Data / restraints / parameters	2753 / 0 / 157	
Goodness-of-fit on F ²	1.006	
Final R indices [I > 2σ(I)]	R1 = 0.0389, wR2 = 0.0975	
R indices (all data)	R1 = 0.0613, wR2 = 0.1128	
Largest diff. peak and hole	0.217 and -0.181 e.Å ⁻³	

Table 2. Atomic coordinates ($\times 10^4$) and equivalent isotropic displacement parameters ($\text{\AA}^2 \times 10^3$). For ligand **(36)** $U(\text{eq})$ is defined as one third of the trace of the orthogonalized U^{ij} tensor.

	x	y	z	U(eq)
C(1)	9043(1)	3109(2)	5559(1)	32(1)
N(1)	9675(1)	4034(2)	6187(1)	37(1)
C(2)	10097(1)	2192(3)	6645(1)	34(1)
C(3)	9716(1)	192(2)	6291(1)	29(1)
N(2)	9037(1)	801(2)	5592(1)	25(1)
C(4)	8368(1)	-751(2)	5031(1)	30(1)
C(5)	7438(1)	-1794(2)	5430(1)	30(1)
C(6)	6619(1)	-39(2)	5642(1)	28(1)
N(3)	5682(1)	-1188(2)	5920(1)	27(1)
C(7)	5147(1)	-173(2)	6427(1)	25(1)
C(8)	4174(1)	-1216(2)	6686(1)	24(1)
C(9)	3579(1)	-56(2)	7224(1)	29(1)
C(10)	2635(1)	-976(3)	7456(1)	33(1)
C(11)	2269(1)	-3090(3)	7145(1)	33(1)
C(12)	2845(1)	-4293(2)	6618(1)	30(1)
C(13)	3803(1)	-3385(2)	6388(1)	25(1)
O(1)	4352(1)	-4607(2)	5875(1)	33(1)

Table 3. Bond lengths [Å] and angles [°] for ligand (**36**).

C(1)-N(1)	1.3172(19)	N(3)-C(7)	1.2756(16)
C(1)-N(2)	1.3501(17)	C(7)-C(8)	1.4584(18)
N(1)-C(2)	1.372(2)	C(8)-C(9)	1.3972(18)
C(2)-C(3)	1.359(2)	C(8)-C(13)	1.4116(18)
C(3)-N(2)	1.3683(18)	C(9)-C(10)	1.3824(19)
N(2)-C(4)	1.4609(17)	C(10)-C(11)	1.388(2)
C(4)-C(5)	1.5228(18)	C(11)-C(12)	1.382(2)
C(5)-C(6)	1.5118(19)	C(12)-C(13)	1.3929(19)
C(6)-N(3)	1.4613(17)	C(13)-O(1)	1.3531(16)
N(1)-C(1)-N(2)	112.66(13)	N(3)-C(7)-C(8)	120.94(12)
C(1)-N(1)-C(2)	104.04(12)	C(9)-C(8)-C(13)	118.70(12)
C(3)-C(2)-N(1)	111.08(13)	C(9)-C(8)-C(7)	120.28(12)
C(2)-C(3)-N(2)	105.57(12)	C(13)-C(8)-C(7)	121.01(12)
C(1)-N(2)-C(3)	106.65(12)	C(10)-C(9)-C(8)	121.34(13)
C(1)-N(2)-C(4)	126.95(12)	C(9)-C(10)-C(11)	119.19(13)
C(3)-N(2)-C(4)	126.22(12)	C(12)-C(11)-C(10)	120.93(13)
N(2)-C(4)-C(5)	111.77(11)	C(11)-C(12)-C(13)	120.15(13)
C(6)-C(5)-C(4)	113.13(12)	O(1)-C(13)-C(12)	118.82(12)
N(3)-C(6)-C(5)	109.95(11)	O(1)-C(13)-C(8)	121.50(12)
C(7)-N(3)-C(6)	119.42(12)	C(12)-C(13)-C(8)	119.67(12)

Table 4. Anisotropic displacement parameters ($\text{\AA}^2 \times 10^3$) for ligand (36). The anisotropic displacement factor exponent takes the form: $-2\pi^2 [h^2 a^{*2} U^{11} + \dots + 2 h k a^* b^* U^{12}]$

	U ¹¹	U ²²	U ³³	U ²³	U ¹³	U ¹²
C(1)	31(1)	24(1)	41(1)	2(1)	4(1)	2(1)
N(1)	35(1)	31(1)	46(1)	-7(1)	5(1)	-3(1)
C(2)	29(1)	43(1)	30(1)	-4(1)	5(1)	-1(1)
C(3)	27(1)	33(1)	29(1)	5(1)	7(1)	2(1)
N(2)	23(1)	23(1)	28(1)	0(1)	8(1)	-1(1)
C(4)	29(1)	31(1)	31(1)	-6(1)	8(1)	-5(1)
C(5)	27(1)	28(1)	35(1)	-5(1)	8(1)	-5(1)
C(6)	24(1)	30(1)	30(1)	1(1)	5(1)	-3(1)
N(3)	24(1)	29(1)	29(1)	-1(1)	4(1)	-1(1)
C(7)	24(1)	23(1)	26(1)	-1(1)	0(1)	0(1)
C(8)	22(1)	26(1)	23(1)	2(1)	1(1)	1(1)
C(9)	28(1)	29(1)	28(1)	-1(1)	1(1)	4(1)
C(10)	29(1)	41(1)	28(1)	0(1)	7(1)	7(1)
C(11)	26(1)	41(1)	33(1)	8(1)	7(1)	-1(1)
C(12)	28(1)	29(1)	32(1)	3(1)	1(1)	-4(1)
C(13)	25(1)	26(1)	25(1)	2(1)	1(1)	2(1)
O(1)	33(1)	29(1)	39(1)	-8(1)	11(1)	-4(1)

Table 5. Hydrogen coordinates ($\times 10^4$) and isotropic displacement parameters ($\text{\AA}^2 \times 10^{-3}$) for ligand (36).

	x	y	z	U(eq)
H(1)	8636	3972	5129	38
H(2)	10591	2300	7143	41
H(3)	9885	-1313	6488	35
H(4A)	8837	-1992	4862	36
H(4B)	8058	97	4529	36
H(5A)	7051	-2938	5049	36
H(5B)	7751	-2603	5940	36
H(6A)	6972	983	6082	33
H(6B)	6366	906	5151	33
H(7)	5386	1283	6640	29
H(9)	3829	1395	7434	34
H(10)	2241	-171	7825	39
H(11)	1614	-3719	7295	39
H(12)	2587	-5743	6413	36
H(10)	4969(15)	-3650(30)	5786(11)	50

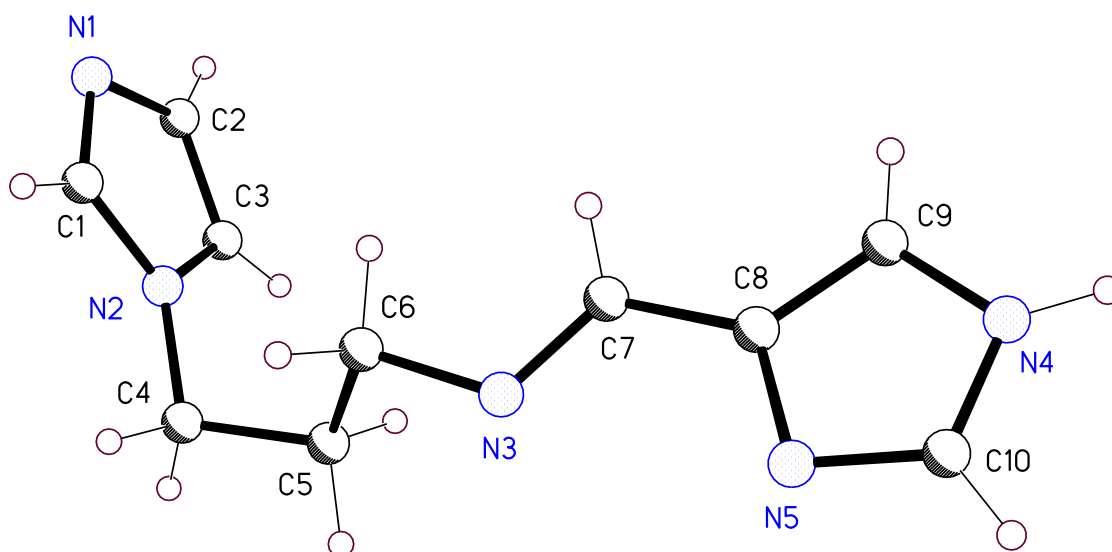
Table 6. Torsion angles [°] for ligand (36).

N(2)-C(1)-N(1)-C(2)	0.18(16)
C(1)-N(1)-C(2)-C(3)	-0.15(16)
N(1)-C(2)-C(3)-N(2)	0.07(16)
N(1)-C(1)-N(2)-C(3)	-0.14(16)
N(1)-C(1)-N(2)-C(4)	175.20(12)
C(2)-C(3)-N(2)-C(1)	0.04(15)
C(2)-C(3)-N(2)-C(4)	-175.35(11)
C(1)-N(2)-C(4)-C(5)	-105.86(15)
C(3)-N(2)-C(4)-C(5)	68.62(17)
N(2)-C(4)-C(5)-C(6)	63.96(15)
C(4)-C(5)-C(6)-N(3)	172.61(11)
C(5)-C(6)-N(3)-C(7)	151.33(12)
C(6)-N(3)-C(7)-C(8)	176.83(12)
N(3)-C(7)-C(8)-C(9)	-178.22(12)
N(3)-C(7)-C(8)-C(13)	0.60(2)
C(13)-C(8)-C(9)-C(10)	-1.00(2)
C(7)-C(8)-C(9)-C(10)	177.86(12)
C(8)-C(9)-C(10)-C(11)	-0.30(2)
C(9)-C(10)-C(11)-C(12)	1.00(2)
C(10)-C(11)-C(12)-C(13)	-0.40(2)
C(11)-C(12)-C(13)-O(1)	179.75(12)
C(11)-C(12)-C(13)-C(8)	-0.90(2)
C(9)-C(8)-C(13)-O(1)	-179.09(12)
C(7)-C(8)-C(13)-O(1)	2.07(19)
C(9)-C(8)-C(13)-C(12)	1.60(19)
C(7)-C(8)-C(13)-C(12)	-177.25(12)

Table 7. Hydrogen bonds for ligand (36) [\AA and $^\circ$].

D-H...A	d(D-H)	d(H...A)	d(D...A)	$\angle(\text{DHA})$
O(1)-H(10)...N(3)	0.970(19)	1.685(19)	2.5791(15)	151.3(16)

Appendix 2



Data were collected at 150(2)K on a Bruker SMART 1000 CCD diffractometer. The structure was solved by direct methods and refined on F^2 using all the reflections*. All the non-hydrogen atoms were refined using anisotropic atomic displacement parameters and hydrogen atoms were inserted at calculated positions using a riding model. Parameters for data collection and refinement are summarised in Table 1.

This one is not as advertised and you didn't tell us what went into the mix, so we have gone for total analysis by X-ray. The data are good enough to distinguish C from N, so we believe we have the atom types assigned correctly. There is a short imine bond between N3 and C7. There is a respectable H-bond from N4 to the imine nitrogen of a neighbouring molecule (under $\frac{1}{2}-x, \frac{1}{2}+y, \frac{1}{2}-z$), and a less convincing one from the same NH to N5 of the same neighbour (the DHA angle is a bit low for this one). These interactions link the molecules into chains. There is also a C-H \cdots N H-bond from C10 to N1 (imidazole lone pair) of a second neighbour (under $x, y, z+1$) – this is longer but that is always true for CH H-bonds – and including this interaction gives sheets of molecules in the plane perpendicular to the a axis.

* G.M. Sheldrick, SHELXTL Version 6.12, Bruker AXS, Madison WI, 2001.

Table 1. Crystal data and structure refinement for (37).

Identification code	(37)
Empirical formula	C ₁₀ H ₁₃ N ₅
Formula weight	203.25
Temperature	150(2) K
Wavelength	0.71073 Å
Crystal system	Monoclinic
Space group	P2(1)/n
Unit cell dimensions	
a = 8.6001(10) Å	$\alpha = 90^\circ$.
b = 10.1425(12) Å	$\beta = 103.131(2)^\circ$.
c = 12.3976(14) Å	$\gamma = 90^\circ$.
Volume	1053.1(2) Å ³
Z	4
Absorption coefficient	0.084 mm ⁻¹
F(000)	432
Crystal size	0.37 x 0.17 x 0.0 mm ³
Crystal description	colourless block
Theta range for data collection	2.62 to 25.00°.
Index ranges	-10 ≤ h ≤ 10, -12 ≤ k ≤ 11, -14 ≤ l ≤ 14
Reflections collected	7349
Independent reflections	1848 [R(int) = 0.0267]
Completeness to theta = 25.00°	99.9 %
Absorption correction	Semi-empirical from equivalents
Max. and min. transmission	1.00000 and 0.843689
Refinement method	Full-matrix least-squares on F ²
Data / restraints / parameters	1848 / 0 / 136
Goodness-of-fit on F ²	1.091
Final R indices [I > 2σ(I)]	R1 = 0.0359, wR2 = 0.0794
R indices (all data)	R1 = 0.0516, wR2 = 0.0885

Largest diff. peak and hole 0.165 and -0.232 e.Å⁻³

Table 2.

Atomic coordinates (x 10⁴) and equivalent isotropic displacement parameters (Å²x 10³) for (37). U(eq) is defined as one third of the trace of the orthogonalized U^{ij} tensor.

	X	y	z	U(eq)
C(1)	1591 (2)	-316(2)	-3846(1)	27(1)
C(1)	1591 (2)	-316(2)	-3846(1)	27(1)
N(1)	2077 (2)	497(1)	-4530(1)	31(1)
C(2)	3700(2)	553(2)	-4141(1)	35(1)
N(2)	2808(2)	-780(1)	-3051(1)	26(1)
C(3)	4166(2)	-220(2)	-3238(1)	34(1)
C(4)	2709(2)	-1672(2)	-2143(1)	34(1)
C(5)	3042(2)	-985(2)	-1022(1)	33(1)
C(6)	1804(2)	50(2)	-943(1)	29(1)
N(3)	1973(2)	484(1)	202(1)	26(1)
C(7)	2230(2)	1702(2)	418(1)	25(1)
C(8)	2356(2)	2243(2)	1515(1)	23(1)
C(9)	2823(2)	3483(2)	1883(1)	27(1)
N(4)	2749(2)	3517(1)	2967(1)	27(1)
C(10)	2236(2)	2321(2)	3213(1)	27(1)
N(5)	1980(2)	1511(1)	2364(1)	27(1)
C(6)	1804(2)	50(2)	-943(1)	29(1)
N(3)	1973(2)	484(1)	202(1)	26(1)
C(7)	2230(2)	1702(2)	418(1)	25(1)
C(8)	2356(2)	2243(2)	1515(1)	23(1)
C(9)	2823(2)	3483(2)	1883(1)	27(1)

N(4) 2749(2) 3517(1)	2967(1)	27(1)
C(10) 2236(2) 2321(2)	3213(1)	27(1)
N(5) 1980(2) 1511(1)	2364(1)	27(1)

Table 3. Bond lengths [Å] and angles [°] for (37).

C(1)-N(1)	1.317(2)
C(1)-N(2)	1.349(2)
N(1)-C(2)	1.371(2)
C(2)-C(3)	1.350(2)
N(2)-C(3)	1.365(2)
N(2)-C(4)	1.462(2)
C(4)-C(5)	1.523(2)
C(5)-C(6)	1.514(2)
C(6)-N(3)	1.4616(19)
N(3)-C(7)	1.272(2)
C(7)-C(8)	1.448(2)
C(8)-C(9)	1.367(2)
C(8)-N(5)	1.385(2)
C(9)-N(4)	1.360(2)
N(4)-C(10)	1.350(2)
C(10)-N(5)	1.314(2)
N(1)-C(1)-N(2)	112.43(15)
C(1)-N(1)-C(2)	104.25(14)
C(3)-C(2)-N(1)	110.77(16)
C(1)-N(2)-C(3)	106.40(14)
C(1)-N(2)-C(4)	127.38(14)
C(3)-N(2)-C(4)	126.19(14)
C(2)-C(3)-N(2)	106.14(15)
N(2)-C(4)-C(5)	112.79(14)

C(6)-C(5)-C(4)	112.80(14)
N(3)-C(6)-C(5)	110.82(13)
C(7)-N(3)-C(6)	118.05(13)
C(9)-C(8)-N(5)	109.95(13)
C(9)-C(8)-C(7)	128.05(14)
N(5)-C(8)-C(7)	122.01(14)
N(4)-C(9)-C(8)	106.10(14)
C(10)-N(4)-C(9)	106.96(13)
N(5)-C(10)-N(4)	112.62(14)
C(10)-N(5)-C(8)	104.37(13)

Table 4. Anisotropic displacement parameters ($\text{\AA}^2 \times 10^3$) for (37).

The anisotropic displacement factor exponent takes the form: $-2\pi^2 [h^2 a^{*2} U^{11} + \dots + 2 h k a^* b^* U^{12}]$

	U ¹¹	U ²²	U ³³	U ²³	U ¹³	U ¹²
C(1)	28(1)	31(1)	23(1)	-2(1)	5(1)	1(1)
N(1)	34(1)	35(1)	25(1)	2(1)	7(1)	0(1)
C(2)	33(1)	42(1)	32(1)	1(1)	12(1)	-3(1)
N(2)	32(1)	28(1)	19(1)	-2(1)	7(1)	3(1)
C(3)	25(1)	45(1)	31(1)	-3(1)	5(1)	2(1)
C(4)	54(1)	26(1)	23(1)	1(1)	10(1)	6(1)
C(5)	46(1)	31(1)	21(1)	1(1)	7(1)	7(1)
C(6)	38(1)	29(1)	19(1)	-1(1)	6(1)	1(1)
N(3)	33(1)	24(1)	21(1)	-1(1)	7(1)	2(1)
C(7)	30(1)	23(1)	23(1)	5(1)	8(1)	3(1)
C(8)	27(1)	20(1)	23(1)	3(1)	6(1)	3(1)
C(9)	34(1)	22(1)	28(1)	1(1)	11(1)	1(1)

N(4)	33(1)	20(1)	27(1)	-6(1)	5(1)	-2(1)
C(10)	37(1)	22(1)	23(1)	0(1)	6(1)	1(1)
N(5)	37(1)	21(1)	22(1)	0(1)	6(1)	0(1)

Table 5. Hydrogen coordinates ($\times 10^4$) and isotropic displacement parameters ($\text{\AA}^2 \times 10^{-3}$) for (37).

	x	y	z	U(eq)
H(1)	505	-550	-3907	33
H(2)	4402	1065	-4462	42
H(3)	5226	-348	-2818	41
H(4A)	3488	-2397	-2118	41
H(4B)	1629	-2067	-2289	41
H(5A)	3069	-1652	-435	39
H(5B)	4106	-563	-888	39
H(6A)	1930	816	-1411	34
H(6B)	722	-319	-1223	34
H(7)	2344	2277	-164	30
H(9)	3136	4180	1466	33
H(4)	2989	4191	3421	32
H(10)	2077	2090	3923	33

Table 6. Torsion angles [°] for (37).

N(2)-C(1)-N(1)-C(2)	-0.11(18)
C(1)-N(1)-C(2)-C(3)	0.03(19)
N(1)-C(1)-N(2)-C(3)	0.15(18)
N(1)-C(1)-N(2)-C(4)	178.48(14)
N(1)-C(2)-C(3)-N(2)	0.1(2)
C(1)-N(2)-C(3)-C(2)	-0.12(18)
C(4)-N(2)-C(3)-C(2)	-178.47(15)
C(1)-N(2)-C(4)-C(5)	-107.99(18)
C(3)-N(2)-C(4)-C(5)	70.0(2)
N(2)-C(4)-C(5)-C(6)	64.6(2)
C(4)-C(5)-C(6)-N(3)	168.12(14)
C(5)-C(6)-N(3)-C(7)	121.28(17)
C(6)-N(3)-C(7)-C(8)	177.58(14)
N(3)-C(7)-C(8)-C(9)	170.99(17)
N(3)-C(7)-C(8)-N(5)	-9.4(2)
N(5)-C(8)-C(9)-N(4)	0.45(18)
C(7)-C(8)-C(9)-N(4)	-179.89(15)
C(8)-C(9)-N(4)-C(10)	-0.45(18)
C(9)-N(4)-C(10)-N(5)	0.31(19)
N(4)-C(10)-N(5)-C(8)	-0.04(18)
C(9)-C(8)-N(5)-C(10)	-0.26(17)
C(7)-C(8)-N(5)-C(10)	-179.95(15)

Table 7. Hydrogen bonds for (37) [\AA and $^\circ$].

D-H...A	d(D-H)	d(H...A)	d(D...A)	$\angle(\text{DHA})$
N(4)-H(4)...N(3)#1	0.88	2.15	2.9902(18)	160.4
N(4)-H(4)...N(5)#1	0.88	2.55	3.0799(19)	119.6
C(10)-H(10)...N(1)#2	0.95	2.51	3.383(2)	153.2

Symmetry transformations used to generate equivalent atoms:

#1 $-x+1/2, y+1/2, -z+1/2$ #2 $x, y, z+1$

C(2)-C(3)-N(2)	106.14(15)
N(2)-C(4)-C(5)	112.79(14)
C(6)-C(5)-C(4)	112.80(14)
N(3)-C(6)-C(5)	110.82(13)
C(7)-N(3)-C(6)	118.05(13)



Epilogue

What lies behind us and what lies before us are tiny matters compared to what lies within us.

Ralph Waldo Emerson

